

Mechanistic insights into AMP-activated protein kinase-dependent gene expression

Thèse N° 9374

Présentée le 22 mars 2019
à la Faculté des sciences de la vie
Programme doctoral en approches moléculaires du vivant

pour l'obtention du grade de Docteur ès Sciences

par

Caterina COLLODET

Acceptée sur proposition du jury
Prof. J. Lingner, président du jury
Dr P. Descombes, Prof. B. Deplancke, directeurs de thèse
Prof. L. Fajas Coll, rapporteur
Dr B. Viollet, rapporteur
Prof. E. Meylan, rapporteur

2019

To my loved ones

"Success is not final.

Failure is not fatal.

It is the courage to continue that counts."

Winston Churchill

Acknowledgements

I would like to express my deepest gratitude to **Kei** and **Patrick** for the opportunity to perform my doctoral studies under their supervision. To Kei, for being a motivation with your hardworking attitude, always offering a rigorous problem-solving approach. Moreover, special thanks for supporting the foundation and growth of the NIHS Student Association, which has offered a platform to build a PhD community and promote the career development of many young scientists. To Patrick, for being so enthusiastic and for showing me the importance of creating cohesion within a team. You both trusted me, developing a project that I loved for its stimulating mixture of genomics and biochemistry approaches. I also thank my co-supervisor **Bart**, for being such an inspiring model and for his insightful advices along the journey.

I am grateful for our collaborators, **Benoit** and **Marc** for their help providing us with mouse primary hepatocytes. My heartfelt thanks to the Zebrafish team, to **Philipp G.** for all his insights and support, always willing to try new approaches. A thank also to **Joy** for being so lovely and competent. I will also keep in my heart **Phung**, it was a pleasure working with such a talented and motivated master student, I am so thankful for your banh bao cooking lesson. Un grazie al resto del gruppo, sapete quanto mi piaceva venirvi a trovare. A **Gabriele**, per tutte le dritte riguardo TFEB, credo un angelo ti abbia messo sulla mia strada. A **Giulia** per aver reso le mie gene ontology migliori ed avermi fatto scoprire la tiggella. Ad **Alice** per l'aiuto lavorativo e spirituale, per i brunch domenicali e i consigli, soprattutto per essere diventata un'amica in questi quattro anni.

Un grand merci également à toute l'équipe de Genomic pour avoir si bien réussi à créer un environnement positif (avec un canapé, des plantes, des croissants et des petits déjeuners, pour n'en citer que quelques-uns), où vous m'avez permis d'améliorer mon niveau de français. Une mention spéciale pour l'aide, en laboratoire et pour l'analyse, à **Frederic, Gregory, Julien et Sylviane**.

Wholehearted thanks to **Elisa G.** and **Claire DD.**, who trained and inspired me in the past, fueling my love for science. All my gratitude also to **Sandra VdC.** for having been a great mentor, positive and caring while helping me creating plans out of dreams.

Special thanks to all the colleagues and friends of the Sakamoto lab, which I have seen evolving so much during these four years. A special thanks to **Batman/Laurent**, you have been so patient while teaching how to perform the perfect western blot, always brightening the lab with your laughs, so cheerful and helpful, you are a real super hero. To the omniscient **Roger**, the perfect mixture of witty humor and genius, thanks for all the scientific discussions and for having honored me with the "bloody student" appellation. To **Laura E.**, we started this adventure together and I am so grateful you were here spreading positivity, I am even more glad we became good friends and kept in touch since then! Thanks also to **Saif** for your tips on presentations and for having passed your teaching-baton to me. To **Maria D.**, you are one of the smartest and strongest characters I have ever met, thanks for being a great inspiration on top of being our Cloning & Shortcut Queen. I would like to express my deepest appreciation to **Matthew (Matta)**, for being a great scientist and for having been my pillar/gatekeeper for the quality of my English throughout the thesis (and beyond) writing process. Together with **Robin**, thanks also for introducing me to the concept of British politeness, PG tips tea and the art of making scones.

Thanks to **Eva** and **Sonia** for having made the lab life moving forward smoothly. Thanks also to **Mayuko**, **Nicolas** and **Katyayanee**, even though we had less time to spend together, you still contributed at making the lab a special place. **Philipp R.**, you know few words will not be able to give justice to all the shared (dis)adventures. Thanks for the jokes, the beverages, the fun being secretaries, accountants, parking people, drivers and movers. Moreover, you made such a robust contribution to the success of the FIR symposium. Thanks also to **Margherita**, **Christopher**, **Olha** and **Laura C.** for supporting and making this event possible! Thanks to the scientists with whom I enjoyed chatting over the long hours in the cell culture room **Christian**, **El Hadji**, **Eija**, **Claudia**, **Julien**. Also many thanks to our neighbor **Canto's team**, to **Carles** for the advice along the thesis, to **Magali** for the help and laughs, which were shared first with **Sameer**, **Maria** and **Asia** and then with **Miriam**, **Angelique** and **Julie**. Thanks also to **Umji** and **Mapi** for being so cheerful! Thanks also to **Jonathan** and **Laurent D.** for their help during submission or pc emergency time.

I am also extremely grateful for the friendships that originated from being at the same PhD recruitment. To **Isabelle**, the Queen of Orchids, for having been the most supportive and joyful friend to share adventures with (like biking for hundreds of km, becoming lizards at the beach, surviving the PhD). Thanks also for introducing me to the full of energy and best storyteller **Sebastian**, you guys became like a second family. To **Omid**, thanks for being such a joyful, trustworthy, resilient and smart man, I am honored to call you friend. All my love to **Maria C.** for being such a brave and strong woman, I am so glad I met you and **Jake** and we had worldwide adventures together (now I know "it's all about that baste"). My gratitude goes also to the science-lovers and enthusiastic **Kathleen** and **Simone**, as well as the cute couples of **Tanja** and **Felix** as well as **Radek** and **Lucie**. Thanks to the BSNL team, especially **Galina**, **Sandra** and **Aleksandra**, being part of this association was a real blessing. I would like to thank also two other special friends, **Jessica** and **Biren**, meeting you directed my interest towards a research linked to metabolism long time ago. Un grazie anche agli amici italiani a Losanna, **Luca** che sono felicissima di aver ritrovato qui dopo Padova, **Daniel** per le chiacchierate culturali, **Lorenzo G.** per trovare le migliori news svizzere, **Edoardo** per la cultura cinematografica ed **Enrico** per tutte le risate. Un grazie speciale anche a **Simona**, sei stata la migliore coloc del mondo. Thanks also to all the other people who made me feel home in the various flats, **Lorenzo** (che spesso si palesava per la Simo), **Paloma** for the deep conversations as well as **Alejandro**, **Pedro** and **Shirani** for the shared dinners. Un grazie speciale anche a **Giulia** e **Lucia** per essere da 15 anni le mie due confidenti, a suon di spritz e sushi. Grazie anche a **Fabio** e gli antipodi, **Silvia**, **Debora**, e **Federico** per le chiacchierate. Grazie alla famiglia allargata fatta dai **Brun** e tutti gli altri ex colleghi.

Serge, it is difficult to decide where to add your name in these acknowledgements, it feels like confining you somewhere. You started as an amazing lab mate, always helpful and kind, reminding me to not be fearful but only curious about the experiments outcome. Few years later, you are now my lover and my rock, thanks for bringing out the best in me and making me see the world from a different perspective.

Grazie infine alla mia famiglia, a nonno **Luigi**, che mi ha trasmesso la passione per i libri e la conoscenza, quanto darei per poterti abbracciare e mostrarti questa tesi. A nonna **Celestina**, non potrò mai sdebitarmi per tutte le tue preghiere e le scorte infinite di cibo ma soprattutto amore. Grazie anche al fratello **Nicola** per le avventure condivise e per tutte quelle che verranno! Grazie specialmente a mamma **Eleonora** e papà **Giuseppe**, per avermi accompagnata e sostenuta in questo viaggio, senza di voi nulla sarebbe mai potuto accadere.

Riassunto

La proteina chinasi attivata dall'AMP (AMPK) è un enzima che svolge un ruolo cruciale nel mantenere l'omeostasi metabolica in condizioni di ridotta disponibilità energetica. AMPK è attivata da vari stress metabolici, quali possono essere la deprivazione di glucosio, l'ipossia e l'esercizio fisico, grazie alla sua capacità di rilevare diminuzioni dei livelli di ATP, nonché l'associato aumento di AMP ed ADP. Una volta stimolata, AMPK induce una rapida cascata di eventi che favoriscono la produzione di ATP, ad esempio promuovendo il consumo di zuccheri e grassi, ed al contempo la diminuzione del suo utilizzo. In aggiunta, AMPK permette un adattamento a prolungati periodi di stress energetico, modulando l'espressione genica.

Per approfondire le basi molecolari relative alla regolazione genica da parte di AMPK, in questo studio abbiamo confrontato l'effetto, a livello trascrittomico, di due attivatori appartenenti a diverse classi: 991, che si lega ad AMPK attivandola in modo selettivo, ed AICAR (5-aminoimidazolo-4-carbossamide-1- β -D-ribofuranoside), un farmaco che mima AMP. L'impatto di 991 ed AICAR è stato studiato tramite microarray eseguito su cellule embrionali di topo (MEFs) ed epatociti primari murini, dotati o privi di AMPK, dopo trattamento con i due composti. Inizialmente, i dati sono stati analizzati con lo scopo di individuare i geni modulati dai due attivatori nei diversi modelli cellulari. Da questo primo approccio è emerso che 991 è un composto altamente selettivo per AMPK, a differenza di AICAR. Conseguentemente, attraverso un'analisi bioinformatica, ci siamo focalizzati nella caratterizzazione dei trascritti modulati da 991. Abbiamo quindi scoperto che l'attivazione di AMPK è correlata a geni coinvolti in processi metabolici e lisosomiali, ed è mediata, almeno in parte, dai due fattori di trascrizione SREBP (proteina che lega l'elemento regolatore dello sterolo) e TFEB (fattore di trascrizione EB). Tra i trascritti modulati, abbiamo inoltre individuato i geni codificanti il soppressore tumorale folliculin (*Fln*) ed una delle proteine che vi interagiscono (*Fnip*), confermando il loro aumento in seguito ad attivazione farmacologica di AMPK, sia in MEFs che epatociti. Servendoci di un nuovo modello di *Danio rerio*, knockout per entrambe le subunità catalitiche della chinasi, abbiamo confermato che anche l'attivazione fisiologica di AMPK comporta l'aumento di *Fln* e *Fnip*. Abbiamo inoltre dimostrato che TFEB media l'incremento di *Fln* a seguito dell'attivazione di AMPK, attraverso un meccanismo indipendente dal bersaglio della rapamicina nei mammiferi (mTORC1).

In conclusione, il nostro studio ha permesso di confrontare l'impatto di diversi tipi di attivatori a livello trascrizionale, mettendo in luce l'importanza di favorire composti che agiscono in modo selettivo. Tramite un'analisi bioinformatica abbiamo inoltre individuato nuovi geni modulati da AMPK, tra i quali sono emersi *Fln* e *Fnip*. Questi ultimi sono stati ulteriormente caratterizzati, portando alla scoperta di un nuovo meccanismo molecolare, comprendente l'aumento di FLCN in risposta all'attivazione di AMPK, mediato da TFEB in modo indipendente da mTOR.

Parole chiave:

AMPK, proteina chinasi attivata dall'AMP, FLCN, folliculina, fattore di trascrizione EB, TFEB, sindrome metabolica, diabete di tipo 2, metabolismo

Abstract

AMP-activated protein kinase (AMPK) is a fundamental enzyme that controls energy homeostasis, through orchestrating the cellular response to a reduction in energy availability. Under conditions of cellular energy stress AMPK senses the decrease in ATP levels and responds by activating catabolic pathways, which will generate ATP, and switching off ATP-consuming ones, in order to restore the energy balance. AMPK regulates several signaling cascades linked to metabolism, overall favoring cellular consumption of glucose and lipid, allowing the cell to adapt to sustained energetic challenges through modulation of gene transcription. The aim of this thesis is to investigate the role that AMPK plays in the adaptive reprogramming of metabolism through transcriptional control. To identify genes and pathways regulated in an AMPK-dependent mechanism, we performed a whole-genome transcriptome profiling using microarray technology and compared the effects of two small molecule AMPK activators acting via distinct mechanisms, namely 991, which binds at the allosteric drug and metabolite site, and the AMP mimetic, 5-aminoimidazole-4-carboxamide-1- β -D-ribofuranoside (AICAR). The impact on gene expression of 991 and AICAR was investigated using two cellular and genetic models, mouse embryonic fibroblasts (MEFs) and mouse primary hepatocytes, either wild-type or AMPK-deficient. Statistical analysis of differential gene expression, followed by pathway analysis, revealed compound- and model-specific gene expression signatures. Notably we found that in contrast to AICAR, 991 affected gene expression almost exclusively in an AMPK-dependent manner. Interestingly, we identified that 991 modulated genes involved in the metabolic and lysosomal pathways, and that a number of these genes are under the control of the sterol regulatory element-binding protein (SREBP) and transcription factor EB (TFEB).

We identified the tumor suppressor folliculin (*Flcn*) and its binding partners, folliculin interacting protein (*Fnip*), as novel transcriptional targets of AMPK. We confirmed the upregulated expression of *Flcn* in response to pharmacological activation of AMPK in MEFs and primary hepatocytes. Furthermore, by taking advantage of a novel zebrafish whole-body knockout model of AMPK, we confirmed that physiological activation of AMPK partly mediates the increase in expression of *Flcn* and *Fnip*. We further identified TFEB as a mediator of the AMPK transcriptional response, accounting for the increase in *Flcn* expression through modulating its promoter activity. Moreover, we revealed the existence of a novel mechanism by which AMPK regulates TFEB through promoting dephosphorylation and nuclear translocation, independently of mammalian target of rapamycin complex 1 (mTORC1).

Taken together, we identified several new AMPK-dependent/-regulated genes and pathways that are differentially modulated in a cell type- and compound-specific manner. Most importantly, we discovered a novel and conserved AMPK-TFEB-FLCN axis in cellular and *in vivo* models. This work contributes to advance our understanding of AMPK-mediated regulation of transcriptional programs, nevertheless future studies will be required to elucidate the physiological relevance of the AMPK-TFEB-FLCN cascade.

Key words:

AMPK, AMP-activated protein kinase, FLCN, Folliculin, transcription factor EB, TFEB, transcription, metabolic syndrome, type 2 diabetes, energy metabolism

Table of content

Acknowledgements	5
Riassunto	7
Abstract	9
Table of content	11
List of figures	15
List of tables	17
List of appendix figures	19
List of appendix tables	19
1 Introduction	21
1.1 General introduction	21
1.2 Structure and regulation of AMPK	22
1.2.1 Isoform expression	23
1.2.2 Regulation by T-loop phosphorylation	24
1.2.3 Regulation by nucleotides	26
1.2.4 Regulation by ADaM-site binders	29
1.2.5 Physiological stimulation	31
1.2.6 Pharmacological activation	31
1.2.7 Clinical relevance as drug target	39
1.3 AMPK role in transcriptional regulation	41
1.3.1 Nuclear localization of AMPK	41
1.3.2 AMPK transcriptional regulation in muscle	44
1.3.3 AMPK transcriptional regulation in liver	49
1.3.4 Other transcriptional targets	53
1.3.5 TFEB - emerging lysosomal and metabolic regulator	57
2 Rationale and aim of the thesis	63

3	<i>Introduction to the results</i>	65
4	<i>Results, part I: transcriptome profiling reveals the AMPK-regulated genes in response to small molecule activators</i>	67
4.1	AMPK activation in the models chosen to investigate the role of AMPK on transcriptional regulation	67
4.2	991- and AICAR-mediated transcriptomic response	70
4.3	Pathways and transcription factors modulated by AMPK	74
4.4	Validation by qPCR of selected AMPK-regulated genes	78
4.5	Characterization of <i>Flcn</i> as transcriptional target of AMPK	81
5	<i>Discussion, part I</i>	85
5.1	991 and AICAR effect at gene expression level	85
5.2	<i>Flcn</i> and <i>Fnip</i>	86
6	<i>Results, part II: TFEB is regulated by AMPK and mediates the increase of Flcn</i>	91
6.1	An AMPK-TFEB/3 axis mediates the increase of <i>Flcn</i>	91
6.2	AMPK activation induces TFEB nuclear translocation independently of mTOR	95
6.3	In mouse hepatocytes, the stimulation of AMPK leads to TFEB nuclear translocation independently of mTOR	100
6.4	TFEB nuclear localization following 991-treatment is conserved in zebrafish	103
7	<i>Discussion, part II</i>	105
	AMPK promotes TFEB/3 nuclear translocation independently of mTORC1	105
8	<i>Conclusion and future perspectives</i>	109
8.1	General conclusion	109
8.2	Future perspectives	111
9	<i>Appendices</i>	113
9.1	Personal contributions	113
9.2	List of co-authored articles	114
9.3	Additional results	115

9.3.1	Materials & Methods	115
9.3.2	Establishing the treatment conditions in MEFs	116
9.3.3	PCA plots of the microarray samples	117
9.3.4	Lysosomal genes modulation by 991 activation of AMPK	118
9.3.5	Time course to monitor <i>Fln</i> pre-mRNA levels in response to AMPK	120
9.3.6	Determining if there is a direct interaction between FLCN-FNIP1-AMPK in U2OS	121
9.3.7	Generation and validation of the FLCN Ser62 phosphorylation site-specific antibody	122
9.3.8	Further characterization of TFEB	123
9.4	Manuscript published on BioRxiv	124
9.5	List of genes regulated by 991 in MEFs	173
9.6	List of genes regulated by 991 in mouse primary hepatocytes	176
	<i>Bibliography</i>	185
	<i>Glossary</i>	201
	<i>Curriculum Vitae</i>	207

List of figures

Figure 1. Schematic representation of the AMP-activated protein kinase (AMPK) subunits.	27
Figure 2. Representation of the canonical mechanisms of AMPK activation.	28
Figure 3. Crystal structure of the human AMPK $\alpha 2\beta 1\gamma 1$ complex.	30
Figure 4. Structure of AMPK activators inhibiting cellular ATP synthesis.	33
Figure 5. Structure of the AMPK activators AICAR and C13, pro-drugs converted in AMP analogs.	35
Figure 6. Structure of small-molecule AMPK activators binding to the ADaM site.	37
Figure 7. Effect of 991 on activity of a panel of 139 kinases.	39
Figure 8. Schematic representation of AMPK transcriptional targets in muscle.	47
Figure 9. Schematic representation of AMPK transcriptional targets in liver.	51
Figure 10. TFEB domains and phosphorylation sites.	60
Figure 11. Schematic depicting how TFEB transitions from an inactive to an active state.	61
Figure 12. Activation of AMPK in samples used for the microarrays.	69
Figure 13. Hierarchical clustering of the transcriptomic data.	72
Figure 14. Venn diagrams indicating the transcripts modulated by AMPK after 991 and AICAR treatment.	73
Figure 15. Gene enrichment analysis across the AMPK-regulated genes.	76
Figure 16. Confirmation of selected AMPK-target genes by qPCR.	80
Figure 17. Time course characterization of <i>Flcn</i> and <i>Fnip1</i>	83
Figure 18. Physiological activation of AMPK in zebrafish leads to <i>Flcn</i> increase.	84
Figure 19. Venn diagrams comparing different datasets of AMPK-regulated genes.	90
Figure 20. <i>Flcn</i> promoter activity in response to 991 treatment.	93
Figure 21. TFEB/3 mediate <i>Flcn</i> increase after AMPK activation.	94
Figure 22. AMPK regulation of TFEB in mouse embryonic fibroblasts.	99
Figure 23. AMPK regulation of TFEB in mouse primary hepatocytes.	102
Figure 24. AMPK activation promotes TFEB nuclear translocation in zebrafish larvae.	104
Figure 25. Schematic representation of TFEB regulation based on our results and hypothesis.	110

List of tables

Table 1. Nuclear transcriptional targets of AMPK.....	43
Table 2. Transcriptional targets of AMPK in muscle.....	48
Table 3. Transcriptional targets of AMPK in liver.	52
Table 4. Additional transcriptional targets of AMPK.....	56
Table 5. List of predicted transcription factors mediating AMPK transcriptional response.	77

List of appendix figures

Appendix Figure 1. Characterization of the MEFs model used for the microarray study.....	116
Appendix Figure 2. Principal component analysis (PCA) score plots.	117
Appendix Figure 3. Lysosomal genes enriched in MEFs after activation of AMPK by 991.....	118
Appendix Figure 4. Lysosomal genes enriched in primary hepatocytes after 991 stimulation of AMPK.	119
Appendix Figure 5. Pre-mRNA levels of <i>Flcn</i> in MEFs AMPK α 1 α 2 ^{+/+} after AMPK activation.....	120
Appendix Figure 6. FLCN and FNIP1 do not directly interact with AMPK.	121
Appendix Figure 7. FLCN Ser62 is not an AMPK-phosphorylation site in our model.	122
Appendix Figure 8. Further characterization of TFEB.....	123

List of appendix tables

Appendix Table 1. List of genes regulated by 991 in MEFs.	173
Appendix Table 2. List of genes regulated by 991 in mouse primary hepatocytes.....	176

1 Introduction

1.1 General introduction

Mammals require a constant supply of energy in order to grow and develop, reproduce, repair and move, as well as maintaining intracellular homeostasis. This means that organisms must obtain and then use this energy in order to survive. In general, mammals obtain this energy by ingesting and absorbing organic compounds and converting the nucleotide adenosine diphosphate (ADP) and phosphate ions (Pi) into adenosine triphosphate (ATP) which is regarded as the universal energy currency of the cell. Under normal/unstressed conditions, the equilibrium for the reaction that interconverts ATP and ADP + Pi lies in favor of ATP hydrolysis¹. However, by coupling ATP synthesis to oxidation of reduced compounds, most cells maintain ATP concentrations around 10-fold higher than those of ADP, which is many orders of magnitude away from the equilibrium position of the hydrolysis reaction. A useful analogy can be drawn between ATP and ADP and the chemicals in a rechargeable battery: catabolism “charges up the battery” by converting ADP to ATP, while the majority of other cellular functions require energy and are mainly driven by being coupled to the conversion of ATP back to ADP^{1,2}. Accordingly, to sustain life this battery needs to be fully charged (ratio of ATP to ADP of the order of 10:1), which requires that the rate of ATP production by catabolism is balanced by the rate at which ATP is consumed by energy-demanding processes, including the biosynthesis of macromolecules (*e.g.* protein synthesis) required for cellular growth. Given the critical requirement of the maintenance of appropriate ratios of ATP:ADP and AMP:ATP, it is reasonable that sophisticated mechanisms to regulate this ratio are equipped and conserved. One of the most important of these is the AMP-activated protein kinase (AMPK), which forms the main topic of this thesis.

AMPK is an evolutionary conserved enzyme found in all eukaryotes and acts as a guardian of the energy status at the cellular and whole-body level³. AMPK is activated by different stress conditions, including low glucose⁴, hypoxia, ischemia^{5,6} and exercise⁷, which diminish cellular ATP levels. Under these conditions, the intracellular AMP and ADP levels increase and these nucleotides activate AMPK leading to stimulation of catabolic, ATP-generating processes (such as glucose uptake, glycolysis and fatty acid oxidation), and inhibition of anabolic, ATP-consuming processes (*e.g.* fatty acid and protein synthesis). Overall, AMPK plays a critical role to adapt to changing energy demands and help ensure cell survival under various stress conditions⁸. AMPK regulates carbohydrate and lipid metabolism in a number of tissues, including the liver, heart, skeletal muscle and adipose tissue. Importantly, AMPK can regulate glucose and lipid homeostasis

independently of insulin-signalling and activation of AMPK has also been shown to improve insulin-sensitivity⁹, which places AMPK as an important drug target for treating diabetes and insulin-resistance¹⁰. Consistent with this AMPK-deficient animal models displayed insulin-resistance and defects in glucose homeostasis¹¹. AMPK came to prominence as a potential drug target after the widely prescribed type 2 diabetic drug, metformin, was shown to activate AMPK in the liver *in vivo*, raising the possibility that the beneficial effects of metformin are mediated, at least in part, by activation of AMPK. Recently, a number of potent direct activators of AMPK have been developed that display beneficial effects in diabetic rodent and non-human primate models, and these effects were dependent on the expression/activity of AMPK^{12,13}. Taken together, there is clear evidence for the potential of AMPK as a therapeutic target for treating various metabolic disorders¹⁴.

AMPK achieves its effects by rapid and direct targeting a number of substrates involved in energy metabolism, as well as initiating metabolic reprogramming events by regulating various transcription factors. Through its ability to target gene transcription, AMPK allows the cell to adapt to a prolonged change in nutrient availability. For example, activation of AMPK leads to inhibition of genes involved in glucose production¹⁵ and lipogenesis^{16,17} in the liver¹⁸. Furthermore, chronic activation of AMPK has been demonstrated to induce mitochondrial biogenesis in muscle through regulation of gene transcription¹⁹ and increase in glucose transporter expression allowing cells to increase the uptake glucose into muscle²⁰. Whilst research has been performed into the effects of AMPK on transcription factors and gene expression, a number of studies have used non-specific activators of AMPK and lacked complementary experiments in AMPK-deficient cells. With the recent advent of potent and selective activators of AMPK and a vast number of AMPK-deficient models available, it is now possible to re-evaluate the contribution of AMPK to various metabolic programming events.

1.2 Structure and regulation of AMPK

Key to developing specific and potent activators of AMPK is understanding the structure and regulation of each AMPK complex. AMPK is a heterotrimeric serine/threonine kinase, composed of a catalytic α subunit and two regulatory subunits (β and γ). In mammals there are 12 heterotrimeric complexes possible due to the existence of a number of different isoforms of each subunit; there are two isoforms of the α subunit ($\alpha 1$ and $\alpha 2$), two of the β subunit ($\beta 1$ and $\beta 2$) and three of the γ subunit ($\gamma 1$, $\gamma 2$ and $\gamma 3$)²¹. AMPK is activated primarily by phosphorylation on the activation loop of the α subunit kinase domain, by upstream kinases. Ligand binding to two distinct regulatory sites on AMPK has been shown to maintain the phosphorylated, active form of AMPK

as well as causing allosteric activation. In this section, I will describe the regulation of AMPK by these phosphorylation and ligand binding events. I will conclude by providing a summary of the existing activators, underlying the knowledge in support of the relevance of targeting AMPK in the clinic.

1.2.1 Isoform expression

There is a preferential pattern of expression of the different subunit isoforms between various tissues, which may suggest a tissue-specific role for these complexes. While $\alpha 1$, $\beta 1$ and $\gamma 1$ are ubiquitously and uniformly expressed across tissues/cell-types, other subunit isoforms show characteristic distributions. For instance, $\alpha 2$ is predominantly expressed in skeletal muscle²², but also highly expressed in heart and liver, whereas $\beta 2$ is expressed primarily in skeletal muscle and to a lesser extent in heart²³. The subunits $\gamma 3$ is exclusively expressed in glycolytic (fast-twitch, type II) skeletal muscle²⁴⁻²⁶. Notably, it has been shown that $\gamma 3$ -containing complexes are necessary for mediating the effects of AMPK on increasing glucose uptake in response to an AMP-mimetic compound 5-aminoimidazole-4-carboxamide-1- β -D-ribofuranoside (AICAR) and energy stress (*e.g.* hypoxia)^{24,27}. Although whether $\gamma 3$ is required in mediating exercise-/contraction-stimulated glucose uptake in skeletal muscle is controversial and under debate²⁸, AMPK $\alpha 2\beta 2\gamma 3$ is uniquely activated during high intensity exercise in human skeletal muscle²⁹. Furthermore, a naturally occurring gain-of-function mutation of $\gamma 3$ in human (R225W)³⁰, originally identified in purebred Hampshire pigs (R200Q), was associated with an increase in muscle glycogen content³¹. Additional support for the causative role of the R200Q mutation in the elevated muscle glycogen levels has been provided by transgenic mouse models overexpressing equivalent mutant (R225Q)²⁴, demonstrating the conserved and key role of this subunit isoform in muscle glucose and glycogen metabolism. $\gamma 2$ is present in many tissues including heart, brain, pancreas and liver³², while its role is intensively studied in heart, because of its potential implication on the metabolic syndrome and cardiomyopathy. Interestingly, human gain-of-function mutations in the gene encoding $\gamma 2$ were discovered in patients with congenital hypertrophic cardiomyopathy and familial pre-excitation syndrome, termed Wolff-Parkinson-White syndrome³³. These mutations were shown to cause an aberrant accumulation of glycogen within the heart (*i.e.* cardiomyocytes), which is tightly linked to the cardiac phenotype observed in these humans³⁴⁻³⁶. Although $\gamma 2$ is expressed in a number of tissues, these naturally-occurring mutations may reveal a potential $\gamma 2$ subunit isoform specific role in the heart.

There is major interest in generating isoform-specific AMPK activators to allow for selective activation of AMPK in a particular cell-type/tissue. This may be important when trying to

avoid activation of AMPK that may lead to a detrimental effect, for example, activation of γ 2-complexes in the heart may lead to a cardiac phenotype. Research is focused on understanding the precise regulation of these 12 heterotrimeric AMPK complexes by natural and synthetic activators in an attempt to exploit these tissue-specific roles. There is also considerable interspecies variation in AMPK isoform expression. For instance, AMPK α 1 β 2 γ 1 predominates in human hepatocytes, whereas AMPK α 2 β 1 γ 1 is the major complex in rat and pig liver³⁷.

Therefore, it is particularly important to complement the work performed in rodent models with human models/samples depending on the tissue of interest. It is also important to note that a major progress has been made during the last decade in delineating the distinct pathophysiological function of AMPK and its isoforms, largely due to the generation of whole-body and conditional gain-/loss-of function mouse models. This aspect is elegantly and extensively covered in a recent review article³⁸.

1.2.2 Regulation by T-loop phosphorylation

The α subunit includes an N-terminal Ser/Thr kinase domain that contains a conserved activation loop (also called the T-loop) (Figure 1). Phosphorylation of site Thr172³⁹ (numbered according to the rat sequence) in the activation loop is required for maximal AMPK activity. Indeed, the negatively charged phosphate group of the phosphorylated Thr172 and residues located within the kinase domain stabilize the T-loop, promoting the substrate binding and optimal positioning of key residues involved in kinase catalytic activity. Downstream from the kinase domain (KD) lies an auto-inhibitory domain (AID, shown in Figure 1), which binds to elements within the kinase domain, maintaining AMPK in an inactive conformation. It is proposed that activation of AMPK by nucleotides leads to dissociation of this domain, relieving this inhibition⁴⁰⁻⁴².

Two kinases have been demonstrated to phosphorylate Thr172, namely liver kinase B1 (LKB1) and Ca^{2+} -calmodulin-dependent protein kinase kinase β (CAMKK β). In contrast, the phosphatases responsible for Thr172 dephosphorylation under physiological conditions are still unknown (Figure 2). LKB1 was the first kinase to be shown to phosphorylate Thr172⁴³⁻⁴⁶. LKB1 is a tumor suppressor that exists in complex with two accessory subunits STE20-related kinase adaptor α and β (STRAD α/β) and mouse protein 25 α and β (MO25 α/β). LKB1 is crucial for muscle-AMPK stimulation in response to pharmacological (*e.g.* AICAR) and physiological (*e.g.* fiber contraction) stimuli⁴⁷. LKB1 is believed to be constitutively active since its activity is not altered by energy stress conditions that promote AMPK activity⁴⁶. Instead, adenine nucleotides binding to AMPK can facilitate the phosphorylation by making it a better substrate for LKB1 and by inhibiting

dephosphorylation, thereby maintaining AMPK in its active state. The details of this process will be further explored below (section 1.2.3 - Regulation by nucleotides).

Even though LKB1's role as a modulator of AMPK is well established, recent discoveries suggest that the complexity of this relationship may be more complicated than originally expected. It has been reported that, in response to low nutrient availability, an AXIN-LKB1-AMPK complex localizes on the lysosome surface and facilitates the phosphorylation of Thr172⁴⁸. Interestingly Zhang *et al.*, demonstrated that the formation of the AXIN-LKB1-AMPK complex requires LAMTOR1 (late endosomal/lysosomal adaptor, MAPK and mTOR Activator-1), a component of the Ragulator machinery, which is known to recruit mammalian target of rapamycin (mTORC1) to the lysosomal membrane under energy-rich conditions. This regulatory cascade suggested for the first time a dual role for the Ragulator complex that could act as a lysosomal sensor capable of stimulating different signaling cascades (*i.e.* mTORC1 and AMPK) depending on nutrient availability⁴⁹. Moreover indicating that the activation of AMPK may be dependent on recruitment by other factors, which can place this enzyme and its activation at specific loci.

The second confirmed upstream kinase for Thr172 is CAMKK β , which has a high sequence homology with LKB1 and responds to an increase in cytosolic-free calcium (Ca^{2+})⁵⁰⁻⁵². Intracellular Ca^{2+} can act as a secondary messenger in response to signals, and indeed several stimuli have been shown to raise Ca^{2+} levels and consequently stimulate AMPK through CAMKK β . The physiological relevance of this cascade and the signals that trigger it, are going to be further discussed (section 1.2.5 - Physiological stimulation).

In addition to phosphorylation of Thr172, AMPK can also be phosphorylated on a number of additional sites throughout the α and β subunits. Some of these sites have been attributed to autophosphorylation events that occur, including Ser108 on β ⁵³, Ser485/491 sites on $\alpha 1/\alpha 2$ ⁵⁴ and Ser377 on $\alpha 2$. The precise physiological role of these autophosphorylation sites on AMPK function is unclear. Phosphorylation of Ser108 is important for high affinity binding of small molecule activators of AMPK (see section 1.2.4 - Regulation by ADaM-site binders) and maintaining basal AMPK activity⁵⁵, and some of the other sites have been implicated in subcellular localization of AMPK⁵⁶. Furthermore, other kinases have been shown to directly phosphorylate AMPK outside of the KD. For example, phosphorylation of $\alpha 1/\alpha 2$ on Ser485/491 by protein kinase B ((PKB) also known as Akt)⁵⁴ as well as Ser377 on $\alpha 2$ by CDK4⁵⁷ have been shown to alter the kinase activity of AMPK. These phosphorylation sites were reported to have an inhibitory effect on AMPK activity, however the physiological role of these inhibitory events is not well defined.

1.2.3 Regulation by nucleotides

AMPK is activated by a decrease in ATP levels within the cell, and a concomitant increase in AMP and ADP levels, providing a mechanism for the cell to sense adenine nucleotide changes (see Figure 2). Binding of AMP and ADP to the γ subunit promotes Thr172 phosphorylation of AMPK as well as preventing its dephosphorylation and inactivation. In addition, AMP, but not ADP, can allosterically activate AMPK, and all of these processes are inhibited by the ATP, allowing AMPK to be activated when ATP levels fall while AMP and ADP levels rise. AMP, ADP and ATP⁵⁸ bind to the cystathionine β -synthase (CBS) repeats in the γ subunit. The CBS are organized into two structures referred to as Bateman domains⁵⁹, which provide four potential adenine-nucleotide binding sites (Figure 1). Studies indicate that while sites 1 and 3 can bind the three adenine nucleotides in a competitive manner, site 4 has a tightly bound AMP that appears to be non-exchangeable, whereas site 2 remains unoccupied due to a missing aspartate residue that causes it to be non-binding⁶⁰. An α -linker within the C-terminal domain (CTD) of the α subunit contacts the CBS domains within the γ subunit through two α subunit-interacting regulatory motifs (*i.e.* α -RIM1 and 2)⁶¹⁻⁶³. This provides a mechanism for how the enzyme activity, located in the α subunit, can be altered by the nucleotide status of the γ subunit. There are three isoforms of the γ subunit and they differ in their sequences by virtue of differing N-terminal lengths, with γ 2- and γ 3- containing an N-terminal extension that is absent in the γ 1 subunit isoform. It is not clear the precise role of these N-terminal extensions and they may play a role in localization of AMPK within the cell⁶⁴. Recently, it was reported that the N-terminal of γ 2 may influence the ability of AMPK to respond to activators at the allosteric drug and metabolite binding site (ADaM-site) on AMPK (section 1.2.4 - Regulation by ADaM-site binders).

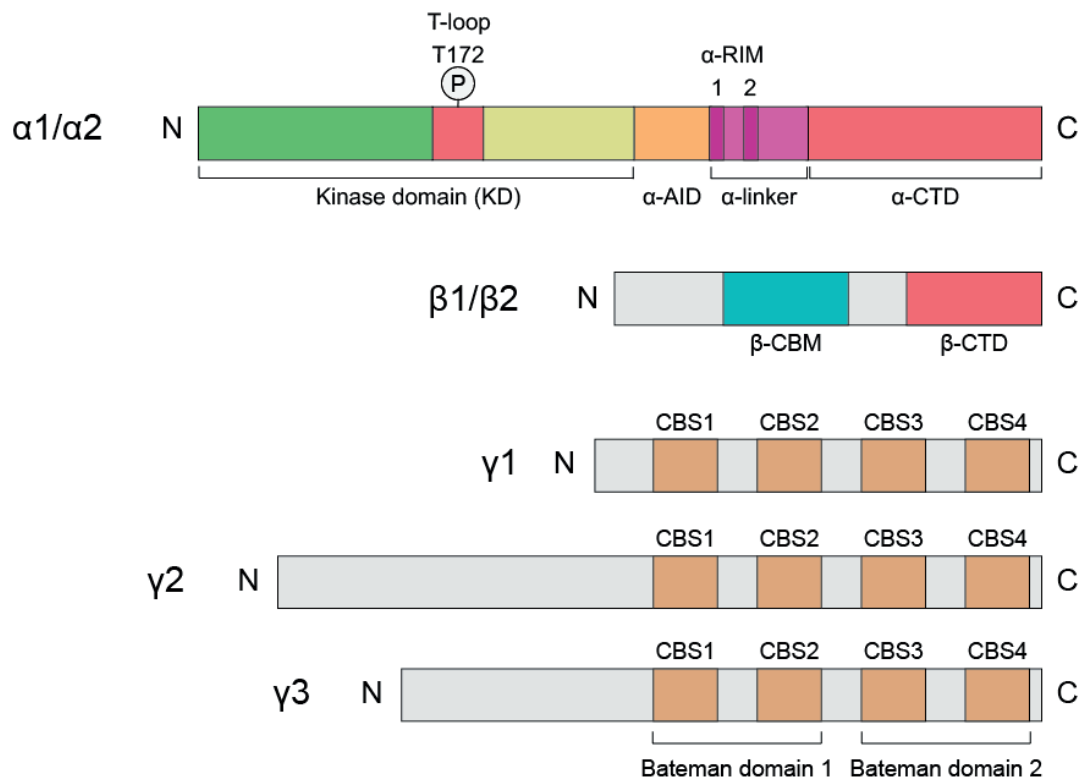


Figure 1. Schematic representation of the AMP-activated protein kinase (AMPK) subunits.

AMPK is a heterotrimeric protein composed of a catalytic subunit (α) and two regulatory ones (β and γ). The **α subunit** exists as two isoforms ($\alpha1$, $\alpha2$) with a highly similar structure, that from the N- to the C-terminus comprises: the kinase domain (KD) with a large lobe (in green), the activation loop (T-loop) with the Thr(T)172, whose phosphorylation is required for the kinase activity, and a small lobe (yellow). These elements are followed by an α -autoinhibitory domain (α -AID, in orange), the α -linker with the two subunit-interacting regulatory motifs (α -RIM1 and 2, in violet) and the α -C terminal domain (α -CTD, in red). The **β subunit** has also two similar isoforms ($\beta1$, $\beta2$) with a carbohydrate-binding module (β -CBM, in light blue) and the β -C terminal domain (β -CTD, in red). The **γ subunit** presents three isoforms ($\gamma1$, $\gamma2$, $\gamma3$) all having two Bateman domains with two cystathionine β -synthase domains (CBS, in brown) each, where AMP, ADP and ATP can bind. From G. Hardie *et al.*⁶⁵

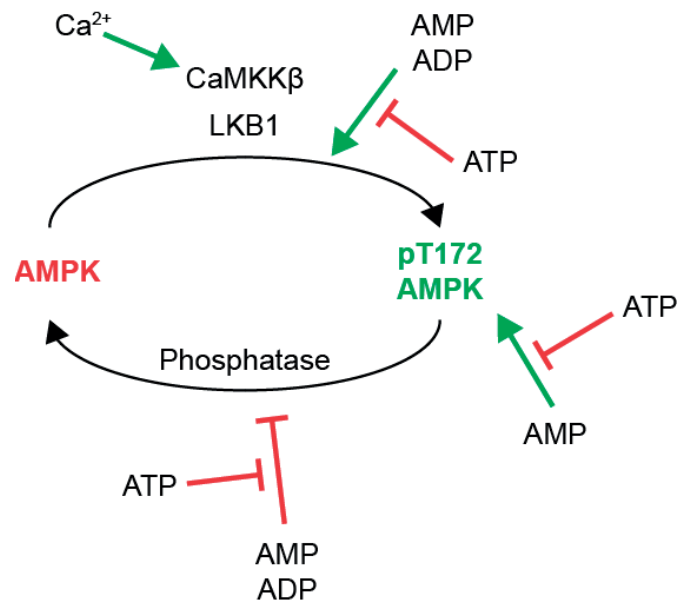


Figure 2. Representation of the canonical mechanisms of AMPK activation.

AMPK can be present in the cells in a dephosphorylated and inactive form (in red) or in a phosphorylated at Thr172 (pT172, in green) and active form. AMPK can be stimulated by increase in AMP/ATP or ADP/ATP ratio as well as Ca^{2+} concentration. The conversion from inactive to active status is catalyzed by at least two upstream kinases, namely LKB1 that is constitutively active, and CaMKK β , that requires an increase in Ca^{2+} levels. Increases in AMP or ADP stimulate AMPK by causing a conformational change that promotes phosphorylation by upstream kinases and by protecting AMPK from dephosphorylation by phosphatases. ATP on the contrary antagonizes the events promoted by AMP/ADP, inhibiting AMPK activity. Color code for the arrows: red indicates inhibition and green activation. Adapted from G. Hardie *et al.*⁶⁶

1.2.4 Regulation by ADaM-site binders

In 2006, Abbott laboratories identified the first direct AMPK activator through a high-throughput screen, termed A-769662, a thienopyridone⁶⁷, which allosterically activated AMPK possibly through a different mechanism to AMP⁶⁸. Subsequently, it was demonstrated that activation of AMPK by A-769662 depended on the carbohydrate-binding module (β -CBM) located within the β subunit of AMPK⁶⁹ (Figure 1 and 3). The β -CBM was identified in AMPK due to its similarity to other domains present in proteins that have been shown to bind to starch, such as the N-terminal domains of *E. coli* glycogen branching enzyme and *Pseudomonas* isoamylase⁷⁰. Whilst AMPK has been shown to bind to carbohydrates⁵⁶ and this may regulate its activity, the physiological role of this domain is unclear.

Mutations in the γ subunit of AMPK that interfere with AMP regulation did not affect regulation of A-769662 suggesting that there was an additional site on AMPK, separate to the nucleotide binding ones. A number of further direct activators were identified, including 991 (benzimidazole derivative), and all were shown to share the same requirement for binding to the β -CBM of AMPK^{12,61}. Structural studies revealed that there is an additional binding site formed between the α kinase domain and the β -CBM, termed ADaM-site⁶¹. Additionally, there is an autophosphorylation site (Ser108 on β 1) located within the β -CBM that is required for maximal AMPK stimulation by A-769662 and 991 (as well as other activators, such as salicylate)⁷¹. The ADaM-site has now been a major focus of attention for developing direct AMPK activators for use in a clinical setting (read more in section 1.2.7 - Clinical relevance as drug target). Moreover, a number of these activators have been shown to have preferential activation of different AMPK complexes. For example, A-769662 has been demonstrated to mainly activate β 1-containing complexes⁷². This allows the ability to activate specific AMPK complexes in tissues which have preferential expression of β 1-containing complexes. Interestingly, γ 2-containing complexes were shown to have enhanced Thr172 protection from dephosphorylation in response to treatment with 991. This allows γ 2-containing AMPK to become activated to a greater extent compared to γ 1- or γ 3- containing heterotrimers⁷³. The precise mechanism for how the N-terminal extension of γ 2 is able to influence the activation of AMPK at the ADaM site is unclear. Further studies are required since our current understanding of the regulation of AMPK is based off of γ 1-containing structures, which lack an N-terminal extension.

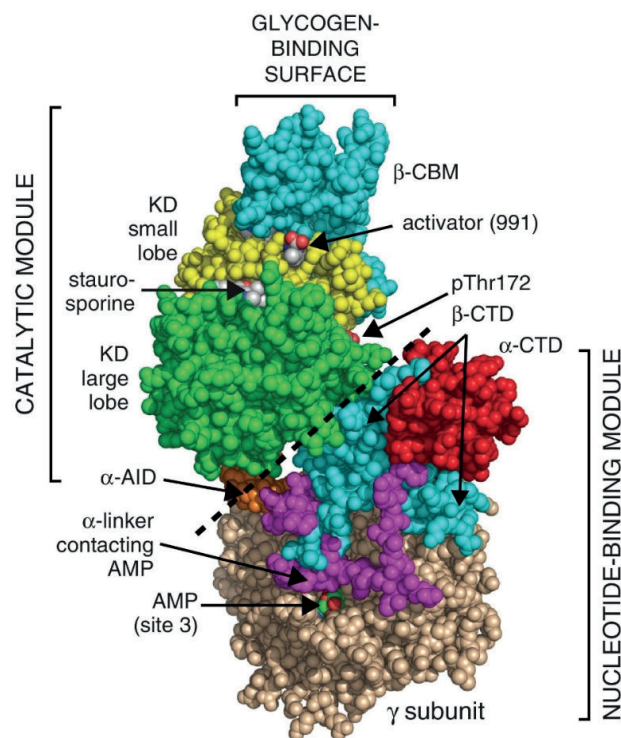


Figure 3. Crystal structure of the human AMPK $\alpha 2\beta 1\gamma 1$ complex.

The human AMPK $\alpha 2\beta 1\gamma 1$ complex was crystallized in the presence of AMP, the kinase inhibitor staurosporine and the ADaM-site binder activator 991, visible in the cleft between the β subunit carbohydrate binding module (β -CBM) and the kinase domain (KD) small lobe. The complex was additionally phosphorylated on Thr172. The diagonal dotted line divides the catalytic module and the adenine-nucleotides binding module. All the domains are color-coded and labeled as in figure 1. From G. Hardie *et al.*⁷⁴.

1.2.5 Physiological stimulation

AMPK has been demonstrated to be activated in response to a number of physiological and pathophysiological conditions, as a consequence of its ability to sense changes in the adenine nucleotide levels within the cell. As described previously, activation of AMPK through nucleotides is thought to be mediated through LKB1-dependent phosphorylation. Increase of the AMP/ATP and ADP/ATP ratios can be caused by various metabolic stress such as glucose deprivation⁴, oxidative stress⁵, hypoxia and ischemia. Importantly, the most physiological mean leading to AMPK activation is skeletal muscle contraction, during exercise⁷⁵. Throughout physical activity, the ATP turnover has a dramatic increase, which has been shown to activate AMPK in rodents⁷⁶ and humans⁷⁷ in an intensity-dependent⁷⁸ manner. To sustain the energy request during high ATP demand, AMPK promotes oxidative and non-oxidative phosphorylation.

Additionally, AMPK supports the whole-body energy homeostasis integrating cell non-autonomous mechanisms of activation (hormonal and systemic)⁶³, which are typically mediated by alterations in intracellular Ca^{2+} through $\text{CaMKK}\beta$ ⁷⁹. For example, during fasting periods the gut-released hormone ghrelin can activate AMPK in the hypothalamus⁷⁹, via binding to G-protein-coupled receptor GHSR1 (growth hormone secretagogue receptor type 1), initiating the production of inositol trisphosphate and release of intracellular Ca^{2+} . Adiponectin, an adipokine secreted by adipocytes, which increases insulin sensitivity of peripheral tissues, can also activate AMPK inducing Ca^{2+} influx through its receptor 1 (AdipoR1⁸⁰). Adiponectin-dependent stimulation of AMPK promotes the organism food intake⁸¹ while increasing mitochondrial biogenesis in muscle⁸⁰ and reducing gluconeogenesis in liver⁸². Notably, increase in Ca^{2+} levels, and consequent $\text{CaMKK}\beta$ -dependent activation, happen also during neuronal depolarization and have been linked with a neuroprotective function of AMPK⁵⁰. The beneficial effect of Ca^{2+} -dependent stimulation of AMPK has also been observed in T lymphocytes. For instance, during inflammation the activation of T cell antigen receptor triggers a Ca^{2+} -mediated signaling pathway that activates AMPK, favoring ATP production and ensuring energy supply for an efficient immune response⁸³.

1.2.6 Pharmacological activation

In order to assess the contribution of AMPK in mediating signaling pathways and phenotypes, researchers have been using various methods to activate AMPK. These mechanisms range from a) non-specific activation of AMPK through inhibition of ATP synthesis, b) molecules that mimic the effects of its natural activating ligand (AMP-mimetics) and more recently c) more selective direct activators targeting the ADaM-site on AMPK. These advances in the ability to specifically target

AMPK, alongside advances in our ability to genetically manipulate the expression of AMPK, have revealed the AMPK-dependent processes in energy homeostasis.

Activators inhibiting cellular ATP synthesis

By virtue of its ability to sense changes in AMP and ATP levels of the cell, AMPK is activated by inhibition of mitochondrial respiration or glycolysis, processes that would normally generate ATP. In cells relying on glycolysis for ATP generation, the activation of AMPK can be achieved by treatment with inhibitors of this process, such as 2-deoxyglucose (2-DG). It is also possible to block ATP generated through mitochondrial oxidative phosphorylation, using compounds that target this process. These compounds act on the mitochondrial complexes, for example R419⁸⁴, metformin and phenformin inhibit complex I, antimycin A inhibits complex III and resveratrol or oligomycin inhibit ATP synthase (some examples can be found in Figure 4). In addition, a number of natural products (over 100) have been reported to activate AMPK⁸⁵ and whilst the molecular mechanism has not been defined for most of them, they are thought to activate AMPK through inhibition of mitochondrial complexes, *e.g.* berberine and arctigenin. One very important consideration when using these non-specific activators of AMPK, is that they will have multiple effects within the cell. Therefore, it is important to substantiate any claims with these activators, with complementary experiments in knockout models of AMPK, to distinguish the AMPK-dependent effects of these activators from potential AMPK-independent effects of the compounds.

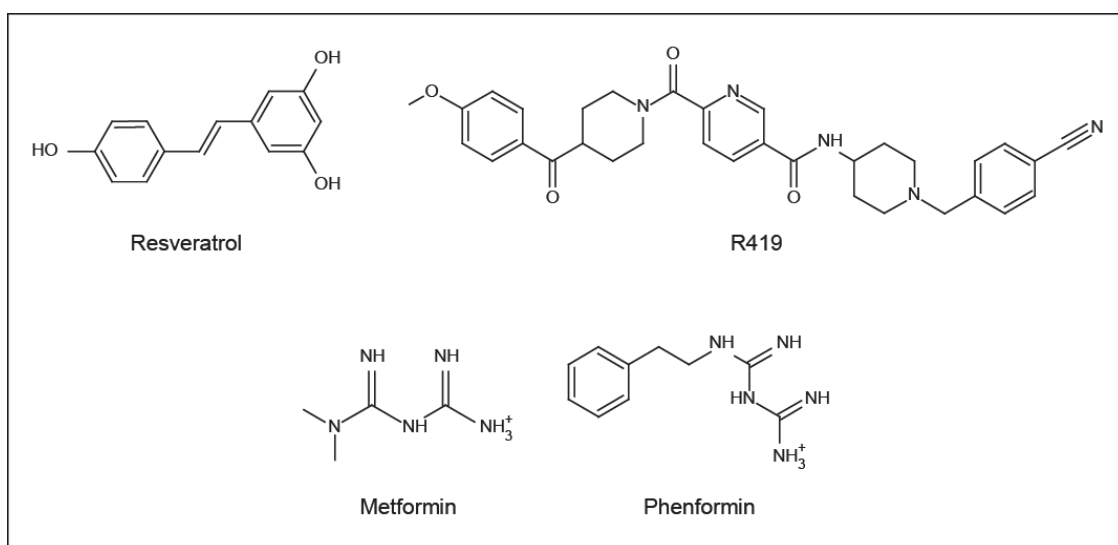


Figure 4. Structure of AMPK activators inhibiting cellular ATP synthesis.

Example of molecules activating AMPK by lowering/blocking cellular ATP generation, namely resveratrol, R419 and the antidiabetic drugs metformin and phenformin.

Pro-drugs converted into AMP-analogs

Before the identification of the ADaM-site on AMPK, the main method for activating AMPK was to use classes of compounds that mimicked the natural activating ligand, AMP. Notably, cell-permeable AMP analogues do not exist, since the negatively charged phosphate group on the nucleotides hinders their entry into the cell. AICAR is absorbed by the cells via nucleoside transporters⁸⁶ and consequently phosphorylated into AICAR monophosphate (ZMP) (Figure 5), an intermediate of the pathway for the purine nucleotide synthesis, by cytoplasmic adenosine kinase. ZMP activates AMPK in almost all cells and tissues but to a lower extent compared to AMP due to its weaker binding affinity. The capability of ZMP to nevertheless stimulate AMPK is due to the fact that its conversion rate is much faster than the metabolization rate, allowing an accumulation of ZMP within cells. Importantly, ZMP has also been proven to modulate the activity of other AMP-sensitive enzymes. This has the potential drawback that when studying the effects of AMPK using AICAR treatment, the observed results may or may not be due to activation of AMPK, but through activation of these other AMP-regulated proteins. Similar to ATP-synthesis inhibitors, it is important to complement experiments using AICAR with AMPK-deficient cell/model systems.

Recently, a synthetic compound named compound 13 (C13), was developed. C13 is a phosphonate diester that once uptaken by the cells is then metabolized by esterases into C2 (compound 2, furan-2-phosphonic acid derivative, Figure 5)⁸⁷. C13 has a higher potency compared to ZMP and due to its more unique properties, it is assumed that it has more specificity to AMPK compared to ZMP, although the potential off-target effects have not yet been fully investigated.

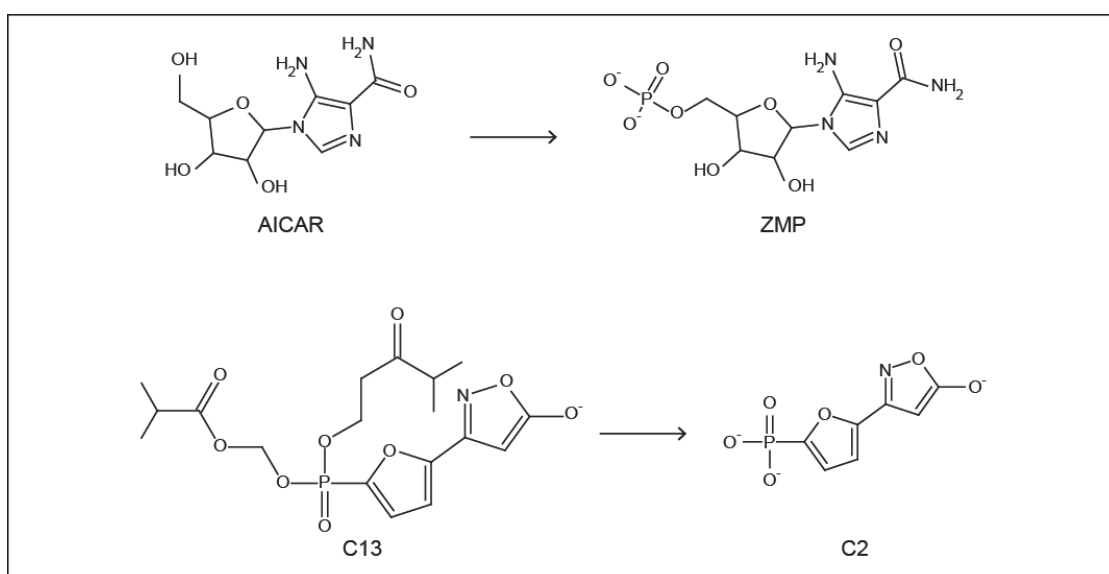


Figure 5. Structure of the AMPK activators AICAR and C13, pro-drugs converted in AMP analogs.

5-aminoimidazole-4-carboxamide-1-β-D-ribofuranoside (AICAR) and compound 13 (C13) are firstly absorbed by the cells and then transformed into AICAR monophosphate (ZMP) and C2, respectively. ZMP and C2 stimulate AMPK acting as AMP analogs.

Allosteric activators that bind at sites distinct from AMP sites

Activators binding to a site located between the α subunit kinase domain and the β -CBM, termed ADaM site, constitute the third class⁸⁸ (some examples are in Figure 6). These compounds stimulate AMPK allosterically as well as by protecting it from dephosphorylation. The first compound identified was A-769662, a thienopyridone developed by Abbott laboratories through a high-throughput screen⁶⁷ that preferentially activates β 1-containing complexes⁶⁹. The discovery of A-769662 led to the synthesis of several compounds with a comparable mode of action, such as PF-06409577¹³, PF-249¹² and MT 63-78⁸⁹. Despite being a very promising activator of AMPK, A-769662 has been reported to cause several off-target effects, through a still unknown mechanism(s), in isolated mouse skeletal muscle and in other cells/tissues^{90,91} when used at high concentrations⁷². An additional drawback is that A-769662 has poor oral availability and it cannot activate β 2-containing complexes, which is the predominant isoform expressed in muscle, a tissue of particular interest to stimulate AMPK.

More recently a cyclic benzimidazole named 991 (also known as ex229), was developed by Merck. 991 binds AMPK 10-times tighter than A-769662 in cell-free assays⁶¹ and activates both β 1- and β 2-containing AMPK (with a higher affinity to β 1 complexes²⁶). 991 appears to have a high specificity towards AMPK since, as we show (Bultot...Collodet *et al.*) by using a cell-free assay against a panel of protein kinases, 991 promoted the exclusive activation of AMPK²⁶ (Figure 7). Importantly there are no known off-target effects of 991, although one caveat is its limited bioavailability. Recently MK-8722⁹² and PF-739¹², two similar benzimidazole compounds, were discovered. Similar to 991, both derivatives are pan-AMPK activators with a preference towards β 1-containing heterotrimers. However, MK-8722 and PF-739 differ from 991 because of their high bioavailability, a key feature which allowed their use for preclinical trials in rodents and non-human primates (section 1.2.7 - Clinical relevance as drug target).

The identification of the ADaM-site on AMPK posed the open question of whether natural ligands/metabolites, possibly endogenous, can similarly up-regulate AMPK. For the moment only salicylate, a natural product extracted from plants and a major component of aspirin, has been shown to bind at the ADaM site. It will be interesting to investigate whether this new regulatory site on AMPK has any physiological relevance aside from targeting it for drug discovery.

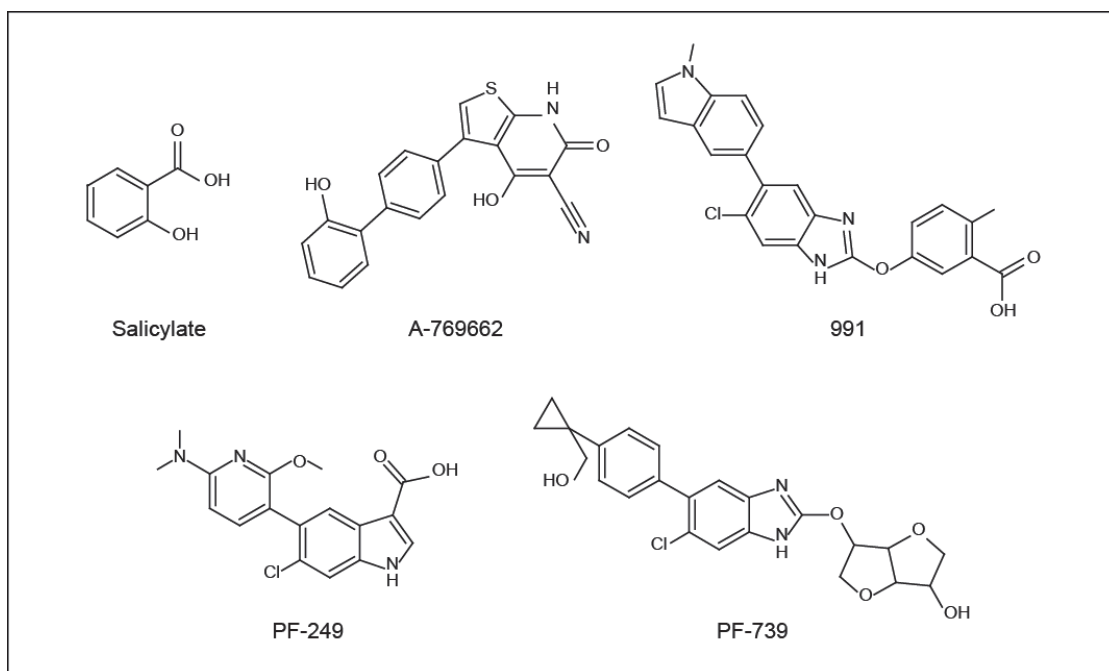


Figure 6. Structure of small-molecule AMPK activators binding to the ADaM site.

Example of compounds binding to the ADaM site, located between the α subunit kinase domain and the β -CBM. Salicylate is the only known natural ligand, A-769662 was the first chemically synthesized, whereas 991, PF-249 and PF-739 have been produced more recently.

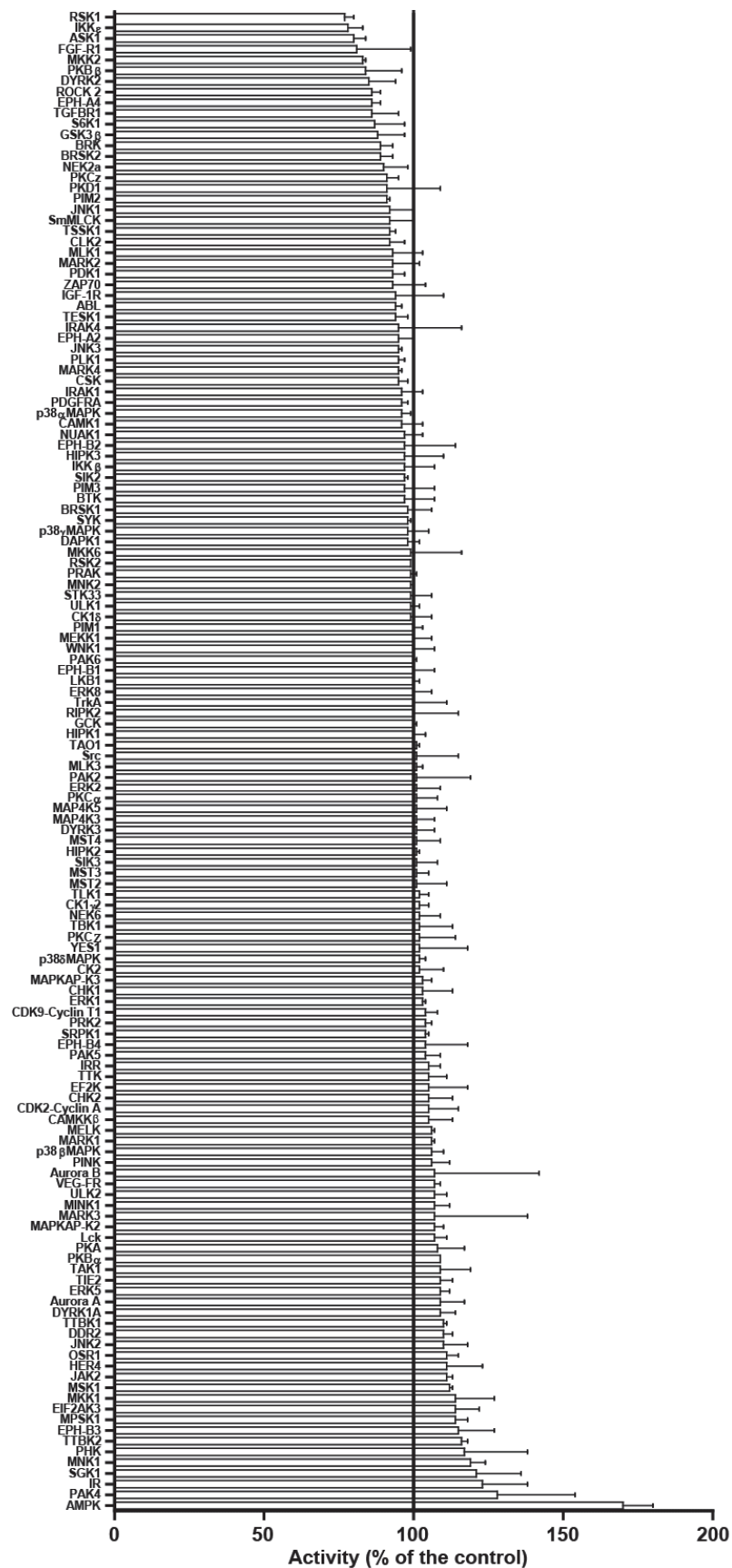


Figure 7. Effect of 991 on activity of a panel of 139 kinases.

A kinase screen was performed by the International Centre for Kinase Profiling (University of Dundee). The assays were performed in the presence of 1 μ M 991. The results are shown in rank order as mean percent activity compared with controls in the absence of compound \pm SD. Adapted from L. Bultot *et al.*²⁶.

1.2.7 Clinical relevance as drug target

First-line therapies for the treatment of metabolic disorders include diet improvement, weight control and regular exercise. Importantly, physical activity is associated with numerous beneficial effects such as increased insulin sensitivity, improved glycemic control and lipid profile. As it is often difficult to implement a suitable exercise regime for many patients, due to both physiological and psychological reasons, research has focused on understanding molecular processes that may mediate the beneficial effects of exercise, in an attempt to exploit them as therapeutic targets. Studies have shown that these health benefits are partly mediated by insulin-independent AMPK stimulation, which takes place in skeletal muscle as well as in liver and adipose tissue⁹. For this reason, AMPK has emerged as an attractive therapeutic target to counteract the abnormalities associated with obesity, insulin resistance, and type 2 diabetes^{93,94}.

The most widely used drug to treat type 2 diabetes, metformin, was shown to inhibit the mitochondrial respiratory complex and consequently reported to indirectly activate AMPK via increases in the AMP/ATP ratio in the liver and hepatocytes. Zhou *et al.* claimed that AMPK stimulation is responsible for the therapeutic effects of metformin and reported data supporting a mechanism involving AMPK-dependent inhibition of hepatic glucose production and lipogenesis⁹⁵. This notion has recently been supported by Fullerton *et al.* who demonstrated that inhibitory phosphorylation of acetyl CoA carboxylase (ACC, a key regulator of lipid synthesis and oxidation) by AMPK plays an important role in metformin-induced improvements in insulin action via maintaining hepatic lipid homeostasis⁹⁶. However, the significance of AMPK in metformin's acute action on glucose-lowering effect/inhibition of hepatic glucose production has been challenged in experiments using mice lacking either hepatic AMPK or its upstream activating enzyme LKB1⁹⁷. Moreover, recently it has been demonstrated that a key contributor to metformin therapeutic action is mediated by the inhibition of fructose-1,6-bisphosphatase-1 (FBP1) by AMP, in an AMPK-independent manner⁹⁸. Overall, it is likely that AMPK plays a role in mediating some of the beneficial effects of metformin.

The AMP-mimetic AICAR has been shown to improve the metabolic phenotypes of several rodent models of insulin resistance. For example, continuous AICAR administration in Zucker diabetic fatty (ZDF) rats prevented hyperglycemia, delayed β -cells dysfunction and ameliorated

insulin sensitivity in muscle⁹⁹⁻¹⁰³. Furthermore, type 2 diabetic patients receiving intravenously AICAR had ameliorated glycaemia and hepatic fatty acid oxidation, which correlated with a lower plasma concentration of non-esterified fatty acid¹⁰⁴. However, it has been shown that AICAR leads to several AMPK-independent/off-target cellular responses raising the possibility that the beneficial effects observed *in vivo* may not be entirely AMPK-dependent. These effects include inhibition of FBP1 in the liver and glycogen phosphorylase in muscle. Given that AICAR is not a specific activator and shows limited promising results for clinical use (due to poor oral availability and only modest effect on glucose metabolism in human when intravenously infused), new compounds targeting specifically AMPK have been generated. Therefore, the beneficial effects of several activators binding to the ADaM site have been investigated.

Initially A-769662 showed positive metabolic effects (*i.e.* lowered plasma triglyceride, and gluconeogenic gene expressions) when administered intraperitoneally in rodent models⁶⁷. Similarly, the effect of 991 has been linked to desirable effects as increased glucose uptake and fatty acid oxidation, together with inhibited protein synthesis, in treated rat skeletal muscles. However, pre-clinical studies using A-769662 and 991 were limited by the low bioavailability of the two compounds.

The new generation of ADaM-site activators developed by Merck and Pfizer have shown much more promise *in vivo*. Chronic administration of synthetic activators with β 1-isoform selectivity a) reduced proteinuria levels in ZSF rats with diabetic nephropathy (PF-04609577), b) inhibited prostate cancer growth through the blockage of lipogenesis (MT 63-78⁸⁹), c) down-regulated *de novo* lipogenesis and lowered triglycerides in rodents without affecting glucose metabolism in rats (PF-249¹²) and d) decreased lipid and cholesterol levels in liver and whole-body of rodent and Cynomolgus monkey (PF-06409577¹⁰⁵). The two compounds PF-739¹² and MK-8722⁹², which target both β 1- and β 2-containing complexes, showed the potential promise of the use of pan-AMPK activation. PF-739 has been shown to ameliorate hepatic metabolism, similar to PF-249, and to improve muscle glucose uptake, reversing elevated blood glucose concentrations in rodents and non-human primates through activation of AMPK *in vivo*¹². MK-8722 effects has been studied in diabetic mice and rhesus macaque monkeys, where it promoted insulin-independent glucose uptake in muscle and a general improvement in glycaemia. However, the advantageous effects were accompanied by a side-effect of cardiac hypertrophy and increased glycogen content⁹². Whilst this was likened to the hypertrophic effect observed in elite athletes¹⁰⁶, there remains the concern that strong activation of AMPK in humans could bring about a detrimental effect in the heart.

To conclude, strong evidence exists in support of the therapeutic role of AMPK for treating metabolic disorders. Preliminary studies also suggest that AMPK may have a possible importance in the context of renal pathologies and prostate cancer. Until now, no activators have reached the clinical stage, possibly due to the concern of the potential deleterious consequences caused by the broad AMPK activation in all tissues, including the heart. Scientists are now searching for more isoform-specific activators that will help in targeting specific tissues (*i.e.* muscle, liver)¹⁰.

1.3 AMPK role in transcriptional regulation

Traditionally AMPK is known to orchestrate metabolic changes through acute regulation of enzymes/proteins via phosphorylation. In addition, AMPK can also modulate transcription and have a long-term effect on reprogramming of gene expression as an adaptive response to long-term changes in nutrient availability. In yeast, the AMPK homolog sucrose non fermenting (SNF1) complex is important for survival in the presence of different carbon sources¹⁰⁷. When there is a shortage of glucose, SNF1 modulates gene expression of genes involved in metabolism of alternative carbon sources. In mammalian cells, AMPK has been shown to regulate gene transcription and promote energy homeostasis by several studies. The next sections will explore the means by which AMPK can regulate transcription, controlling differential responses across tissues. Firstly, there will be a review of the pieces of evidence in support of a nuclear localized AMPK, proposed to act as histone kinase and capable of rearranging chromatin accessibility. Afterwards, there will be a description of AMPK-mediated modulation of transcription factors/co-factors in different tissues (*i.e.* muscle, liver). To conclude, additional insights will be given in regards of underexplored biological functions that AMPK can regulate at the gene expression level.

1.3.1 Nuclear localization of AMPK

There is a continuing debate within the AMPK field about whether AMPK can mediate its effects via nuclear translocation. Some studies demonstrate that AMPK can regulate a number of transcription factors, although it is unknown whether AMPK does this in the cytosol or the nucleus. Additional evidence suggest a potential role of AMPK in the nucleus since it has been shown to target histone proteins within nucleosomes. A nucleosome is the basic structural element of chromatin, consisting of approximately 150 base pairs of DNA coiled around an octamer of histones, which comprises two copies of each histone protein (*i.e.* H2A, H2B, H3 and H4). The nucleosome has a globular core structure with additional protruding elements, the histone tails, which can undergo various post-translational modifications (PTMs), referred to as epigenetic modifications, such as acetylation, methylation, ubiquitination and phosphorylation. These PTMs

affect the overall chromatin structure, fine-tuning the transcriptional rate across genomic regions. Notably, both SNF1¹⁰⁸ and AMPK¹⁰⁹ have been shown to modify histone tails through their direct phosphorylation (on H3 Ser10 and H2B Ser36, respectively). This histone kinase activity promotes the recruitment of histone acetyltransferases, which acetylate histones and thus initiate the transcription of a specific subset of genes¹⁰⁸⁻¹¹⁰. Furthermore, nuclear AMPK has been shown to indirectly promote histone acetylation and transcription by suppressing type 2A histone deacetylases (HDACs)¹¹¹.

The physiological relevance of the role of nuclear AMPK in the modulation of PTMs has been explored mostly in muscle models, where it has been shown to promote the transcription of genes related to glucose homeostasis (*i.e.* glucose transporter 4, *Glut4*)¹¹¹⁻¹¹³ and fatty acid oxidation (*i.e.* peroxisome proliferator-activated receptor α , *Ppara*)¹¹⁴. For instance, McGee *et al.* reported that an acute bout of exercise can cause the preferential translocation of AMPK α 2 isoforms in human muscle¹¹², an event which is promoted by low glycogen content¹¹³. This, as revealed by a study performed on human primary myotubes, results in the phosphorylation of HDAC5 (Ser259 and Ser498) by AMPK, an event that promotes HDAC5 association with the adaptor protein 14-3-3 and its consequent nuclear export, leading to an increase in *Glut4* gene expression¹¹¹.

Recently nuclear AMPK has been shown to regulate another epigenetic modification by phosphorylating and stabilizing ten-eleven translocation-2 (TET2 on Ser99), a tumor suppressor that catalyzes the conversion from DNA 5-methylcytosine to 5-hydroxymethylcytosine. Importantly, Wu *et al.* demonstrated that glucose can affect DNA 5-hydroxymethylome, which is usually perturbed in cancer, through a deregulation of the AMPK-TET and 5-hydroxymethylome, suggesting a connection between diabetes and cancer¹¹⁵.

A clear mechanistic explanation for the AMPK nuclear translocation is still missing. Firstly, there are some controversial indications concerning a preferential AMPK isoform-specific nuclear localization. Indeed, studies done in muscle¹¹¹⁻¹¹³ and in a pancreatic β -cell line (INS-1)¹¹⁶ suggested that AMPK activation leads to a predominant AMPK α 2 nuclear translocation. However, experiments conducted in several cell models (*i.e.* MEFs, HeLa and HEK-293) revealed an AMPK α 1 nuclear localization in response to stress (*e.g.* heat, energy depletion)¹¹⁷ or genotoxic agents¹¹⁸. This discrepancy may suggest the existence of an isoform-specific localization dependent on the cellular context. Secondly, it is still unclear how AMPK is allowed to shuttle between the cytoplasm and the nucleus. A study done in C2C12 demonstrated that there are some factors required for the nuclear relocalization, namely a) a nuclear localization signal located at Lys223 to Arg226 (in human α 2), b) the phosphorylation of α 2 on Thr172 as well as c) the presence of β 2 and

γ 1 subunits¹¹⁴. These results raise two critical questions that only future studies may answer. A query concerns the absence of a nuclear localization signal (NLS) in the AMPK α 1 isoform, suggesting that a possible non-canonical signal may mediate its translocation. It should be noted that such discrepancy within isoforms does not exist on the export process, since α 1 and α 2 both contain a nuclear export signal (NES)¹¹⁹. Another question regards how AMPK can diffuse through the nuclear pore structure, a complex that allows the import and export of protein into and from the nucleus. For a long time the limit for protein diffusion was thought to be around 60 kDa¹²⁰. However it has been demonstrated that larger proteins (90-110 kDa)¹²¹ can also move across the nuclear pore. Since the whole AMPK complex is required also in the nucleus, it would be interesting to clarify if the heterotrimer, which has a molecular weight of ~140 kDa hence higher than the maximum allowed, has to disassemble prior the entrance and reassemble once in the nucleus. However, this explanation raises questions regarding the translocation of the two regulatory subunits β and γ that, once separated from α , would lack the NLS required to enter the nucleus. Future studies, possibly focusing on endogenous AMPK, in order to avoid artificial results that may arise from an overexpression system, would be required to shed light onto the AMPK nuclear translocation.

In conclusion, several inputs which trigger AMPK activation promote an isoform-specific translocation to the nucleus, possibly in a tissue-/cell-dependent manner. Once in the nucleus AMPK modulates histone PTMs, directly via phosphorylation and indirectly through the modulation of histone acetylases, deacetylases and of the enzymes responsible for hydroxymethylation (Table 1). Currently only a few genes related to glucose and lipid metabolism are known to be affected by this epigenetic modulation. Further work will be required to clarify the mechanism allowing AMPK translocation as well as additional gene networks modulated by this cascade.

Target	Genes or epigenetic modifications	Changes	Model	AMPK specificity	Activator	Ref.
H2B (Ser36)	<i>Cpt1c, p21</i>	↗	MEFs AMPK α 1-/- α 2-/-	Yes	Glucose withdrawal	109
HDAC5 (Ser259, Ser498)	<i>GLUT4</i>	↗	Human myotubes	No	AICAR	111
HAT1 (Ser190) RBBP7 (Ser314)	<i>PGC1α, NRF1, NRF2, Tfam, UCP2, UCP3</i>	↗	MEFs AMPK α 1-/- α 2-/-	Yes	AICAR	122
TET2 (Ser99)	5-hydroxymethylome		Human epithelial	Yes	Glucose withdrawal	115

Table 1. Nuclear transcriptional targets of AMPK.

1.3.2 AMPK transcriptional regulation in muscle

AMPK plays a role on the metabolic adaptations that the skeletal muscle undertakes to optimize its energy production. Nutrient scarcity and/or physical exercise activate muscular AMPK and in turns, AMPK promotes glucose and fatty acid uptake, mitochondrial biogenesis and fatty acid oxidation, supporting a general shift from glucose utilization to fatty acid consumption as a main energy source. AMPK mediates these metabolic changes through acute regulation of metabolic enzymes as well as via regulation of gene expression in response to long-term adaptation (*e.g.* exercise, nutrient availability).

From a transcriptional perspective, AMPK activation promotes plasma glucose uptake and oxidation, improving postprandial hyperglycemia and therefore having a beneficial effect on whole body energy metabolism. Firstly, AMPK increases the expression levels of GLUT4, whose up-regulation is accomplished through an AMPK α 2-mediated indirect stimulation of the activity of myocyte enhancer factor-2 (MEF2)^{20,123,124}, combined with a direct phosphorylation and consequent promotion of GLUT4 enhancer factor (GEF)¹²⁵. Secondly, AMPK supports glucose utilization by promoting the expression of the rate-limiting enzyme for the first step of glycolysis, hexokinase II (HKII)¹²⁶. HKII regulation by AMPK is mediated through the direct phosphorylation of the transcription factor cAMP response element-binding protein (CREB)¹²⁷.

In addition to its effect on glucose homeostasis, AMPK boosts fatty acid usage through a complex transcriptional reprogramming that favors an increase in mitochondrial content and promotes the expression of genes related to oxidative metabolism^{128,129}. Skeletal muscle has a high number of mitochondria since these organelles, through oxidative phosphorylation, fulfill the crucial requirement for rapid and sustained ATP production during heightened metabolic demand (*i.e.* contraction). The activation of AMPK increases mitochondrial content through the modulation of a) the transcriptional coactivator PGC1 α (peroxisome proliferator-activated receptor gamma coactivator 1-alpha), which promotes mitochondrial biogenesis and b) some of the transcription factors with which PGC1 α interacts.

AMPK supports the positive feedback loop exerted by PGC1 α on its own expression directly through phosphorylation and indirectly by modulating its acetylation status. Indeed, observations from several studies performed in AMPK loss-of-function or gain-of-function models showed that activation of AMPK closely associates with an increase in *Pgc1 α* mRNA expression. For instance, physiological stimulation (*i.e.* acute exercise) of AMPK in skeletal muscle increased PGC1 α and additional mitochondrial markers, an effect that was abolished in a muscle-specific AMPK α 1 α 2 double knockout model¹³⁰. Similarly, upon treatment with AMPK activators (*i.e.* AICAR,

resveratrol or β -guanidinopropionic acid), models with defective AMPK activity had an impaired or abolished increase in mitochondrial genes and associated protein levels^{19,128,131-133}. An additional study, performed in a muscle specific transgenic model with an inactive form of $\alpha 2$ (Asp157Ala), demonstrated that impaired $\alpha 2$ activity reduced maximal exercise capacity¹¹ and decreased the basal level of mitochondrial protein expression¹²⁸. Still in support of the existence of an AMPK-PGC1 α axis, a gain-of-function model, where a mutant form (Arg225Gln) of the $\gamma 3$ subunit was overexpressed, displayed an increase in mitochondrial biogenesis, associated with a higher level of PGC1 α ¹³⁴.

The precise mechanism through which AMPK can upregulate PGC1 α expression level has been suggested to require the promoter-binding of a) upstream stimulatory factor-1 (USF1)¹³⁵ and MEF2, which are indirectly regulated by AMPK, and b) of PGC1 α itself, that AMPK phosphorylates triggering its positive feedback loop¹³⁶. In addition, AMPK was hypothesized to indirectly promote PGC1 α activity modulating its acetylation state via the NAD⁺-dependent deacetylase sirtuin1 (SIRT1), although the precise mechanism by which AMPK activates SIRT1 is unclear¹³⁷.

In addition, AMPK controls genes related to β -oxidation through some of the transcription factors, MEF2, peroxisome proliferator-activated receptor delta (PPAR δ), that act in concert with PGC1 α . For example, AMPK has been proposed to promote MEF2 activity indirectly through the phosphorylation of HDAC5¹¹¹, a histone deacetylase that can specifically inhibit genes by binding to a subset of transcription factors (*e.g.* MEF2¹³⁸). Upon phosphorylation by AMPK, HDAC5 dissociates from MEF2²⁰, which can then increase genes related to mitochondria oxidation, such as *Pgc1 α* and lactate dehydrogenase, an enzyme that converts lactate to pyruvate, providing fuel for mitochondria oxidation. PPAR δ is another transcription factor mediating the PGC1 α response that AMPK has been proposed to control. This hypothesis originated from a transcriptomic study where Narkar *et al.* compared the genes changing after PPAR δ stimulation with the ones responding to chronic (four weeks) pharmacological AMPK-stimulation with AICAR. AICAR treatment alone led to enhanced running endurance in mice and was therefore associated to an endurance-related gene expression signature, consisting of 32 up-regulated genes linked to oxidative metabolism. The majority of these transcripts (*i.e.* 30 out of 32) were also increased in a model with constitutively active PPAR δ and did not respond to AICAR in PPAR δ -null cell, globally suggesting that those could be a pool of genes modulated by AMPK via PPAR δ ¹³⁹. A drawback of this study is the absence of an AMPK knockout in the experimental design, a factor that raises the question of whether the identified genes may distinguish an AICAR-PPAR δ axis independent of AMPK. It would be interesting to rule out which proportion of the endurance-related genes identified upon AICAR treatment represents an off-target/AMPK-independent population.

Recently, a transcriptomic analysis investigated the impact of AMPK stimulation by a small molecule acting through the ADaM site (*i.e.* PF-739), on mouse gastrocnemius muscle after short (4 h) or long-term (32 days) treatment. Cokorinos *et al.* results were in line with previous observation, showing an AMPK-mediated regulation of mRNA linked to mitochondrial biogenesis, oxidative phosphorylation and glucose metabolism¹². It should be noted, that a knockout model was not included within the experimental design and therefore the presence of AMPK-independent transcriptional changes cannot be ruled out. Nevertheless, this study represents an important step forward in the field by offering the first gene expression study based on an allosteric activator.

To summarize, AMPK favors muscle energy homeostasis, acting via a broad network of transcriptional reprogramming. As illustrated in Figure 8, AMPK has been shown to modulate several targets, both directly or indirectly, overall favoring mitochondrial biogenesis and increasing oxidative phosphorylation and glucose metabolism. Notably, since an important number of studies have been performed relying on indirect activators and sometimes missing a knockout control (see Table 2), future research taking advantage of novel/selective activators will be required to confirm some of the previously identified targets.

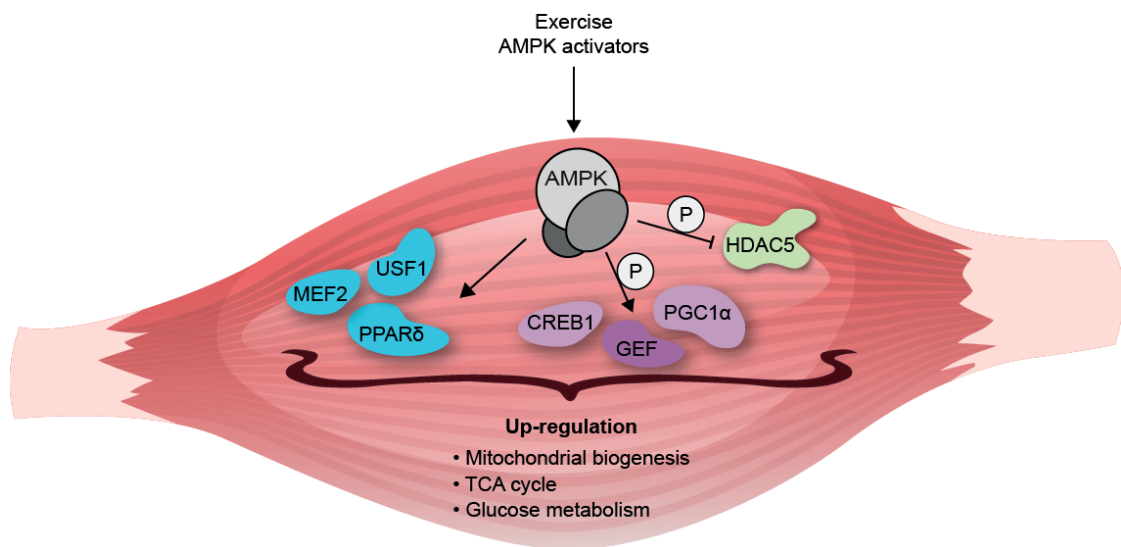


Figure 8. Schematic representation of AMPK transcriptional targets in muscle.

Physiological and pharmacological activation of AMPK leads to an increased expression of genes related to mitochondrial biogenesis, tricarboxylic acid cycle (TCA) cycle and glucose metabolism. Targets are color-coded: light blue for indirectly promoted, purple for directly promoted or green if directly inhibited.

Target	Regulated genes	Changes	Model	Specificity	Tissue	Activator	Notes	Ref.
CREB1 (Ser133)			Mouse muscle-specific LKB1-/-	Partially	Heart Skeletal muscle	AICAR		127
GEF (Ser?) MEF2	<i>Glut4</i>	↗	Rat	No	Skeletal muscle	AICAR		125
HDAC5, MEF2	<i>Glut4</i>	↗	Mouse AMPKα2-/-	Yes	Skeletal muscle	Exercise		20 123
MEF2	<i>Glut4</i>	↗	Mouse	No	Skeletal muscle	Creatine		140
MEF2	<i>Glut4</i>	↗	Rat	No	Myocardium	AICAR		124
PGC1α (Thr177, Ser538)	<i>Pgc1α, Glut, Cyt, Ucp2</i>	↗	C2C12 and mouse pgc1α-/-	Partially		AICAR, metformin		136
PPARδ	30 genes endurance-related		Mouse pparδ-/-	Partially		AICAR, PPARδ-agonist	Available microarray	139
USF1	<i>Pgc1α</i>	↗	C2C12	No		AICAR		135
-	<i>Cyt, δ-ALA-S</i>	↗	Rats	No	Skeletal muscle	AICAR (1 h or 28 days)		133
-	<i>Glut4, HKII, Cyt, COX-1, CS</i>	↗	Mouse AMPKα2-/-	Yes		AICAR or exercise (28 days)	Exercise-induced changes were not affected by ko	128
-	<i>Glut4, COX-1, VEGF</i>	↗	Mouse muscle-specific AMPKα1-/-α2-/-	Yes	Skeletal muscle	Acute (30 min) or chronic exercise (28 days)	Regulated via AMPK after acute but not chronic training	130
-	<i>Glut4, HK</i>	↗	Rat	No	Skeletal muscle	AICAR		126
-	<i>Pgc1α</i>	↗	Mouse muscle-specific dominant negative AMPK	Yes	Skeletal muscle	β-guanidinopropionic acid		131
-	<i>Pgc1α, Ucp3, Myogenin</i>	↗	Rats	No	Skeletal muscle	AICAR (14 days)		132
-	<i>Pgc1α, Pgc18, Cyt, Ucp1, Ucp2, Ucp3</i>	↗	Mouse AMPKα1-/- or AMPKα2-/-	Yes	Skeletal muscle BAT WAT	Resveratrol		19
-	<i>Pgc1α, NRF1, NRF2, TFAM, Cyt, CS, SOD2, Catalase,</i>	↗	Mouse AMPKγ3 (R225Q)	Yes	Skeletal muscle	Gain-of-function mutation		134
-	<i>Pgc1α, Nr4a1, Nr4a3, Hk2, Pdk4</i> TCA cycle, glucose metabolism	↗	Mouse	No	Skeletal muscle	PF-739 4 h PF-739 32 days	Available RNA-seq data done with specific activator	12
-	<i>Ppara</i>	↗	C2C12	No		Leptin		114

Table 2. Transcriptional targets of AMPK in muscle.

1.3.3 AMPK transcriptional regulation in liver

The liver is a central organ governing whole body energy balance, adapting its metabolism daily to alternating fed and fasted states. Under anabolic (energy-rich) condition, the liver converts sugar into pyruvate via glycolysis. Pyruvate can then either be oxidized to supply energy, stored as glycogen or used for lipogenesis. Oppositely, under catabolic (energy-deprived) state, the liver decreases the lipogenesis rate, while increasing fatty acid oxidation and ketogenesis in order to provide energy to extrahepatic organs. In the fasted state or during exercise, hepatic AMPK is activated and plays a major role in maintaining liver energy status, inhibiting lipogenesis, cholesterol synthesis and glucose production while increasing fatty acid oxidation. The action of AMPK is exerted via rapid and direct phosphorylation of enzymes as well as through long term modulation of gene expression.

During fasting AMPK reduces cholesterol synthesis and lipogenesis predominantly in a rapid manner via phosphorylation and inhibition of the rate-controlling enzymes 3-hydroxy-3-methylglutaryl-CoA reductase (HMGCR) and ACC, respectively. The most critical mechanism is the inhibition of ACC, which leads to a decrease in the concentration of its reaction product malonyl-CoA, a key precursor for *de novo* lipogenesis as well as an inhibitor of fatty acid uptake into mitochondria. Indeed, the drop in malonyl-CoA produces a dual effect, lowering *de novo* lipogenesis^{13,141} and allowing an increase in fatty acid oxidation¹⁴², which protects the liver against hepatic steatosis.

In addition, activated-AMPK represses the lipogenic transcriptional program through a reduction in activity and content of the transcription factors sterol regulatory element-binding protein (SREBP-1c), which controls genes associated to fatty acid and triacylglycerol synthesis, and SREBP-2, which promotes genes involved in cholesterol biosynthesis. Indeed, *in vitro* and *in vivo* evidence demonstrated that AMPK directly phosphorylates hepatic SREBP-1c (Ser372) and SREBP-2, inhibiting their cleavage, required for nuclear translocation, and thus blocking their lipogenic transcriptional programs¹⁶. The discovery of a direct inhibition of SREBP members by AMPK helped explain previous observations where increased activity of AMPK, either upon pharmacological activation (*i.e.* AICAR or metformin)^{17,143,144} or by overexpression of a constitutively active form of the $\alpha 2$ catalytic subunit¹⁸, caused a decrease in the level of lipogenic genes. Intriguingly, a recent gene expression study challenged the inhibition of SREBP by stimulated AMPK. Esquejo *et al.* generated transcriptomic data using mice liver from wild-type and liver-specific knockout of AMPK $\alpha 1\alpha 2$, treated for 42 days with a $\beta 1$ -selective activator (*i.e.* PF-06409577). Their analysis indicated an up-regulation of SREBP target genes, which was further confirmed by a proteomic

experiment where the overnight treatment with PF-06409577 was sufficient to increase the level of SREBP target proteins¹³. This novel result may be explained by an activation of SREBP due to the low level of hepatic lipid species, which is caused by AMPK stimulation.

AMPK has also been suggested to promote hepatic fatty acid oxidation and energy production via a PGC1 α -mediated increase in mitochondrial content, as previously described in muscle. This mechanism however still requires additional studies to be confirmed, as it was proposed only following the observation that the model of AMPK liver-specific knockout has a decreased expression of PGC1 α and mitochondrial markers, associated with reduced mitochondrial respiration rate and ATP level in the basal state¹⁴⁵.

In combination with its effect on lipid metabolism, AMPK also regulates glucose homeostasis, mainly by inhibiting gluconeogenesis and glycolysis through a transcriptional mediated repression of key enzymes, namely L-pyruvate kinase (L-PK), phosphoenolpyruvate carboxykinase (PEPCK) and glucose 6-phosphatase (G6Pase). Several studies using pharmacological AMPK activation (*i.e.* AICAR-treatment)^{15,146} or mouse models with gain-of-function^{18,147} mutations, contributed to the discovery that AMPK attenuates gluconeogenesis and thus ameliorates glycaemia. This link has been supported by experiments performed on AMPK liver-specific knockout mice, which showed a reduced hypoglycemic response to AICAR-treatment¹⁴⁸ together with a general hyperglycemia and increased hepatic glucose production¹⁴⁹.

The mechanism by which activated AMPK has been proposed to suppress gluconeogenesis comprises AMPK modulating CREB regulated transcription coactivator-2 (CRTC2)¹⁵⁰ and CREB-binding protein (CBP/p300)¹⁵¹ leading to the loss of their interaction with CREB. The impaired interaction within CREB and its cofactors blocks the transcription, and therefore decreases the level, of the two rate-limiting enzymes PEPCK and G6Pase^{15,18,147,152}. Concomitantly with its effect on gluconeogenesis, AMPK modulates glucose utilization also by repressing glycolytic enzymes expression (*e.g.* L-PK, aldolase) via phosphorylation and consequent inhibition of the two transcription factors carbohydrate-responsive element-binding protein (ChREBP)¹⁵³ and hepatocyte nuclear factor 4 alpha (HNF4 α)^{154,155}.

In conclusion, activation of hepatic AMPK promotes a complex cascade of events (main targets are summarized in Figure 9 and Table 3), which concur to protect liver against hepatic steatosis and hyperlipidemia^{16,147}, highlighting AMPK as a promising therapeutic target for the treatment of fatty liver disease.

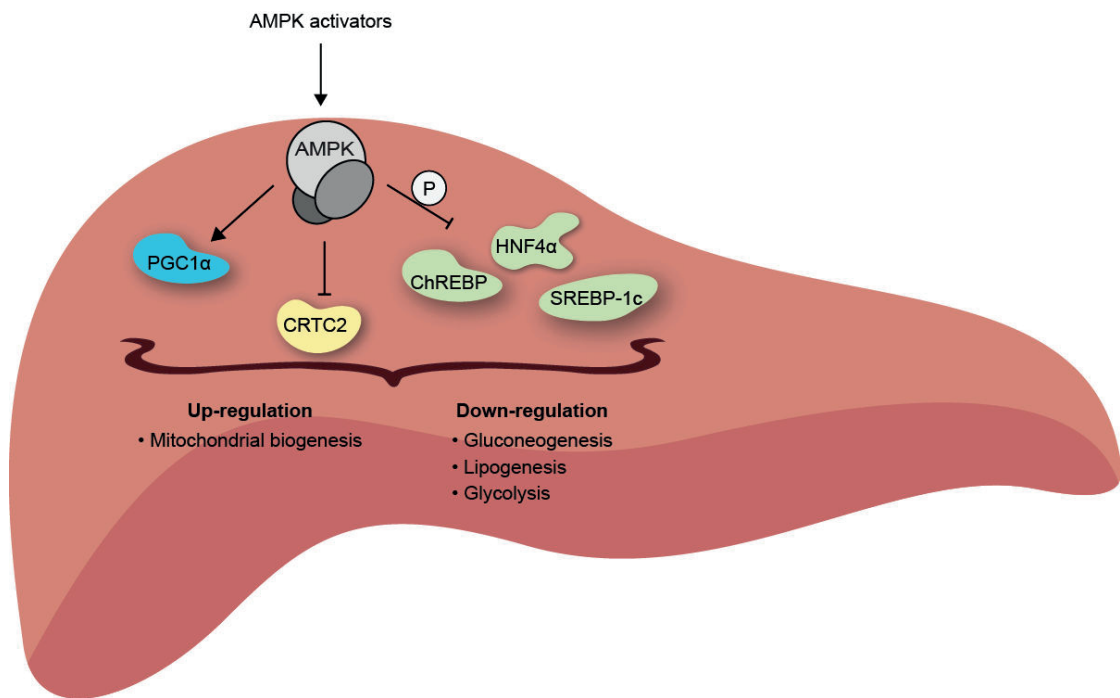


Figure 9. Schematic representation of AMPK transcriptional targets in liver.

Pharmacological activation of AMPK has been associated with up-regulated mitochondrial biogenesis and down-regulated expression of genes related to gluconeogenesis, lipogenesis and glycolysis. Targets are color-coded: light blue for indirectly promoted (PGC1 α), yellow for indirectly inhibited (CRTC2) or green if directly inhibited via phosphorylation (ChREBP, HNF4 α and SREBP-1c).

Target	Regulated genes	Changes	Model	AMPK specificity	Tissue	Activator	Notes	Ref.
CBP/p300 (Ser89)			<i>in vitro</i>				Modulates the affinity of p300 with its partners	151
ChREBP (Ser568)	<i>L-PK</i>	↘	Rat primary hepatocytes	Partially		AICAR		153
CRTC2	<i>Pepck, G6pase</i>	↘	Rat primary hepatocytes	Partially		Metformin, AICAR, overexpression of constitutively active AMPK		150
DUSP4	<i>Egr1</i> <i>Pepck, G6pase</i>	↗ ↘	Hepatocyte cells	No		AICAR		146
HNF4α	<i>Aldo B, ApoB, Glut2, Hnf1α, L-PK</i>	↘	Mouse primary hepatocytes	No		AICAR	Decreased level of HNF4α	155
HNF4α (Ser304)		↘	<i>In vitro</i> and overexpression in cells	Partially		AICAR	Repression of HNF4α	154
PGC1α	<i>ATPase, Cyt, Cox1, CoxIV, Pgc1α</i>	↗	Mouse liver-specific AMPKα1-/-α2-/-	Yes	Liver			145
SREBP-1c (Ser372)	<i>Acc, Fas, Scd1, Hmgcr, Hmgcs</i>	↘	Mouse, HepG2, MEFs AMPKα1-/-α2-/-	Yes	Liver	Polyphenols, metformin	Inhibition of SREBP-1c and lipogenic genes	16
SREBP-1c	<i>Srebp-1c, Fas, Cpt-1, Ppara</i>	↘	Rats	No	Liver	AICAR		17
SREBP-1c ChREBP	<i>Acc, Chrebp, Fas, G6Pase, HMGCR, L-PK, Pepck, SCD-1, Srebp-, Ucp2</i>	↘	Mouse	Partially	Liver	Overexpression of constitutively active AMPKα2	Decrease of gluconeogenic and lipogenic genes	18
-	<i>Fas, L-PK</i>	↘	Rat primary hepatocytes	Yes		AICAR, overexpression of constitutively active AMPK		144
-	<i>Pepck, G6Pase</i>	↘	Rat hepatoma cells	No		AICAR	Inhibition of gluconeogenic genes	15
-	<i>Pepck, G6pase</i>	↘	Mouse	Partially	Liver	Liver-specific gain-of-function		147
-	Hepatic fibrosis genes SREBP-target genes	↘ ↗	Mouse liver-specific AMPKα1-/-α2-/-	Yes	Liver	PF-06409577	No changes detected in SREBP-1c (total and phosphorylated)	13

Table 3. Transcriptional targets of AMPK in liver.

1.3.4 Other transcriptional targets

This section will offer an overview of transcriptional targets of AMPK which have not been fully characterized and/or whose physiological relevance is still uncertain. The targets will be discussed following their listing order in Table 4, which is based on an alphabetical sorting of the process that they influence.

Bile acid and lipid metabolism: FXR

Farnesoid X receptor (FXR) is a member of the nuclear receptor family, highly expressed in liver, intestine and kidney, known as the master regulator of bile acids homeostasis. FXR is triggered by bile acids and modulates their biosynthesis and metabolism in a negative feedback loop¹⁵⁶. This factor has additionally been shown to regulate glucose and lipid metabolism, increasing insulin sensitivity and decreasing *de novo* lipogenesis, via suppression of SREBP-1c¹⁵⁷. Because of its beneficial role, FXR has a substantial pharmacological relevance and its modulation has been proposed to hold therapeutic potential for various metabolic syndromes (e.g. type 2 diabetes, dyslipidemia and non-alcoholic steatohepatitis)¹⁵⁸. To discover novel regulators of FXR, Lien *et al.* performed a mass spectrometry analysis on human hepatoma cells and revealed AMPK as novel interactor of this factor. They demonstrated *in vitro* that AMPK phosphorylates FXR at Ser250 and correlated the activation of AMPK with a negative regulation of FXR transcriptional activity, due to the impaired recruitment of its co-activators. This study identified a cascade of event via which AMPK represses the transcriptional activity of the bile acid sensor FXR. Thus raising the problem of an impinged bile acid homeostasis during *in vivo* activation of AMPK. Nevertheless, these results should be taken with caution as they were obtained using the activators AICAR and metformin, without being validated in a knockout model.

Cell cycle: TP53

AMPK was shown to promote cell cycle arrest at the transcriptional level, through increasing the activity of the tumor suppressor TP53. TP53 is a transcription factor that responds to stressors, such as DNA damage and oxidative stress, inducing the expression of genes responsible for apoptosis, arrest of cell growth and senescence. AMPK has been suggested to favor TP53 action in two ways, firstly via direct phosphorylation and stabilization of the factor and secondly through inhibition of a p53 repressor, mouse double minute 4 (MDM4). The first axis of regulation has been indicated by experiments done in a hepatocytes cell line, where AMPK activation upon AICAR treatment led to phosphorylation of TP53 on Ser15¹⁵⁹. The second axis of regulation has been proven by He *et al.*, who showed that AMPK can directly phosphorylate MDM4 (Ser342), a component of the TP53 repressor complex, causing 14-3-3 binding and the consequent activation of TP53¹⁶⁰. These investigations

indicate that metabolic stress can cause cell cycle arrest through AMPK-dependent mechanisms, however further studies are required to confirm the exact regulatory targets.

Circadian rhythm: CRY1

AMPK is within the metabolic sensors that convey energy-dependent signals to the circadian clock, affecting its function. Circadian clocks regulate mammalian physiology (*e.g.* optimizing gluconeogenesis and insulin secretion) according to daily environmental cycles. This is possible thanks to a molecular oscillator, consisting of transcriptional activators and repressors, which can receive inputs (*i.e.* light, nutrients) from the environment and coordinate a pulsing transcriptional program accordingly. The clock consists of a self-sustained feedback loop with a positive and negative component. The positive axis comprises the increased expression of period genes (*i.e.* *Per1*, *Per2* and *Per3*) and cryptochrome genes (*i.e.* *Cry1* and *Cry2*) by the transcriptional activators CLOCK and brain and muscle ARNT-like 1 (BMAL1). The negative axis is mediated by PER and CRY direct association with CLOCK-BMAL1, which leads to the inhibition of its transcriptional activity.

AMPK can contribute to the regulation of the mammalian clock through direct and indirect destabilization of two core elements, CRY and PER. In more detail, AMPK can a) directly phosphorylate CRY1 on Ser71, reducing its stability and promoting its degradation¹⁶¹ and b) indirectly cause PER degradation by phosphorylating and increasing the enzymatic activity of casein kinase I epsilon (CKIε on Ser389), that is responsible for PER destabilization¹⁶². The importance of AMPK as regulator of the circadian clock genes has been further supported by studies where knockout models of AMPK (*i.e.* α2 or γ3) or of its upstream regulator LKB1, presented an altered expression of clock genes in muscle¹⁶³ or liver^{161,162} in response to pharmacological AMPK stimulation.

Gene expression in β-cells

Functional β-cells ensure a correct glucose homeostasis and their compromised activity leads to impaired insulin production and hyperglycemia, which can progress to diabetes. AMPK role in glucose-dependent insulin secretion is controversial^{164,165} and it is still uncertain whether AMPK effect is beneficial or detrimental for β-cells. In order to investigate if AMPK plays a role on β-cells gene expression, a transcriptomic study was performed on a mouse model carrying β-cells-specific deletion of both AMPK catalytic subunits^{166,167}. Data mining of the sequencing results¹⁶⁶ revealed that AMPK concurs at maintaining a correct differentiation status of the β-cells, suppressing the expression of neuronal genes among other sequences usually not transcribed in these cells¹⁶⁸. Further analysis of the data set highlighted AMPK also as a regulator of various (*i.e.* 23) microRNAs¹⁶⁷. Overall, these results emphasize a novel role of AMPK in regulating the β-cells gene expression. Future studies are required to reveal the mechanisms contributing to this regulation and their physiological relevance.

Longevity and redox state: FOXO

Oxidative stress is a detrimental cellular status characterized by an elevated content of reactive oxygen species (ROS). Increased ROS level contributes to the establishment of many pathological conditions such as neurological and cardiovascular diseases, cancer and aging. Because of the therapeutic interest of increasing ROS detoxifying mechanisms, the implied regulatory pathways represent an important area of research. Among the beneficial players of antioxidant reactions, the family of transcription factor forkhead box O (FOXO) has emerged as promoter of stress resistance, via regulation of genes implied in the detoxification processes. AMPK has been suggested to promote FOXO action and therefore lower ROS content. Mechanistically AMPK was shown to phosphorylate two members of the FOXO family, FOXO1 and FOXO3, respectively at Thr649¹⁶⁹ and Ser413/Ser588¹⁷⁰, stabilizing and thus up-regulating them. The physiological relevance of the AMPK-mediated activation of FOXOs factors, has been associated with increased expression of antioxidant enzymes¹⁶⁹ which seems to contribute at increased lifespan. Greer *et al.*, who showed how dietary restriction in *C. elegans* requires an AMPK-dependent regulation of FOXO/DAF-16 to extend life duration¹⁷¹, suggested the latter. Overall, by lowering ROS levels via FOXO action, AMPK may contribute to increased longevity and delay age-dependent diseases. Future studies, potentially taking advantage of specific AMPK activators are required to confirm these intriguing observations.

rRNA synthesis: TIF-1A

Transcription initiation factor 1A (TIF-1A) is required for the recruitment of RNA polymerase I (Pol I) to the promoters of ribosomal RNA (rRNA) genes. Using HEK293, Hoppe *et al.* showed that, under glucose restriction, AMPK decreases rRNA synthesis via phosphorylation of TIF-1A on Ser635, precluding the formation of the transcription initiator complex¹⁷². These results suggest that AMPK can adjust rRNA synthesis to nutrient availability. However, as the conclusions were drawn from experiments done *in vitro* and using AICAR solely in wild-type cells, further studies are required to confirm the reported observations.

Pathway/Mechanism	Target	Genes modifications	Changes	Model	Specificity	Tissue	Activator	Ref.
Bile acid, lipid and glucose metabolism	FXR (Ser250)	FXR-regulated genes \downarrow		HepG2, mouse FXR-/-	No		AICAR, metformin	173
	TP53 (Ser15)			HepG2	No		AICAR	159
	MDMX (Ser342)		Stabilizes P53	MEFs AMPK α 1-/- α 2-/-	Yes		AICAR, metformin, salicylate	160
Circadian rhythm	CRY1 (Ser71)		Degrades CRY1	Mouse, MEFs AMPK α 1-/- α 2-/-	Yes	Liver	AICAR	161
	CKI ϵ (Ser389)	<i>Per2</i> , <i>Per1</i>	Shifted expression	Mouse AMPK α 2-/-	Yes	Heart	Metformin	162
		<i>Cry2</i> , <i>Nr1d1</i> , <i>Bhlhb2</i> , <i>Per1</i>	Shifted expression	Mouse AMPK γ 3-/-	Yes	Skeletal muscle	AICAR	163
	-	<i>Slc16a1</i> , <i>Ldha</i> , <i>Mgst1</i> , <i>Pdgfra</i> \downarrow		Mouse β -cell specific AMPK α 1-/- α 2-/-	Yes			166
Gene expression in β -cells	-	23 miRNAs modulation			Yes			167
Longevity	<i>FOXO3</i> (Ser413 Ser588)	Microarray	Promotes FOXO3	MEFs FOXO3-/-	No		2-DG	170
	<i>FOXO1</i> (Thr649)	Antioxidant enzymes \uparrow	Stabilizes FOXO1	AMPK dominant negative	Yes		Resveratrol, AICAR	169
rRNA synthesis	TIF-1A (Ser635)	Ribosomal RNA genes \downarrow	Blocks the assembly of transcriptional initiation complex	HEK293	No		AICAR, glucose deprivation	172

Table 4. Additional transcriptional targets of AMPK.

1.3.5 TFEB - emerging lysosomal and metabolic regulator

The lysosomes are membrane-bound vesicles containing hydrolytic enzymes, present in every eukaryotic cell and mostly known for their cellular waste disposal function. In the past years, various new roles have been assigned to this organelle, such as nutrient sensor as well as regulator of transcription and metabolic homeostasis¹⁷⁴. Remarkably, the lysosome has been shown to be a hub for the integration of the anabolic and catabolic signaling pathways through mTORC1 and more recently via AMPK. For instance, Zhang *et al.* reported a mechanism by which the lysosomal protein v-ATPase (vacuolar-type H⁺-ATPase), known to regulate mTORC1¹⁷⁵, coordinates the activation of AMPK via AXIN, that acts as scaffold protein for the LKB1-mediated stimulation of AMPK on the lysosome surface⁴⁹. In addition, AMPK itself has been reported to control lysosomal gene expression, since its knockout in embryonic stem cells (ESCs) impairs the transcriptional program of this organelle¹⁷⁶. This aberrant gene regulation occurs because the lack of AMPK causes an elevated mTORC1 signaling, which leads to a constitutive cytoplasmic retention of the transcription factor EB (TFEB), the master regulator of lysosomal transcriptional program. The next section will offer an overview of TFEB structure, regulation and physiological relevance, especially in light of its connection with AMPK.

TFEB is a member of the microphthalmia (MiT) family, which comprises also microphthalmia-associated transcription factor (MITF), TFE3 and TFEC¹⁷⁷. MiT members share a similar structure having as key elements an activation domain (AD), a basic helix-loop-helix (bHLH) domain and a leucine zipper (Zip) motif, required for the factors dimerization as well as DNA-binding to the CACGTG E-boxes sequence motif¹⁷⁸. Distinct from other bHLH-Zip transcription factors, MiT proteins also bind TCATGTG M-box sequence¹⁷⁹. MiT transcriptions bind DNA in the form of both homodimers and heterodimers with any other family member¹⁸⁰. In pathological context, MiT members are generally reported as proto-oncogenic, since their aberrant overexpression can promote the initiation and/or survival of various tumor types, such as melanoma (*Mitf*)¹⁸¹, sarcomas (*Tfe3*)¹⁸², and subtypes of renal cell carcinomas (*Tfeb*, *Tfe3*). Physiologically, the MiT members control cell growth and differentiation, for example TFEC¹⁸⁴ is involved in embryonic hematopoiesis, by modulating the expression of various cytokines, and MITF acts as a critical player in development and maintenance of melanocytes and osteoclasts, with mice carrying *Mitf* mutations presenting coat color defects and abnormal bone growth¹⁷⁷. Acting in a mutually redundant way with MITF, TFE3 has also been shown to regulate osteoclast development^{185,186}. Additionally TFE3 has a role partially redundant with the one of TFEB as both have been shown to a) favor autophagy and lysosomal biogenesis^{187,188}, b) modulate metabolic reprogramming during physical exercise, for example controlling PGC1 α expression^{189,190}, and c) promote the immune

response in macrophages^{191,192}. Even though TFEB- and TFE3-regulated gene networks can partially overlap, there is evidence of diverse roles for these two factors. For instance, while *Tfe3* knockout mice are viable, despite having mitochondrial abnormalities and compromised lipid metabolism¹⁹³, *Tfeb* knockout mice suffer from embryonic lethality¹⁹⁴, due to defective placental vascularization and disrupted endodermal specification. Impaired lysosomal activity and the consequent disruption of Wnt signaling have been proposed as causative for the compromised endodermal lineage differentiation in ESCs lacking *Tfeb*¹⁷⁶, suggesting a unique function for TFEB in controlling lysosomes.

TFEB was initially identified as the key regulator of the lysosomes, central organelles required for the degradation and recycling of cellular waste material, by orchestrating the expression program of genes related to lysosomal biogenesis¹⁹⁵, fusion with the autophagosome¹⁸⁸ and exocytosis. Promoter analysis of lysosomal genes revealed that they share a common 10 base E-box-like sequence, the so-called coordinated lysosomal expression and regulation (CLEAR) motif. TFEB has been shown to directly bind to CLEAR elements, as a consequence enhancing the expression of the whole network of genes that possesses the CLEAR motif in their promoter¹⁹⁶. Indeed, TFEB overexpression results in an increased number of lysosomes and higher levels of lysosomal enzymes, thus enhancing lysosomal catabolic activity¹⁹⁷. These findings demonstrate that lysosomal biogenesis and function are globally coordinated by transcriptional regulation.

Apart from lysosomal regulation, recent studies demonstrated that TFEB also controls metabolic processes, such as liver lipid catabolism during starvation¹⁸⁹ and metabolic reprogramming in muscle, following acute exhausting and chronic exercise. In the latter study, it has been reported that TFEB up-regulates the expression of genes related to glucose homeostasis (*e.g. Glut1/4*), as well as mitochondrial content and function (*e.g. citrate synthase and various respiratory chain complex*)¹⁹⁸. These recent studies have identified TFEB as a key mediator of metabolic functions.

The activity of TFEB is primarily regulated through PTMs, protein-protein interactions and spatial organizations¹⁷⁸, as illustrated in Figure 10 and 11. In resting and nutrient rich cells, TFEB is inactive and phosphorylated on several sites by mTORC1 (*e.g. Ser122*¹⁹⁹, Ser142 and Ser211^{200,201}, Figure 10). These PTMs occur at the lysosomal surface and, especially the one at Ser211²⁰², serve as docking events for the adapter 14-3-3, which maintains TFEB largely cytoplasmic probably by masking the NLS^{188,197} (Figure 11, Inactive TFEB). Notably, Ser142 is a common site for mTORC1 and mitogen-activated protein kinase (MAPK also known as ERK2) that for a long time was thought to act in a manner similar to Ser211, allowing the nuclear entrance of TFEB only when

dephosphorylated¹⁷⁸. Only recently a novel model was suggested by Li *et al.*, with Ser142 being a site that regulates the nuclear-cytoplasmic shuttling together with Ser138, a residue phosphorylated by glycogen synthase kinase 3 β (GSK3 β), primed for phosphorylation by Ser142²⁰³ (Figure 10). In this new model, the presence of both phosphorylated Ser138 and Ser142 allows TFEB nuclear import, however the retention in the nucleus happens only if Ser138 is dephosphorylated, otherwise TFEB is exported via the chromosomal maintenance-1 (CRM1, also known as exportin 1) receptor, bound to the Ran-GTPase. The dephosphorylation of Ser138 is possible only under low glucose conditions, which stimulate an mTORC2-dependent activation of PKB/Akt, leading to the inhibition of GSK3 β ²⁰³ (Figure 10). Overall, TFEB nuclear localization and retention result from a coordinate sensing of amino acid and glucose withdrawal, with the absence of the latter causing an eventual export of TFEB from the nucleus.

Activation of TFEB occurs after a combined a) reduction of phosphorylation, when mTORC1 and GSK3 β are inhibited, upon limited amino acids and glucose availability respectively, and b) increased dephosphorylation (Figure 11, Active TFEB). The dephosphorylation events are mediated by the calcium/calmodulin-activated serine/threonine phosphatase calcineurin (also known as protein phosphatase 2B) that is triggered by a release of lysosomal Ca²⁺, through the Ca²⁺-channel mucolipin 1 (MCOLN1), in response to nutrient deprivation and exercise²⁰⁴ (Figure 11, Active TFEB). Additionally the endoplasmatic reticulum stress can also induce nuclear translocation of TFEB via a eukaryotic translation initiation factor 2 α kinase 3 (EIF2AK3)-dependent activation of calcineurin²⁰⁵.

In the past two years AMPK has emerged as an indirect promoter of TFEB transcriptional activity by suppressing mTORC1¹⁷⁶, and in parallel promoting the nuclear localization of acetyl-CoA synthetase 2 (ACSS2), which can then interact with TFEB and support its function. By using AMPK-deficient ESCs, Young *et al.* revealed that AMPK is required for TFEB localization and consequent correct lysosomal function, which are crucial to ensure the embryoid body formation. The authors suggested this AMPK-dependent regulation of TFEB to be mediated via mTORC1-dependent inhibition. Moreover AMPK has been shown to directly phosphorylate ACSS2 at Ser659, leading to its translocation into the nucleus, where ACSS2 forms a complex with TFEB and produces acetyl CoA for histone H3 acetylation, favoring the promoter accessibility and thus the transcription of lysosomal genes²⁰⁶.

The novel link within AMPK and TFEB is an appealing topic for future research, especially in light of TFEB potential as therapeutic target for a broad range of pathologies. For instance, enhanced TFEB activity showed beneficial effects in various murine models of lysosomal storage disorders (LSDs)^{207,208} and neurodegenerative diseases²⁰⁹, such as Parkinson²¹⁰, owing to its

capability to increase cellular waste clearance. Additionally, TFEB activation may represent a strategy to treat metabolic disorders, since its overexpression can prevent weight gain and metabolic syndrome, in genetic and diet-induced models of obese mice¹⁸⁹.

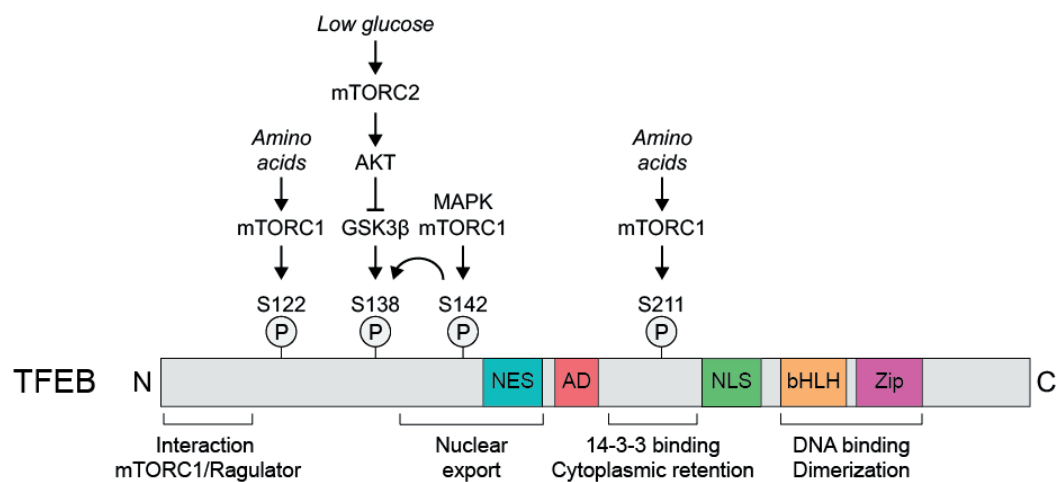


Figure 10. TFEB domains and phosphorylation sites.

TFEB structure main elements are an N-terminal domain mediating its interaction with the mTORC1/Ragulator complex, a nuclear export signal (NES, in blue), an activation domain (AD, in red) which precedes a region required for the 14-3-3 adapter binding, responsible for TFEB cytoplasmic retention. There are also a nuclear localization signal (NLS, in green) and the basic helix-loop-helix (bHLH, in orange) leucine zipper (Zip, in violet) domains, allowing TFEB dimerization and DNA binding. TFEB is regulated by phosphorylations on serine (S) residues. In nutrient rich conditions mTORC1 senses amino acids and phosphorylates TFEB at S122, S142 (site shared with MAPK) and S211. Additionally GSK3β phosphorylates S138, an event that is primed by S142. Low glucose conditions trigger mTORC2 which stimulates AKT that in turns inhibits GSK3β-dependent S138 phosphorylation, favoring TFEB nuclear translocation. Adapted from Li *et al.*²⁰³.

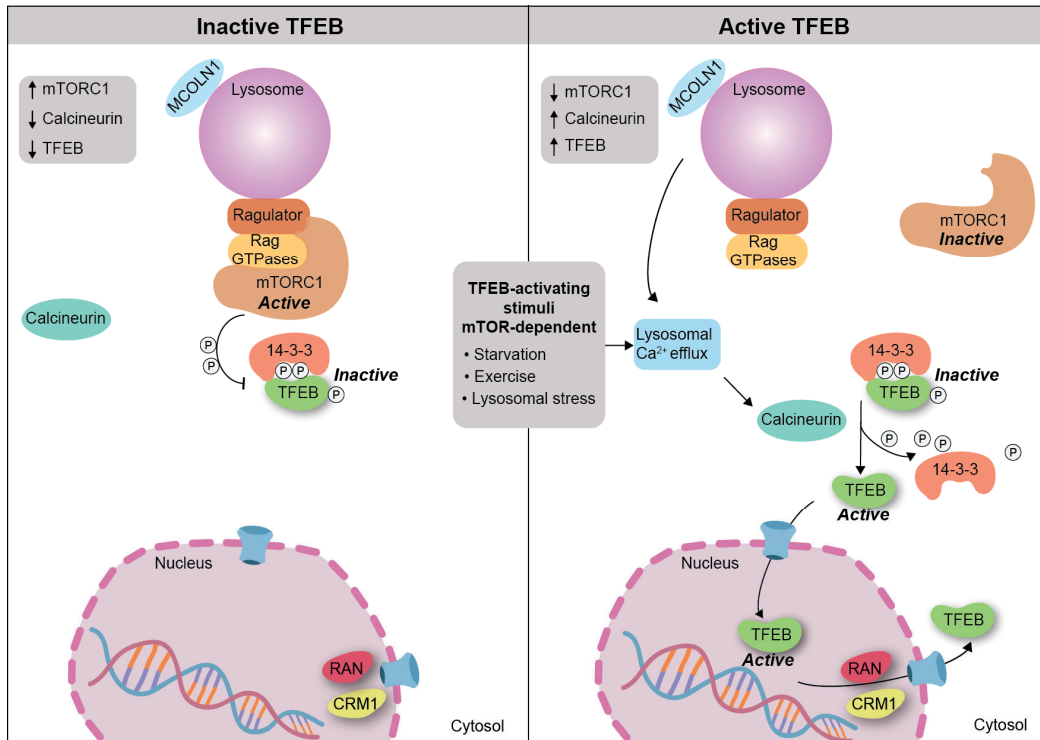


Figure 11. Schematic depicting how TFEB transitions from an inactive to an active state.

Under nutrient-rich conditions, mTORC1 is active and localizes to the lysosome surface, while in complex with the Ragulator complex and the RagGTPases. Active mTORC1 phosphorylates TFEB, promoting 14-3-3 adapter protein binding and the consequent cytoplasmic retention of TFEB (**Inactive TFEB**). Various stimuli, such as starvation, exercise and lysosomal stress, can activate TFEB by inhibiting the mTORC1 cascade and favoring the release of lysosomal Ca^{2+} , which triggers the calcineurin-dependent dephosphorylation of TFEB. Dephosphorylated TFEB enters the nucleus where it regulates a transcriptional program linked to lysosome, autophagy as well as glucose and lipid metabolism (**Active TFEB**). Nuclear export is then mediated by CRM1 receptor bound to the Ran-GTPase. Adapted from Napolitano *et al.*¹⁷⁸.

2 Rationale and aim of the thesis

AMPK represents an important target to develop drugs for the treatment of metabolic disorders. Since medications to cure metabolic diseases need to be administered continuously, triggering diverse and complex patterns of gene expression changes, it is fundamental to understand AMPK-dependent effects on long-term metabolic adaptations. The involvement of AMPK in reprogramming of metabolism is being studied intensively. However, whether described changes in gene expression are mediated through an AMPK-dependent mechanism still remains unclear. This notion is based on the fact that conclusions are often drawn from experiments only using promiscuous non-selective AMPK inhibitor (*i.e.* Compound C) and/or activator (*e.g.* AICAR, metformin) without having loss-of-function (*e.g.* AMPK knockout) control. In addition, some studies employed AMPK knockout models and substantiated the role of AMPK in control of only a small subset of genes.

The aim of this thesis is to investigate the role that AMPK plays in the adaptive reprogramming of metabolism through transcriptional control. To do so I will initially compare the effect on gene expression of AICAR and 991, two pharmacological AMPK activators with distinct mechanisms of action, performing a transcriptomic study in mouse embryonic fibroblasts and mouse primary hepatocytes, either wild-type or AMPK-deficient.

The first axis of the thesis will explore the data originated from a transcriptome profiling using microarrays, with a special emphasis on the bioinformatic investigation of the gene expression results. In this section, I will present some novel AMPK-regulated genes and a comprehensive *in silico* analysis that will provide a) a global overview of the transcriptional responses associated to distinct treatments, b) information on the metabolic processes impacted and c) a prediction of the transcription factors acting as mediators of AMPK action.

In the second axis of the thesis, I will follow-up on the microarray dataset. Initially I will present the example of a novel AMPK-regulated gene whose promoter analysis supported the discovery of a link between AMPK and one of the predicted transcription factors (TFEB). This will be followed by detailed cellular and biochemical studies providing potential mechanistic insights by which AMPK regulates specific gene expression. Additionally, I will use zebrafish as an *in vivo* model to investigate the conserved transcriptional response to AMPK stimulation, by physiological or pharmacological means.

3 Introduction to the results

AMPK is a Ser/Thr kinase and is a heterotrimeric complex consisting of a catalytic α subunit and β - and γ -regulatory subunits. AMPK is activated by phosphorylation of AMPK on a conserved threonine residue (Thr172) in the activation loop of the α subunit mediated by the upstream kinases LKB1 or CaMKK β . AMP and ADP binding to the γ subunit maintains this phosphorylated and activated form of AMPK, and in the case of AMP, AMPK can be further activated through an allosteric mechanism⁷⁴. The effects of AMP on AMPK can be mimicked within the cell by the actions of AICAR, as a consequence of its conversion to ZMP. The use of AICAR *in vitro* and *in vivo* has implicated AMPK as playing a central role in regulating a number of metabolic pathways²¹¹, however, AICAR has a number of additional targets by virtue of its ability to mimic the effects of AMP within the cell²¹². With the advent of genetic models lacking a functional AMPK complex, the contribution of AMPK to the actions of AICAR has been challenged in several studies^{97,98,213}. In recent years more specific and potent AMPK activators have been developed including A-769662 and 991^{61,67}. These compounds also work by maintaining the phosphorylated and active form of AMPK, as well as allosterically activating the enzyme. Importantly, the major advantage of these compounds is that they do not mimic the actions of AMP, and instead activate AMPK through a distinct binding site, termed the ADaM-site³⁰. Given that these compounds are expected to have fewer off-target effects compared to AICAR, this has prompted researchers to re-examine the contribution of AMPK to regulating pathways involved in central metabolism and adaptive metabolic reprogramming at the transcriptional level.

In this study, we performed a transcriptome profiling of mouse embryonic fibroblasts and primary hepatocytes in order to identify genes and transcription factors/co-activators that are directly and/or indirectly regulated by AMPK. Our studies using AMPK-deficient cells highlight the problem with using AICAR as an activator of AMPK since a profound number of genes were regulated in an AMPK-independent manner. In contrast, treatment of cells with the ADaM-site activator, 991, resulted in almost exclusively AMPK-dependent regulation of gene transcription. We discovered that AMPK plays a central role in regulating the dephosphorylation and subsequent nuclear-translocation of TFEB. Importantly, we show that these effects are independent of the activity of mTOR, which has been previously reported to play a central role in the regulation of TFEB^{202,214}. We show that AMPK regulation of TFEB leads to increased transcription and protein expression of folliculin (FLCN), a tumor suppressor which has been proposed to regulate the lysosome functions and more recently metabolic responses²¹⁵⁻²¹⁷. Taken together, we provide

evidence for the importance of AMPK in mediating the translocation of TFEB into the nucleus and we suggest that this AMPK-TFEB axis may play a key role in regulation of the lysosome through the action of FLCN.

Part of the work presented in this thesis forms a manuscript, is available in the Appendix section 9.4, which has been prepared and published on BioRxiv (doi.org/10.1101/499921), in preparation for publication in a peer-reviewed journal:

Collodet C., Foretz M., Deak M., Bultot L., Metairon S., Viollet B., Lefebvre G., Raymond F., Parisi A., Civiletto G., Gut P., Descombes P., Sakamoto K. (2019). AMPK promotes induction of a tumor suppressor FLCN through activation of TFEB independently of mTOR. *Manuscript in preparation*.

4 Results, part I: transcriptome profiling reveals the AMPK-regulated genes in response to small molecule activators

4.1 AMPK activation in the models chosen to investigate the role of AMPK on transcriptional regulation

In order to specifically identify genes regulated by AMPK we first established two working models that have been widely used within the AMPK field, namely mouse primary hepatocytes and mouse embryonic fibroblasts (MEFs). Primary hepatocytes represent a physiologically relevant cell model but are more challenging to obtain and culture. In contrast, MEFs have the advantage that they can be continuously cultured although their differentiation status is less defined. In order to specifically identify genes induced by AMPK, we exploited two distinct genotypes, namely cells harboring a functional AMPK, and cells lacking both isoforms of the catalytic α subunit, AMPK α 1 α 2^{-/-} herein referred to as AMPK-WT and AMPK-KO, respectively. Mouse primary hepatocytes were isolated from AMPK-WT and liver-specific AMPK-KO mice whereas AMPK-WT and AMPK-KO MEFs were derived from WT and AMPK-KO mice, respectively²¹⁸. In addition, AMPK activation was triggered in both models with two activators that have distinct modes of action, namely AICAR and 991 (schematic representation in Figure 12A, B). AICAR has been the most widely used activator in AMPK studies for decades. However, AICAR presents the major drawback of having off-target effects due to its ability to mimic the effects of AMP within the cell^{213,219}. In contrast, 991 is an activator that has been specifically developed to target AMPK directly through the ADaM-pocket⁶¹, and is therefore expected to exert a much more AMPK-specific response²⁶. In summary, our experimental strategy presents the major advantage of monitoring gene changes in both the AMPK-WT and AMPK-KO MEFs and hepatocytes, allowing us to accurately determine which transcriptional changes occur upon AMPK activation.

For MEFs, the dose of 991 (10 μ M, a near saturating concentration) was selected based on dose-response curves previously generated within our laboratory. For AICAR, a range of doses were tested and the phosphorylation of AMPK itself and its *bona fide* substrate ACC were monitored by western blot analysis as proxies for AMPK activation (Appendix Figure 1A). A dose of 2 mM was chosen since it corresponds to an increase in AMPK activation after 1 h of treatment. We observed that AMPK activation is maintained after treatment of MEFs between 1 and 12 h following both 991 and AICAR stimulations (Appendix Figure 1B, C respectively). In order to focus

on the acute transcriptional responses following an AMPK activation, and assuming a transcriptional readout in a 2 to 8 h time frame, we chose to harvest the cells at the 4 h time-point following treatment. Similar treatment conditions were used for studying AMPK activation in mouse primary hepatocytes with the exception that lower concentrations of activators were used, 300 μ M AICAR and 3 μ M 991, based on previous data generated in our laboratory which showed that primary hepatocytes respond better to treatment with these compounds²⁶.

To generate the samples for the transcriptome analysis, cells were treated and harvested by two methods, in order to obtain protein and total RNA samples. Before proceeding to the transcriptome profiling, the activation of AMPK was confirmed by analyzing from cell lysates the phosphorylation profiles of AMPK and its substrates ACC and Raptor, in both MEFs (Figure 12C) and primary hepatocytes (Figure 12D). The results showed that both compounds activated AMPK, as demonstrated by the increase in phosphorylation of the AMPK substrates ACC and Raptor, in AMPK-WT MEFs and mouse primary hepatocytes. Notably, although treatment with 991 or AICAR caused a similar increase of ACC phosphorylation in both MEFs and hepatocytes, 991-induced Raptor phosphorylation was stronger in MEFs but lower in hepatocytes compared to AICAR. Activation of AMPK was also monitored in AMPK-KO MEFs and hepatocytes. Western blot analysis confirmed that the catalytic α subunit is absent in these models. Consequently, the levels of phosphorylation of AMPK and its substrates ACC and Raptor are absent. Taken together, these results confirm that AICAR and 991 activate AMPK in our two model systems and that these effects are completely abolished in MEFs and hepatocytes lacking AMPK α 1 α 2.

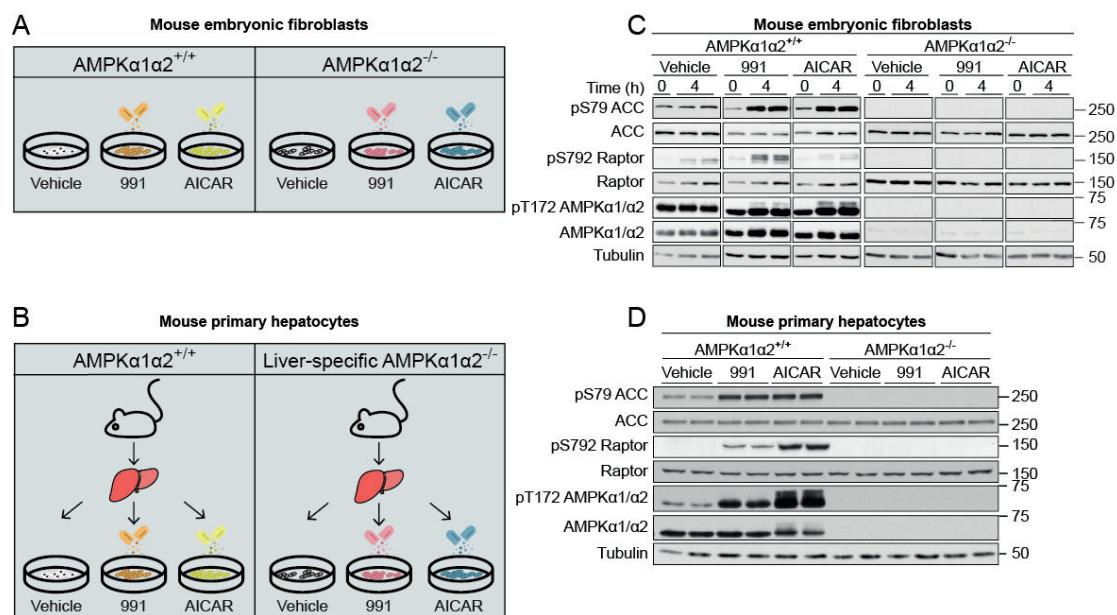


Figure 12. Activation of AMPK in samples used for the microarrays.

(A) Schematic representation of the experimental design in mouse embryonic fibroblasts. Control (AMPK α 2^{+/+}) or knockout (AMPK α 2^{-/-}) cells were treated with vehicle (DMSO), 2 mM AICAR or 10 μ M 991 for 4 h. (B) Schematic representation of the experimental design using primary hepatocytes. Primary hepatocytes were isolated from AMPK α 2 liver-specific knockout (AMPK α 2^{-/-}) mice and control AMPK α 1^{lox/lox} α 2^{lox/lox} mice littermates (AMPK α 2^{+/+}). Plated cells were treated for 4 h with vehicle (DMSO), 3 μ M 991 or 300 μ M AICAR. MEFs (C) and mouse primary hepatocytes (D) cell lysates (20 μ g) were subjected to western blot analysis with the indicated antibodies, figures show a representative blot of n=3 and n=2, respectively.

4.2 991- and AICAR-mediated transcriptomic response

Following the confirmation of AMPK stimulation, total RNA was extracted from crude lysates and used for a whole-genome transcriptome profiling with Affymetrix MOE430 arrays, following manufacturer's protocol. Briefly, RNA integrity was first monitored by capillary electrophoresis. Labeled copy RNA was produced by oligo dT-primed double-strand cDNA synthesis from total RNA, followed by *in vitro* transcription/amplification in presence of biotinylated ribonucleotide analogs. Purified labeled copy RNA was hybridized to Affymetrix MOE430 GeneChips, followed by washing/staining and scanning. The resulting intensity files (CEL files) were imported into Partek Genomics Suite software for initial raw data quality assessment, followed by robust multi-array average (RMA) normalization and statistical analysis to identify differentially expressed genes.

We performed a first quality assessment by principal component analysis (PCA), to investigate the pattern of segregation within MEFs and primary hepatocytes samples (Appendix Figure 2A and B, respectively). In MEFs, the PCA analysis showed a clear segregation of data based on genotypes, explaining almost 30% of the variability intra-samples. The PCA also suggested a distinct treatment-dependent pattern within genotypes. Indeed, the second component revealed that in MEFs AMPK-WT, the AICAR-treated samples segregate further than the 991-treated samples, as compared to vehicle-stimulated samples, suggesting that AICAR either affects a greater number of genes and/or induces greater fold-changes in gene expression. In addition, we observed an overlap between vehicle- and 991-treated samples in the MEFs AMPK-KO, suggesting that 991 has an almost undetectable effect in the absence of AMPK. In primary hepatocytes in contrast, the treatment was the main cause of variance, followed by a lower variance explained by the genotypes. AICAR in particular elicited a much greater response than 991. These conclusions were corroborated by the hierarchical clustering (Figure 13A, B). This later analysis, based on transcripts having a false discovery rate P -value < 0.0001 , first depicts a clear distinction between AICAR- and 991-treated samples. Second, the more subtle transcriptional changes between treatment and vehicle control are clearly illustrated for both AICAR and 991 in AMPK-WT cells, with a much greater difference for AICAR as compared to 991. Finally, we also observe that the absence of functional AMPK leads to greater differences as compared to WT cells in MEFs than in primary hepatocytes.

In order to identify genes specifically and exclusively regulated following AMPK activation, we first selected transcripts by pairwise differential expression analysis of MEFs and primary hepatocytes treated with vehicle as compared to AICAR or 991. P -values were corrected for multiple testing by use of the false-discovery rate (FDR) method of Benjamini and Hochberg²²⁰ and

we applied a conservative significance threshold of 5% FDR associated with fold-change value of 1.3 or more, given the global moderate fold changes detected. The list of transcripts significantly modulated are represented in Venn diagrams, highlighting the number of mRNA either up- or down-regulated following the treatment with 991 or AICAR in AMPK-WT and AMPK-KO MEFs and primary hepatocytes (Figure 14A, B), respectively.

Following 991 treatment, the vast majority of differentially expressed transcripts required a functional AMPK (184 out of 199 for MEFs and 670 out of 684 for primary hepatocytes, respectively (Figure 14A, B), complete gene list in appendix table 1 and 2 (Appendix section 9.5 and 9.6)). This observation confirms the nearly exclusive specificity of 991 for AMPK in both MEFs and primary hepatocytes. In contrast, AICAR globally induced a much larger transcriptional response compared to 991, with a majority of the transcripts differentially regulated in absence of functional AMPK (1026 out of 2053 in MEFs and 754 out of 1718 in primary hepatocytes, respectively). This result is not surprising since AICAR leads to an increase in ZMP (AMP analog) concentration and is therefore expected to globally influence numerous cellular processes in addition to AMPK-dependent cellular events. Notably, despite having similar trends of specificity across the models, the compounds affected different set of genes in MEFs and primary hepatocytes. For instance, considering the total number of transcripts regulated by 991, only 8% were shared across MEFs and hepatocytes AMPK-WT, and similar percentage were found when looking at commonly modulated genes by AICAR in AMPK-WT (7.3%) or in AMPK-KO (11.2%). Altogether, our findings strongly suggest that 991 elicits a much more AMPK-specific transcriptional response than AICAR, and corroborate the results of the PCA and the hierarchical clustering.

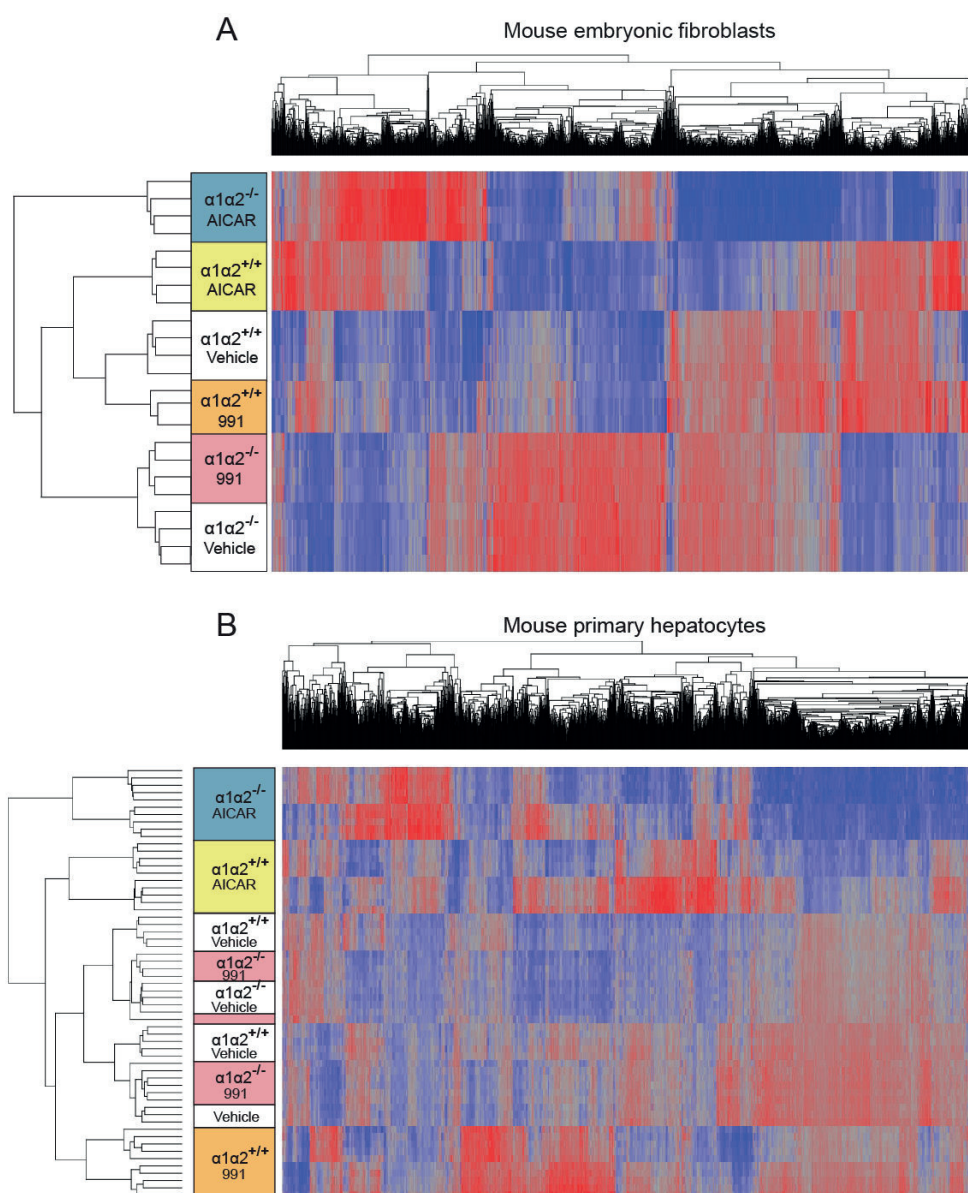


Figure 13. Hierarchical clustering of the transcriptomic data.

Overview of the hierarchical clustering analyses in mouse embryonic fibroblasts (A) and mouse primary hepatocytes (B). Mean-centered gene expression ratios are depicted by a log2 pseudo color scale. Red and blue indicate gene over- and under-expressed, respectively, compared to the mean value. The data were analyzed by two-way analysis of variance (ANOVA) with the factors of genetic background, treatment and interaction. Selected genes having a false discover rate (FDR) P -value < 0.0001 for the interaction are shown.

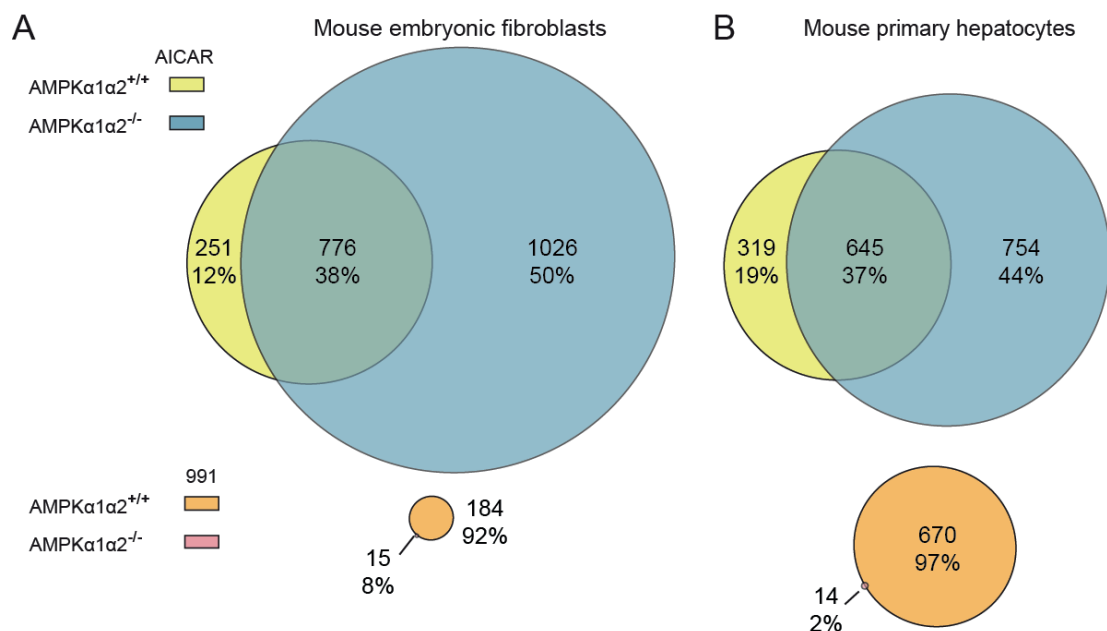


Figure 14. Venn diagrams indicating the transcripts modulated by AMPK after 991 and AICAR treatment.

Venn diagrams showing 991 and AICAR specificity in mouse embryonic fibroblasts (**A**) and mouse primary hepatocytes (**B**) transcriptome profiling, respectively. Two-way ANOVA with Benjamini & Hochberg multiple testing correction was applied to discriminate 991 versus control and AICAR versus control conditions. The moderated *P*-value was set at 0.05 for the interaction within genetic background and treatment as well as for the pairwise comparisons. In addition, a fold-change cutoff of 1.3 was applied. Each group of genes is shown with a color code, as specified in the legend. The numbers correspond to the numbers of transcripts altered and the percentage contribution to the total number of transcripts identified for each treatment in the correspondent model.

4.3 Pathways and transcription factors modulated by AMPK

We next sought to investigate which pathways were impacted in response to AMPK stimulation. We focused our analyses on the transcripts modulated following 991 treatment only, as they appeared to be transcriptional effects almost exclusively AMPK-dependent (184 transcripts modulated in MEFs and 670 in hepatocytes, respectively). The gene ontology analysis was conducted using the Database for Annotation, Visualization and Integrated Discovery (DAVID) program^{221,222}. This analysis revealed the metabolic and lysosomal pathways as common pathways between the both cell types (Figure 15A, B). Considering the function of AMPK as master regulator of metabolic homeostasis, the observed enrichment in metabolic pathway provided a confirmation of the key relevant role of AMPK in this context. In contrast, the conserved effect of AMPK on the lysosomal pathway appeared more surprising. Indeed, six and 13 upregulated transcripts were linked to lysosomal processes in MEFs and hepatocytes, respectively (Appendix Figures 3 and 4). Interestingly, three of these transcripts were upregulated in both hepatocytes and MEFs: *Mcoln1*, *Gns* and *Neu1*. *Mcoln1*, a nonselective cation channel has been proposed to regulate lysosome trafficking, exocytosis and autophagy²²³, together with two genes encoding for enzymes located in the lysosomal lumen. N-acetylglucosamine-6-sulfatase (*Gns*), is involved in the breakdown of glycosaminoglycans²²⁴ and Neuraminidase-1 (*Neu1*) cleaves sialic acid from substrates such as glycoproteins and glycolipids²²⁵.

We observed a higher number of significantly modulated pathways in primary hepatocytes compared to MEFs. This result is likely to be due to the fact that more transcripts were affected by 991-treatment in hepatocytes compared to MEFs. The AMPK signaling pathway was also predicted by the *in silico* analysis, given the identified changes in expression for transcripts previously shown to be controlled by the AMPK, such as *Hmgcr*, *G6pc* and *Ppargc1a*. Similarly, a number of pathways related to transcription factors known to be substrates of AMPK, such as FOXO¹⁷¹ and TP-53¹⁵⁹, were enriched.

In order to better define the mechanisms by which AMPK regulates gene expression, we next performed an analysis aimed at identifying potential transcription factors that could be direct or indirect AMPK substrates and be responsible of the AMPK-induced transcriptional output. One method for identifying these new targets was to perform an *in silico* analysis, for which we focused on 991-responsive transcripts identified in MEFs and hepatocytes. We took advantage of Ingenuity Pathway Analysis (IPA) software, which comprises an approach that correlates the observed gene expression changes with potential upstream transcriptional regulators²²⁶. The transcription factor

prediction highlighted 11 candidates in MEFs and 12 in hepatocytes, respectively (Table 5). Of particular interest, only two transcription factors were identified in both MEFs and primary hepatocytes, namely SREBP1, previously reported to be regulated by AMPK¹⁶, and TFEB a master regulator of lysosomal biogenesis¹⁷⁸. Additionally, and in line with the pathway analysis, we identified transcription factors that have previously been reported to be regulated by AMPK, including FOXO3¹⁷⁰, TP53¹⁵⁹ in MEFs and CREB1¹²⁷, in primary hepatocytes. Given its implication in regulating energy metabolism, we focused on TFEB for subsequent analysis (chapter 6 - Results, part II).

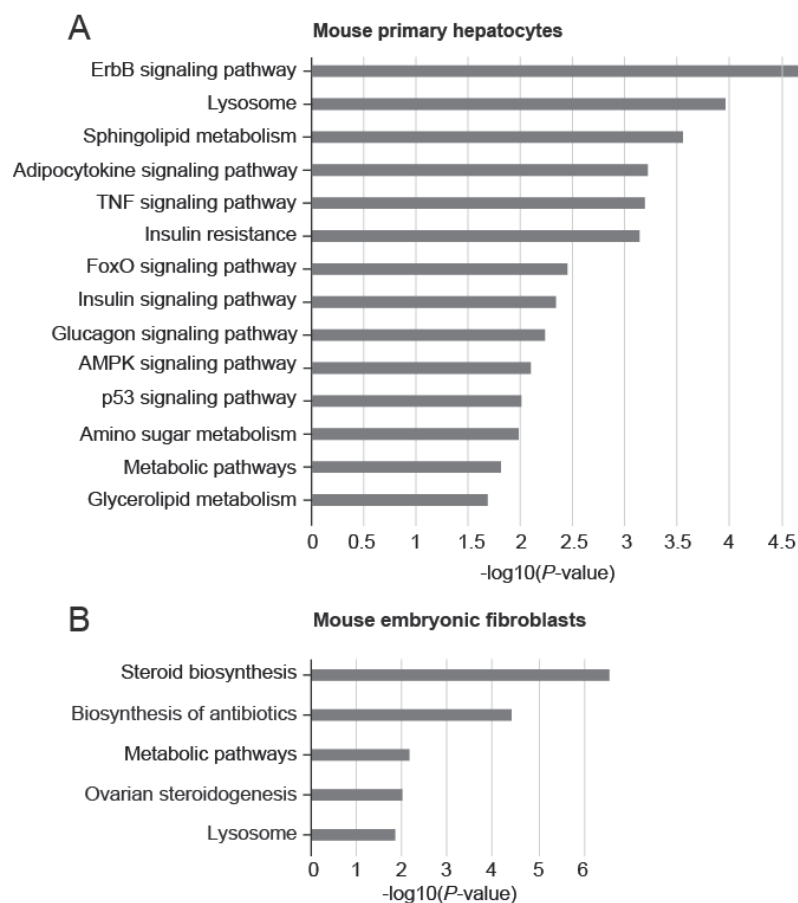


Figure 15. Gene enrichment analysis across the AMPK-regulated genes.

Gene enrichment analysis of the 991-responsive signature in mouse embryonic fibroblasts (A) and mouse primary hepatocytes (B). DAVID was used to explore the gene ontology terms associated to the AMPK-regulated genes. The bars represent the negative $\log_{10}(P\text{-value})$ of enriched terms, referring to how significant is the association within the gene list and an indicated ontology term.

Mouse embryonic fibroblasts		Mouse primary hepatocytes	
Transcriptional regulator	<i>P</i> -value	Transcriptional regulator	<i>P</i> -value
SREBP1	1E-14	NUPR1	2E-08
SREBP2	8E-12	CREB1	3E-08
STAT4	2E-08	TFEB	6E-08
SIRT2	7E-08	SREBP1	6E-07
SRC2	7E-06	Miz-1	1E-05
TFEB	2E-04	ATF4	1E-04
FOXO3	3E-04	ATF2	3E-04
TP53	4E-04	TCF3	3E-04
NFATc2	9E-04	MITF	3E-03
IRF7	3E-03	TAF7L	1E-02
IRF3	4E-03	HOXD10	1E-01
		HNF-1B	2E-01

Table 5. List of predicted transcription factors mediating AMPK transcriptional response.

The 991-responsive genes in mouse embryonic fibroblasts and primary hepatocytes were used to perform an upstream regulator analysis in IPA. The figure shows the predicted transcription factors together and the associated *P*-value.

4.4 Validation by qPCR of selected AMPK-regulated genes

We next aimed to validate by qPCR the robustness of the expression level detected by microarray at the 4 h time point for selected AMPK-regulated genes. The candidates were prioritized by applying the following parameters: magnitude of the fold-change in expression, previous implication in the AMPK response and function of the gene. The latter was investigated with IPA software, which allowed us to perform functional, pathway, causal network and gene regulatory analyses, using a manually curated database of gene and protein interactions²²⁶. This combined exploration led to an initial selection of 27 targets for subsequent validation by qPCR.

The qPCR results validated 13 genes as AMPK-responsive targets in MEFs, whereas the other 14 were not confirmed as significantly regulated transcripts (Figure 16A). These transcripts changed level after 991 and/or AICAR treatment in the AMPK-WT cells, whereas their variation in the AMPK-KO genetic background were either completely blunted or still present after AICAR stimulation but significantly decreased compared to the AMPK-WT counterpart.

Numerous confirmed targets in our selection encode enzymes important for the metabolism of cholesterol and which are known to be regulated by the transcription factor SREBP. For example, *Acss2* encodes an enzyme that activates acetate making it available for lipid synthesis²²⁷ and methylsterol monooxygenase-1 (*Msmo1*), encoding an enzyme involved in the cholesterol biosynthesis²²⁸. SREBP also regulates the genes low-density lipoprotein receptor (*Ldlr*), a cell surface protein that plays a role in cholesterol homeostasis²²⁹ as well as *Hmgcr*, the rate-limiting enzyme in cholesterol biosynthesis that converts HMG-CoA to mevalonate²³⁰. Interestingly, *Hmgcr* and lipin-1 (*Lpin1*) emerged from the transcriptome analysis of the MEFs and mouse primary hepatocytes as induced by activation of AMPK, providing strong support for the role of AMPK in their regulation (Figure 16A, B). Taken together, these data suggest that AMPK may play an important role in regulating the SREBP transcription factor and thereby the genes involved in lipid and cholesterol homeostasis.

Additionally, we identified various target genes linked to diverse cellular functions which were increased in response to 991-treatment. For example a) the *Lpin* and CREB3 regulatory factor (*Crebrf*) genes, which are involved in transcriptional regulation^{231,232}, b) thioredoxin interacting protein (*Txnip*), an α -arrestin family protein, originally characterized as a regulator of cell redox state²³³ and c) toll interacting protein (*Tollip*), which has been demonstrated to promote ubiquitin-dependent autophagy²³⁴, leading to the elimination of protein aggregates and counteracts the cytotoxicity caused by misfolded proteins in neurodegenerative diseases.

Fln and its interacting protein *Fnip1*, which showed increased expression in both cellular models (Figure 16A, B), were of particular interest since both have been previously linked with AMPK^{235,236}. We found these results intriguing, especially because FLCN tumor suppressor function has been suggested to take place via a FLCN-mediated inhibition of AMPK^{216,237}. Based on our observations, we hypothesized that there may be a more complex relationship between the activities of AMPK and FLCN, with AMPK potentially modulating the expression of FLCN at the transcriptional level. Given the link between AMPK and FLCN, we decided to further investigate the relationship between AMPK activity and FLCN expression.

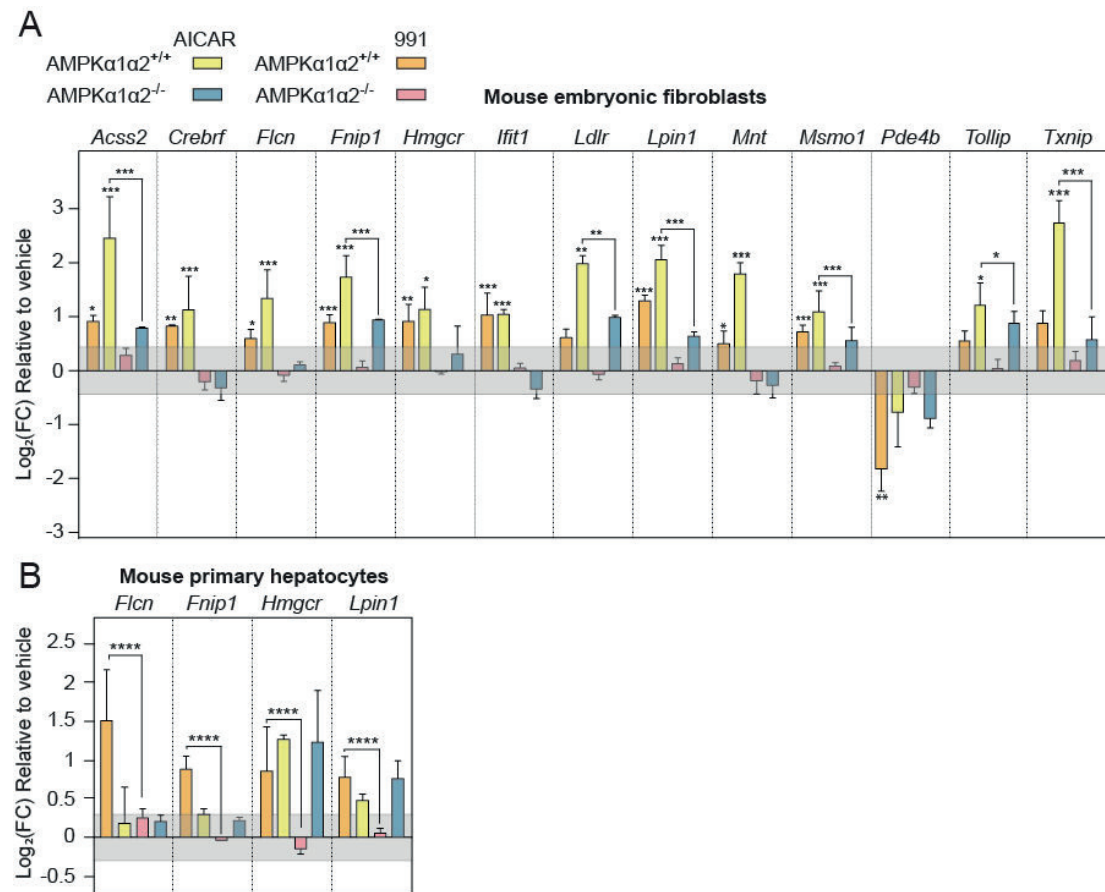


Figure 16. Confirmation of selected AMPK-target genes by qPCR.

Relative mRNA levels of the indicated genes, respectively in mouse embryonic fibroblasts (**A**) and primary hepatocytes (**B**) as measured by qPCR. The color code is indicated in the legend. MEFs AMPK α 1 α 2^{+/+} or AMPK α 1 α 2^{-/-} were stimulated with 10 μ M 991 or 2 mM AICAR for 4 h, and AMPK α 1 α 2^{+/+} or AMPK α 1 α 2^{-/-} hepatocytes were treated for 4 h with 3 μ M 991 or 300 μ M AICAR. Two normalization genes were used (β 2 microglobulin *B2m*, Peptidylprolyl isomerase-a *Ppia*), selected based on their stability following assessment with GeNorm (M value < 0.6)²³⁸. Values are represented as log₂ fold-change \pm SD (n=9). Grey lines indicate log₂ fold-change threshold of \pm 0.37. For the analysis, two-way ANOVA with interaction was fit to log-transformed data, **P*-value < 0.05, ***P*-value < 0.01, ****P*-value < 0.001.

4.5 Characterization of *Flcn* as transcriptional target of AMPK

We next performed a time course experiment to investigate the kinetics of *Flcn* and *Fnip1* expression changes in response to AMPK activation. MEFs were treated with 991 and AICAR for various time-points (0.5, 1, 2, 4, 8, 12 and 24 h), cells were harvested to isolate total RNA for qPCR analysis (Figure 9A, B). The mRNA levels of both *Flcn* and *Fnip1* increased after 991 treatment only in AMPK-WT cells but not in AMPK-KO cells (Figure 17A, B), confirming their AMPK-dependent induction. 991 induced an approximately 1.5-fold increase in both *Flcn* and *Fnip1* expression after 2 h of treatment, which was maintained throughout the 24 h of experiment. AICAR stimulated a higher level of induction for both genes (~3-fold for *Fnip1* and ~2.5-fold for *Flcn*), although there was some increase in gene expression in the AMPK-KO cells, albeit at later time points compared to AMPK-WT cells. This suggests that the contribution of AICAR to the induction of *Fnip1* and *Flcn* is, at least partially, AMPK-independent.

Subsequently, we sought to determine whether the detected *Flcn* and *Fnip1* mRNA changes were associated with an increase in the respective protein levels. MEFs AMPK-WT and AMPK-KO cells were treated with vehicle, 991 or AICAR for 4, 12, 24 or 36 h and harvested for western blot analysis (Figure 17C). FLCN was significantly increased after around 12 h following treatment with both 991 and AICAR in AMPK-WT MEFs, whereas FNIP1 levels did not change over time (*data not shown*). In contrast, there was no detectable change in FLCN expression in AMPK-KO MEFs treated with 991 or AICAR. Taken together, these data indicate that treatment of MEFs with 991 and AICAR induces an increase in expression at both mRNA and protein levels of FLCN in an AMPK-dependent manner. We also confirmed that the increased levels of *Flcn* mRNA were due at least partly to enhanced gene transcription, since pre-mRNA levels of *Flcn* were also significantly up-regulated in response to 991 and AICAR treatment, as measured by increased levels of an intron of this gene (Appendix Figure 5A, B).

In order to study the role of AMPK in a number of physiological processes, we took advantage of the zebrafish (*Danio rerio*), which represents a powerful vertebrate model in biomedical research, due to the genetic similarities with humans together with its high fecundity, rapid development and the optical transparency of embryos and larvae²³⁹. An additional advantage of using zebrafish as a physiological model is the ability to study exercise metabolism *in vivo* as one can exercise and train the fish through modulating their swimming behavior. Parisi *et al.* generated *prkaa1/prkaa2*, the zebrafish paralogues of human/mouse AMPK α 1 and α 2, double knockout (DKO) zebrafish using CRISPR-Cas9 genome editing (*manuscript in preparation*).

The knockdown of AMPK was confirmed by qPCR and western blot analysis, which showed the absence of both AMPK catalytic subunits and related AMPK-activity. Using this model, we investigated whether *Flcn* and *Fnip1* expression were regulated in an AMPK-dependent manner after exercise training, a physiological and established condition that has been previously shown to activate AMPK primarily in skeletal muscle in mouse and human studies.

First, we established an acute exercise training protocol in order to stimulate AMPK in zebrafish skeletal muscle, which is summarized in Figure 18A. A mixed population of WT and knockout fish was used to perform the exercise study, to ensure consistency between the experimental groups. The control group was placed in the swim tunnel and subjected to a low flow speed (5 cm/s) for 3 h. For the exercise group, an acclimatization period of 20 min at a low flow speed (5 cm/s) was followed by a gradual increase of water velocity up to 80% of maximum speed capacity, 60 cm/s for this cohort of fish, which was maintained for approximately 2 h. Notably, the maximum speed of the fish, defined as the maximum sustainable swimming speed, was determined in a previous grouped endurance test following the existing guidelines²⁴⁰. Subsequently, zebrafish were sacrificed and the muscles were extracted as quickly as possible, to avoid AMPK activation due to cellular stress (*e.g.* hypoxia). AMPK activation in the WT exercise fish was confirmed by western blot analysis of the phosphorylated AMPK and its substrate ACC (Figure 18B). We have not been able to validate additional substrates used in our MEFs and mouse hepatocytes experiments (*e.g.* Raptor) since the only commercially available antibodies recognize an epitope which is not conserved in zebrafish. We also determined by qPCR the mRNA levels of *flcn* and *fnip2*, the paralogue of *Fnip1*. These analyses showed an increased level of expression of both genes after physical exercise in WT zebrafish, whereas the increase was significantly diminished in *prkaa1/prkaa2* DKO zebrafish (Figure 18C). Taken together, these data suggest that exercise can increase the activity of AMPK in zebrafish muscle, resulting in an increase in *flcn* and *fnip* expression at least in part mediated by AMPK.

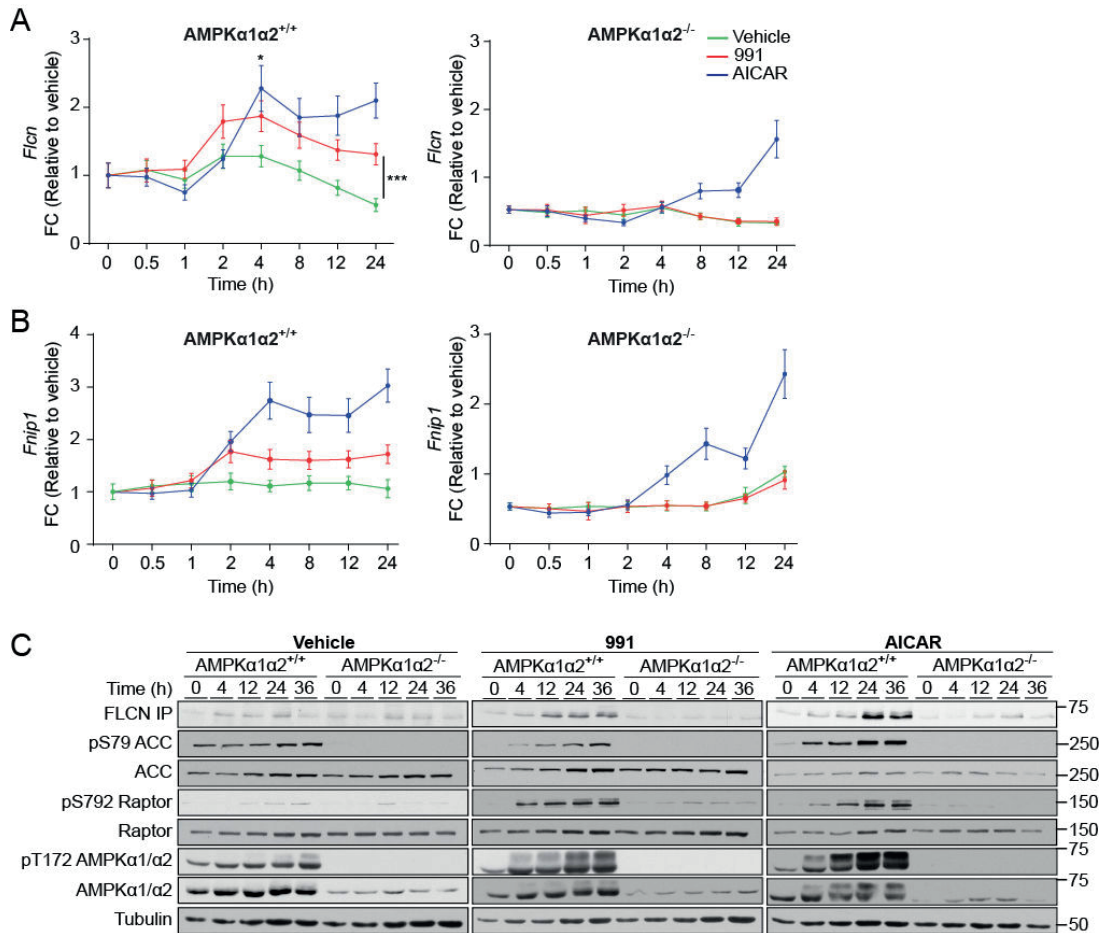


Figure 17. Time course characterization of *Flcn* and *Fnip1*.

(A and B) Relative *Flcn* and *Fnip1* mRNA quantity was assessed with a Biomark gene expression 192.24 IFC delta gene assay. MEFs AMPKα1α2^{+/+} or AMPKα1α2^{-/-} were treated with vehicle (DMSO), 10 μM 991 or 2 mM AICAR, for 0, 0.5, 1, 2, 4, 8, 12 and 24 h. Two normalization genes (*Ppia*, *Tbp*) were used. For the analysis, two-way ANOVA with interaction was fit to log-transformed data, * *P*-value < 0.05, *** *P*-value < 0.001. Each data point represents the mean ± SEM (n=12). (C) Western blot analysis of the indicated antibodies, FLCN was immunoprecipitated (IP) from 500 μg of cell lysate with 1 μg of anti-Folliculin antibody. MEFs AMPKα1α2^{+/+} or AMPKα1α2^{-/-} were treated with 991 10 μM or AICAR 2 mM for the indicated time points. The image is representative of three independent experiments.

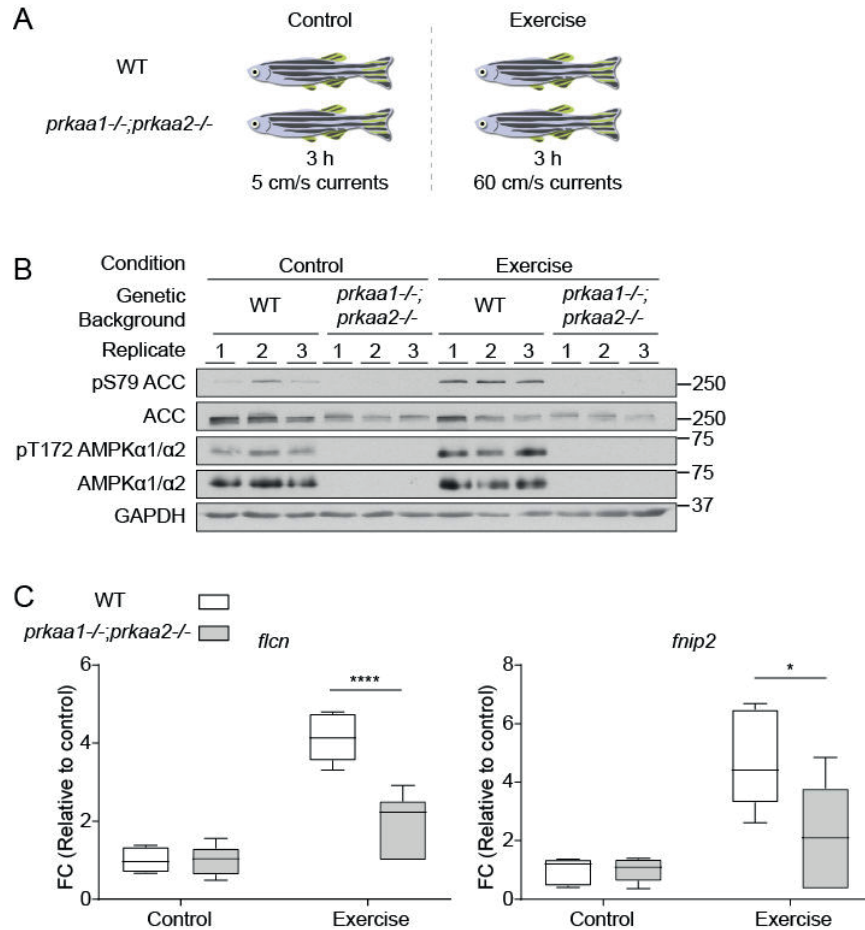


Figure 18. Physiological activation of AMPK in zebrafish leads to *Flcn* increase.

(A) The figure summarizes the experimental scheme implemented to acutely exercise WT and *prkaa1*^{-/-};*prkaa2*^{-/-} adult zebrafish. An electronic controller and a motor-driven propeller were used to adjust the water velocity to the indicated speed. (B) Immediately after the 3 h of training, muscle samples were collected from the zebrafish. Tissue lysates (20 µg) were used to perform western blot analysis with the indicated antibodies. (C) mRNA transcript levels of *flcn* and *fnip2* were determined after normalization with the reference genes *ef1a* and *nrf1*. Data are shown as box-and-whisker plot (min to max) of values normalized to control WT (n=6). Two-way ANOVA with the factors of genetic background, exercise and interaction was performed, the graph shows the significance of the interaction, * *P*-value < 0.05, **** *P*-value < 0.0001.

5 Discussion, part I

5.1 991 and AICAR effect at gene expression level

Global gene expression changes

In this study, using two different AMPK loss-of-function cellular models we have compellingly demonstrated that 991 affects gene expression almost entirely in an AMPK-dependent manner. This observation is consistent with our previous *in vitro* data, indicating the high selectivity of 991 towards AMPK. Indeed, by using a cell-free assay against a panel of 139 protein kinases, we showed that 991 exclusively increased the activity of AMPK without affecting other kinases²⁶. We also observed that AICAR induced a large number of gene expression changes in MEFs and primary hepatocytes that lacked AMPK, indicating that there are multiple off-target effects of this compound. This is not entirely surprising given that AICAR works by conversion to ZMP and mimics the effects of AMP on regulation of AMPK, as well as other AMP-sensitive proteins. Given that there are multiple AMP-regulated enzymes within the cell, it is likely that these effects persist in cells lacking AMPK²¹². Our result complements the knowledge on several AICAR's off-target effects, which previously has included inhibition of FBP1 in the liver²⁴¹ and glycogen phosphorylase in muscle²⁴². In most previous studies the transcripts modulated by AMPK have mostly been identified upon treatment with AICAR^{139,243,244}, mainly due to lack of specific direct AMPK activators and AMPK knockout models. Our data underline the importance for future studies to utilize activators that bind AMPK at the ADaM-site (distinct from the AMP ones, as 991) and include AMPK knockout models as gold standard controls in the experimental design. It may be necessary to revisit the work that has previously implicated AMPK in a number of transcriptional processes, in studies that have used AICAR and lacked AMPK knockout cell lines/models.

Pathways and transcription factors modulated by AMPK

We furthermore explored the dataset of AMPK-regulated transcripts in order to determine which cellular processes were specifically modulated by AMPK. More pathways were significantly enriched in the hepatocyte dataset compared to the MEFs dataset (14 and 5, respectively), suggesting that a broader spectrum of intracellular processes are impacted by 991-treatment in primary hepatocytes. These data challenge the use of immortalized cell lines as models to monitor the role of AMPK, and potentially other proteins, in regulating gene expression. Given that cell lines have already undergone reprogramming events in order to allow for continuous sustained growth in cell culture, they may not represent the most physiologically-relevant model.

We performed a number of complementary analyses to identify pathways and potential transcription factors that mediate the effects of AMPK on gene expression. We identified genes related to the regulation of the transcription factor FOXO^{170,245} as upregulated in response to AMPK activation. This pathway has previously been shown to be regulated by AMPK, and may promote transcriptional programs related to antioxidant response and cell cycle control²⁴⁶. In addition, we discovered a number of transcripts associated with the SREBP-class of transcription factors that were upregulated following AMPK activation. SREBPs family comprises transcription factors which modulate lipid homeostasis by controlling the expression level of several key enzymes involved in synthesis of cholesterol, fatty acid and phospholipid²⁴⁷. SREBPs are present as inactive precursors anchored to the endoplasmatic reticulum membrane²⁴⁸. A decrease in sterol levels results in the cleavage of the transmembrane segment, thereby triggering the activation and nuclear translocation of active SREBPs^{249,250}. Notably, three isoforms exist (SREBP-1a, SREBP-1c and SREBP-2)²⁵¹ and are associated with distinct and specific gene expression programs. For instance, while SREBP-1a/-1c have been shown to regulate fatty acid synthesis²⁵², SREBP-2 has been linked to the modulation of cholesterol synthesis²⁵³. Previously, AMPK has been reported to directly phosphorylate both SREBP-1c and -2 precursors, repressing their processing towards an active form and therefore inhibiting the associated transcriptional programs¹⁶. In contrast, Esquejo *et al.* reported recently that treatment with an ADaM-binding site activator, PF-06409577, led to an increased expression level of SREBPs target genes¹³. Our microarray analysis supports the latest observations from Esquejo *et al.* since we could observe, and confirm by qPCR, an increase in the expression of genes controlled by active SREBPs. A possible explanation is that AMPK stimulation causes a decrease in cholesterol level and/or lipid species, which initiates the SREBPs proteolytic cleavage and consequent activation. Future studies are required to further investigate the molecular relationship within AMPK and SREBPs. In addition, given that AMPK controls lipid metabolism through ACC, HMG-CoA reductase, as well as SREBPs, it would be of major interest to perform lipidomics profiling in response to 991 (and using AMPK-KO models) to reveal how AMPK orchestrates hepatic lipid homeostasis.

5.2 *Flcn* and *Fnip*

Both *Flcn* and its interacting protein *Fnip1* showed an increased mRNA and protein expression (exclusively for FLCN) in both MEFs and primary hepatocytes in response to AMPK activation. *Flcn* encodes a tumor suppressor protein and mutations of this gene cause an autosomal dominant syndrome called Birt-Hogg-Dubé (BHD)²⁵⁴. The BHD predisposes patients to lung cysts, fibrofolliculomas and increased risk of developing kidney tumors. The function of FLCN has so far

been linked to a variety of cellular processes such as epithelial polarization²⁵⁵, autophagy²⁵⁶ and ciliogenesis²⁵⁷. However, the precise molecular mechanism linking the mutation of *Fln* to the BHD symptoms is still unclear and represents an intensive field of research.

Fln was of our particular interest because previous studies have proposed that FLCN could act as a negative regulator of AMPK^{216,237}. Indeed *Fln* knockout models (*i.e.* mice and *C. elegans*) reported a higher basal activity of AMPK compared to their WT counterparts^{216,217,237,258,259}. Interestingly, the capability of FLCN to repress AMPK has been proposed to account for the tumor suppressor role of this protein. In support of this hypothesis, a study from Yan *et al.* showed that in FLCN-null MEFs, active AMPK conferred a tumorigenic advantage via the activation of hypoxia-inducible factor- α (HIF α), responsible for the Warburg metabolic transformation²¹⁶. In contrast, a mouse model with adipose-tissue specific deletion of *Fln* was characterized by chronic hyperactivation of AMPK that induced, via PGC1 α /ERR α the up-regulation of mitochondrial biogenesis and activity in white and beige adipose tissues, protecting the mice from high fat diet-induced obesity²¹⁷. This suggests that there may be a complex and potentially tissue-specific role and association between FLCN and AMPK, which in different context can be beneficial or detrimental.

The function of FLCN is modulated by the interaction with the two paralogous proteins FNIP1 and FNIP2, which occurs via the FLCN c-terminal domain²⁶⁰. These two proteins are required for FLCN regulation, since mice carrying kidney-specific inactivation of both (but not of the single *Fnip1* or *Fnip2*) recapitulate the kidney-targeted FLCN-null mice phenotype²⁶⁰, which is characterized by the presence of cystic kidneys, elevated PGC1 α activity and mitochondrial biogenesis. Similar to *Fln*, there have also been previous reports linking the expression of *Fnip1* to the level of AMPK activity. FNIP1-null mice showed an increased AMPK activity at the basal level²⁶¹, which appeared to favor a switch to type I/slow-twitch fibers²⁶¹, due to an increased oxidative capacity and mitochondria number. FNIP1-knockout mice also displayed enhanced γ 2-specific (but not γ 1-specific) activity in the myocardium of neonatal hearts, which led to cardiomyopathy and was associated with increased glycogen accumulation. Interestingly, this phenotype is similar to that reported in humans with cardiac gain-of-function mutations in AMPK γ 2²³⁵. It should be noted that both γ 1- and γ 2-specific AMPK activity in hepatocytes was comparable between WT and FNIP1-knockout mice, again highlighting cell-/tissue-specific regulatory relationship between FNIP1 and AMPK.

Previous studies showed that FNIP1/2 can directly interact with AMPK, mediating its binding to FLCN^{236,262}. In the present study, we performed FLCN, FNIP1 and AMPK co-

immunoprecipitation experiments following treatment of cells with or without 991. We were able to demonstrate binding between FLCN and FNIP1, however, we did not observe any detectable interaction between FNIP1 or FLCN and AMPK itself (Appendix Figure 6). This discrepancy may be due to the fact that previous studies used particular immortalized cell lines (*i.e.* HEK293) and were based on overexpression of the proteins of interest. Baba *et al.* reported that both FLCN and FNIP1 could be directly phosphorylated by AMPK. Ser62 was proposed as an AMPK-regulated phosphorylation site on FLCN, promoting the interaction within FLCN, FNIP and AMPK²⁶³. To investigate whether Ser62 on FLCN is an AMPK-regulated phosphorylation site, we generated a phospho-specific antibody in-house. Following confirmation of the antibody specificity with Ser62Ala mutant as control (Appendix Figure 7A), we performed western blot analysis on immunoprecipitated endogenous FLCN from U2OS AMPK-WT or AMPK-KO cells treated with vehicle or 991. Our data showed no detectable differences in Ser62 phosphorylation across these conditions (Appendix Figure 7B), suggesting that the phosphorylation site Ser62 may not be regulated by AMPK in this cell line and context (pharmacological stimulation with 991). Furthermore, to evaluate the presence of additional AMPK-regulated phosphorylation sites, we performed a phospho-proteomic analysis on ectopically expressed FLCN in the presence or absence of 991. Based on our pilot results, we could not identify any additional candidate AMPK-dependent phosphorylation site on FLCN. Further work may be required to identify potential AMPK phosphorylation sites on FLCN (*data not shown*).

Flcn and *Fnip* as transcriptional targets of AMPK

Our transcriptome profiling experiments allowed us to identify *Flcn* and *Fnip1* within the 49 commonly regulated transcripts following 991 treatment in AMPK-WT MEFs and primary hepatocytes. By monitoring the mRNA levels longitudinally (up to 24 h) upon AMPK stimulation, we observed a consistent increase of *Flcn* and *Fnip1* in MEFs AMPK-WT. In the case of FLCN this up-regulation corresponded to an enhanced protein content. Moreover, we could confirm the conservation of this transcriptional program across species, by measuring the increase of *flcn* and *fnip2* mRNA level in zebrafish muscle following physiological activation of AMPK, achieved through an acute bout of swimming exercise. The role of AMPK as mediator of the transcripts up-regulation was supported by the significantly compromised up-regulation of both *Flcn* and *Fnip2* in *prkaa1/prkaa2* DKO zebrafish.

Additional evidence of a conserved increase of *Flcn*, *Fnip1* and *Fnip2* in response to AMPK stimulation comes from a comparative analysis which we performed across our data sets and the ones recently published by Cokorinos *et al.*. In their study, the authors treated WT mice with the

ADaM binding drug PF-739, which can activate both β 1- and β 2- containing complexes, similarly to 991¹². They performed a transcriptome profiling by RNA-sequencing on gastrocnemius muscle either 4 h after a single oral dose or following 32 days of daily PF-739 treatment. Strikingly we observed that *Flcn* and *Fnip2* are the only two common transcripts across the data sets originated from MEFs and primary hepatocytes 991-treated, and skeletal muscle collected 4 h or 32 days of dosage with PF-739 (Figure 19). Interestingly *Fnip1*, which we detected up-regulated upon 991 treatment, was also shown to increase in muscle, after 32 days of treatment with PF-739 (Figure 19). We cannot exclude that the mRNA increase observed in response to PF-739 is AMPK-dependent, since a knockout was absent in the experiment.

To the best of our knowledge, we report here for the first time an increase of *Flcn* and *Fnip1/2* transcripts following AMPK activation. Our data complement the existing literature regarding these genes, showing for the first time an additional layer of regulation exerted by AMPK on *Flcn* and *Fnip1/2* at the transcriptional level. Considering the previously suggested role of FLCN and FNIP1/2 as negative regulators of AMPK, one could wonder whether AMPK is promoting the increase of its own regulators in a feedback loop. This possibility together with the functional and physiological significance of this potential cross-regulation will require future studies to be elucidated.

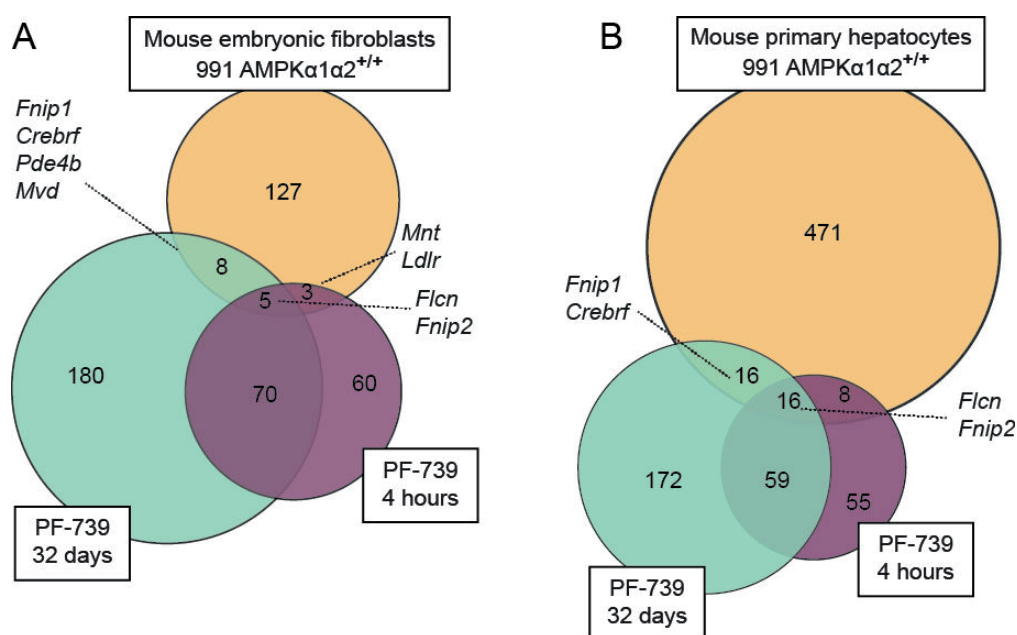


Figure 19. Venn diagrams comparing different datasets of AMPK-regulated genes.

Venn diagrams showing the comparison of genes regulated in muscle by 4 h (purple) or 32 days (green) of treatment with PF-739 and 991 treatment in MEFs (A) or primary hepatocytes (B). The moderated *P*-value was set at 0.05 and a fold-change cutoff of 1.3 was applied. A note should be made to clarify the different total number of 991-regulated transcripts in the Venn diagrams in Figure 14 and in Figure 19. In Figure 14 the graphs were produced considering the Affymetrix probesets, while in Figure 19 we took into account the gene name, a necessary conversion in order to compare data originated from microarray and RNA-sequencing studies.

6 Results, part II: TFEB is regulated by AMPK and mediates the increase of *Flcn*

6.1 An AMPK-TFEB/3 axis mediates the increase of *Flcn*

Following our results showing that AMPK can modulate mRNA and protein expression of *Flcn*, we studied the *Flcn* promoter to identify which transcription factor(s) may mediate its AMPK-dependent increase. To do this, we measured the luciferase activity associated with *Flcn* promoter sequences of various lengths (*i.e.* 8000, 6000, 1200, 200, 150, 100 and 50 bp) upstream of the predicted transcription start site (TSS), in response to 991 stimulation. The promoter activity was measured in MEFs AMPK-WT and AMPK-KO transiently transfected with the constructs expressing the reporter under various lengths of promoter sequences. Subsequently, these cells were stimulated for 12 h with 991 or vehicle (DMSO) and the promoter/luciferase activity was measured. Overall, the 991-treatment induced an increase in promoter activity compared to vehicle stimulation only in AMPK-WT cells, whereas it did not produce any significant effect in AMPK-KO MEFs. Figure 20A shows that the response to 991 in AMPK-WT cells led to a comparable promoter activity with various promoter lengths from 8000 to 150 bp. A significantly impaired response to 991 stimulation was only detected when removing the sequence located between 150 and 50 bp upstream of the TSS. Consequently, to identify the transcription factor(s) regulating *Flcn* expression we performed a bioinformatic analysis searching for binding site(s) in the 150 bp upstream of the TSS, as this region appeared to be crucial to ensure a response to AMPK activation. In the region of interest, we detected a CLEAR-motif binding site in the position -40 with respect to the TSS. The CLEAR-motif is recognized by members of the MiT family¹⁷⁸, which includes the transcription factors TFEB and TFE3. This finding corroborates the results of our transcription factor analysis, where TFEB was predicted as a candidate (chapter 4 - Results, part I). Furthermore, both TFEB and TFE3 are involved in the regulation of lysosomal gene expression, which is a pathway that emerged from our transcriptome analysis in both MEFs and primary hepatocytes (chapter 4 - Results, part I). To investigate the role of this promoter site, the predicted TFEB and TFE3-binding motif was subjected to mutagenesis. Figure 20B shows that the mutation of four bases located in the CLEAR-motif led to a reduction of around 50% in the promoter response to AMPK-activation. This result was reproducible with two different promoter lengths, 1200 and 100 bp, suggesting that this motif potentially represents a crucial element mediating AMPK regulation of *Flcn* gene transcription.

To assess whether AMPK controls changes in *Flcn* via TFEB/3, we took advantage of MEFs deficient for both transcription factors (TFEB/3-KO)²⁰⁵, since a functional redundancy has been reported for TFE3 and TFEB¹⁹¹. TFEB/3-WT and TFEB/3-KO MEFs were treated with vehicle (DMSO), 991 or AICAR and the mRNA as well as protein levels of *Flcn* were measured. qPCR analysis was performed to compare mRNA expression levels after 4, 12 or 24 h of treatment, and the results showed that there was a significant increase in expression upon AMPK activation solely in TFEB/3-WT cells (Figure 21A). Next, western blot analysis (Figure 21B) was performed after treatment for 24 or 36 h. After treatment of TFEB/3-WT cells with both 991 and AICAR, we observed an increase in FLCN at both time points. Interestingly, this increase in FLCN expression in response to AMPK activation was completely abolished in the TFEB/3-KO MEFs. Importantly, we confirmed the absence of protein expression of both transcription factors in the TFEB/3-KO cells and that these cells had normal AMPK activation as monitored by phosphorylation of ACC. Taken together, this evidence strongly supports the existence of an AMPK signaling cascade that can lead to the up-regulation of *Flcn* in a TFEB/3-dependent manner.

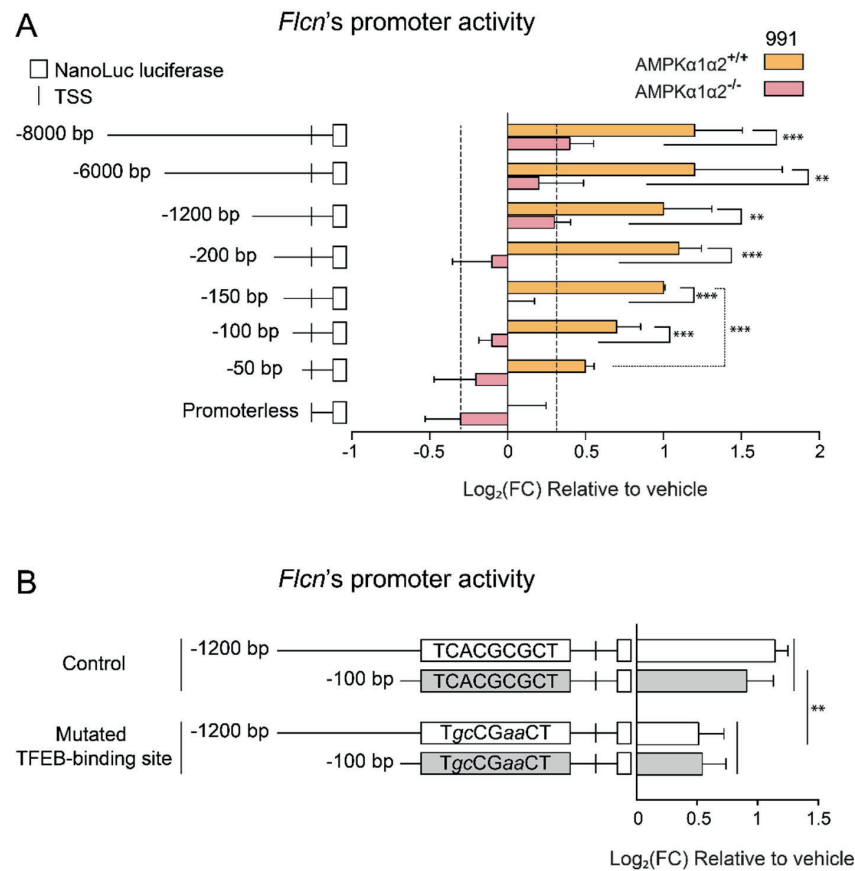


Figure 20. *Flcn* promoter activity in response to 991 treatment.

(A) Schematic representation of *Flcn*-NanoLuc luciferase reporter plasmid and the correspondent luciferase activity profile. Several lengths of *Flcn* promoter region (8000, 6000, 1200, 200, 150, 100 and 50 bp) were inserted upstream of the NanoLuc luciferase reporter gene. The constructs, along with a firefly luciferase plasmid which served as internal control, were transiently transfected into MEFs AMPKα1α2^{+/+} or AMPKα1α2^{-/-}. Cells were then treated with vehicle (DMSO) or 30 μM 991. Values were first normalized by transfection efficiency, and then represented as log₂ fold-change ± SD, relative to control (vehicle-treated cells) (n=6). Dashed lines indicate log₂ fold-change threshold of ±0.37. Data were analyzed by two-way ANOVA with the factors of genetic background, promoter length and interaction. Significance of the genetic background is indicated, *** *P*-value < 0.001, ** *P*-value < 0.01. (B) MEFs control were transiently transfected with *Flcn*-NanoLuc luciferase (-1200 or -100 bp) control or with a mutation on TFEB binding site (position -40 bp), together with a firefly luciferase plasmid. Afterwards, cells were treated as in the previous point. Values were first normalized by transfection efficiency, and then represented as log₂ fold-change ± SD, relative to control (vehicle-treated cells) (n=6). Data were analyzed by two-way ANOVA with the factors of promoter length, TFEB binding site status (control or mutated) and interaction. Significance of the TFEB binding site status is indicated, ** *P*-value < 0.01.

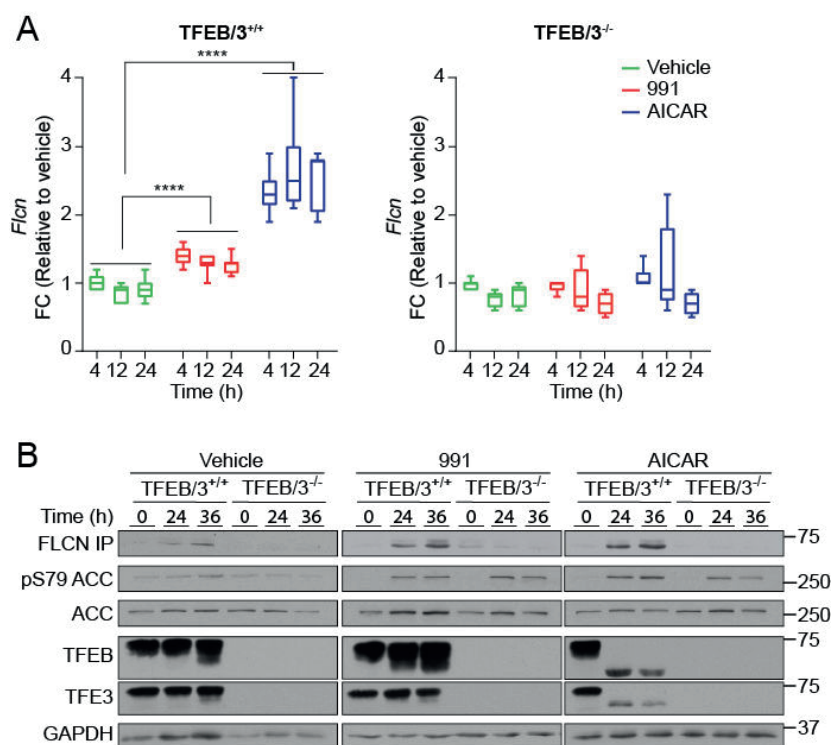


Figure 21. TFEB/3 mediate *Flcn* increase after AMPK activation.

(A) mRNA levels of *Flcn* in MEFs TFEB/TFE3 control (TFEB/3^{+/+}) or knockout (TFEB/3^{-/-}), treated with 10 μ M 991 or 2 mM AICAR for 4, 12 and 24 h. Data are presented with box-and-whisker plot (min to max) of values normalized to control (vehicle-treated cells at 4 h). Data were analyzed by two-way ANOVA with the factors of time, treatment and interaction (n=9). Significance of the treatment factor is indicated, **** *P*-value < 0.0001. (B) MEFs TFEB/3^{+/+} and TFEB/3^{-/-} were lysed after 0, 24 and 36 h of treatment with 10 μ M 991 or 2 mM AICAR. Laemmli extracts (20 μ g) were subjected to western blot analysis using the indicated antibodies. FLCN was immunoprecipitated (IP) from 500 μ g of cell lysate with 1 μ g of anti-Folliculin antibody. Images are representative of n=2.

6.2 AMPK activation induces TFEB nuclear translocation independently of mTOR

Like many transcription factors, intracellular localization of TFEB and TFE3 can be controlled via post-translational modifications. Previously, it has been reported that TFEB and TFE3 are found in a phosphorylated form predominantly in the cytoplasm and dephosphorylated form mostly in the nucleus²⁶⁴. These two forms can be distinguished to a certain degree by monitoring a band shift on a western blot, due to the differing molecular weight and electrophoretic properties of the two species. We first performed experiments to determine whether the activation of AMPK would alter the phosphorylation status of TFEB and TFE3, and as a consequence its cytoplasmic/nuclear distribution (Figure 22A). We treated AMPK-WT and AMPK-KO MEFs with 991 or AICAR for 1 h and generated cytosolic and nuclear fractions/extracts prior to western blot analysis. We confirmed successful separation of the nuclear and cytosolic extracts by detecting the presence of Lamin A/C in the nuclear extract, and both GAPDH and ACC in the cytosolic extracts. Under vehicle-treated conditions, only the phosphorylated form of TFEB was detected in both the nuclear and cytosolic extracts, as evidenced by the presence of the higher molecular weight (phosphorylated) species.

Interestingly, after treatment with 991 or AICAR we observed a clear band shift of TFEB to the lower molecular weight species and enrichment of this dephosphorylated form in the nuclear extracts of AMPK-WT MEFs (Figure 22A). Importantly, this increase in dephosphorylated TFEB in the nucleus was not observed in MEFs lacking AMPK. Taken together, this suggests that activation of AMPK by both 991 and AICAR leads to dephosphorylation of TFEB and nuclear translocation or sequestration of this form within the nucleus in an AMPK-dependent manner. In contrast to TFEB, the band shift of TFE3 is less clear in this western blot analysis, but there appears to be a slight but complete down-shift of the TFE3 band present in cytosolic and nuclear extracts of AMPK-WT MEFs treated with 991 and AICAR. Importantly, this lower molecular weight species does not appear in AMPK-KO cells in response to these activators (Figure 22A). This suggests that AMPK may have a more profound effect on promoting the dephosphorylation of TFE3, since this species is the only one detected in AMPK treated cells in both cytosolic and nuclear extracts.

During the course of this study, a report was published implicating AMPK in the nuclear translocation of TFEB during endoderm lineage specification. In that study, the authors reported that the ability of AMPK to promote nuclear translocation of TFEB occurred in a manner dependent on mTORC1¹⁷⁶. Therefore, we investigated the possibility that the effects of AMPK on TFEB nuclear translocation that we have observed in MEFs is mediated through AMPK regulation

of mTORC1. Thus, we designed experiments to monitor the translocation of TFEB in response to AMPK activation or in the presence of inhibitors of the mTORC1 signaling cascade, Rapamycin and Torin-2 (Figure 22B and C, respectively). Rapamycin forms a complex with FK506-binding protein-12 (FKBP12) which then specifically binds to mTORC1 allosterically inhibiting it²⁶⁵, whereas Torin-2 acts as an ATP-competitive drug, potent and selective towards both mTORC1 and mTORC2²⁶⁶.

Firstly, we tested the effect of 991 and AICAR alone on the AMPK and mTORC1 pathways after treatment of AMPK-WT and AMPK-KO MEFs, for 1 and 4 h (Figure 22B). AMPK activation was achieved after treatment with both 991 and AICAR, as shown by the increased phosphorylation of its activation site and its substrate ACC. As AMPK is well known to regulate and inhibit the mTORC1-signaling cascade, we compared the phosphorylation of some mTOR downstream substrates, p70-S6 kinase 1 (p70 S6K) and S6 ribosomal protein (S6RP), in response to 991 and AICAR. Whilst treatment with both drugs did not lead to a complete inhibition of phosphorylation of mTORC1 substrates after 1 h of treatment, only AICAR caused a clear reduction of the mTORC1-signaling cascade after 4 h of treatment, which occurred in an AMPK-dependent manner. Interestingly, already after 1 h of AMPK stimulation and despite the absence of a reduction of mTORC1 signaling, we observed the TFEB band shift. This suggests that the ability of AMPK to modulate the dephosphorylation, and likely nuclear translocation, of TFEB can occur in absence of AMPK's effect on the mTORC1-signalling cascade.

We next tested whether direct inhibition of mTORC1 by compounds alone affected the band shift of TFEB. Rapamycin inhibited the mTORC1 signaling cascade at all doses and at both time points, as demonstrated by the reduced phosphorylation profiles of the downstream targets P70 S6K and S6RP (Figure 22B). We did not detect a TFEB band shift after treatment with Rapamycin alone in either AMPK-WT or AMPK-KO MEFs, suggesting that inhibition of the mTORC1 pathway alone is not sufficient to mediate TFEB dephosphorylation. Given that Torin-2 (which will be referred to as Torin) mechanism of action for inhibiting the mTORC pathway is distinct from Rapamycin, we also tested the effect of this compound on the TFEB band shift. Figure 22C shows the consequences of Torin (5 and 10 nM), 991 and AICAR on mTORC1 and AMPK pathways after 1 or 4 h of treatment in MEFs. Torin inhibited the mTORC1 cascade and promoted the presence of a very small lower band shift on TFEB at the 10 nM dose, although this effect was much less pronounced compared to the effect of both 991 and AICAR treatment (Figure 22C). Taken together, our data suggest that inhibition of mTOR by two different compounds resulted in little or no effect on TFEB dephosphorylation.

As next step, in order to determine whether the presence of active mTOR is required for the AMPK-dependent TFEB translocation, we inhibited the mTOR pathway prior stimulation of AMPK (Figure 22D). We pre-treated MEFs AMPK-WT and AMPK-KO with vehicle, Rapamycin or Torin for 1 h and subsequently added either vehicle or 991 for an additional hour. Figure 22D illustrates the inhibition of mTORC1 pathways in cells pre-treated with Rapamycin or Torin, as well as the activation of AMPK in stimulated wild-type cells. The results show that the pre-treatment did not cause any significant variation in terms of TFEB band shift pattern, suggesting that the activity of mTOR is not having any impact on the AMPK-promoted dephosphorylation of TFEB.

In order to get more insights into the mechanism mediating TFEB nuclear translocation, we raised a phosphorylation site-specific antibody (pS142) for one of the key residues known to influence TFEB localization. To validate the antibody's specificity, Flag-tagged TFEB (wild-type or mutated to alanine at the residue 142) were over-expressed in COS1 cells. Afterwards, the ectopically expressed proteins were immunoprecipitated and western blot analysis was performed to monitor total and Ser142-phosphorylated TFEB. We confirmed that this antibody specifically detected the phosphorylation of TFEB in the WT but not the S142A mutant TFEB protein (Appendix Figure 8A). Subsequently, this antibody was used to monitor the (de)phosphorylation status of TFEB in cells in response to various treatment conditions. As shown in Figure 22B, C and D, this antibody confirmed the dephosphorylated status of TFEB at this residue correlating to the previously described band shift.

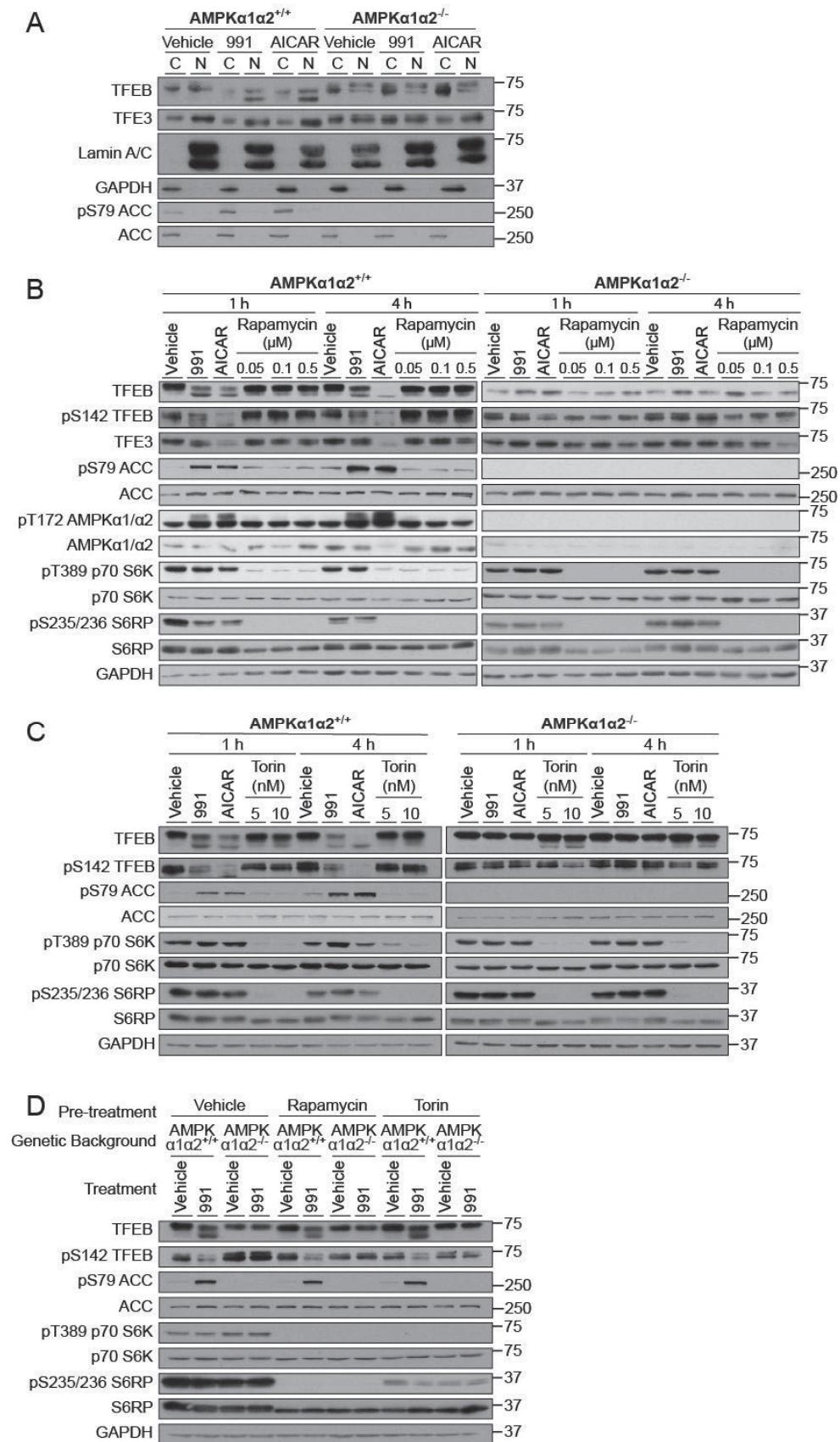


Figure 22. AMPK regulation of TFEB in mouse embryonic fibroblasts.

(A) MEFs AMPK α 1 α 2^{+/+} or AMPK α 1 α 2^{-/-} were stimulated with vehicle (DMSO), 10 μ M 991 or 2 mM AICAR for 1 h. The cytoplasmic and nuclear fractions were separated, accordingly to the NE-PER kit manufacturers' instruction. The lysates (20 μ g) were used for a western blot analysis of the indicated proteins. (B) Western blot analysis of the transcription factors TFEB and TFE3 together with signaling components of mTOR and AMPK pathways. Cells were treated with AMPK activators (10 μ M 991 or 2 mM AICAR) or different doses of the mTOR inhibitor Rapamycin (0.05, 0.1 and 0.5 μ M) for 1 or 4 h. Cell lysates (20 μ g) were separated by SDS-PAGE and western blot was performed using the indicated antibodies. (C) The experiment was performed as described in the previous point, however Torin (5 nM or 10 nM) was used as mTOR inhibitor. (D) MEFs AMPK α 1 α 2^{+/+} or AMPK α 1 α 2^{-/-} were pre-treated for 1 h with vehicle (DMSO), 0.05 μ M Rapamycin or 5 nM Torin. After 1 h cells were stimulated for an additional hour with vehicle (DMSO) or 10 μ M 991. Laemmli extracts (20 μ g) were subjected to western blot analysis using the indicated antibodies. Figures are representative of n=2.

6.3 In mouse hepatocytes, the stimulation of AMPK leads to TFEB nuclear translocation independently of mTOR

As mention above, previous studies have reported that AMPK can regulate TFEB nuclear translocation through its ability to inhibit the mTORC1 signaling pathway. Our work with MEFs provided a more detailed mechanistic insight into the AMPK-TFEB relationship and potentially challenges the previous observation that the ability of AMPK to mediate TFEB nuclear translocation is mTORC1-dependent. In an attempt to substantiate our new findings, we used a more physiologically relevant cellular model and performed parallel experiments in mouse primary hepatocytes. Firstly, we compared the effect of three AMPK activators, 991, AICAR and also C13, a recently identified $\alpha 1$ selective AMPK activator²⁶⁷, on the mTORC1 signaling pathway and TFEB/3 band shifts in AMPK-WT and AMPK-KO hepatocytes (Figure 23A). As previously shown, treatment of hepatocytes for 1 h and 4 h with AMPK activators increased the activity of AMPK in WT but not KO hepatocytes. Importantly, we could also demonstrate that as expected Rapamycin inhibited the mTORC1 signaling at both time points. Consistent with the results observed in MEFs, activation of AMPK by all three compounds resulted in a complete band shift of TFEB and TFE3 in AMPK-WT hepatocytes (Figure 23A). These effects were completely dependent on the presence of AMPK for 991 and C13, although there appears to be a small effect of AICAR on TFE3 band shift in AMPK-KO hepatocytes.

In contrast to activation of AMPK, inhibition of mTORC1 after treatment of hepatocytes with Rapamycin did not have any effect on phosphorylation status of TFEB and TFE3, again consistent with our previous observations in MEFs. AICAR and C13 diminished the phosphorylation of mTORC1 targets after 1 h and completely abolished it after 4 h suggesting that activation of AMPK by these activators can inhibit the mTORC1-signaling pathway. Unexpectedly, C13 treatment still induced inhibition of mTORC1 signaling in AMPK-KO hepatocytes, suggesting for the first time that C13 has effects in cells independent of AMPK. Based on the fact that inhibition of mTORC1 with Rapamycin alone has no effect on the TFEB and TFE3 band shift, it is unlikely that the ability of AICAR and C13 to induce TFEB/TFE3 dephosphorylation is as a consequence of their inhibition of mTORC1. Moreover, 991 activation of AMPK did not appear to alter mTORC1 cascade, although this activator can still induce the TFEB and TFE3 band shift to a similar extent to AICAR and C13 (Figure 23A). Taken together, these data strongly support the results generated in MEFs that AMPK can induce the band shift, influencing their phosphorylation status, in TFEB and TFE3 independently of mTORC1. One particular point to note is to approach

studies using AICAR and C13 alone with caution since they display some AMPK-independent effects in cells, likely as a consequence of the non-specific nature of these activators (AMP-mimetics).

One important consideration when performing experiments in the AMPK-KO hepatocytes is that the lack of effect on the band shift of TFEB does not result from a loss of ability of these cells to regulate translocation of TFEB to the nucleus. To address this potential concern, we performed experiments in AMPK-KO hepatocytes in which we rescued the expression of AMPK by infection with an adenovirus containing a sequence for the $\alpha 2\beta 1\gamma 1$ complex (Figure 23B). AMPK-WT and AMPK-KO hepatocytes were used as controls. Figure 23B shows that the subunits expression was successfully restored through viral infection. Importantly, treatment of cells with 991 resulted in a similar level of AMPK activation in AMPK-KO cells infected with $\alpha 2\beta 1\gamma 1$ complex compared to AMPK-WT cells. Interestingly, 991 activation of AMPK led to a complete band shift of both TFEB and TFE3 in AMPK-WT and AMPK-KO $\alpha 2\beta 1\gamma 1$ -complex rescued hepatocytes (Figure 23B). Taken together, these data demonstrate that the effect of 991 on inducing the lower band shift of TFEB and TFE3, was dependent on AMPK expression/activity in hepatocytes. Finally, we generated nuclear and cytosolic fractions of hepatocytes AMPK-WT in order to monitor the cellular distribution of TFEB in response to AMPK activation (Appendix Figure 8B). Our method for separating the cytosolic and nuclear fractions was successful as indicated by the detection of H3 in the nuclear fractions and pACC in the cytosolic fractions. Activation of AMPK by 991 resulted in increases in pACC and this was associated with an enrichment of TFEB in the nuclear fractions.

Taken together, our data obtained from both mouse primary hepatocytes and MEFs, support a role for AMPK to promote a band-shift at least partly through dephosphorylation of TFEB and TFE3, which results in the nuclear translocation of TFEB. Importantly, this effect does not appear to be mediated by inhibition of the mTORC1 signaling cascade.

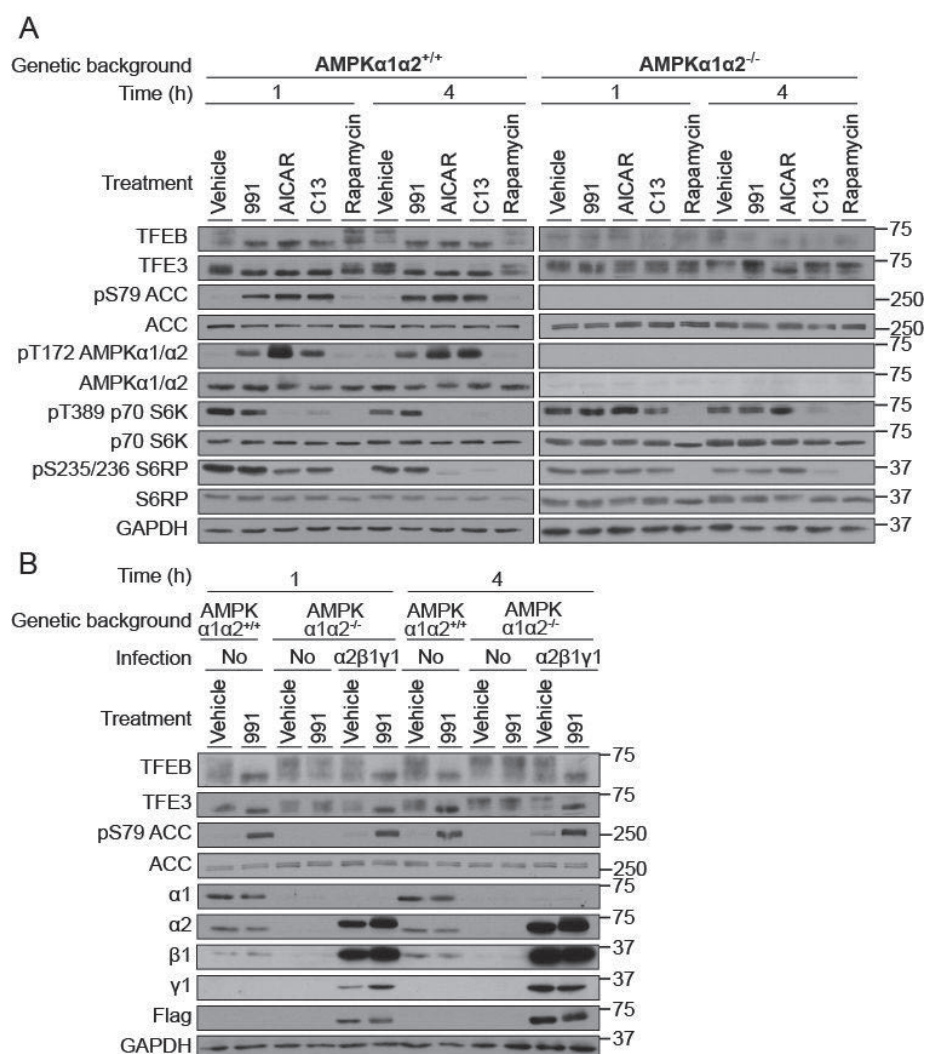


Figure 23. AMPK regulation of TFEB in mouse primary hepatocytes.

(A) Western blot analysis of the indicated proteins was performed on primary hepatocytes lysates AMPK $\alpha 1\alpha 2^{+/+}$ or AMPK $\alpha 1\alpha 2^{-/-}$. Plated cells were treated with 10 μ M 991, 300 μ M AICAR, 30 μ M C13 or Rapamycin 0.05 μ M, for 1 or 4 h. (B) Primary hepatocytes were isolated from AMPK $\alpha 1\alpha 2^{-/-}$ mice. Cells were plated and 4 h later they were either non-infected or co-infected (MOI of 3) with three adenovirus, in order to rescue the expression of the three subunits of AMPK ($\alpha 2$, $\beta 1$ and $\gamma 1$). 16 h post infection, the primary hepatocytes were treated for 1 h with vehicle (DMSO) or 10 μ M 991. Cell lysates (20 μ g) were used for western blot analysis with the indicated antibodies.

6.4 TFEB nuclear localization following 991-treatment is conserved in zebrafish

In the final part of this study, we wanted to understand if the nuclear translocation of TFEB in response to AMPK activation is present in zebrafish. Unfortunately, it was not possible to perform a western blot on endogenous TFEB in zebrafish due to the lack of suitable antibodies. We therefore took advantage of a zebrafish model, which has been generated in-house expressing a ZsGreen-tagged version of TFEB, as well as mCherry associated to a NLS, both under the actin alpha cardiac muscle 1b (*actc1b*) promoter, which drives gene expression in skeletal muscle. As previously discussed (section 4.5), zebrafish has major benefits, with one being the optical transparency of embryos and larvae²⁶⁸. Taking advantage of this feature, we can perform fluorescence-based confocal microscopy allowing us to monitor the translocation of TFEB into the nucleus in response to activation of AMPK.

Fluorescence based confocal microscopy was performed on embryos 3 days post fertilization (dpf), after treatment with vehicle (DMSO) or 991 for 24 h (Figure 24). Under basal conditions, the ZsGreen-tagged Tfeb is distributed throughout the entire cell likely due to cytosolic localization of Tfeb. In support of this, merging this image with the mCherry-NLS image shows that there is no clear nuclear localization of Tfeb. We previously confirmed that 991 can activate AMPK in zebrafish (data not shown). Under similar treatment conditions, we observed a change in the distribution pattern of ZsGreen-Tfeb going from a diffuse pattern throughout the cell, to forming puncta within the cell. Merging this image with the mCherry-NLS shows that these punctae superimpose with the image from the mCherry-NLS signal. This suggests that treatment of zebrafish with 991 leads to the translocation of ZsGreen-Tfeb to the nucleus (Figure 24). Taking everything together, our findings in cells and the whole organism, zebrafish, support the hypothesis that activation of AMPK leads to dephosphorylation and nuclear translocation of Tfeb, where it can regulate gene expression. We provide strong evidence that this effect is likely completely independent of the ability of AMPK to inhibit the mTOR signaling cascade. Further work will be required to explore the AMPK-TFEB axis in more detail particularly in the context of the role of AMPK in regulating the lysosome and what new therapeutic opportunities emerge for the treatment of metabolic disorders.

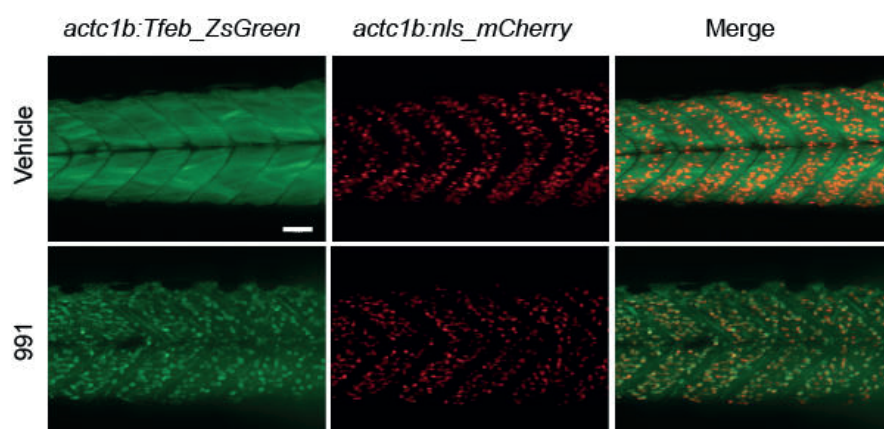


Figure 24. AMPK activation promotes TFEB nuclear translocation in zebrafish larvae.

Tg(actc1b:tfeb-ZsGreen);Tg(actc1b:nls-mCherry) embryos at 3 dpf were treated with 10 μ M 991 or vehicle (DMSO) for 24 h. Embryos were mounted live in water containing 0.016% tricaine and imaged with ImageXpress confocal system at 20X magnification, the scale bar corresponds to 50 μ m.

7 Discussion, part II

AMPK promotes TFEB/3 nuclear translocation independently of mTORC1

The cellular localization and activity of TFEB are primarily regulated by its phosphorylation status. Two serine residues, Ser142 and Ser211, in the TFEB have mainly been proposed to play a key role in determining its subcellular localization^{178,200}. When both sites are phosphorylated, TFEB is kept inactive in the cytosol, while mutation of either Ser142 or Ser211 to non-phosphorylatable alanine residue rendered TFEB constitutively active through keeping it within the nucleus. mTOR and ERK2 are the main protein kinases known to phosphorylate TFEB under nutrient-rich conditions (supplemented cells with conventional cell culture medium) in most cell types. AMPK inhibits mTOR through multiple mechanisms²⁶⁹⁻²⁷¹, and it has recently been reported that AMPK controls endolysosomal function through suppression of mTOR and its subsequent regulation of TFEB¹⁷⁶. Therefore, we initially hypothesized that 991- or AICAR-induced activation of TFEB, via dephosphorylation and nuclear localization, is mediated through the AMPK-dependent inhibition of mTOR. Contrary to our hypothesis, we observed that acute treatment with a specific AMPK activator, 991^{26,61}, promoted TFEB dephosphorylation in the absence of detectable inhibition of mTOR (as judged by phosphorylation of p70 S6K and S6RP) in primary hepatocytes. In a previous study, it has been shown that phosphorylation of TFEB at Ser142 represents a Rapamycin-resistant, but Torin-sensitive site²⁰⁰. In line with this, we observed that the Ser142 phosphorylation was not affected by Rapamycin. However, in contrast to the previous observation, Torin displayed only a marginal effect on TFEB dephosphorylation (*i.e.* appearance of a minor faster-migrating form of the total TFEB and reduced Ser142 phosphorylation), and notably this was not only observed in WT, but also in AMPK-KO MEFs. Collectively, in MEFs and primary hepatocytes, a) we have demonstrated that acute inhibition of mTOR (*i.e.* 1-4 h) does not modulate TFEB phosphorylation, and b) 991-induced dephosphorylation of TFEB is unlikely to be mediated through AMPK-dependent suppression of mTOR. However, it would be important to assess if other phosphorylation sites (*e.g.* Ser211, Ser138), which are proposed to play key roles for cellular distribution of TFEB²¹⁴, are regulated upon AMPK activation.

The mechanism by which AMPK dephosphorylates and activates TFEB is unknown. It has been demonstrated that nutrient deprivation induces the release of lysosomal Ca^{2+} through the Ca^{2+} channel MCONL1. This activates calcineurin, which binds to and dephosphorylates TFEB, thus

promoting its nuclear localization and induction of autophagy²⁰⁴. It would be interesting to determine if AMPK-mediated activation of TFEB regulates the catalytic activity of calcineurin and/or the interaction between TFEB and calcineurin. It has also been shown that nutrient/glucose deprivation-induced AMPK activation regulates lysosomal and autophagy gene expression through phosphorylation at Ser659 and nuclear localization of ACSS2²⁰⁶. Phosphorylated ACSS2 forms a complex with TFEB, which modulates lysosomal and autophagosomal genes by locally producing acetyl CoA for histone H3 acetylation in the promoter regions of these genes. Therefore, AMPK indirectly modulates the transcriptional activity of TFEB after its nuclear translocation via inhibition of mTOR in response to energy stress. Nonetheless, in the current study we found *Acss2* as one of the AMPK-dependent genes upregulated at mRNA levels in response to both 991 and AICAR. Whether this upregulation of *Acss2* is linked to an increase in its protein/phosphorylation levels needs to be determined.

Although TFEB is an established master regulator of lysosomal biogenesis^{188,197}, emerging evidence suggests that it also acts as key controller for various other cellular and metabolic responses, including lipid metabolism in liver¹⁸⁹, mitochondrial biogenesis in muscle¹⁹⁸, as well as modulation of the immune response²⁷². In support of this, we identified genes that are involved in lipid/cholesterol signaling and metabolism (*Acss2*, *Crebrf*, *Hmgcr*, *Ldlr*, *Lpin1*, *Msmo1*, *Pde4b*) and immunity (*Ifit1*, *Tollip*). It would be of interest to determine if these genes are regulated through the AMPK-TFEB axis, as we have shown for *Flcn*. The tumor suppressor FLCN, responsible for the BHD renal neoplasia syndrome, is an AMPK-interacting partner, which has recently been proposed to function as a negative regulator of AMPK^{216,258}. It has been reported that ablation of FLCN expression or loss of FLCN binding to AMPK cause constitutive activation of AMPK, which was associated with enhanced osmotic stress resistance and Warburg metabolic transformation. Notably, genetic inactivation of FLCN in adipose tissue led to a metabolic reprogramming characterized by enhanced mitochondrial biogenesis and browning of white adipose tissue²¹⁷. Mechanistically, adipose-specific deletion of FLCN results in induction of the PGC1 α transcriptional coactivator through relieving mTORC1-dependent cytoplasmic retention of TFE3²⁷³ and/or activation of AMPK²¹⁷. It has been shown that exercise promotes TFEB translocation into the myonuclei, which then regulates glucose/glycogen metabolism by controlling expression of glucose transporters, glycolytic enzymes, as well as pathways linked to glucose homeostasis¹⁹⁸. Moreover, muscle-specific overexpression of TFEB mimics the effects of exercise training and promotes metabolic reprogramming through induction of gene expression involved in mitochondrial biogenesis and function. We showed *in vivo* using zebrafish that exercise induces *Flcn* and *Fnip2* expression at least partially through an AMPK-dependent mechanism. Moreover,

we proved that activation of AMPK by 991 induces Tfeb translocation to the nucleus, suggesting that the increased gene transcription of *Flcn* and *Fnip2* observed after exercise are likely mediated through the ability of AMPK to promote Tfeb translocation in skeletal muscle. Whether FLCN mediates part of metabolic responses downstream of TFEB/3 or increased expression of FLCN functions as negative feedback loop to suppress AMPK to avoid its prolonged activation of AMPK is unknown.

In summary, we demonstrated in fibroblasts, hepatocytes, as well as at whole organism levels, *in vivo* using zebrafish, that pharmacological activation of AMPK promoted nuclear translocation of TFEB. This appeared to be through an apparent effect on dephosphorylation of TFEB, independent of mTORC1, and was associated with induction of a tumor suppressor FLCN through activation of its promoter activity. Future studies using gain-of-function models of FLCN in skeletal muscle and other tissues (*e.g.* liver) could reveal the physiological significance of the AMPK-TFEB-FLCN pathway.

8 Conclusion and future perspectives

8.1 General conclusion

In the studies covered in this thesis, we have investigated the effect and role that AMPK has on the regulation of gene expression, taking advantage of different classes of activators, and tested it in various AMPK loss-of-function models. Additionally, we identified novel AMPK-regulated transcripts/pathways and provided mechanistic insights into AMPK-dependent transcriptional responses through the regulation of TFEB.

In the first part of the study, we performed a transcriptome profiling of wild-type and AMPK-knockout MEFs and primary hepatocytes, which were treated with two distinct classes of AMPK activators, 991 and AICAR. This strategy allowed us to identify cell- and compound-specific transcriptional responses, clearly showing an important AMPK-independent effect of AICAR and a high specificity of 991. AICAR has been used for a number of decades as a valuable and powerful tool to investigate AMPK functions, and over 1,500 articles have been published during this period using AICAR as an activator of AMPK. Our research complements previous studies reporting off-target effects of this AMP-mimetic. Furthermore, our comprehensive transcriptome comparison of two activators acting with distinct mode of actions, highlights the importance of a) favoring drugs binding to the ADaM site and b) including knockout control in the experimental design. Moreover, our analyses allowed us to identify AMPK-regulated transcripts and pathways, pointing to a conserved enrichment of genes involved in the lysosomal pathway and regulated by TFEB.

In the second part of the study, we robustly characterized *Flcn* and its interacting protein *Fnip* as AMPK-dependent transcriptional targets. In particular, we showed that *Flcn*, which encodes the tumor suppressor and nutrient sensor FLCN, is upregulated in an AMPK- and TFEB/3-dependent manner. We provided compelling evidence that activation of AMPK promotes dephosphorylation of endogenous TFEB and its subsequent translocation into the nucleus, independently of the activity of mTORC1 (Figure 25). We confirmed in zebrafish that this AMPK-TFEB-FLCN axis is conserved and can be activated in response to physical exercise and pharmacological stimulation of AMPK *in vivo*.

In conclusion, we have revealed a key role of AMPK in regulating the TFEB-FLCN signaling pathway, and this may represent an important physiological pathway for regulating the lysosome, autophagy and other metabolic processes. Future work is required to elucidate the physiological

role of these events and whether they represent a desirable output in response to AMPK activation, by physiological or pharmacological means. Our results contribute to advance the understanding of the methodologies (*e.g.* drugs, models) used to investigate AMPK, while allowing us to reveal further insights on the regulation of gene expression by the kinase, which could occur in case of pharmacological activation for the treatment of metabolic diseases.

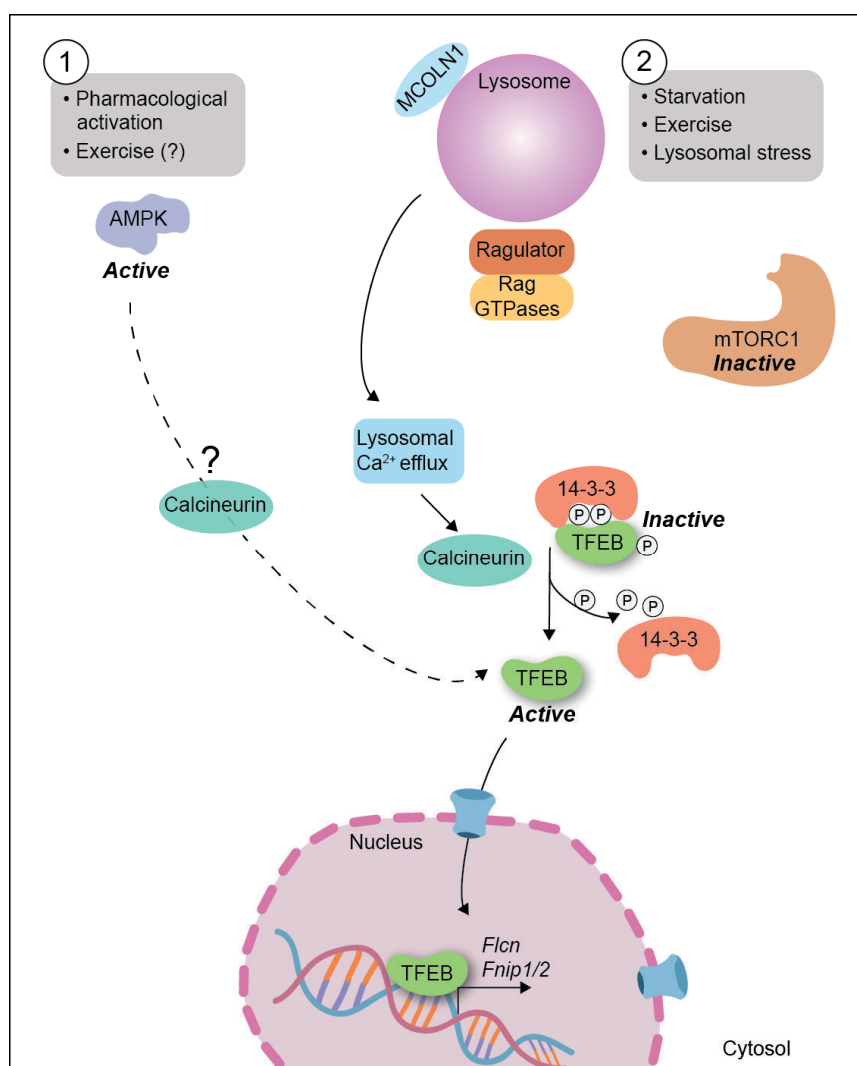


Figure 25. Schematic representation of TFEB regulation based on our results and hypothesis.

TFEB activation can be promoted via (1) the pharmacological activation of AMPK, in an mTORC1-independent manner, leading to an increased expression of *Flcn* and its interacting partners *Fnp1/2*. This novel mechanism complements the canonical model (2), where mTORC1 inhibition upon starvation, exercise or lysosomal stress, leads to a Ca^{2+} -dependent activation of the phosphatase calcineurin and the consequent dephosphorylation and nuclear translocation of the factor.

8.2 Future perspectives

In the work encompassed in this thesis, we discovered a novel link within AMPK and the transcription factors TFEB/3, which emerged as regulators of the tumor suppressors *Flcn*. We envisage future studies focusing on the two main questions raised by our results, regarding a) the mechanism responsible for AMPK-dependent regulation of TFEB/3 and b) the physiological relevance of this novel cascade. To answer point a), we would focus on characterizing how AMPK mediates the dephosphorylation event(s) of TFEB/3, allowing their nuclear relocalization. We showed in this study that Ser142 on TFEB loses its phosphorylation upon AMPK stimulation, however it still has to be determined if additional sites are involved and which phosphatases eventually enable this process. To discover further phosphorylation sites, we would perform a mass spectrometry experiment on ectopically-expressed TFEB in wild-type and AMPK knockout cells, treated with vehicle or the highly specific activator 991. To identify the phosphatase(s) regulating the translocation event, we would initially focus on the candidate calcineurin using well-validated pharmacological inhibitor (*e.g.* cyclosporine), as it was shown to modulate TFEB phosphorylation status²⁰⁴. Moreover, we would like to determine if AMPK-mediated dephosphorylation promotes dissociation of 14-3-3 adaptor proteins from TFEB.

To address point b), that is the physiological significance of the novel axis, we would first study the general AMPK-TFEB cascade and then focus on its specific role in the context of *Flcn* regulation. Initially, we would investigate, in cellular and *in vivo* models, if AMPK-dependent TFEB nuclear translocation could increase lysosomal activities, since these are well-established processes known to be regulated by TFEB¹⁷⁸. Importantly, confirming these hypotheses would suggest that AMPK activation could bring about beneficial effects in pathologies characterized by an accumulation of misfolded proteins (*e.g.* LSDs, Alzheimer's disease). Moreover, as TFEB activity in muscle was recently shown to control metabolic flexibility, favoring glucose and lipid utilization¹⁹⁸, we would try to understand whether AMPK contributes to this function of TFEB. In parallel, we would proceed at the generation of a knockout model with ablated *Flcn* expression, to explore the impact of this genetic modification onto signaling cascades (*i.e.* AMPK, mTOR, TFEB) and physiological settings, such as metabolism of glucose and lipids as well as lysosomal/autophagic flux.

9 Appendices

9.1 Personal contributions

I performed all the treatments in cell lines and the promoter activity assay, prepared and analyzed MEFs, zebrafish and hepatocytes samples. I contributed to the microarray and general data analysis and interpretation. I generated almost all the figures (except Figure 24) in the main and appendix results of the thesis. I contributed to the design of the experiments and to the writing of the manuscript with Prof. Sakamoto.

Dr. Civileto generated and performed experiments on the *tfeb-ZsGreen;nls-mCherry* double transgenic zebrafish.

Dr. Deak performed molecular cloning and mutagenesis on TFEB and *Fln* promoter.

Dr. Lefebvre contributed to the statistical analysis, performing ANOVA analysis fit to log-transformed data.

Sylviane Metairon executed the microarray and contributed to total mRNA preparation.

Dr. Parisi generated the AMPK *prkaa1^{-/-};prkaa2^{-/-}* zebrafish line and together we performed the fish exercise.

Dr. Raymond and I analyzed the microarray data.

Dr. Viollet and Dr. Foretz generated liver-specific AMPK KO mouse model and AMPK KO mouse embryonic fibroblasts. Dr. Foretz performed the hepatocytes isolation, viral infection, compound treatments and cell collection.

Prof. Sakamoto and Dr. Descombes supervised me and conceived the project, assisted by a) Dr. Viollet for the design of the hepatocytes study b) Dr. Bultot for the setup of the gene expression study and c) Dr. Gut for the zebrafish study design and interpretation of results.

9.2 List of co-authored articles

Collodet C, Foretz M, Deak M, Bultot L, Metairon S, Viollet B, Lefebvre G, Raymond F, Parisi A, Civiletto G, Gut P, Descombes P, Sakamoto K. AMPK promotes induction of a tumor suppressor FLCN through activation of TFEB independently of mTOR. *BioRxiv*. 2018 Dec 20. doi: <https://doi.org/10.1101/499921>. Preprint.

Ducommun S, Deak M, Zeigerer A, Göransson O, **Collodet C**, Madsen AB, Jensen TE, Viollet B, Foretz M, Gut P, Sumpton D, Sakamoto K. Chemical genetic screen identifies Gapex-5/GAPVD1 and STBD1 as novel AMPK substrates. *Cell Signal*. 2019 Feb 14. PMID: 30772465.

Kfoury A, Armaro M, **Collodet C**, Sordet-Dessimoz J, Giner MP, Christen S, Moco S, Leleu M, de Leval L, Koch U, Trumpp A, Sakamoto K, Beermann F, Radtke F. AMPK promotes survival of c-Myc-positive melanoma cells by suppressing oxidative stress. *EMBO J*. 2018 Feb 12. PMID: 29440228.

Lopez-Mejia IC, Lagarrigue S, Giral A, Martinez-Carreres L, Zanou N, Denechaud PD, Castillo-Armengol J, Chavey C, Orpinell M, Delacuisine B, Nasrallah A, **Collodet C**, Zhang L, Viollet B, Hardie DG, Fajas L. CDK4 Phosphorylates AMPK α 2 to Inhibit Its Activity and Repress Fatty Acid Oxidation. *Mol Cell*. 2017 Oct 19. PMID: 29053957.

Theret M, Gsaier L, Schaffer B, Juban G, Ben Larbi S, Weiss-Gayet M, Bultot L, **Collodet C**, Foretz M, Desplanches D, Sanz P, Zang Z, Yang L, Vial G, Viollet B, Sakamoto K, Brunet A, Chazaud B, Mounier R. AMPK α 1-LDH pathway regulates muscle stem cell self-renewal by controlling metabolic homeostasis. *EMBO J*. 2017 Jul 3. PMID: 28515121.

Bultot L, Jensen TE, Lai YC, Madsen AL, **Collodet C**, Kviklyte S, Deak M, Yavari A, Foretz M, Ghaffari S, Bellahcene M, Ashrafian H, Rider MH, Richter EA, Sakamoto K. A benzimidazole derivative small molecule 991 enhances AMPK activity and glucose uptake induced by AICAR or contraction in skeletal muscle. *Am J Physiol Endocrinol Metab*. 2016 Aug 30. PMID: 27577855.

9.3 Additional results

9.3.1 Materials & Methods

For the materials and methods regarding the main result sections and the majority of the appendix figures, we refer to the enclosed manuscript (appendix 9.4 - Manuscript published on BioRxiv). We include below additional information on materials and methods used solely for the appendix figures.

Materials

SiRNA targeting *Flcn* (D-050651-01 and D-050651-02) and *Fnip1* (D-063588-01 and D-063588-02) were purchased from Dharmacon. Scramble siRNA constructs were purchased from Sigma, namely MISSION siRNA Control (SIC001 and SIC002). Constructs were transfected using Lipofectamine RNAiMAX Transfection Reagent (13778075, ThermoFisher). General and specific cell culture reagents were obtained from Life Technologies.

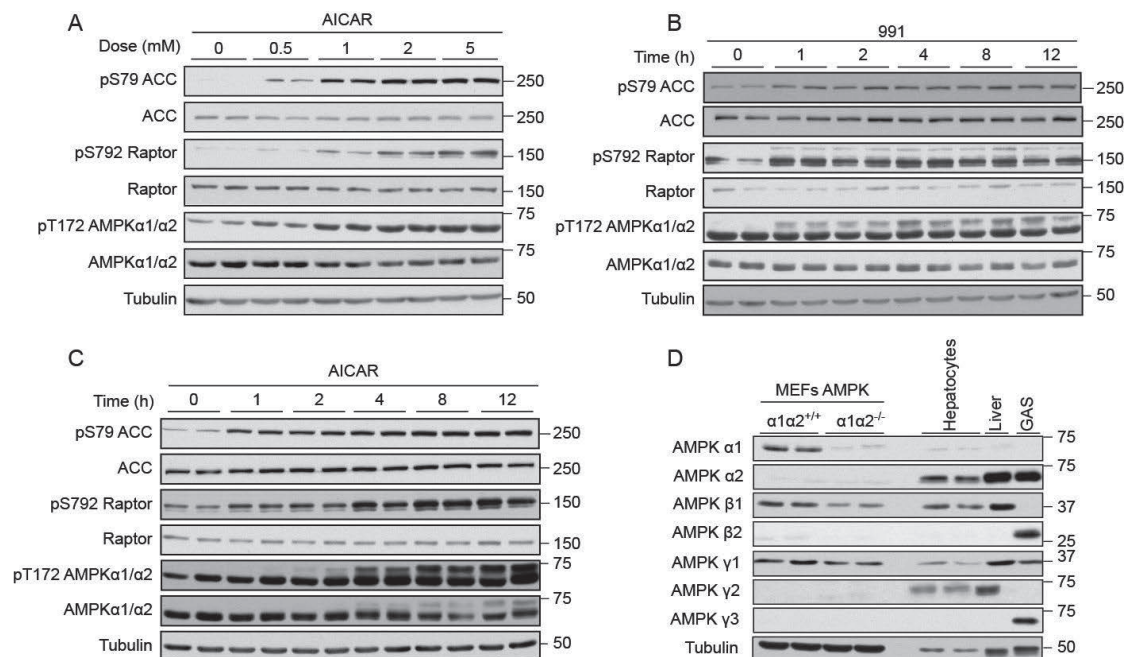
Antibodies

Total AMPK β 1/ β 2 (#4150) and H3 (#4499) antibodies were obtained from Cell Signaling Technology. Total FNIP1 antibody was obtained from Abnova (#PAB12367). AMPK γ 2 was obtained from Santa Cruz Biotechnology (#sc-19141). The following polyclonal antibodies were generated by YenZym Antibodies (South San Francisco, CA, USA) by rabbit immunization with the following listed peptides. For the site-specific phospho-FLCN (Ser62) a phosphorylated peptide of the human sequence, highly conserved with mouse, was used (CQMNSRMRAH-*S-PAEG, the prefix *denotes the phosphorylated residue). For AMPK γ 1, a peptide from the mouse sequence was employed (CESSPALENEHFQETPESNNS). For AMPK γ 3, a combination of human (CS-SERIRGKRRRAKALRWTRQKS) and mouse peptides (CSSERT-CAIRGVKASRWTRQEA) were used.

Cell culture

Human osteosarcoma (U2OS) cell line containing the Flp-In T-REx system (Thermo Fisher Scientific) were a generous gift from Prof. John Rouse (University of Dundee). U2OS were cultured in Dulbecco's modified eagle medium (DMEM)-Glutamax supplemented with 1 mM sodium pyruvate, 10% fetal calf serum and 1% penicillin streptomycin, 10 μ g/ml Blasticidin and 100 μ g/ml Zeocin. Cells were seeded at ~80% confluence and treated the following day as described in the figures.

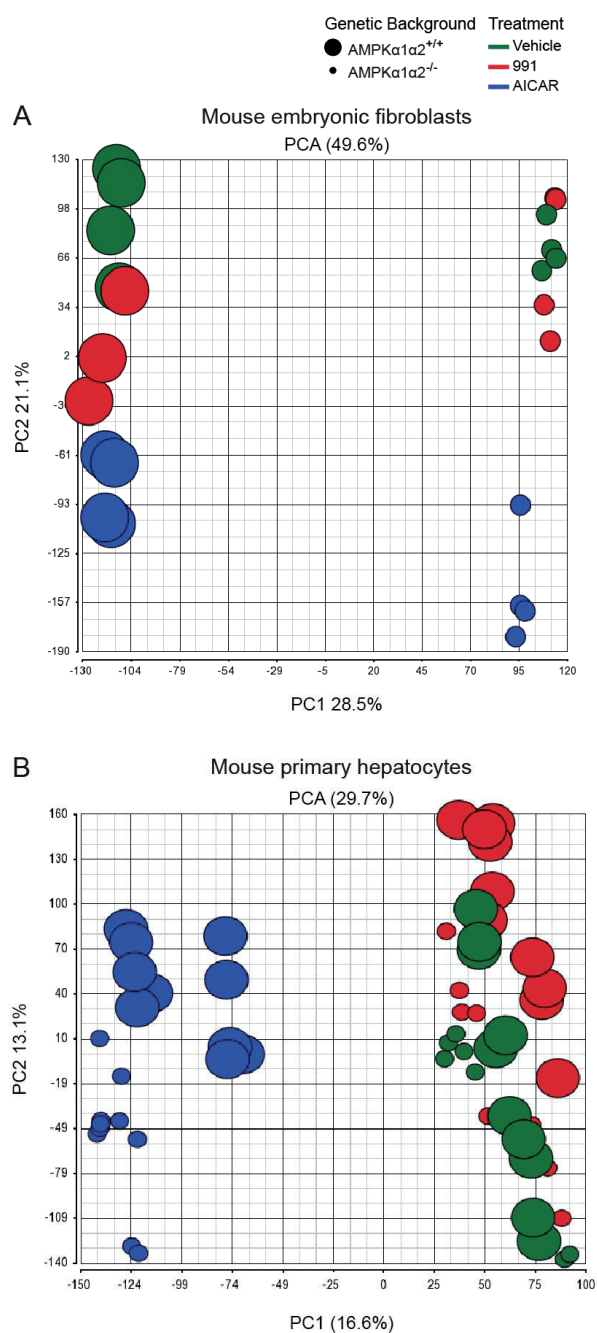
9.3.2 Establishing the treatment conditions in MEFs



Appendix Figure 1. Characterization of the MEFs model used for the microarray study.

(A) AMPK stimulation following an AICAR dose-response was monitored by western blot on cell lysates from MEFs AMPKα1α2^{+/+}, treated with 0.5, 1, 2 or 5 mM AICAR for 1 h. (B) Time course experiment of 991 activation of AMPK was performed on cell lysates from MEFs AMPKα1α2^{+/+}, treated with 10 μM 991 and harvested after various periods of stimulation (0, 1, 2, 4, 8, 12 h). (C) Time course experiment of AICAR effects onto AMPK activation was performed on MEFs AMPKα1α2^{+/+}, treated with 2 mM AICAR and harvested at various timings (0, 1, 2, 4, 8, 12 h). (D) AMPK subunits expression was checked by western blot analysis in MEFs AMPKα1α2^{+/+} or AMPKα1α2^{-/-}, primary hepatocytes, liver and gastrocnemius (GAS) tissues from wild-type mice. For all figures, cell lysates (20 μg) were used for western blot analysis with the indicated antibodies (n=2).

9.3.3 PCA plots of the microarray samples

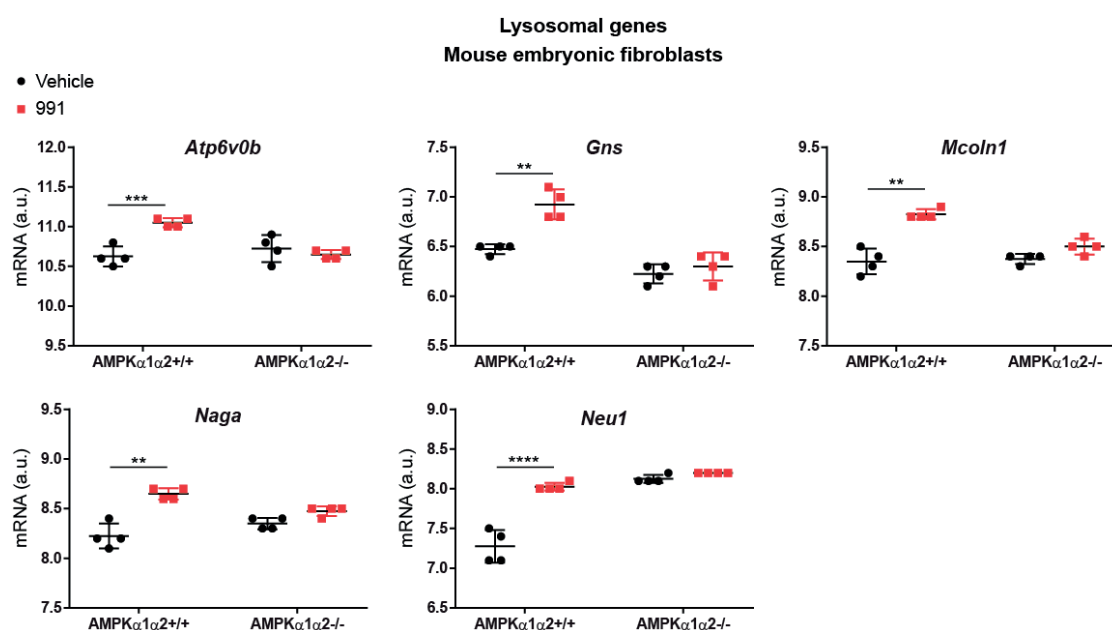


Appendix Figure 2. Principal component analysis (PCA) score plots.

(A) PCA score plot based on gene expression dataset generated from mouse embryonic fibroblasts treated with vehicle (DMSO), 10 μ M 991 or 2 mM AICAR for 4 h. The first two principal components (PC1 and PC2) explain 28.5% and 21.1% of total variance in the data, due to genetic background and treatment, respectively. (B) PCA score plot obtained from the gene expression dataset of mouse primary hepatocytes

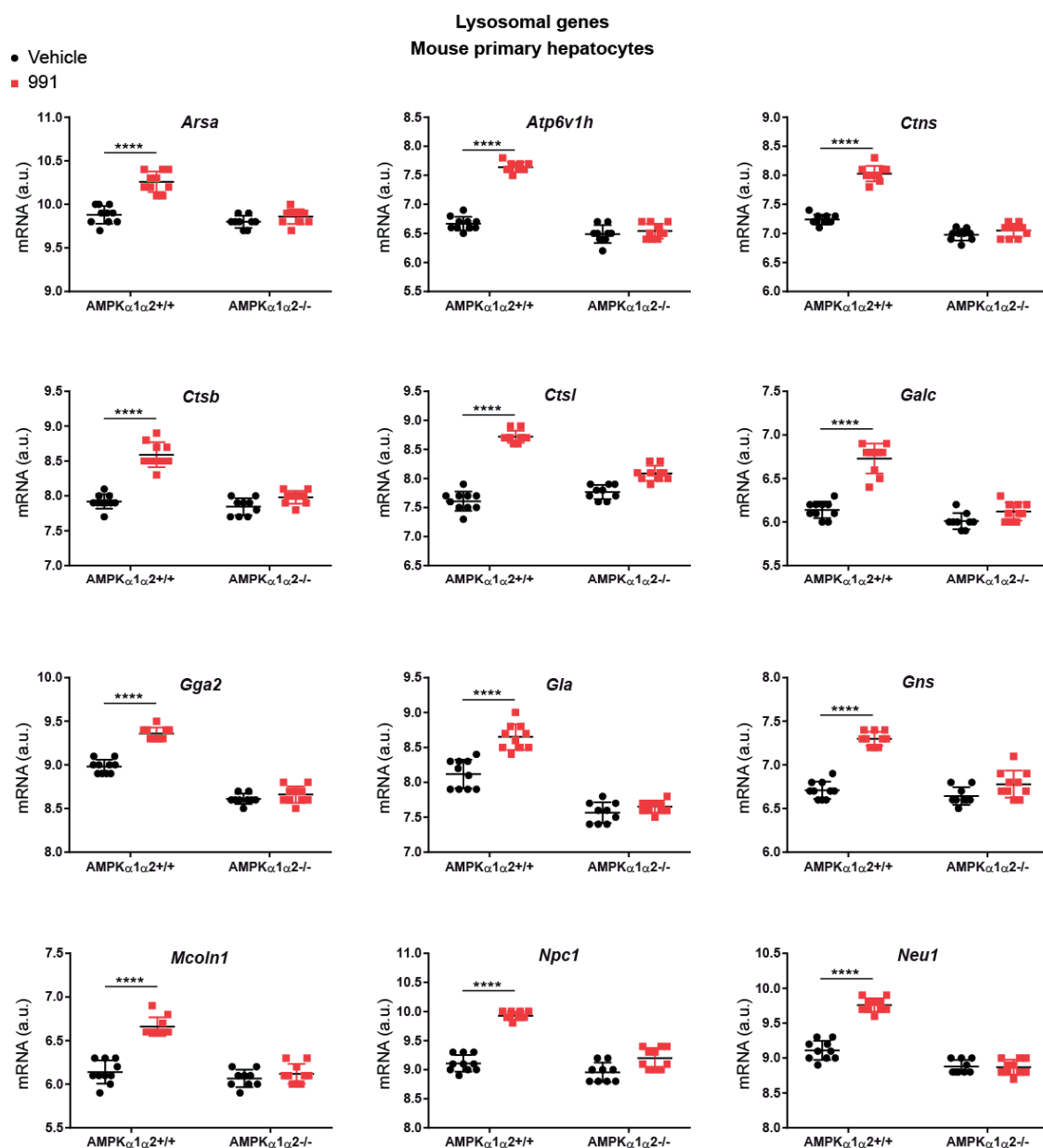
treated with vehicle (DMSO), 3 μ M 991 or 300 μ M AICAR for 4 h. AICAR and 991 treatment are responsible for 16.6% and 13.1% of the total variance in the data, respectively, represented by the two principal components (PC1 and PC2). Samples are depicted as indicated in the legend.

9.3.4 Lysosomal genes modulation by 991 activation of AMPK



Appendix Figure 3. Lysosomal genes enriched in MEFs after activation of AMPK by 991.

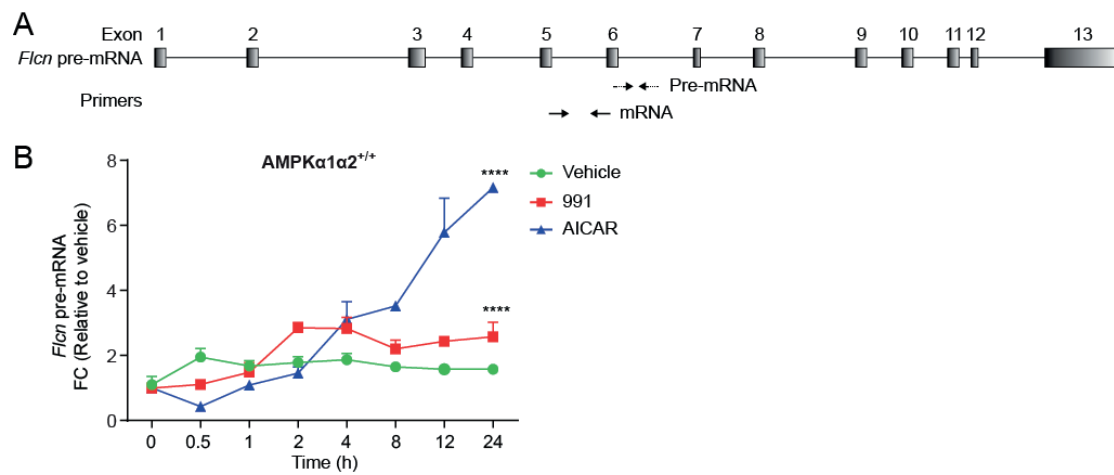
Plot of individual lysosomal genes in microarray analysis following RMA normalization, n=4 samples per group. MEFs $AMPK\alpha1\alpha2^{+/+}$ or $AMPK\alpha1\alpha2^{-/-}$ were treated with vehicle (DMSO) or 10 μ M 991 for 4 h. Color code: black indicates vehicle-treated and red 991-stimulated samples.



Appendix Figure 4. Lysosomal genes enriched in primary hepatocytes after 991 stimulation of AMPK.

Plot of individual lysosomal genes in the microarray analysis following RMA normalization, n=4 samples per group. Mouse primary hepatocytes AMPK α 1 α 2^{+/+} or AMPK α 1 α 2^{-/-} were treated with vehicle (DMSO) or 3 μ M 991 for 4 h. Color code: black indicates vehicle-treated and red 991-stimulated samples.

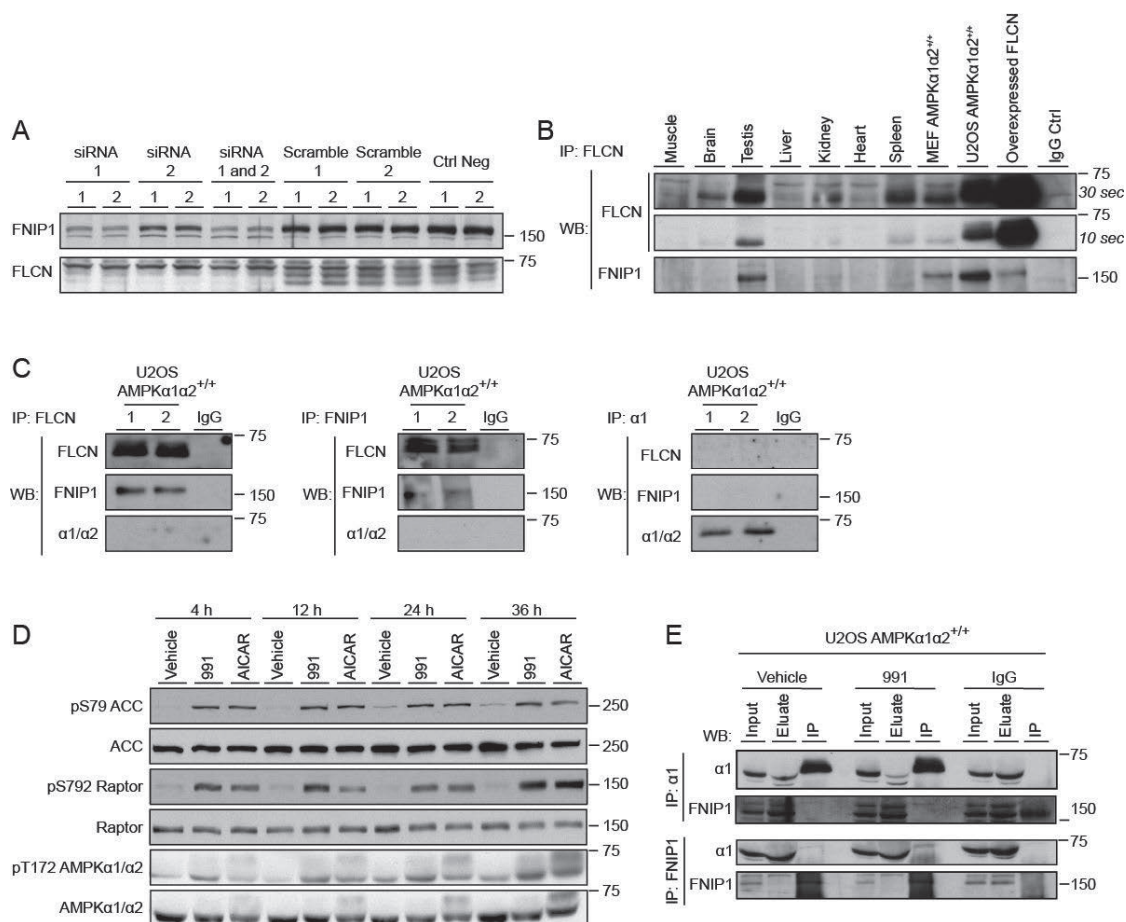
9.3.5 Time course to monitor *Fln* pre-mRNA levels in response to AMPK



Appendix Figure 5. Pre-mRNA levels of *Fln* in MEFs *AMPKα1α2^{+/+}* after AMPK activation.

(A) Schematic representation of the *Fln* pre-mRNA and position of the primers designed to measure *Fln* pre-mRNA (exon-intron) and mRNA (exon-exon). (B) Pre-mRNA level of *Fln* in MEFs *AMPKα1α2^{+/+}* treated with vehicle (DMSO), 10 μ M 991 or 2 mM AICAR for 0, 0.5, 1, 2, 4, 8, 12 and 24 h. Data were analyzed by two-way ANOVA with the factors of time and treatment, plus the interaction between these two factors ($n=3$). Significance of the treatment factor is indicated, **** P -value < 0.0001 .

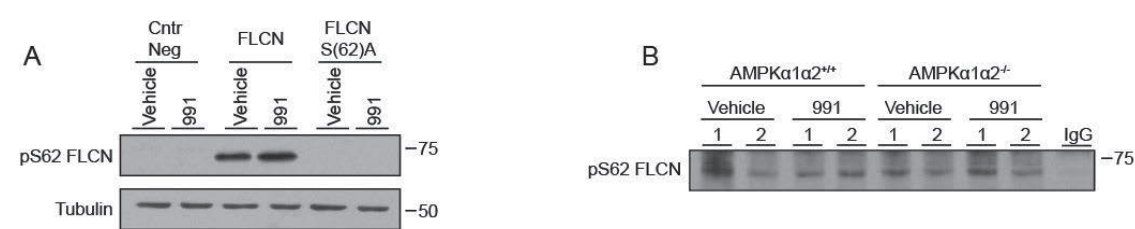
9.3.6 Determining if there is a direct interaction between FLCN-FNIP1-AMPK in U2OS



Appendix Figure 6. FLCN and FNIP1 do not directly interact with AMPK.

(A) Validation by western blot analysis of the FLCN and FNIP1 antibodies. MEFs AMPK-WT were lysed after expressing for 72 h two different siRNA (indicated as 1 and 2) targeting either *Fln*, *Fnip1*, or scramble sequences, non-transfected (control negative, Ctrl Neg) cells were used as an additional control. (B) 300 μ g of total lysates were immunoprecipitated using the FLCN antibody to compare by western blot (WB) the endogenous levels of FLCN and the interacting protein FNIP1, across a panel of tissues and cell lines (MEFs, U2OS and COS1 overexpressing FLCN). (C) Co-immunoprecipitation of FLCN, FNIP1 and AMPK ($\alpha1/\alpha2$) from U2OS AMPK $\alpha1\alpha2^{+/+}$ was performed starting from 300 μ g of total cell lysate, IgG control was added to each western blot. (D) Western blot analysis to measure AMPK activation in a time course experiment in U2OS AMPK $\alpha1\alpha2^{+/+}$ treated with vehicle (DMSO), 10 μ M 991 or 2 mM AICAR for 4, 12, 24 or 36 h. Cell lysates (20 μ g) were used for western blot analysis with the indicated antibodies (n=2). (E) Co-immunoprecipitation (IP) of AMPK $\alpha1$ and FNIP1 from U2OS AMPK $\alpha1\alpha2^{+/+}$ treated with vehicle (DMSO) or 991 for 4 h, after overnight IP western blot analysis (WB) was performed using the indicated antibodies (n=2).

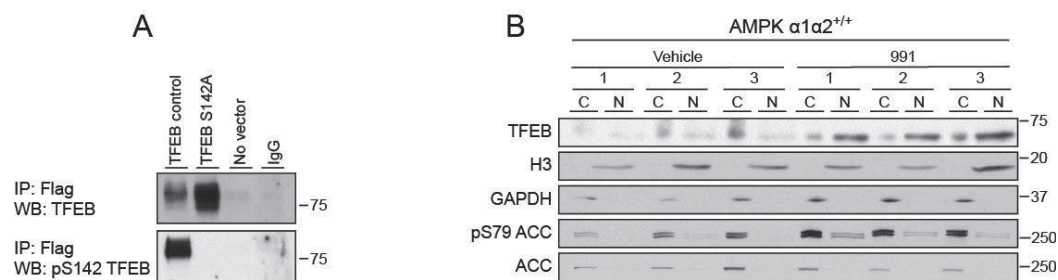
9.3.7 Generation and validation of the FLCN Ser62 phosphorylation site-specific antibody



Appendix Figure 7. FLCN Ser62 is not an AMPK-phosphorylation site in our model.

(A) Validation of the Ser62 phospho-specific antibody. COS1 cells were transfected for 48 h with no vector (control negative, Cntr Neg), FLCN control Flag-tagged or FLCN Flag-tagged mutated on the phosphorylation site (S62A). FLCN was immunoprecipitated (IP) from 500 µg of cell lysate with 1 µg of anti-Flag antibody, and subjected to western blot analysis with anti pS42 FLCN antibody. Images are representative of n=2. (B) Endogenous FLCN was IP from MEFs AMPKα1α2^{+/+} or AMPKα1α2^{-/-} following 4 h of treatment with vehicle (DMSO) or 991, western blot analysis was then done using the FLCN (Ser62) phospho-specific antibody.

9.3.8 Further characterization of TFEB



Appendix Figure 8. Further characterization of TFEB.

(A) COS1 cells were transfected for 48 h with no vector (negative control), TFEB control Flag-tagged or Flag-tagged mutated on the phosphorylation site (S142A). TFEB was immunoprecipitated (IP) from 500 μ g of cell lysate with 1 μ g of anti-Flag antibody, and subjected to western blot analysis (WB) with total TFEB or anti-pS142 TFEB-antibodies. Images are representative of $n=2$. **(B)** Primary hepatocytes from AMPK $\alpha 1\alpha 2^{+/+}$ mice were treated with vehicle (DMSO) or 10 μ M 991 for 1 h. Harvested cells were processed using the NE-PER kit, in order to separate cytoplasmic and nuclear fractions. Laemmli extracts (20 μ g) were separated by SDS-PAGE and western blot was performed using the indicated antibodies.

9.4 Manuscript published on BioRxiv

Following a copy of the work published on BioRxiv (doi.org/10.1101/499921), in preparation for publication in a peer-reviewed journal:

Collodet C., Foretz M., Deak M., Bultot L., Metairon S., Viollet B., Lefebvre G., Raymond F., Parisi A., Civiletto G., Gut P., Descombes P., Sakamoto K. (2019). AMPK promotes induction of a tumor suppressor FLCN through activation of TFEB independently of mTOR. *Manuscript in preparation*.

AMPK promotes induction of a tumor suppressor FLCN through activation of TFEB independently of mTOR

Caterina Collodet^{1,2}, Marc Foretz^{3,4,5}, Maria Deak¹, Laurent Bultot⁶, Sylviane Metairon¹, Benoit Violette^{3,4,5}, Gregory Lefebvre¹, Frederic Raymond¹, Alice Parisi¹, Gabriele Civiletto¹, Philipp Gut¹, Patrick Descombes^{1,2#}, Kei Sakamoto^{1,2#*}

¹Nestlé Research, EPFL Innovation Park, Bâtiment G/H, 1015 Lausanne, Switzerland

²School of Life Sciences, Ecole Polytechnique Fédérale de Lausanne (EPFL), 1015 Lausanne, Switzerland

³INSERM U1016, Institut Cochin, Paris, France

⁴CNRS UMR 8104, Paris, France

⁵Université Paris Descartes, Sorbonne Paris Cité, Paris, France

⁶Nestlé Research, EPFL Innovation Park, Bâtiment G, 1015 Lausanne, Switzerland; current address: Université catholique de Louvain, Institut de Recherche Expérimentale et Clinique, Pole of Cardiovascular Research, Brussels, Belgium

#These authors contributed equally.

*Correspondence:

Nestlé Research, EPFL Innovation Park, Bâtiment H, 1015 Lausanne, Switzerland

Email: Kei.Sakamoto@rd.nestle.com

Tel.: + 41 216326133; fax: + 41 216326499

Running title: AMPK-dependent regulation of TFEB

Key words: AMP-activated protein kinase; AMPK; AICAR; 991; Folliculin; FLCN; mTOR; zebrafish

Abbreviations: ACC; acetyl-CoA carboxylase, AICAR; 5-aminoimidazole-4-carboxamide ribonucleotide, AMPK; 5'-AMP-activated protein kinase, FLCN; Folliculin, TFEB; transcription factor EB

ABSTRACT

AMP-activated protein kinase (AMPK) is a central energy sensor and master regulator of energy homeostasis. AMPK not only elicits acute metabolic responses, but also promotes metabolic reprogramming and adaptations in the long-term through regulation of specific transcription factors/co-activators. We performed a whole-genome transcriptome profiling in wild-type and AMPK-deficient mouse embryonic fibroblasts (MEF) and mouse primary hepatocytes that had been treated with two distinct classes of small-molecule AMPK activators, namely 5-aminoimidazole-4-carboxamide ribonucleotide (AICAR) or 991. This led to the identification of distinct compound-dependent gene expression signatures and to the discovery of several AMPK-regulated genes, including folliculin (*Flcn*), a gene encoding for a tumor suppressor and nutrient sensor. Gene set enrichment and pathway analyses identified the lysosomal pathway and the associated transcription factor EB (TFEB) as key transcriptional mediator responsible for AMPK-dependent gene expression changes. AMPK-induced *Flcn* expression was abolished in TFEB/TFE3 double knockout MEF and the promoter activity of *Flcn* was profoundly reduced when its putative TFEB-binding site was mutated. Mechanistically, we have found that AMPK promotes the dephosphorylation and nuclear localization of TFEB independently of mTOR activity.

Collectively, we identified the AMPK-TFEB-FLCN axis as a potential key regulator for cellular and metabolic homeostasis. Moreover, data from zebrafish with physiologically and pharmacologically activated AMPK confirmed the AMPK-TFEB-FLCN cascade *in vivo*.

INTRODUCTION

AMP-activated protein kinase (AMPK) is an evolutionary conserved energy sensor which functions to maintain energy homeostasis through coordinating effective metabolic responses to reduced energy availability^{1,2}. Low-energy conditions under various pathophysiological settings (*e.g.* nutrient deprivation, physical activity, ischemia), characterized by elevated AMP:ATP or ADP:ATP ratios, trigger AMPK activation. Once activated, AMPK promotes ATP-producing, catabolic pathways and decreases ATP-consuming, anabolic pathways to restore and maintain cellular ATP at a constant level.

AMPK is a heterotrimeric complex composed of a catalytic α -subunit and two regulatory β and γ subunits. Two to three isoforms exist for each subunit (α 1 and α 2, β 1 and β 2, and γ 1, γ 2, and γ 3), giving rise to 12 distinct combinations of the heterotrimeric complexes. In general α 1, β 1, and γ 1 appear to be the ubiquitously expressed isoforms of AMPK. There are cell- and tissue-specific distributions of some isoforms (*e.g.* exclusive expression of γ 3 in skeletal muscle^{3,4}), and they may target AMPK complexes to particular subcellular locations to phosphorylate specific substrates^{5,6}. The γ subunits contain four tandem cystathionine β -synthase (CBS) repeats that provide adenine nucleotide binding⁷. AMPK activity increases >100-fold on phosphorylation of a conserved threonine residue within the activation loop (Thr172). Binding of ADP and/or AMP causes conformational changes that favor net Thr172 phosphorylation by the promotion of Thr172 phosphorylation and the inhibition of Thr172 dephosphorylation⁸⁻¹⁰. In addition, the binding of AMP (but not ADP) further promotes AMPK activity by >10-fold by allosteric activation⁸. The major upstream kinase catalyzing AMPK α Thr172 phosphorylation in most mammalian cells/tissues, including skeletal muscle and liver, is the tumor suppressor kinase LKB1¹¹. In some cell types, Thr172 can be phosphorylated in a Ca^{2+} -mediated process catalyzed by Ca^{2+} /calmodulin-dependent protein kinase kinases¹².

AMPK is considered an attractive therapeutic target for metabolic disorders since AMPK activation brings about metabolic responses anticipated to counteract the metabolic abnormalities associated with obesity, insulin resistance, and type 2 diabetes^{13,14}. Indeed several compounds, which can be divided into three categories¹², have been reported to activate AMPK and elicit metabolic effects in cellular and pre-clinical studies. The first class comprises indirect activators which, through inhibition of mitochondrial respiration and eventual suppression of ATP synthesis, increase cellular AMP:ATP or ADP:ATP ratios (*e.g.* metformin, resveratrol)¹⁵. The second class includes pro-drugs converted to AMP analogs inside the cells, and the most well characterized and commonly used compound is 5-aminoimidazole-4-carboxamide-1- β -D-

ribofuranoside (AICAR)^{16,17}. The allosteric activators, binding to a site located between the α -subunit kinase domain and the β -subunit carbohydrate binding module (CBM) termed “allosteric drug and metabolite (ADaM)” site, constitute the third class. The first compound identified through a high-throughput screen¹⁸ as an allosteric AMPK activator is A769662, a thienopyridone that preferentially activates β 1-containing complexes¹⁹. More recently 991 was developed, a cyclic benzimidazole which binds AMPK 10 times tighter than A769662 in cell-free assays²⁰ and activates both β 1- and β 2-containing complexes (with a higher affinity to the β 1 complexes)^{4,21}. It has been reported that A769662 causes several off-target effects, for example in isolated mouse skeletal muscle when used at high concentration²² and also in other cells/tissues^{23,24} and was reported to have poor oral availability¹⁸. Notably, an emerging new generation of ADaM site-binding compounds, including MK-8722 and PF-739, have been shown to be effective in reversing elevated blood glucose concentrations in rodents and non-human primates through activation of AMPK *in vivo*^{25,26}.

It is well established that AMPK elicits a plethora of acute metabolic responses through phosphorylation of serine residues surrounded by the well characterized recognition motif²⁷. There has been much effort into the identification of AMPK substrates, and several targeted and untargeted proteomics studies have been performed²⁸⁻³², which led to a mechanistic understanding of AMPK-mediated metabolic responses and the discovery of new roles for AMPK beyond conventional metabolic regulation (*e.g.* cell cycle, autophagy). Growing evidence suggests that in the long-term AMPK promotes metabolic reprogramming via effects on gene expression at least partly through regulation of specific transcription factors and transcriptional co-activators^{1,12}.

In the current study we initially performed a comprehensive transcriptomic profiling in wild-type (WT) and AMPK-deficient (AMPK α 1/ α 2 double knockout (AMPK KO)) mouse embryonic fibroblasts (MEF) and primary hepatocytes treated with AICAR and 991, which led to the identification of distinct compound-dependent gene expression signatures and to the discovery of several AMPK-regulated genes. Gene set enrichment and pathway analyses prompted us to hypothesize that the transcription factor EB (TFEB) is a potential key transcription factor responsible for AMPK-mediated gene expression. We found that expression of *Flcn*, a gene which encodes the tumor suppressor folliculin (FLCN), was abolished in both AMPK KO and TFEB/TFE3 double KO MEF and the promoter activity of *Flcn* was profoundly reduced when the putative TFEB-binding site was mutated. Finally, we found that AMPK

activates TFEB through promotion of dephosphorylation and nuclear translocation independently of mTOR signaling.

RESULTS

Whole-genome transcriptome profiling revealed distinct gene expression profiles in response to AMPK activators in MEF and primary hepatocytes

To identify genes and pathways regulated in an AMPK-dependent mechanism, we performed a whole-genome transcriptome profiling using microarray technology (Affymetrix Mouse GeneChips). Taking cell type-specific roles and isoform-/compound-selective responses of AMPK into account, we used two different cell models and genotypes, namely AMPK WT and AMPK KO in both MEF and mouse primary hepatocytes, and treated them with two different AMPK activators (991 and AICAR) known to target distinct regulatory sites/mechanisms²⁷. MEF and mouse primary hepatocytes were treated with vehicle, 991 or AICAR at the indicated concentrations for 4 hours. Following treatment, one set of the samples was subjected to transcriptome profiling and the other set was used for immunoblotting to assess the effect of compounds on AMPK activity. We initially confirmed by immunoblot analysis that treatment of WT MEF with 991 (10 μ M) or AICAR (2 mM) resulted in an increase in phosphorylation of AMPK (Thr172) and its *bona fide* substrates acetyl CoA carboxylase (ACC) (Ser79) and raptor (Ser792) (Fig. 1A). Similar results were obtained when WT mouse primary hepatocytes were treated with 991 (3 μ M) or AICAR (300 μ M) (Fig. 1B). Notably, although treatment with 991 or AICAR resulted in a comparable elevation of ACC phosphorylation in both MEF and hepatocytes, 991-induced raptor phosphorylation was higher in MEF but lower in hepatocytes compared to AICAR (Fig. 1A, B). As previously demonstrated³³⁻³⁵, there was no detectable phosphorylation of AMPK, ACC and raptor in vehicle- and 991-/AICAR-treated AMPK KO MEF and hepatocytes (Fig. 1A, B). Taken together, we validated a complete ablation of AMPK activity in both AMPK KO MEF and hepatocytes, and observed differential responses in commonly used surrogate markers for cellular AMPK activity (i.e. phosphorylation of ACC and raptor) following the treatment with 991 or AICAR.

We next performed a whole transcriptome profiling using Affymetrix MOE430 arrays. A principal component analysis (PCA) was conducted for initial evaluation of data quality and assessment of the effect of genotype and treatment on the transcriptome (Supplementary Fig. 1A, B). In MEF the PCA clarified that genotype was the primary factor responsible for variance, followed by treatment, and that globally AICAR caused a greater transcriptional response

compared to that induced by 991. It also implied that 991 induced a rather limited, but potentially more specific transcriptional responses compared to AICAR. In contrast, in primary hepatocytes, treatment was the main cause of variance, followed by a lower variance explained by genotype. AICAR consistently produced a much greater response than that driven by 991. These observations were well corroborated by the hierarchical clustering (Fig. 2A, B).

Identification and validation of AMPK-dependent genes and pathways

To clarify genes specifically regulated following AMPK activation, we first selected genes by pairwise differential analysis of MEF and primary hepatocytes treated with AICAR or 991 as compared to vehicle. *P*-values were corrected for multiple testing using the false-discovery rate (FDR) method of Benjamini and Hochberg³⁶ and we applied a conservative significance threshold of 5% FDR associated with a fold change value of 1.3 or more, given that moderate fold changes were observed. Following 991 treatment, the vast majority of differentially expressed transcripts (>92%) required a functional AMPK, with 184 out of 199 for MEF and 670 out of 684 for primary hepatocyte transcripts regulated in an AMPK-dependent fashion, respectively (Fig. 3A, B and Supplementary Table 1). This observation confirms the nearly exclusive specificity of 991 for targeting AMPK in MEF and hepatocytes consistent with the *in vitro* (cell-free) observation in our previous study⁴. In contrast, AICAR induced a much greater transcriptional response with a majority (~50%) of the transcripts differentially regulated in the absence of AMPK (1026 out of 2053 in MEF and 754 out of 1718 in primary hepatocytes, respectively) (Fig. 3A, B). Altogether, these findings suggest that 991 elicits much more AMPK-specific transcriptional responses compared to AICAR, an observation which is corroborated by the results of PCA (Supplementary Fig. 1) and hierarchical clustering (Fig. 2A, B).

To illuminate the pathways regulated by AMPK, we performed a gene ontology analysis on the genes differentially expressed upon 991 treatment in primary hepatocytes and MEF using the Database for Annotation, Visualization and Integrated Discovery (DAVID) program^{37,38} (Fig. 4 A, B). This analysis revealed a commonly shared signature of biological/metabolic pathways (*e.g.* lysosomes) observed in both cell types, as well as additional cell type-specific pathways such as ErbB signaling, sphingolipid metabolism and adipocytokine signaling for primary hepatocytes, and steroid biosynthesis and biosynthesis of antibiotics for MEF, respectively (Fig. 4A, B). In order to validate the microarray data, we performed quantitative real-time PCR (qPCR) analyses on several genes that are known to be involved in

lipid/cholesterol signaling and metabolism (*Acss2*, *Crebrf*, *Hmgcr*, *Ldlr*, *Lpin1*, *Msmo1*, *Pde4b*), glucose transport (*Txnip*), immunity (*Ifit1*, *Tollip*), and cell growth/cancer (*Flcn*, *Fnip1*, *Mnt*) (Fig. 4C, D). Overall, we observed a strong correlation between the microarray and qPCR data. Additionally, we also found cell type-/compound-specific responses. For example, AICAR had a more profound effect on gene expression compared to 991 in MEF (*Acss2*, *Flcn*, *Ldlr*, *Lpin1*, *Mnt*, *Tollip*, *Txnip*), but this was not the case in primary hepatocytes (Fig. 4C, D). Interestingly, while AICAR exhibited significant and greater effects on expression of *Flcn* and *Fnip1* in MEF compared to 991, it had no significant effect in primary hepatocytes. In addition, AICAR elicited an AMPK-dependent effect on *Hmgcr* and *Lpin1* expression in MEF, which was absent in primary hepatocytes. Collectively, we identified AMPK-dependent genes (involved in metabolism, immunity and cell growth) that demonstrate cell type- and compound-specific responses in MEF and mouse primary hepatocytes.

991-/AICAR-stimulated *Flcn* expression is AMPK-TFEB/TFE3 dependent

To shed light on the mechanism by which AMPK modulates expression of specific genes, we next conducted an *in silico* analysis to identify potential transcription factors responsible for the AMPK-dependent responses upon compound treatment. To this end, we performed a search for correlation in expression between the 991-responsive transcripts identified in MEF (184 targets) and hepatocytes (670 targets), and the expression of potential upstream regulators using the Ingenuity Pathway Analysis (IPA) tool³⁹ (Table 1). The IPA revealed that there were around 10 candidates and only two of these, sterol regulatory element binding protein 1 (SREBP1) and TFEB, were identified in both MEF and hepatocytes (Table 1). SREBP1 is a master transcriptional regulator of lipid synthesis and its activity is known to be regulated by AMPK-mediated phosphorylation⁴⁰. TFEB and TFE3 are members of the microphthalmia (MiT/TFE) family of HLH-leucine zipper transcription factors that play an important role in the control of cell and organismal homeostasis through regulating lysosomal biogenesis and autophagy⁴¹. TFEB is also known to be indirectly regulated by AMPK in the control of lineage specification in embryoid bodies⁴². Interestingly, it was recently reported that TFEB/TFE3 regulate energy metabolism, although the underlying mechanism remains elusive^{43,44}. Among the genes regulated specifically in an AMPK-dependent manner (Fig. 4C, D), we focused on *Flcn*, which encodes the tumor suppressor folliculin (FLCN). FLCN and its binding partner FLCN-interacting protein (FNIP) are known to interact with AMPK and this FLCN-FNIP-AMPK interaction/complex has been proposed to control various metabolic functions⁴⁵⁻⁴⁷. We first determined the kinetics of the effects of 991 and AICAR on the expression of *Flcn* in time-

course experiment over 24 hours, followed by qPCR analysis. We observed that 991 and AICAR induced significant and prolonged expression of *Flcn* throughout the time points measured in an AMPK-dependent manner compared to the vehicle control, except the 24 hour time point where AICAR caused an increase in *Flcn* expression in AMPK KO MEF (Fig. 5A). We confirmed that the increased levels of *Flcn* mRNA were due at least partly to enhanced gene transcription, since pre-mRNA levels of *Flcn* were also significantly elevated in response to 991 and AICAR treatment (Supplementary Fig. 2A, B). Moreover, we confirmed that the elevated levels of *Flcn* transcripts were translated into an increase in FLCN protein levels in a time- and AMPK-dependent manner in response to 991 or AICAR treatment (Fig. 5B). We next wanted to determine if TFEB is required for mediating AMPK-induced expression of FLCN at both mRNA and protein levels. Since TFEB and TFE3 have been proposed to be at least partially redundant⁴¹, TFEB/TFE3 double KO MEF were employed. As anticipated 991 or AICAR significantly increased expression of *Flcn* at both mRNA and protein levels in WT, but not in TFEB/TFE3 double KO MEF (Fig. 5C, D). We hypothesized that TFEB regulates *Flcn* expression through enhancing its promoter activity, especially based on the fact that the *Flcn* promoter contains a putative TFEB binding site, which is conserved between humans and mice. To test this hypothesis, we cloned and placed fragments of various length (8000, 1200, and 100 bp) of the mouse *Flcn* promoter region upstream of the luciferase gene and transfected the resulting reporter construct individually into WT or AMPK KO MEF. 991 increased the promoter activity of all three constructs when introduced into WT MEF, while in contrast no or only a marginal increase was seen when they were introduced into AMPK KO MEF (Supplementary Fig. 2C). Notably, when the putative TFEB binding site was mutated in the 1200 and 100 bp fragments and the corresponding reporter constructs introduced in WT MEF, 991-induced promoter activity was significantly reduced (Supplementary Fig. 2D). Taken together, these results demonstrate that AMPK promotes *Flcn* transcription through activation of TFEB/TFE3.

AMPK promotes dephosphorylation and nuclear translocation of TFEB independently of mTOR

It has been reported that the transcriptional activity of TFEB is coupled to its subcellular localization and is regulated by reversible phosphorylation. We thus wanted to determine if AMPK-induced activation of TFEB occurs as a consequence of its dephosphorylation and nuclear localization. To test this hypothesis, we treated WT and AMPK KO MEF with 991 or

AICAR for 4 hours and prepared cytoplasmic and nuclear fractions followed by immunoblot analysis (Fig. 6A). ACC was only detected in the cytoplasm as anticipated and its phosphorylation was increased (~2 fold) after treatment with the compounds. In WT MEF both 991 and AICAR similarly decreased and increased TFEB levels in cytoplasmic and nuclear fractions, respectively, whereas the levels of TFEB were not altered in both fractions upon treatment with 991 or AICAR compared to control (vehicle) in AMPK KO MEF. Notably, both compound treatments resulted in a marked increase in a faster-migrating form of TFEB, indicative of TFEB dephosphorylation, in the nuclear fraction in WT but not in AMPK KO MEF (Fig. 6A). To examine if the faster migration of TFEB was associated with dephosphorylation, we generated a phospho-specific antibody against Ser (S)142, one of the key phosphorylation sites impacting cellular localization and activity of TFEB⁴⁸. We verified and confirmed the specificity of the phospho-S142 TFEB antibody by immunoblotting using recombinant WT and non-phosphorylatable Ala (A) mutant form (S142A) of N-terminus Flag-tagged mouse TFEB (Fig. 6B). Given that mTOR has been demonstrated to act as a key upstream regulator of TFEB and that AMPK is known to modulate mTOR activity, we also wanted to address if AMPK-mediated dephosphorylation and nuclear localization of TFEB were dependent on mTOR (Fig. 6C). Consistent with the results shown in Fig. 6A, both 991 and AICAR treatment (for 1 and 4 hours) resulted in a downward band-shift of total TFEB in WT, which was associated with a decrease in S142 phosphorylation. In contrast, compound treatment had no effect on both band-shift and S142 phosphorylation in AMPK KO MEF (Fig. 6C). AICAR induced a robust decrease in mTOR activity as evidenced by a decrease in phosphorylation of p70 S6K (Thr389, a known mTOR-target site) and its downstream substrate ribosomal protein S6 (S6RP) in WT (notably at 4 hours post treatment), but not in AMPK KO MEF. 991 treatment showed only a modest decrease in S6RP phosphorylation in WT, but not in AMPK KO MEF. Treatment with Rapamycin, an mTOR complex 1 (mTORC1) inhibitor, for 1 or 4 hours at three doses (0.05, 0.1, and 0.5 μ M) caused a robust decrease in phosphorylation of p70 S6K and S6RP in both WT and AMPK KO MEF. In sharp contrast to this observation, Rapamycin did not lead to any notable band-shift or dephosphorylation (S142) of TFEB in both WT and AMPK KO MEF (Fig. 6C). It has previously been demonstrated that nutrient-induced S142 phosphorylation was resistant to Rapamycin but sensitive to a novel class of mTOR inhibitor (Torin) targeting catalytic site of mTOR⁴⁸. Torin (5 or 10 nM for 1 or 4 hours) inhibited mTOR activity (*i.e.* ablated phosphorylation of p70 S6K and S6RP) to a similar degree compared to Rapamycin. Of note, Torin treatment (10 nM, 4 hours) caused a modest

downward band-shift and dephosphorylation (S142) of TFEB, although this was not AMPK-dependent since it was observed in both WT and AMPK KO MEF (Fig. 6D).

We next wanted to determine if the AMPK-dependent and mTOR-independent dephosphorylation and nuclear enrichment of TFEB in response to AMPK activators could also be observed in mouse primary hepatocytes (Fig. 7A, B). As anticipated, treatment of hepatocytes with AMPK activators (991, AICAR, and also C13, a recently identified α 1-selective AMPK activator^{34,49}) for 1 or 4 hours robustly increased phosphorylation of AMPK and ACC in WT, which was totally ablated in AMPK KO hepatocytes (Fig. 7A). AICAR and C13, but not 991, potentially reduced phosphorylation of p70 S6K and S6RP in an AMPK-dependent mechanism, except that C13 (4 hours) displayed an AMPK-independent inhibition of mTOR. In control (vehicle-treated) hepatocytes, total TFEB appeared as doublets in WT, whereas in AMPK KO hepatocytes TFEB band was fainter and smeary compared to WT. Consistent with our observations using MEF (Fig. 6A, C and D), AMPK activators resulted in disappearance of the upper band and increased the amount of the lower/faster-migrating form of TFEB in WT, while no apparent change/band-shift in TFEB was observed in AMPK KO hepatocytes. We also observed that treatment of WT hepatocytes with the AMPK activators decreased and increased TFEB levels in cytoplasmic and nuclear fractions, respectively (data not shown). Of note, we attempted to assess TFEB S142 phosphorylation, however it was not detectable most likely due to the low abundance of total TFEB in mouse primary hepatocytes (data not shown). In line with the observations in MEF (Fig. 6C), Rapamycin had no apparent effect on TFEB band-shift/-migration (Fig. 7A). To demonstrate that a loss of band-shift/dephosphorylation of TFEB observed in AMPK KO hepatocytes is intrinsic to AMPK deficiency, we reintroduced AMPK subunits (Flag- α 2, β 1, γ 1) back in AMPK KO cells using adenovirus (Fig. 7B). Genetic deletion of AMPK α 1 and α 2 catalytic subunit (AMPK KO) resulted in profound reductions in other regulatory subunits (β 1 and γ 1). When AMPK α 2, β 1, γ 1 were introduced/expressed in the AMPK KO hepatocytes, the effect of 991 (following both 1 and 4 hours) on ACC phosphorylation, as well as a downward band-shift of TFEB, was totally restored. Collectively, we demonstrate that AMPK activators promote dephosphorylation and nuclear localization of TFEB in an AMPK-dependent and mTOR-independent mechanism in MEF and mouse primary hepatocytes.

***In vivo* evidence that AMPK activation promotes nuclear localization of TFEB and *Flcn* expression using zebrafish.**

Zebrafish (*Danio rerio*) represents a powerful vertebrate model in biomedical research, given its genetic similarities with humans together with its high fecundity, rapid development and the optical transparency of embryos and larvae. Taking advantage of the zebrafish model, we sought to address if AMPK activation promotes nuclear localization of TFEB at organismal/tissue levels and across species. To this end, we employed zebrafish transgenically-expressing zebrafish Tfeb fused to ZsGreen (ZsGreen-Tfeb), as well as mCherry fused to a nuclear localization signal (NLS) under the actin alpha cardiac muscle 1b *actc1b* promoter, which drives gene expression in skeletal muscle. Fluorescence-based confocal microscopy was performed on embryos 3 days post fertilization following treatment with vehicle (DMSO) or 991 (10 μ M) for 24 hours (Fig. 8A). We verified that 991 (10 μ M for 24 hours) increases the phosphorylation of AMPK and ACC by immunoblot analysis using larvae protein extracts (data not shown). Under vehicle-treated condition, the ZsGreen-Tfeb was distributed throughout the entire cell likely due to cytosolic localization of Tfeb. In support of this, merging the ZsGreen-Tfeb with the mCherry-NLS images showed that there was no apparent nuclear localization of Tfeb (Fig. 8A). We observed a change in the distribution pattern of ZsGreen- Tfeb going from a diffuse pattern to a forming puncta within the cell. Merging this image with the mCherry-NLS shows that these puncta superimpose with the signal from the mCherry-NLS image. This suggests that treatment of zebrafish larvae with 991 leads to translocation of ZsGreen- Tfeb to the nucleus, which is consistent with results obtained with cell fractionation and immunoblot analysis in MEF (Fig. 6A). Altogether, these results compellingly demonstrate AMPK plays an important role in the regulation and activation of TFEB across species.

Having demonstrated that pharmacological activation of AMPK promotes nuclear localization of TFEB and its transcriptional activation leading to induced *Flcn* expression, we wanted to study if a physiological activation of AMPK, such as physical exercise, would also increase *Flcn* expression *in vivo*. For this purpose, we generated loss of function of *prkaa1/prkaa2* (which encodes paralogue of human/mouse AMPK α 1 and α 2, respectively) double KO zebrafish using CRISPR-Cas9 genome editing (Parisi *et al.*, in preparation). Using this model, we investigated whether expression of *Flcn* and *Fnip2*, the paralogue of *Fnip1*, alters in response to an acute bout of swimming exercise. We initially established an acute exercise training protocol which stimulates AMPK in zebrafish (as summarized in Fig. 8B). The control and exercise groups comprised a mixed population of WT and knockout fish, to

ensure consistency between the experimental groups. The control group was placed in the swim tunnel and subjected to a low flow speed (5 cm/s) for 3 hours. For the exercise group, an acclimatization period of 20 min at a low flow speed (5 cm/s) was followed by a gradual increase of water velocity up to 80% of maximum speed capacity (*i.e.* 60 cm/s for this cohort of fish), which was maintained for approximately 2 hours. Notably, the maximum speed of the fish, defined as the maximum sustainable swimming speed, was determined in a previous grouped endurance test following the existing guidelines⁵⁰. Subsequently, the skeletal muscles were rapidly extracted to avoid AMPK activation due to cellular stress (*e.g.* hypoxia). The loss of expression/function of AMPK in the knockout fish was assessed by immunoblotting, which confirmed the absence of expression and activity of the AMPK catalytic subunits (Fig. 8C). We confirmed that an acute bout of exercise increased AMPK activity as judged by an increase in phosphorylation of AMPK and ACC in WT muscle (Fig. 8C). Finally, we compared by qPCR the levels of *flcn* and *fnip2*, the paralogue of *fnip1*. The results showed an increased level of expression of both genes after physical exercise in WT zebrafish, and that this increase was significantly decreased in *prkaa1/prkaa2*-deficient zebrafish (Fig. 8D). Taken together, these data suggest that exercise increases the activity of AMPK in zebrafish, which is associated with an increase in *flcn* and *fnip2* expression that is at least in part mediated through AMPK.

DISCUSSION

It is well documented that AMPK not only elicits a plethora of acute metabolic responses, but also promotes metabolic reprogramming by modulating gene expression through regulation of specific transcription factors and transcriptional co-activators^{12,27,51}. In the current study, we performed whole-genome transcriptome profiling in AMPK-intact or -deficient mouse embryonic fibroblasts and hepatocytes. We identified several new AMPK-dependent/-regulated genes and pathways that are differentially regulated in a cell type- and a compound-specific manner. The major finding of this study was that we found TFEB, a transcription factor and emerging regulator of lysosomal biogenesis/autophagy⁵², as one of the key mediators of AMPK-dependent transcriptional responses.

We performed transcriptome profiling using two different AMPK activators (AICAR and 991), known to target distinct regulatory sites/mechanisms. AICAR is a valuable and the most commonly used pharmacological AMPK activator, which significantly contributed to uncover critical metabolic functions of AMPK for decades⁵³⁻⁵⁵. In recent years, with the development and availability of genetic technologies/tools (*i.e.* AMPK KO models), as well as highly-specific AMPK activators targeting ADaM site, the specificity of AICAR has been questioned. Several studies have reported AICAR's off-target effects¹⁷, for example on AMP-regulated enzymes such as fructose 1,6-bisphosphatase, a key regulator for hepatic gluconeogenesis^{56,57}. To our knowledge, this is the first study investigating the effect of AICAR on genome-wide gene expression employing AMPK-deficient cell models to dissect AMPK-dependent/-independent effects. It was striking to find out that the vast majority of the transcripts were significantly altered with AICAR in the absence of functional AMPK. This implied that previously claimed signaling, cellular, as well as physiological effects induced by AICAR may not be mediated through AMPK (unless its off-target effects were ruled out using AMPK KO models as a control). In contrast, 991 exhibited nearly exclusive specificity for targeting AMPK in both MEF and hepatocytes consistent with the specificity of this compound that we showed *in vitro* (cell-free) in our previous study⁴. 991 activates both β 1- and β 2-containing complexes (with higher affinity to the β 1 complexes), thus it acts as a pan/total AMPK activator. Given that isoform-specific AMPK activators have recently been identified^{34,58}, it would be of interest to elucidate isoform-specific gene responses and metabolic programming.

The cellular localization and activity of TFEB are primarily regulated by its phosphorylation status. Two serine residues, S142 and S211, in the TFEB have mainly been

proposed to play a key role in determining its subcellular localization^{48,52}. When both sites are phosphorylated, TFEB is kept inactive in the cytosol, while mutation of either S142 or S211 to non-phosphorylatable alanine residue rendered TFEB constitutively active through keeping it within the nucleus. mTOR and ERK2 are the main protein kinases known to phosphorylate TFEB under nutrient-rich conditions supplemented cells with conventional cell culture medium) in most cell types. AMPK inhibits mTOR through multiple mechanisms⁵⁹⁻⁶¹, and it has recently been reported that AMPK controls endolysosomal function through suppression of mTOR and its subsequent regulation of TFEB⁴². Therefore, we initially hypothesized that 991- or AICAR-induced activation of TFEB, via dephosphorylation and nuclear localization, is mediated through the AMPK-dependent inhibition of mTOR. Contrary to our hypothesis, we observed that acute treatment with a specific AMPK activator, 991^{4,20}, promoted TFEB dephosphorylation in the absence of detectable inhibition of mTOR (as judged by phosphorylation of p70 S6K and S6RP) in primary hepatocytes. In a previous study, it has been shown that phosphorylation of TFEB at S142 represents a Rapamycin-resistant, but Torin-sensitive site⁴⁸. In line with this, we observed that the S142 phosphorylation was not affected by Rapamycin. However, in contrast to the previous observation, Torin displayed only a marginal effect on TFEB dephosphorylation (*i.e.* appearance of a minor faster-migrating form of the total TFEB and reduced S142 phosphorylation), and notably this was not only observed in WT, but also in AMPK KO MEF. Collectively, in MEF and primary hepatocytes, 1) we have demonstrated that acute inhibition of mTOR (*i.e.* 1-4 hours) does not modulate TFEB phosphorylation, and 2) 991-induced dephosphorylation of TFEB is unlikely to be mediated through AMPK-dependent suppression of mTOR. However, it would be important to assess if other phosphorylation sites (*e.g.* S211, S138), which are proposed to play key roles for cellular distribution of TFEB⁶², are regulated upon AMPK activation.

The mechanism by which AMPK dephosphorylates and activates TFEB is unknown. It has been demonstrated that nutrient deprivation induces the release of lysosomal Ca^{2+} through Ca^{2+} channel mucolipin 1. This activates calcium/calmodulin-activated serine/threonine phosphatase calcineurin (also known as protein phosphatase 2B), which binds to and dephosphorylates TFEB, thus promoting its nuclear localization and autophagy induction⁶³. It would be interesting to determine if AMPK-mediated activation of TFEB regulates the catalytic activity of calcineurin and/or interaction between TFEB and calcineurin. It has also been shown that nutrient/glucose deprivation-induced AMPK activation regulates lysosomal and autophagy gene expression through phosphorylation at S659 and nuclear localization of acetyl-CoA synthetase 2 (ACSS2)⁶⁴. Phosphorylated ACSS2 forms a complex with TFEB, which modulates

lysosomal and autophagosomal genes by locally producing acetyl CoA for histone H3 acetylation in the promoter regions of these genes. Therefore, AMPK indirectly modulates the transcriptional activity of TFEB after its nuclear translocation via inhibition of mTOR in response to energy stress. Nonetheless, in the current study we found *Acss2* as one of the AMPK-dependent genes upregulated at mRNA levels in response to both 991 and AICAR. Whether this upregulation of *Acss2* is linked to an increase in its protein/phosphorylation levels needs to be determined.

Although TFEB is an established master regulator of lysosomal biogenesis^{65,66}, emerging evidence suggests that it also acts as key controller for various other cellular and metabolic responses, including lipid metabolism in liver⁶⁷, mitochondrial biogenesis in muscle⁴⁴, as well as modulation of the immune response⁶⁸. In support of this, we identified genes that are involved in lipid/cholesterol signaling and metabolism (*Acss2*, *Crebrf*, *Hmgcr*, *Ldlr*, *Lpin1*, *Msmo1*, *Pde4b*) and immunity (*Ifit1*, *Tollip*). It would be of interest to determine if these genes are regulated through the AMPK-TFEB axis, as we have shown for *Flcn*. The tumor suppressor FLCN, responsible for the Birt-Hogg Dubé renal neoplasia syndrome (BHD), is an AMPK-interacting partner which has recently been proposed to function as a negative regulator of AMPK^{46,47}. It has been reported that ablation of FLCN expression or loss of FLCN binding to AMPK cause constitutive activation of AMPK, which was associated with enhanced osmotic stress resistance and metabolic transformation. Notably, genetic inactivation of FLCN in adipose tissue led to a metabolic reprogramming characterized by enhanced mitochondrial biogenesis and browning of white adipose tissue⁴⁵. Mechanistically, adipose-specific deletion of FLCN results in induction of the PGC-1 transcriptional coactivator through relieving mTOR-dependent cytoplasmic retention of TFE3⁶⁹ and/or activation of AMPK⁴⁵. It has been shown that exercise promotes TFEB translocation into the myonuclei, which regulates glucose/glycogen metabolism by controlling expression of glucose transporters, glycolytic enzymes, as well as pathways linked to glucose homeostasis⁴⁴. Moreover, muscle-specific over-expression of TFEB mimics the effects of exercise training and promotes metabolic reprogramming through induction of gene expression involved in mitochondrial biogenesis and function. We showed *in vivo* using zebrafish that exercise induces *Flcn* and *Fnip2* expression at least partially through an AMPK-dependent mechanism. Moreover, we proved that activation of AMPK by 991 induces Tfeb translocation to the nucleus, suggesting that the increased gene transcription of *Flcn* and *Fnip2* observed after exercise are likely mediated through the ability of AMPK to promote Tfeb translocation in skeletal muscle. Whether FLCN mediates part of metabolic responses downstream of TFEB/TFE3 or increased expression of FLCN functions as

negative feedback loop to suppress AMPK to avoid its prolonged activation of AMPK is unknown.

Coincidentally, we noticed that in the dataset generated by Cokorinos *et al*, the mRNA levels of *Flcn* and *Fnip1/2* were elevated in response to acute or chronic treatment with the ADaM site-binding allosteric AMPK activator PF-739 in mouse skeletal muscle²⁵. This strongly supports the findings from our current study that activation of AMPK leads to changes in *Flcn* and *Fnip1/2* *in vivo* across multiple species and tissues. Our study suggests that the ability of PF-739 to increase transcription of *Flcn* and *Fnip1/2* are likely mediated by its ability to regulate TFEB.

In summary, we demonstrated in fibroblasts, hepatocytes, as well as at whole organism levels, *in vivo* using zebrafish, that pharmacological/physiological activation of AMPK promoted nuclear translocation of TFEB. This appeared to be through an apparent effect on dephosphorylation of TFEB, independent of mTOR, and was associated with induction of a tumor suppressor FLCN through activation of its promoter activity. Future studies using gain of function models of FLCN in skeletal muscle and other tissues (*e.g.* liver) could reveal the physiological significance of the AMPK-TFEB-FLCN pathway.

MATERIALS AND METHODS

Materials

The materials used comprise 5-aminoimidazole-4-carboxamide riboside (AICAR, OR1170T, Apollo Scientific), Protein G Sepharose (P3296; Sigma), 991 (5-[[6-chloro-5-(1-methylindol-5-yl)-1H-benzimidazol-2-yl]oxy]-2-methyl-benzoic acid, CAS number 129739-36-2)³¹, Rapamycin (R0395, Sigma) and Torin-2 (SML1224, Sigma). General and specific cell culture reagents were obtained from Life Technologies. All other materials unless otherwise indicated were from Sigma.

Antibodies

Total FLCN antibody was purchased from Proteintech (#11236-2-AP). Flag (#F7425), α -tubulin (#T6074), and GAPDH (#G8795) were obtained from Sigma. AMPK α 1 (#07-350) and AMPK α 2 (#07-363) antibodies were obtained from Merck Millipore. Acetyl-CoA carboxylase (ACC; #3676), phospho-ACC1 (Ser79; #3661), AMPK α (#2532), phospho-AMPK α (Thr172; #2535), AMPK β 1 (#4178), lamin A/C (#4777), p70 S6 kinase (#9202), phospho-p70 S6 kinase (Thr389; # 9206), raptor (#2280), phospho-raptor (Ser792; #2083), S6 ribosomal protein (#5G10), phospho-S6 ribosomal protein (Ser235/236; #2211) and TFE3 (#14779) antibodies were obtained from Cell Signaling Technology. TFEB (#A303-673A) antibody purchased was from Bethyl Laboratories. Horseradish peroxidase-conjugated secondary antibodies were from Jackson ImmunoResearch Europe. AMPK γ 1 (#TA300519) antibody was from OriGene. Site-specific rabbit polyclonal antibody against phospho-TFEB (Ser142) was generated by YenZym Antibodies (South San Francisco, CA, USA) by immunisation with a phosphorylated peptide of the sequence identical between human and mouse was used (*i.e.* PN-*S-PMAMHLHIGSNPC-amide, where the prefix *denotes the phosphorylated residue).

Cell culture

Mouse embryonic fibroblasts (MEF) from wild-type (WT) and AMPK α 1^{-/-}/ α 2^{-/-} mice were generated as described previously⁷⁰. TFEB^{-/-}/TFE3^{-/-} MEF were a kind gift from Rosa Puertollano (NIH). MEF were cultured in DMEM-Glutamax supplemented with 10% fetal calf serum (FCS) and 1% penicillin streptomycin. Cells were seeded at ~80% confluency and treated the following day at the indicated treatments described in the figures. Cells were washed with ice-cold PBS and scraped into lysis buffer (50 mM HEPES, 150 mM NaCl, 100 mM NaF, 10

mM Na-pyrophosphate, 5 mM EDTA, 250 mM sucrose, 1 mM DTT, 1% Triton X-100, 1 mM Na-orthovanadate, 0.5 mM PMSF, 1 mM benzamidine HCl, 1 µg/ml leupeptin, 1 µg/ml pepstatin-A, 1 mM microcystin-LR). Primary hepatocytes were isolated from AMPK α 1/ α 2 liver-specific knockout mice and control AMPK α 1^{lox/lox} α 2^{lox/lox} mice littermates (10-week-old males) by collagenase perfusion and cultured as previously described³⁵. The experiments were performed accordingly with the European guidelines (approved by the French authorisation to experiment on vertebrates (no. 75-886) and the ethics committee from University Paris Descartes (no. CEEA34.BV.157.12). Briefly the cells were plated in M199 medium containing Glutamax and supplemented with 100 U/ml penicillin, 100 µg/ml streptomycin, 10% (v/v) FBS, 500 nM dexamethasone (Sigma), 100 nM triiodothyronine (Sigma), and 10 nM insulin (Sigma). The hepatocytes were allowed to attach (4 hours), and were then maintained in M199 medium with antibiotics and 100 nM dexamethasone for 16 hours. Experiments were performed the following morning by treating hepatocytes with the indicated compounds (*e.g.* AMPK activators, mTOR inhibitors) for 1 or 4 hours. For viral infection, the hepatocytes were co-infected (1:3 MOI) with three individual adenovirus encoding AMPK subunits α 2, β 1, γ 1 into AMPK α 1^{-/-}/ α 2^{-/-} hepatocytes to restore expression of the AMPK trimeric complexes. 16 hours following adenovirus infection, the cells were treated for 1 h with vehicle (DMSO) or 991 (10 µM). Following the above described treatments, media were aspirated and cells lysed on ice in cold lysis buffer. Lysates were snap-frozen in liquid nitrogen and stored at -80°C for subsequent analyses. Lysates were clarified at 3500 g for 15 min at 4 °C and quantified using Bradford reagent and BSA as standard.

RNA extraction, microarray and bioinformatic analysis

Total RNA was extracted from cells using RNeasy Tissue Kit (A32645; Beckman Coulter) and quantified by RiboGreen (R11490; ThermoFisher). RNA integrity was determined by Fragment Analyzer, (DNF-471, Advanced Analytical) and an RNA Quality Number greater than 8 was observed. 300 ng of total RNA were used as input to produce labeled cRNA targets with the TotalPrep-96 RNA amplification kit, following manufacturer's instructions. cRNA quality was analyzed by Fragment Analyzer, subsequently 11 µg of cRNA was fragmented and hybridized onto Affymetrix Gene Chip Mouse 430 2.0 following manufacturer's instructions. Partek Genomics Suite software was used to analyze the data from CEL files. Values were normalized using Robust Multichip Average (RMA) method. The removal batch effect was applied during the analysis of the hepatocytes samples. Based on the normal distribution of the datasets, the parametric Pearson's product moment correlation was applied for quality control.

Two-way analysis of variance (ANOVA) with Benjamini & Hochberg multiple testing correction was applied to discriminate 991 versus control and AICAR versus control conditions. The moderated *P*-value was set at 0.05 for the interaction within genetic background and treatment as well as for the pairwise comparisons. In addition, a fold-change cutoff of 1.3 was applied. Considering the quality test results, two samples emerged as outlier and therefore were excluded from the analysis (*i.e.* MEF WT, 991-treated, technical replicate 1 and hepatocytes AMPK $\alpha 1^{-/-}/\alpha 2^{-/-}$, vehicle-stimulated, technical replicate 4, biological replicate 1). The gene ontology was performed using DAVID ^{37,38} and the transcription factor prediction using the upstream regulator analysis available in Ingenuity pathway analysis³⁹ (QIAGEN Inc., <https://www.qiagenbioinformatics.com/products/ingenuity-pathway-analysis>).

RT-qPCR

For cDNA synthesis, 500 ng of total RNA was used as starting material for the PrimeScript RT Kit (Takara, #RR037A). RT-qPCR reactions were performed on a LightCycler 480 with SYBR Green Assay (Roche, #04707516001), with primers at a final concentration of 0.3 μ M/reaction. All the primers used in this study are summarized with sequences in Supplementary Table 2. For mouse samples, three normalization genes were used, namely Acyl-CoA synthetase short-chain (*Acss*), $\beta 2$ microglobulin (*B2m*), Peptidylprolyl isomerase-a (*Ppia*), and their stability was assessed using GeNorm (M value < 0.6)^{71,72}. For zebrafish samples, two normalization genes were used, being elongation factor 1- α (*ef1a*) and nuclear respiratory factor 1 (*nrf1*). Normalized values were calculated by dividing the average expression value by a factor equal to the geometric mean of the normalization genes⁷¹.

The relative *Flcn* mRNA quantity of the samples used in Fig. 3D was assessed using a Biomark gene expression 192.24 IFC delta gene assay, Fluidigm Biomark, following manufacturer's instruction. Ct values were calculated using the system's software (Biomark Real-time PCR analysis, Fluidigm). For the analysis, two normalization genes were used (*Ppia* and TATA box-binding protein (*Tbp*)), afterwards two-way ANOVA was fit to the log-transformed data.

Generation of *actc1b:tfef-ZsGreen*; *actc1b:nls-mCherry* double transgenic fish

Adult AB zebrafish were raised at 28°C under standard husbandry conditions. All experimental procedures were carried out according to the Swiss and EU ethical guidelines and were approved by the animal experimentation ethical committee of Canton of Vaud (permit VD3177). Transgenic zebrafish *Tg(actc1b:tfef-ZsGreen)^{nei08}* and *Tg(actc1b:nls-mCherry)^{nei09}*

were independently generated using I-SCEI meganuclease mediated transgenic insertion into one-cell stage embryos as previously described⁷³. One founder for each transgenic line was selected and subsequent generations were propagated and expanded. The two lines were crossed to generate double transgenic embryos, which have been raised at 28°C under standard laboratory conditions before treatment. Double transgenic embryos were selected at 3 dpf and treated with 991 10 µM or DMSO in 96 well plates (n=12). After 24 h of treatment embryos were anesthetized with 0.016% tricaine and imaged with ImageXpress confocal system at 20X magnification (Molecular Devices). Z stack images were captured for each embryo and maximal projection images were produced.

Generation of *prkaa1*^{-/-};*prkaa2*^{-/-} double knockout fish

The *prkaa1*^{-/-};*prkaa2*^{-/-} double knockout fish were generated by using the CRISPR/Cas9 approach (manuscript in preparation). Two gRNA targeting *prkaa1* exon 5 and *prkaa2* exon 6 were designed using the Chopchop online tool (<http://chopchop.cbu.uib.no/index.php>) and ordered as DNA gene strings. After PCR amplification and purification, they were used as input for in vitro transcription with the MEGAscript T7 Kit (Thermo Fisher Scientific). Subsequently the transcripts were purified with the RNA Clean & Concentrator kit (Zymo Research) and their concentration was determined by Nanodrop. *prkaa1*^{-/-} and *prkaa2*^{-/-} single mutants were generated by independent co-injection of single cell stage AB embryos with 50 pg of gRNA and 200 pg of the GeneArt™ Platinum™ Cas9 Nuclease (Thermo Fisher Scientific). Injected embryos were grown to adulthood and outcrossed with AB wild-type fish to identify individuals with mutant germline. Putative filial 1 mutants were fin clipped, their genotype was determined by HRM qPCR (see Supplementary Table X for primers sequence) and the mutation identified by sequencing. For *prkaa1*, we selected a 5 bp deletion and for *prkaa2* a 7 bp deletion, both resulting in frameshift and premature stop codons. Single heterozygous animals for the same gene were in-crossed to obtain single *prkaa1*^{-/-} or *prkaa2*^{-/-}. The homozygotes were then crossed to obtain double heterozygous fish (*prkaa1*^{+/-};*prkaa2*^{+/-}). Finally, double knockout animals *prkaa1*^{-/-};*prkaa2*^{-/-} were obtained by double heterozygous incross and their genotype was determined by HRM qPCR.

Acute exercise protocol

Acute exercise was performed using a 5 L swim tunnel by Loligo® Systems (#SW10050). The day before the acute exercise session, 6 wild-type and 6 *prkaa1*^{-/-};*prkaa2*^{-/-} 4 months old siblings

were subjected to an endurance test to determine their exercise speed. Baseline critical speed (Ucrit) was determined as the speed by which the weakest zebrafish fatigued (5 sec at the rear of the tunnel). Based on this result, 6 wild-type and 6 *prkaa1^{-/-};prkaa2^{-/-}* fish were let habituate for 20 min at a low current speed of 10 cm/sec and then trained for 2 h 40 min at 55 cm/sec (75% of baseline Ucrit). As control group, the 6 wild-type and 6 *prkaa1^{-/-};prkaa2^{-/-}* fish were placed in the swim tunnel for 3 h at a low swim speed of 10 cm/s. At the end of the 3 h, fish were euthanized immediately and trunk muscle was isolated, flash frozen in liquid nitrogen and processed for RNA and protein extraction.

Bicistronic luciferase assay

MEF were transfected with Lipofectamine 3000 (L3000001, ThermoFisher), 12 h post transfection cells were treated with 30 μ M 991 for 12 h. After the treatment, cells were washed once with PBS and harvested in Glo Lysis Buffer (Promega, #E2661). Cell lysates were centrifuged at 3500 rpm for 10 min at room temperature. Luciferase assay was measured using a Dual-Luciferase Reporter Assay System STOP and GLO kit (Promega, #E1910). Differences in the ratio of Firefly to NanoLuc luciferase signals were analyzed for statistical significance by 2-way ANOVA.

Immunoprecipitation and immunoblotting

For immunoprecipitation of FLCN, 200 μ g of lysates were incubated with 1 μ g of antibody and 5 μ l of Protein-G Sepharose, on a shaker (1000 rpm), overnight at 4°C. Immunoprecipitates or total lysates were first denatured in SDS sample buffer, separated by SDS-PAGE, and then transferred to nitrocellulose membrane. Membranes were blocked for 1 h in 10 mM Tris (pH 7.6), 137 mM NaCl, and 0.1% (v/v) Tween-20 (TBST) containing skimmed milk 5% (w/v). Membranes were incubated in primary antibody prepared in TBST containing 1% (w/v) BSA overnight at 4°C.

Cloning and mutagenesis

All plasmid constructs were generated using standard molecular biology techniques. The promoter sequences and the TFEB/3 binding site were identified from the EPD promoter database (<https://epd.vital-it.ch/index.php>). The promoter regions were amplified from mouse genomic DNA (Promega), then ligated into a modified pNL 1.2 luciferase vector (Promega). The luciferase assay was carried out according to the company's protocol (Promega).

To express transiently the mouse TFEB cDNA, the clone MR223016 was ordered from Origene. The phospho sites corresponding to human S122, S142 and S211 were mutated to alanine using standard molecular biology methods. The sequences of all constructs were verified in house utilizing the BigDyeR Terminator 3.1 kit and the 3500XL Genetic analyzer (ABI-Invitrogen).

Statistical analysis

For the statistical analysis, two-way ANOVA with interaction was used to analyze the data or was fit to the log-transformed data, as specified in the figure legend. Data are expressed as box-and-whisker plot (min to max), log2 fold-change of the mean \pm SEM or SD, as indicated. Differences between groups were considered statistically significant when *P*-value < 0.05.

Accession numbers

The microarray data were deposited in GEO, the accession number will be publicly available once the article is accepted.

ACKNOWLEDGEMENTS

We thank Dr Rosa Puertollano (National Institute of Health, Bethesda, MD) for her generous gift of the TFEB^{-/-}/TFE3^{-/-} mouse embryonic fibroblasts. We thank Dr Julien Marquis for his technical advice on qPCR execution and analysis and Dr Giulia Lizzo for her advice on the gene ontology analysis. We also thank Dr Matthew Sanders for his critical review and editing of the manuscript.

AUTHOR CONTRIBUTIONS

K.S., P.D. and C.C. designed the study. C.C. performed all the treatments in MEF and the promoter activity assay. C.C. also prepared and analyzed MEF, zebrafish and hepatocytes samples, generated the figures, contributed to analysis and data interpretation. M.F. performed the hepatocytes isolation, viral infection, compound treatments, cell collecting and subcellular fractionation. M.D. performed molecular cloning and mutagenesis on TFEB and FLCN promoter. L.B. supervised C.C. during the setup of the gene expression study. S.M. executed the microarray and contributed to mRNA preparation. B.V. and M.F. generated liver-specific

AMPK KO mouse model and AMPK KO MEF. B.V. assisted the design of the hepatocytes study. G.L. contributed to the statistical analysis performing ANOVA analysis fit to log-transformed data. F.R. analyzed with C.C. the microarray data. A.P. generated the AMPK *prkaa1*^{-/-};*prkaa2*^{-/-} zebrafish line and performed with C.C. the fish exercise. G.C. generated and performed experiments on the *actc1b:tfeb-ZsGreen*;*actc1b:nls-mCherry* double transgenic zebrafish. P.G. supervised A.P. and G.C. and contributed study design and interpretation of zebrafish studies. P.D. supervised the microarray and qPCR experiments design, execution and analysis. K.S and P.D. supervised C.C. C.C. and K.S. wrote the manuscript and all the authors contributed to writing/editing the manuscript.

CONFLICT OF INTEREST

G. Civiletto, C. Collodet, M. Deak, P. Descombes, P. Gut, G. Lefebvre, S. Metairon, A. Parisi, F. Raymond and K. Sakamoto are full time employees of Nestlé Research (Switzerland).

REFERENCES

- 1 Hardie, D. G., Ross, F. A. & Hawley, S. A. AMPK: a nutrient and energy sensor that maintains energy homeostasis. *Nat Rev Mol Cell Biol* **13**, 251-262, doi:10.1038/nrm3311 (2012).
- 2 Steinberg, G. R. & Kemp, B. E. AMPK in Health and Disease. *Physiol Rev* **89**, 1025-1078, doi:10.1152/physrev.00011.2008 (2009).
- 3 Barnes, B. R. *et al.* The 5'-AMP-activated protein kinase gamma3 isoform has a key role in carbohydrate and lipid metabolism in glycolytic skeletal muscle. *J Biol Chem* **279**, 38441-38447, doi:10.1074/jbc.M405533200 (2004).
- 4 Bultot, L. *et al.* Benzimidazole derivative small-molecule 991 enhances AMPK activity and glucose uptake induced by AICAR or contraction in skeletal muscle. *Am J Physiol Endocrinol Metab* **311**, E706-E719, doi:10.1152/ajpendo.00237.2016 (2016).
- 5 Salt, I. *et al.* AMP-activated protein kinase: greater AMP dependence, and preferential nuclear localization, of complexes containing the alpha2 isoform. *Biochem J* **334** (Pt 1), 177-187 (1998).
- 6 Wu, J. *et al.* Chemoproteomic analysis of intertissue and interspecies isoform diversity of AMP-activated protein kinase (AMPK). *J Biol Chem* **288**, 35904-35912, doi:10.1074/jbc.M113.508747 (2013).
- 7 Xiao, B. *et al.* Structural basis for AMP binding to mammalian AMP-activated protein kinase. *Nature* **449**, 496-500, doi:10.1038/nature06161 (2007).
- 8 Gowans, G. J., Hawley, S. A., Ross, F. A. & Hardie, D. G. AMP is a true physiological regulator of AMP-activated protein kinase by both allosteric activation and enhancing net phosphorylation. *Cell Metab* **18**, 556-566, doi:10.1016/j.cmet.2013.08.019 (2013).
- 9 Xiao, B. *et al.* Structure of mammalian AMPK and its regulation by ADP. *Nature* **472**, 230-233, doi:10.1038/nature09932 (2011).
- 10 Oakhill, J. S. *et al.* AMPK is a direct adenylate charge-regulated protein kinase. *Science* **332**, 1433-1435, doi:10.1126/science.1200094 (2011).
- 11 Alessi, D. R., Sakamoto, K. & Bayascas, J. R. LKB1-dependent signaling pathways. *Annu Rev Biochem* **75**, 137-163, doi:10.1146/annurev.biochem.75.103004.142702 (2006).

- 12 Garcia, D. & Shaw, R. J. AMPK: Mechanisms of Cellular Energy Sensing and Restoration of Metabolic Balance. *Mol Cell* **66**, 789-800, doi:10.1016/j.molcel.2017.05.032 (2017).
- 13 Coughlan, K. A., Valentine, R. J., Ruderman, N. B. & Saha, A. K. AMPK activation: a therapeutic target for type 2 diabetes? *Diabetes Metab Syndr Obes* **7**, 241-253, doi:10.2147/DMSO.S43731 (2014).
- 14 Day, E. A., Ford, R. J. & Steinberg, G. R. AMPK as a Therapeutic Target for Treating Metabolic Diseases. *Trends Endocrinol Metab* **28**, 545-560, doi:10.1016/j.tem.2017.05.004 (2017).
- 15 Hawley, S. A. *et al.* Use of cells expressing gamma subunit variants to identify diverse mechanisms of AMPK activation. *Cell Metab* **11**, 554-565, doi:10.1016/j.cmet.2010.04.001 (2010).
- 16 Corton, J. M., Gillespie, J. G., Hawley, S. A. & Hardie, D. G. 5-aminoimidazole-4-carboxamide ribonucleoside. A specific method for activating AMP-activated protein kinase in intact cells? *Eur J Biochem* **229**, 558-565 (1995).
- 17 Guigas, B. *et al.* Beyond AICA riboside: in search of new specific AMP-activated protein kinase activators. *IUBMB Life* **61**, 18-26, doi:10.1002/iub.135 (2009).
- 18 Cool, B. *et al.* Identification and characterization of a small molecule AMPK activator that treats key components of type 2 diabetes and the metabolic syndrome. *Cell Metab* **3**, 403-416, doi:10.1016/j.cmet.2006.05.005 (2006).
- 19 Scott, J. W. *et al.* Thienopyridone drugs are selective activators of AMP-activated protein kinase beta1-containing complexes. *Chem Biol* **15**, 1220-1230, doi:10.1016/j.chembiol.2008.10.005 (2008).
- 20 Xiao, B. *et al.* Structural basis of AMPK regulation by small molecule activators. *Nat Commun* **4**, 3017, doi:10.1038/ncomms4017 (2013).
- 21 Lai, Y. C. *et al.* A small-molecule benzimidazole derivative that potently activates AMPK to increase glucose transport in skeletal muscle: comparison with effects of contraction and other AMPK activators. *Biochem J* **460**, 363-375, doi:10.1042/BJ20131673 (2014).
- 22 Treebak, J. T., Birk, J. B., Hansen, B. F., Olsen, G. S. & Wojtaszewski, J. F. A-769662 activates AMPK beta1-containing complexes but induces glucose uptake through a PI3-kinase-dependent pathway in mouse skeletal muscle. *Am J Physiol Cell Physiol* **297**, C1041-1052, doi:10.1152/ajpcell.00051.2009 (2009).

- 23 Benziene, B. *et al.* AMP-activated protein kinase activator A-769662 is an inhibitor of the Na(+)-K(+)-ATPase. *Am J Physiol Cell Physiol* **297**, C1554-1566, doi:10.1152/ajpcell.00010.2009 (2009).
- 24 Moreno, D., Knecht, E., Viollet, B. & Sanz, P. A769662, a novel activator of AMP-activated protein kinase, inhibits non-proteolytic components of the 26S proteasome by an AMPK-independent mechanism. *FEBS Lett* **582**, 2650-2654, doi:10.1016/j.febslet.2008.06.044 (2008).
- 25 Cokorinos, E. C. *et al.* Activation of Skeletal Muscle AMPK Promotes Glucose Disposal and Glucose Lowering in Non-human Primates and Mice. *Cell Metab* **25**, 1147-1159 e1110, doi:10.1016/j.cmet.2017.04.010 (2017).
- 26 Myers, R. W. *et al.* Systemic pan-AMPK activator MK-8722 improves glucose homeostasis but induces cardiac hypertrophy. *Science* **357**, 507-511, doi:10.1126/science.aah5582 (2017).
- 27 Hardie, D. G., Schaffer, B. E. & Brunet, A. AMPK: An Energy-Sensing Pathway with Multiple Inputs and Outputs. *Trends Cell Biol* **26**, 190-201, doi:10.1016/j.tcb.2015.10.013 (2016).
- 28 Schaffer, B. E. *et al.* Identification of AMPK Phosphorylation Sites Reveals a Network of Proteins Involved in Cell Invasion and Facilitates Large-Scale Substrate Prediction. *Cell Metab* **22**, 907-921, doi:10.1016/j.cmet.2015.09.009 (2015).
- 29 Hoffman, N. J. *et al.* Global Phosphoproteomic Analysis of Human Skeletal Muscle Reveals a Network of Exercise-Regulated Kinases and AMPK Substrates. *Cell Metab* **22**, 922-935, doi:10.1016/j.cmet.2015.09.001 (2015).
- 30 Banko, M. R. *et al.* Chemical genetic screen for AMPKalpha2 substrates uncovers a network of proteins involved in mitosis. *Mol Cell* **44**, 878-892, doi:10.1016/j.molcel.2011.11.005 (2011).
- 31 Ducommun, S. *et al.* Motif affinity and mass spectrometry proteomic approach for the discovery of cellular AMPK targets: Identification of mitochondrial fission factor as a new AMPK substrate. *Cell Signal* **27**, 978-988, doi:10.1016/j.cellsig.2015.02.008 (2015).
- 32 Zibrova, D. *et al.* GFAT1 phosphorylation by AMPK promotes VEGF-induced angiogenesis. *Biochem J* **474**, 983-1001, doi:10.1042/BCJ20160980 (2017).
- 33 Goransson, O. *et al.* Mechanism of action of A-769662, a valuable tool for activation of AMP-activated protein kinase. *J Biol Chem* **282**, 32549-32560, doi:10.1074/jbc.M706536200 (2007).

- 34 Hunter, R. W. *et al.* Mechanism of action of compound-13: an alpha1-selective small molecule activator of AMPK. *Chem Biol* **21**, 866-879, doi:10.1016/j.chembiol.2014.05.014 (2014).
- 35 Foretz, M. *et al.* Metformin inhibits hepatic gluconeogenesis in mice independently of the LKB1/AMPK pathway via a decrease in hepatic energy state. *J Clin Invest* **120**, 2355-2369, doi:10.1172/JCI40671 (2010).
- 36 Green, G. H. & Diggle, P. J. On the operational characteristics of the Benjamini and Hochberg False Discovery Rate procedure. *Stat Appl Genet Mol Biol* **6**, Article27, doi:10.2202/1544-6115.1302 (2007).
- 37 Huang da, W., Sherman, B. T. & Lempicki, R. A. Bioinformatics enrichment tools: paths toward the comprehensive functional analysis of large gene lists. *Nucleic Acids Res* **37**, 1-13, doi:10.1093/nar/gkn923 (2009).
- 38 Huang, D. W., Sherman, B. T. & Lempicki, R. A. Systematic and integrative analysis of large gene lists using DAVID bioinformatics resources. *Nature Protocols* **4**, 44, doi:10.1038/nprot.2008.211
- 39 Kramer, A., Green, J., Pollard, J., Jr. & Tugendreich, S. Causal analysis approaches in Ingenuity Pathway Analysis. *Bioinformatics* **30**, 523-530, doi:10.1093/bioinformatics/btt703 (2014).
- 40 Li, Y. *et al.* AMPK phosphorylates and inhibits SREBP activity to attenuate hepatic steatosis and atherosclerosis in diet-induced insulin-resistant mice. *Cell Metab* **13**, 376-388, doi:10.1016/j.cmet.2011.03.009 (2011).
- 41 Raben, N. & Puertollano, R. TFEB and TFE3: Linking Lysosomes to Cellular Adaptation to Stress. *Annu Rev Cell Dev Biol* **32**, 255-278, doi:10.1146/annurev-cellbio-111315-125407 (2016).
- 42 Young, N. P. *et al.* AMPK governs lineage specification through Tfeb-dependent regulation of lysosomes. *Genes Dev* **30**, 535-552, doi:10.1101/gad.274142.115 (2016).
- 43 Pastore, N. *et al.* TFE3 regulates whole-body energy metabolism in cooperation with TFEB. *EMBO Mol Med* **9**, 605-621, doi:10.15252/emmm.201607204 (2017).
- 44 Mansueto, G. *et al.* Transcription Factor EB Controls Metabolic Flexibility during Exercise. *Cell Metab* **25**, 182-196, doi:10.1016/j.cmet.2016.11.003 (2017).
- 45 Yan, M. *et al.* Chronic AMPK activation via loss of FLCN induces functional beige adipose tissue through PGC-1alpha/ERRalpha. *Genes Dev* **30**, 1034-1046, doi:10.1101/gad.281410.116 (2016).

- 46 Yan, M. *et al.* The tumor suppressor folliculin regulates AMPK-dependent metabolic transformation. *J Clin Invest* **124**, 2640-2650, doi:10.1172/JCI71749 (2014).
- 47 Possik, E. *et al.* FLCN and AMPK Confer Resistance to Hyperosmotic Stress via Remodeling of Glycogen Stores. *PLoS Genet* **11**, e1005520, doi:10.1371/journal.pgen.1005520 (2015).
- 48 Settembre, C. *et al.* A lysosome-to-nucleus signalling mechanism senses and regulates the lysosome via mTOR and TFEB. *EMBO J* **31**, 1095-1108, doi:10.1038/emboj.2012.32 (2012).
- 49 Langendorf, C. G. *et al.* Structural basis of allosteric and synergistic activation of AMPK by furan-2-phosphonic derivative C2 binding. *Nat Commun* **7**, 10912, doi:10.1038/ncomms10912 (2016).
- 50 Gilbert, M. J., Zerulla, T. C. & Tierney, K. B. Zebrafish (*Danio rerio*) as a model for the study of aging and exercise: physical ability and trainability decrease with age. *Exp Gerontol* **50**, 106-113, doi:10.1016/j.exger.2013.11.013 (2014).
- 51 Mihaylova, M. M. & Shaw, R. J. The AMPK signalling pathway coordinates cell growth, autophagy and metabolism. *Nat Cell Biol* **13**, 1016-1023, doi:10.1038/ncb2329 (2011).
- 52 Napolitano, G. & Ballabio, A. TFEB at a glance. *J Cell Sci* **129**, 2475-2481, doi:10.1242/jcs.146365 (2016).
- 53 Merrill, G. F., Kurth, E. J., Hardie, D. G. & Winder, W. W. AICA riboside increases AMP-activated protein kinase, fatty acid oxidation, and glucose uptake in rat muscle. *Am J Physiol* **273**, E1107-1112 (1997).
- 54 Hayashi, T., Hirshman, M. F., Kurth, E. J., Winder, W. W. & Goodyear, L. J. Evidence for 5' AMP-activated protein kinase mediation of the effect of muscle contraction on glucose transport. *Diabetes* **47**, 1369-1373 (1998).
- 55 Winder, W. W. *et al.* Activation of AMP-activated protein kinase increases mitochondrial enzymes in skeletal muscle. *J Appl Physiol (1985)* **88**, 2219-2226, doi:10.1152/jappl.2000.88.6.2219 (2000).
- 56 Hunter, R. W. *et al.* Metformin reduces liver glucose production by inhibition of fructose-1-6-bisphosphatase. *Nat Med* **24**, 1395-1406, doi:10.1038/s41591-018-0159-7 (2018).
- 57 Vincent, M. F., Erion, M. D., Gruber, H. E. & Van den Berghe, G. Hypoglycaemic effect of AICARiboside in mice. *Diabetologia* **39**, 1148-1155 (1996).

- 58 Salatto, C. T. *et al.* Selective Activation of AMPK beta1-Containing Isoforms Improves Kidney Function in a Rat Model of Diabetic Nephropathy. *J Pharmacol Exp Ther* **361**, 303-311, doi:10.1124/jpet.116.237925 (2017).
- 59 Shaw, R. J. *et al.* The LKB1 tumor suppressor negatively regulates mTOR signaling. *Cancer Cell* **6**, 91-99, doi:10.1016/j.ccr.2004.06.007 (2004).
- 60 Gwinn, D. M. *et al.* AMPK phosphorylation of raptor mediates a metabolic checkpoint. *Mol Cell* **30**, 214-226, doi:10.1016/j.molcel.2008.03.003 (2008).
- 61 Inoki, K. *et al.* TSC2 integrates Wnt and energy signals via a coordinated phosphorylation by AMPK and GSK3 to regulate cell growth. *Cell* **126**, 955-968, doi:10.1016/j.cell.2006.06.055 (2006).
- 62 Napolitano, G. *et al.* mTOR-dependent phosphorylation controls TFEB nuclear export. *Nat Commun* **9**, 3312, doi:10.1038/s41467-018-05862-6 (2018).
- 63 Medina, D. L. *et al.* Lysosomal calcium signalling regulates autophagy through calcineurin and TFEB. *Nat Cell Biol* **17**, 288-299, doi:10.1038/ncb3114 (2015).
- 64 Li, X. *et al.* Nucleus-Translocated ACSS2 Promotes Gene Transcription for Lysosomal Biogenesis and Autophagy. *Mol Cell* **66**, 684-697 e689, doi:10.1016/j.molcel.2017.04.026 (2017).
- 65 Sardiello, M. *et al.* A gene network regulating lysosomal biogenesis and function. *Science* **325**, 473-477, doi:10.1126/science.1174447 (2009).
- 66 Settembre, C. *et al.* TFEB links autophagy to lysosomal biogenesis. *Science* **332**, 1429-1433, doi:10.1126/science.1204592 (2011).
- 67 Settembre, C. *et al.* TFEB controls cellular lipid metabolism through a starvation-induced autoregulatory loop. *Nat Cell Biol* **15**, 647-658, doi:10.1038/ncb2718 (2013).
- 68 Brady, O. A., Martina, J. A. & Puertollano, R. Emerging roles for TFEB in the immune response and inflammation. *Autophagy* **14**, 181-189, doi:10.1080/15548627.2017.1313943 (2018).
- 69 Wada, S. *et al.* The tumor suppressor FLCN mediates an alternate mTOR pathway to regulate browning of adipose tissue. *Genes Dev* **30**, 2551-2564, doi:10.1101/gad.287953.116 (2016).
- 70 Laderoute, K. R. *et al.* 5'-AMP-activated protein kinase (AMPK) is induced by low-oxygen and glucose deprivation conditions found in solid-tumor microenvironments. *Mol Cell Biol* **26**, 5336-5347, doi:10.1128/MCB.00166-06 (2006).

- 71 Vandesompele, J. *et al.* Accurate normalization of real-time quantitative RT-PCR data by geometric averaging of multiple internal control genes. *Genome Biol* **3**, RESEARCH0034 (2002).
- 72 Hellemans, J. & Vandesompele, J. Selection of reliable reference genes for RT-qPCR analysis. *Methods Mol Biol* **1160**, 19-26, doi:10.1007/978-1-4939-0733-5_3 (2014).
- 73 Thermes, V. *et al.* I-SceI meganuclease mediates highly efficient transgenesis in fish. *Mech Dev* **118**, 91-98 (2002).

FIGURE LEGEND

Figure 1. AMPK-activation in samples used for transcriptomic analyses. (A) Mouse embryonic fibroblasts control (AMPK α 1 α 2^{+/+}) or knockout (AMPK α 1 α 2^{-/-}) were treated with vehicle (DMSO), 2 mM AICAR or 10 μ M 991 for 4 h. Cell lysates (20 μ g) were subjected to western blot analysis with the indicated antibodies and a representative blot of n=3 is shown. (B) Primary hepatocytes were isolated from AMPK α 1/ α 2 liver-specific knockout (AMPK α 1 α 2^{-/-}) mice and control AMPK α 1^{lox/lox} α 2^{lox/lox} mice littermates (AMPK α 1 α 2^{+/+}). Plated cells were treated for 4 h with vehicle (DMSO), 3 μ M 991 or 300 μ M AICAR. Laemmli extracts (20 μ g) were subjected to western blot analysis using the indicated antibodies (n=2).

Figure 2. Hierarchical clustering of the transcriptomic data. Overview of the hierarchical cluster analyses in mouse embryonic fibroblasts (A) and mouse primary hepatocytes (B). Mean-centered gene expression ratios are depicted by a log2 pseudo color scale, red indicates that the gene is overexpressed compared to the mean value whereas blue specifies that the gene is less expressed. Data were analyzed by two-way ANOVA with the factors of genetic background, treatment and interaction. Only selected genes, having a false discover rate (FDR) $P < 0.0001$ for the interaction, are shown.

Figure 3. Transcriptomic data analysis of the AMPK-activation response following treatment with 991 and AICAR. Venn diagrams showing the transcriptome profiling specificity of 991 and AICAR in mouse embryonic fibroblasts (A) and mouse primary hepatocytes (B). Two-way analysis of variance (ANOVA) with Benjamini & Hochberg multiple testing correction was applied to discriminate 991 versus control and AICAR versus control conditions. The moderated P -value was set at 0.05 for the interaction between the genetic background and treatment, as well as for the pairwise comparisons, and a fold-change cutoff of 1.3 was applied. The color corresponds to the two treatment conditions and two cellular models as indicated in the legend. The numbers correspond to the numbers of transcripts altered and the percentage contribution to the total number of transcripts identified for each treatment.

Figure 4. Identification of pathways and genes modulated by AMPK. Gene enrichment analysis of the 991-responsive signature in mouse embryonic fibroblasts (A) and mouse primary hepatocytes (B). DAVID was used to explore the gene ontology terms associated to the AMPK-regulated genes. The bars represent the negative log10(P -value) of enriched terms, indicating the significance of association between the gene list and an indicated ontology term. Relative

mRNA levels of the indicated genes, in mouse embryonic fibroblasts (C) and primary hepatocytes (D). AMPK α 1 α 2^{+/+} or AMPK α 1 α 2^{-/-} MEF were stimulated with 10 μ M 991 or 2 mM AICAR for 4 h, and AMPK α 1 α 2^{+/+} or AMPK α 1 α 2^{-/-} hepatocytes were treated with 3 μ M 991 or 300 μ M AICAR for 4 h. The color corresponds to the two treatment conditions and two cellular models as indicated in the key. Three normalization genes were used (Acyl-CoA synthetase short-chain 2 *Acss2*, β 2 microglobulin *B2m*, Peptidylprolyl isomerase-a *Ppia*), and their stability was assessed using GeNorm (M value < 0.6). Values are represented as log2 fold-change of the mean \pm SD (n=9). The grey shaded area indicates the log2 fold-change threshold of \pm 0.37. For the analysis, a two-way ANOVA with interaction was fit to log-transformed data, **P* < 0.05, ***P* < 0.01, ****P* < 0.001.

Figure 5. Identification of *Flcn* as an AMPK-regulated gene and TFEB as a transcription factor that mediates this response. (A) Relative *Flcn* mRNA quantity was assessed with a Biomark gene expression 192.24 IFC delta gene assay. AMPK α 1 α 2^{+/+} or AMPK α 1 α 2^{-/-} MEF were treated with vehicle (DMSO), 10 μ M 991 or 2 mM AICAR, for 0, 0.5, 1, 2, 4, 8, 12 and 24 h. For the analysis, two normalization genes (*Ppia*, *Tbp*) were used and a two-way ANOVA with interaction was fit to log-transformed data, **P* < 0.05, ****P* < 0.001. Each data point represents the mean \pm SEM (n=12). (B) AMPK α 1 α 2^{+/+} or AMPK α 1 α 2^{-/-} MEF were treated with 10 μ M 991 or 2 mM AICAR for the indicated time points. FLCN was immunoprecipitated (IP) from cell lysates and subjected to immunoblot analysis with the indicated antibodies. A representative blot of three independent experiments is shown. (C) mRNA level of *Flcn* in TFEB/TFE3 control (TFEB/3^{+/+}) or knockout (TFEB/3^{-/-}) MEF treated with 10 μ M 991 or 2 mM AICAR for 4, 12 and 24 h. Data are presented as a box-and-whisker plots (min to max) of values normalized to control (vehicle-treated cells, 4 h). Data were analyzed by a two-way ANOVA with the factors of time and treatment, plus the interaction between these two factors (n=9). Significance of the treatment factor is indicated, *****P* < 0.0001. (D) TFEB/3^{+/+} and TFEB/3^{-/-} MEF were lysed after 0, 24 and 36 h of treatment with 10 μ M 991 or 2 mM AICAR. Laemmli extracts (20 μ g) were subjected to western blot analysis using the indicated antibodies. FLCN was IP from 500 μ g of cell lysate with 1 μ g of anti-Folliculin antibody. Images are representative of n=2.

Figure 6. TFEB translocates to the nucleus upon AMPK stimulation independently of mTOR in MEF. (A) AMPK α 1 α 2^{+/+} or AMPK α 1 α 2^{-/-} MEF were stimulated with vehicle (DMSO), 10 μ M 991 or 2 mM AICAR for 1 h. The cytoplasmic and nuclear fractions were

generated using the NE-PER kit accordingly to the manufacturers' instructions. The lysates (20 µg) were used for western blot analysis of the indicated proteins. **(B)** COS1 cells were transfected for 48 h with no vector (negative control), TFEB control Flag-tagged or Flag-tagged mutated on the phosphorylation site (S142A). TFEB was immunoprecipitated (IP) from 500 µg of cell lysate with 1 µg of anti-Flag antibody, and subjected to western blot analysis (IB) with total TFEB or anti-pS142 TFEB-antibodies. Images are representative of n=2. **(C)** MEF were treated with AMPK activators (10 µM 991 or 2 mM AICAR) or different doses of the mTOR inhibitor Rapamycin (0.05, 0.1 and 0.5 µM) for 1 or 4 h. Cell lysates (20 µg) were subjected to western blot analysis using antibodies against TFEB together with various components of the mTOR- and AMPK-signaling pathways. **(D)** The experiment was performed as described in **(C)**, however Torin-2 (5 or 10 nM) was used as an mTOR inhibitor in place of Rapamycin. Figures are representative of n=2.

Figure 7. TFEB translocates to the nucleus upon AMPK stimulation independently of mTOR in mouse primary hepatocytes. **(A)** AMPK α 1 α 2^{+/+} or AMPK α 1 α 2^{-/-} mouse primary hepatocytes were isolated and cells were treated with 10 µM 991, 300 µM AICAR, 30 µM C13 or Rapamycin 0.05 µM, for 1 or 4 h. Western blot analysis of the indicated proteins was performed on cell lysates. **(B)** Primary hepatocytes were isolated from AMPK α 1 α 2^{-/-} mice and where indicated were co-infected with three adenoviruses (1:3 MOI) in order to rescue the expression of the three subunits of AMPK (Flag- α 2, β 1 and γ 1). 16 h post infection, the primary hepatocytes were treated for 1 h with vehicle (DMSO) or 10 µM 991. Cell lysates (20 µg) were used for western blot analysis with the indicated antibodies. Figures are representative of n=3.

Figure 8. Activation of AMPK in zebrafish leads to translocation of TFEB to the nucleus and increased expression of *flcn* and *fnip2*. **(A)** *Tg(actc1b:tfef-ZsGreen);Tg(actc1b:nls-mCherry)* embryos at 3 dpf were treated with 991 10 µM or vehicle (DMSO) for 24 h. Embryos were mounted live in water containing 0.016% tricaine and imaged with ImageXpress confocal system at 20X magnification, the scale bar corresponds to 50 µm. **(B)** The figure summarizes the experimental scheme implemented to acutely exercise wild-type and *prkaa1*^{-/-};*prkaa2*^{-/-} zebrafish. An electronic controller and a motor-driven propeller were used to adjust the water velocity to maintain the indicated speed. **(C)** Immediately after the three hours of training, muscle samples were collected from the zebrafish. Tissue lysates (20 µg) were separated by SDS-PAGE and western blot analysis was performed using the indicated antibodies. **(D)** mRNA

transcript levels of *flcn* and *fnip2* were calculated using *efla* and *nrf1* as reference genes. Data are shown as box-and-whisker plots (min to max) of values normalized to control wild-type (n=6). Two-way ANOVA with the factors of genetic background and exercise, plus the interaction between these two factors was performed. The graph shows the significance of the interaction, * $P < 0.05$, **** $P < 0.0001$.

Supplementary Figure 1. Principal component analysis (PCA) score plots.

(A) PCA score plot based on gene expression dataset generated from mouse embryonic fibroblasts treated with vehicle (DMSO), 10 μ M 991 or 2 mM AICAR for 4 h. The first two principal components (PC1 and PC2) explain 28.5% and 21.1% of total variance in the data, due to genetic background and treatment, respectively. (B) PCA score plot obtained from the gene expression dataset of mouse primary hepatocytes treated with vehicle (DMSO), 3 μ M 991 or 300 μ M AICAR for 4 h. AICAR and 991 treatment are responsible for 16.6% and 13.1% of the total variance in the data, represented by the two principal components (PC1 and PC2). Samples are depicted as indicated in the legend.

Supplementary Figure 2. *Flcn* pre-mRNA and promoter activity. (A) Schematic representation of the primers designed to measure the pre-mRNA (exon-intron) and mRNA (exon-exon) of *Flcn* (B) Pre-mRNA level of *Flcn* in MEF AMPK α 1 α 2^{+/+} treated with vehicle (DMSO), 10 μ M 991 or 2 mM AICAR for 0, 0.5, 1, 2, 4, 8, 12 and 24 h. Data were analyzed by two-way ANOVA with the factors of time and treatment, plus the interaction between these two factors (n=3). Significance of the treatment factor is indicated, **** $P < 0.0001$. (C) Schematic representation of *Flcn*-NanoLuc luciferase reporter plasmid and the correspondent luciferase activity profile. Several lengths of *Flcn*'s promoter region (-8000, -1200 and -100 bp) were inserted upstream of the NanoLuc luciferase reporter gene. The constructs, along with a firefly luciferase plasmid which served as internal control, were transiently transfected into MEF AMPK α 1 α 2^{+/+} or AMPK α 1 α 2^{-/-}. Cells were then treated with vehicle (DMSO) or 30 μ M 991. Values were first normalized by transfection efficiency, and then represented as log2 fold-change \pm SD, relative to control (vehicle-treated cells) (n=3). The color corresponds to the three treatment conditions as indicated in the key. The grey shaded area indicates the log2 fold-change threshold of ± 0.37 . Data were analyzed by two-way ANOVA with the factors of genetic background and promoter length, plus the interaction between the two factors. Significance of the genetic background is indicated, *** $P < 0.001$, ** $P < 0.01$. (D) MEF WT were transiently transfected with *Flcn*-NanoLuc luciferase (-1200 or -100 bp) control or with a mutation on

TFEB binding site (position -40 bp from the TSS), together with a firefly luciferase plasmid, and treated as above. Values were first normalized by transfection efficiency, and then represented as log2 fold-change \pm SD, relative to control (vehicle-treated cells) (n=3). The color corresponds to the cellular genotype as indicated in the key. Data were analyzed by a two-way ANOVA with the factors of promoter length and TFEB binding site status (control or TFEB-mutated), plus the interaction between these two factors. Significance of the TFEB binding site status is indicated, $**P < 0.01$.

TABLES

Table 1. List of predicted transcription factors mediating AMPK transcriptional response. The 991-responsive genes in mouse embryonic fibroblasts and primary hepatocytes were used to perform an upstream regulator analysis in Ingenuity Pathway Analysis. The table shows the top predicted transcription factors together with their *P*-value.

Mouse embryonic fibroblasts		Mouse primary hepatocytes	
Transcriptional regulator	<i>P</i> -value	Transcriptional regulator	<i>P</i> -value
SREBP-1	1E-14	NUPR1	2E-08
SREBP-2	8E-12	CREB-1	3E-08
STAT4	2E-08	TFEB	6E-08
SIRT2	7E-08	SREBP-1	6E-07
SRC2	7E-06	Miz-1	1E-05
TFEB	2E-04	ATF-4	1E-04
FOXO3	3E-04	ATF-2	3E-04
TP53	4E-04	TCF-3	3E-04
NFATc2	9E-04	MITF	3E-03
IRF-7	3E-03	TAF7L	1E-02
IRF-3	4E-03	HOXD10	1E-01
		HNF-1B	2E-01

Supplementary Table 1. Transcripts differentially regulated in response to 991 and AICAR.

The excel file containing the complete list is available as a separate document.

Supplementary Table 2. qPCR primers.

Danio rerio					
Gene Name	Symbol	Accession Number	Hybridization	Primer (5' to 3')	Amplicon size (bp)
Elongation factor 1-alpha	efla	ENSDARG00000020850	Forward	CTTCTCAGGCTGACTGTGC	358
			Reverse	CCGCTAGCATTACCCTCC	
Folliculin	flcn	NM_001040373.1	Forward	AGTGCCAACACACAACCAAC	107
			Reverse	AGTAGGCAGAGCGAGACCAC	
Folliculin-interacting protein 2	fnip2	NM_001145618	Forward	CGAGAGAAGAGGACGACAGG	125
			Reverse	GGGGAGTTTGGTTTCATCA	
Nuclear respiratory factor 1	nrf1	NM_131680.2	Forward	TTAACTGGAGTTCGGATGG	183
			Reverse	CTGTTCCAGGGTCACCACTT	
Mus musculus					
Gene Name	Symbol	Accession Number	Hybridization	Primer (5' to 3')	Amplicon size (bp)
Acyl-CoA synthetase short-chain 2	Acss2	NM_019811	Forward	ACTTGGCGACAAAGTTGCTT	125
			Reverse	GAATGCCCTGTTTACGGAGA	
β2 microglobulin	B2m	NM_009735	Forward	GAGCCCAAGACCGTCTACTG	134
			Reverse	GCTATTTCTTCTGCGTGCAT	
CREB3 regulatory factor	Crebrf	NM_029870	Forward	TGGGGCCTCAACACTGAATA	109
			Reverse	CCATGCTGGGTTCTCTCTCT	
Folliculin	Flcn	NM_001271356	Forward	TGGATCGGATCTACCTCATCA	119
			Reverse	TGGACATCCAAACTGCTCTG	
Folliculin interacting protein 1	Fnip1	NM_173753	Forward	GATGCGTGTTTCATGTCAAGG	93
			Reverse	GGAGAGTGGGTGCTTGCTAC	
3-hydroxy-3-methylglutaryl-Coenzyme A reductase	Hmgcr	NM_008255.2	Forward	TGGTGGGACCAACCTTCTAC	126
			Reverse	GCCATCACAGTGCCACATAC	
Interferon-induced protein with tetratricopeptide repeats 1	Ifit1	NM_008331	Forward	GCTCTGCTGAAAACCCAGAG	118
			Reverse	GCTTCCATGTGAAGTGACATCT	
Low density lipoprotein receptor	Ldlr	NM_010700	Forward	CAATCGGAAAACCATTTTGG	126
			Reverse	GTGAGTCGATTGGCACTGAA	
Lipin 1	Lpin1	NM_015763	Forward	CATGCCAAGACCAACATCAG	141
			Reverse	CAGTGGCTCTCTCCAAAAGG	
Max binding protein	Mnt	NM_010813	Forward	GCAGCAACAACAGAGAGCAC	150
			Reverse	AGTGGTGGAGCCTCGATTC	
Methylsterol monooxygenase 1	Msmo1	NM_025436	Forward	GGCTCCCTGATAGTTCACGA	137
			Reverse	AAACACTTCCACTGGCCTTC	
Phosphodiesterase 4B, cAMP specific	Pde4b	NM_019840	Forward	ATCAGGGAACCAGGTGTCTG	71
			Reverse	ATGGGATTTCACATCGTTC	
	Ppia	NM_008907	Forward	AGCATACAGGTCCTGGCATC	127

Peptidylprolyl isomerase-a			Reverse	TTCACCTTCCCAAAGACCAC	
Transferrin receptor	<i>Tfrc</i>	NM_011638	Forward	GGAATCCCAGCAGTTTCTTTTGTG	84
			Reverse	CAATGCCTCATAGGTATCCAATC TAG	
Toll interacting protein	<i>Tollip</i>	NM_001347562	Forward	CGCTGGAACAAAGTCATTCA	114
			Reverse	GATGTGGGTCCAAGCTATGC	
Thioredoxin interacting protein	<i>Txnip</i>	NM_001009935	Forward	ACCAGTGTCTGCCAAAAAGG	132
			Reverse	TCAAAGTCAGCATGGATGGA	

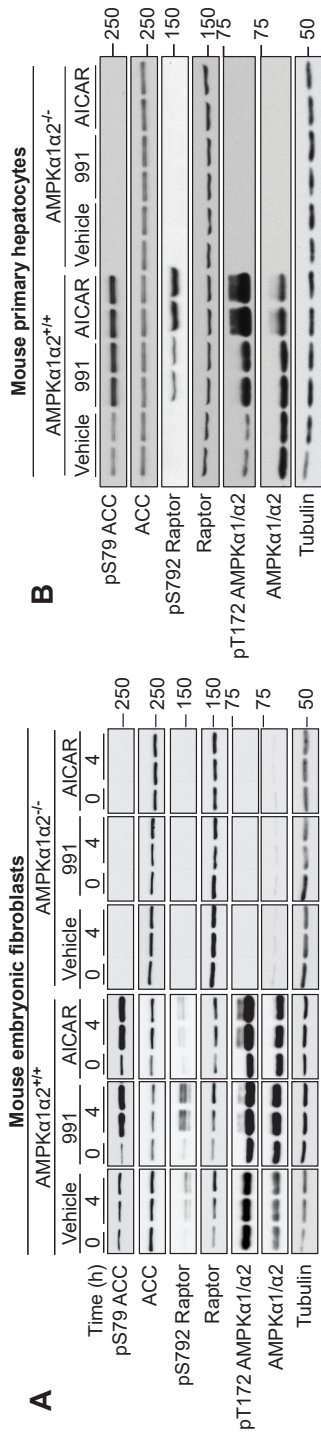


Fig. 1

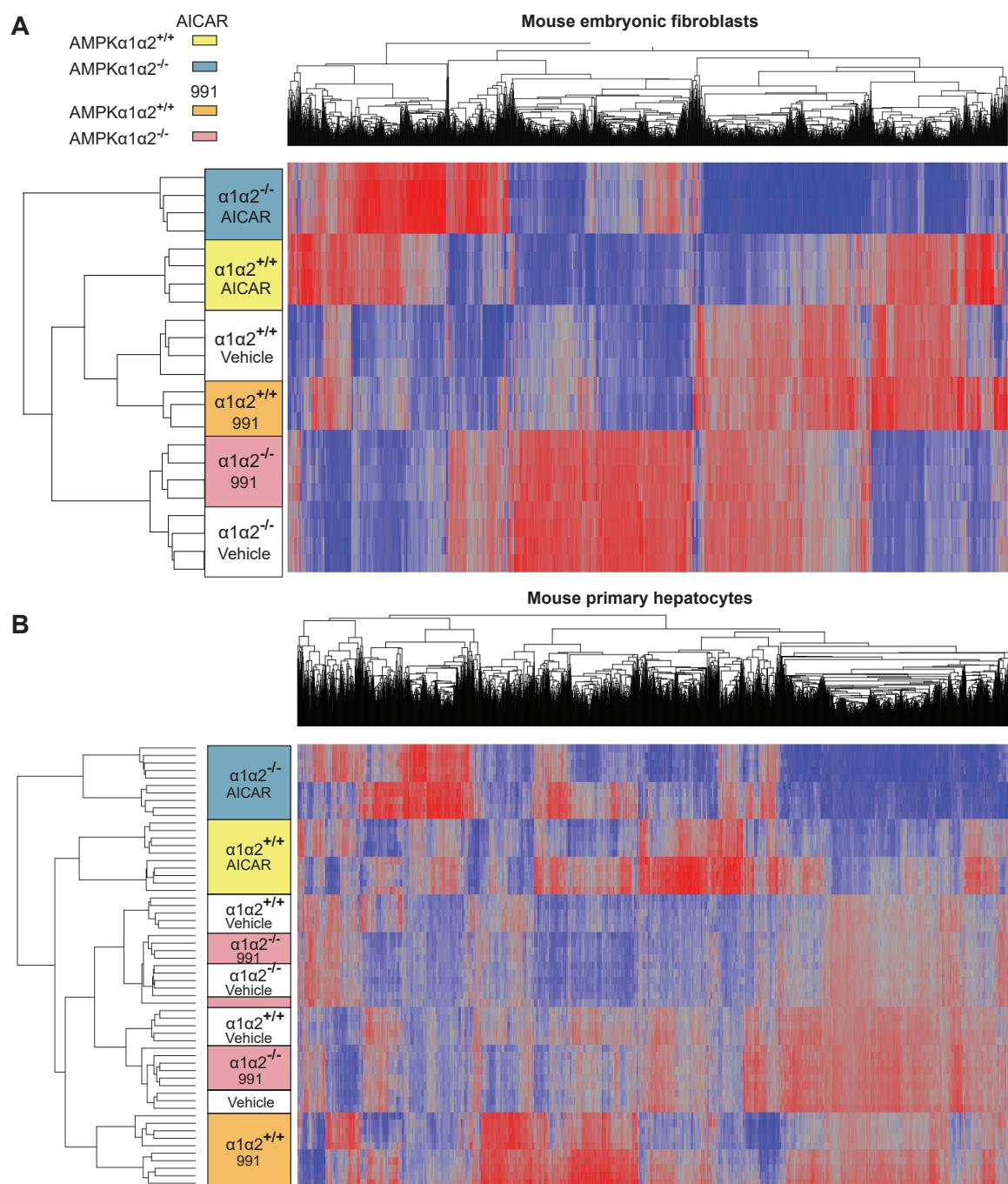


Fig. 2

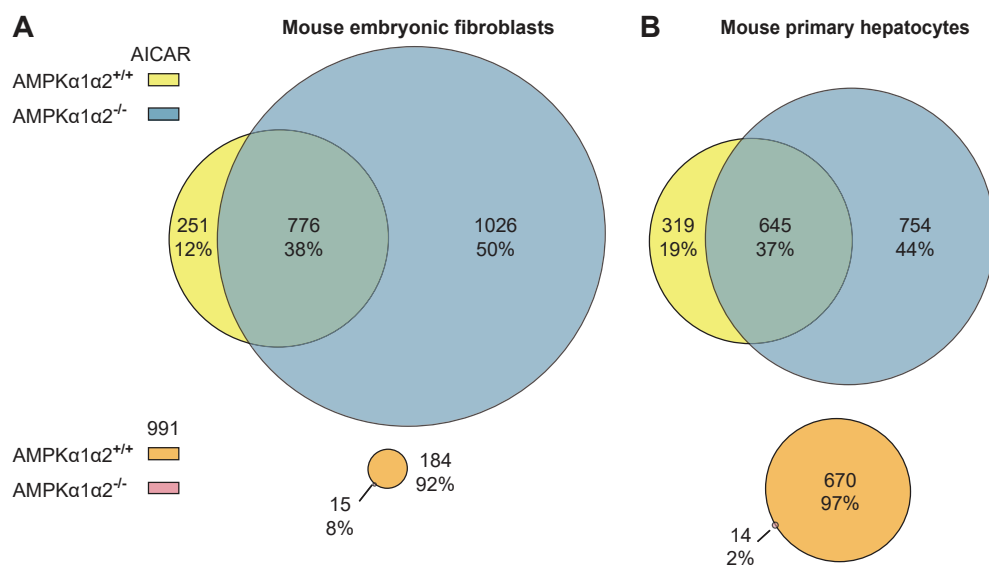


Fig. 3

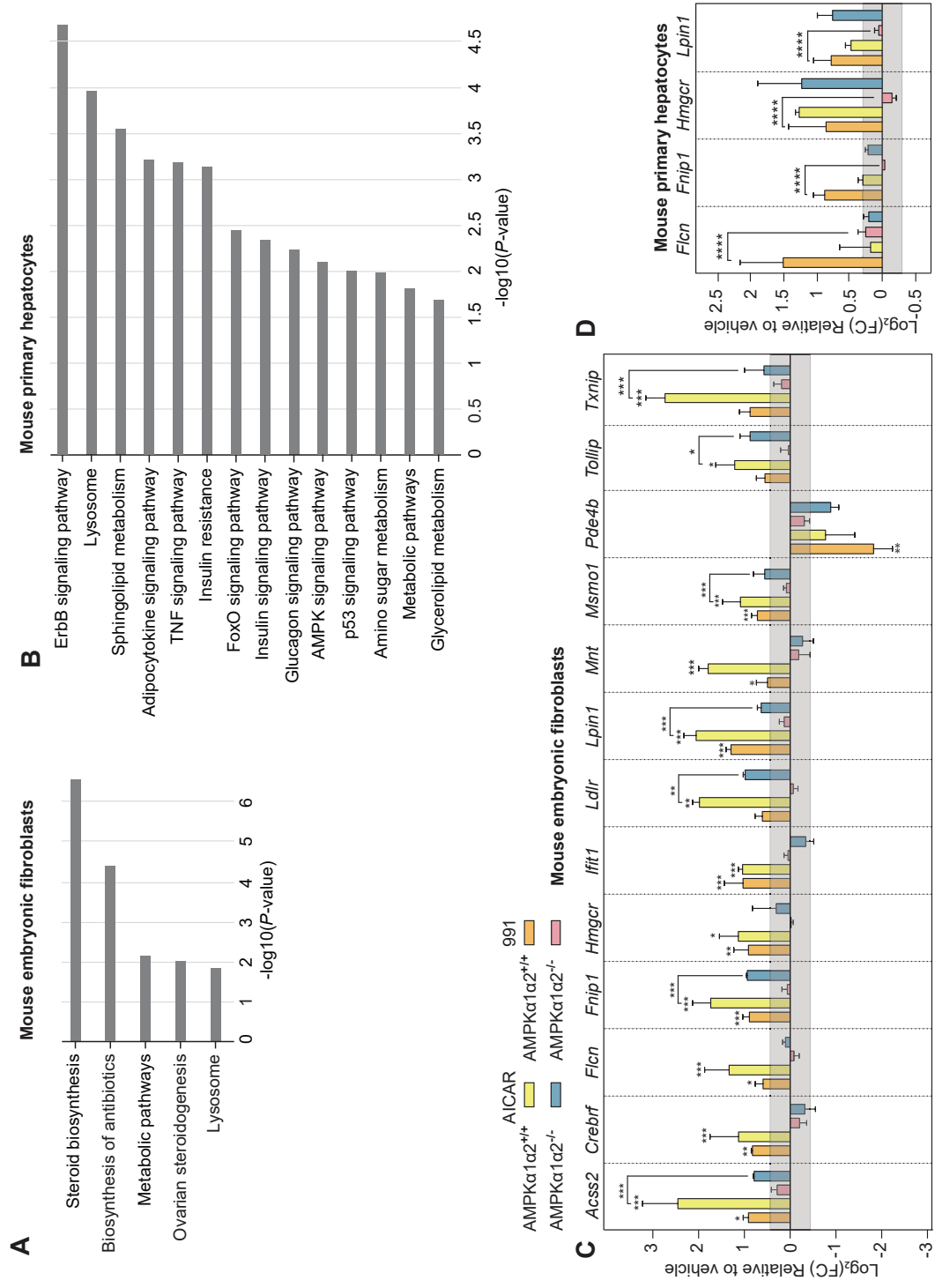


Fig. 4

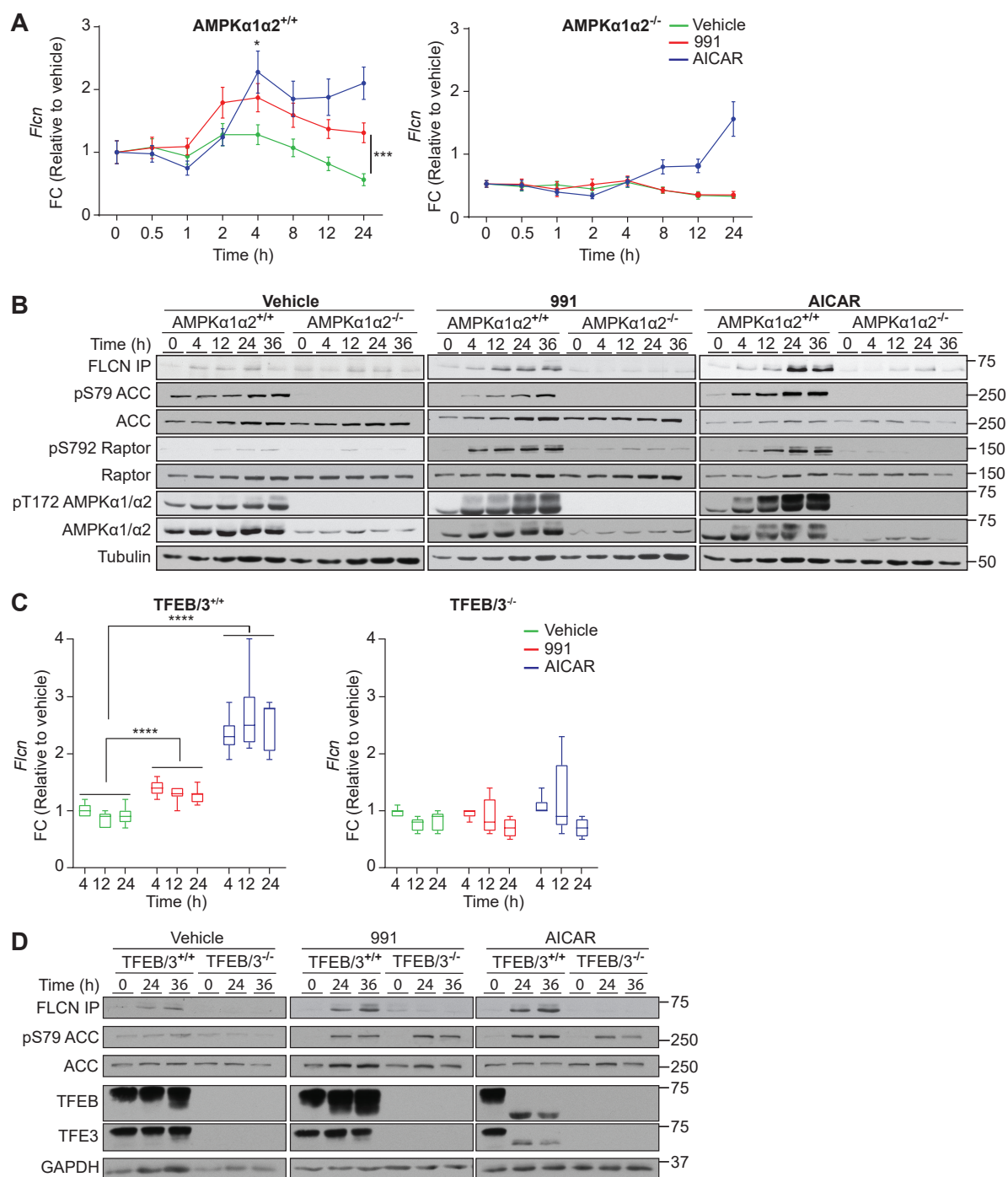


Fig. 5

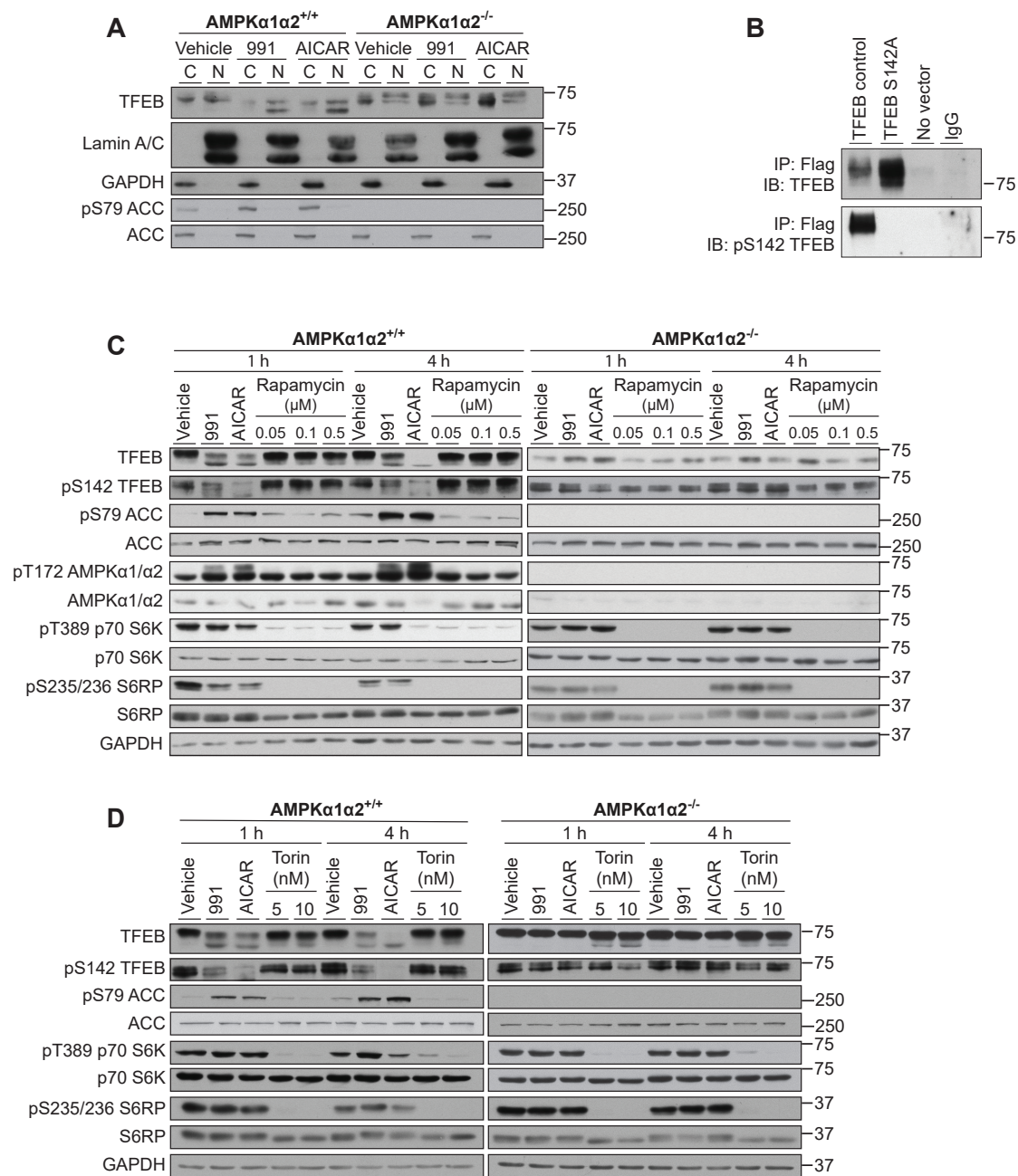


Fig. 6

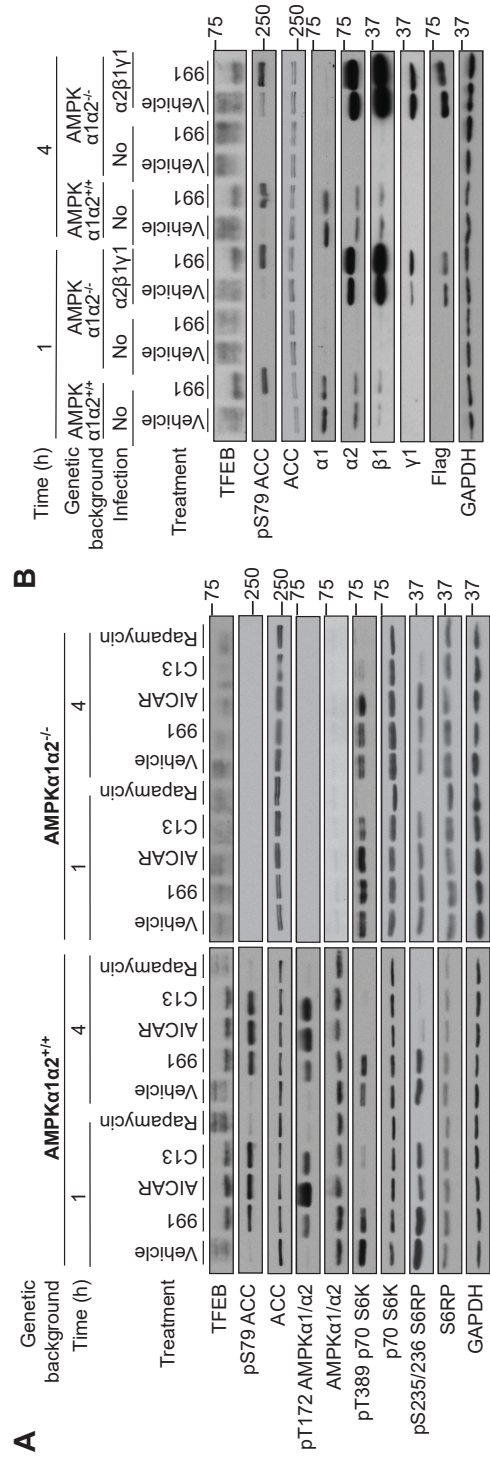


Fig. 7

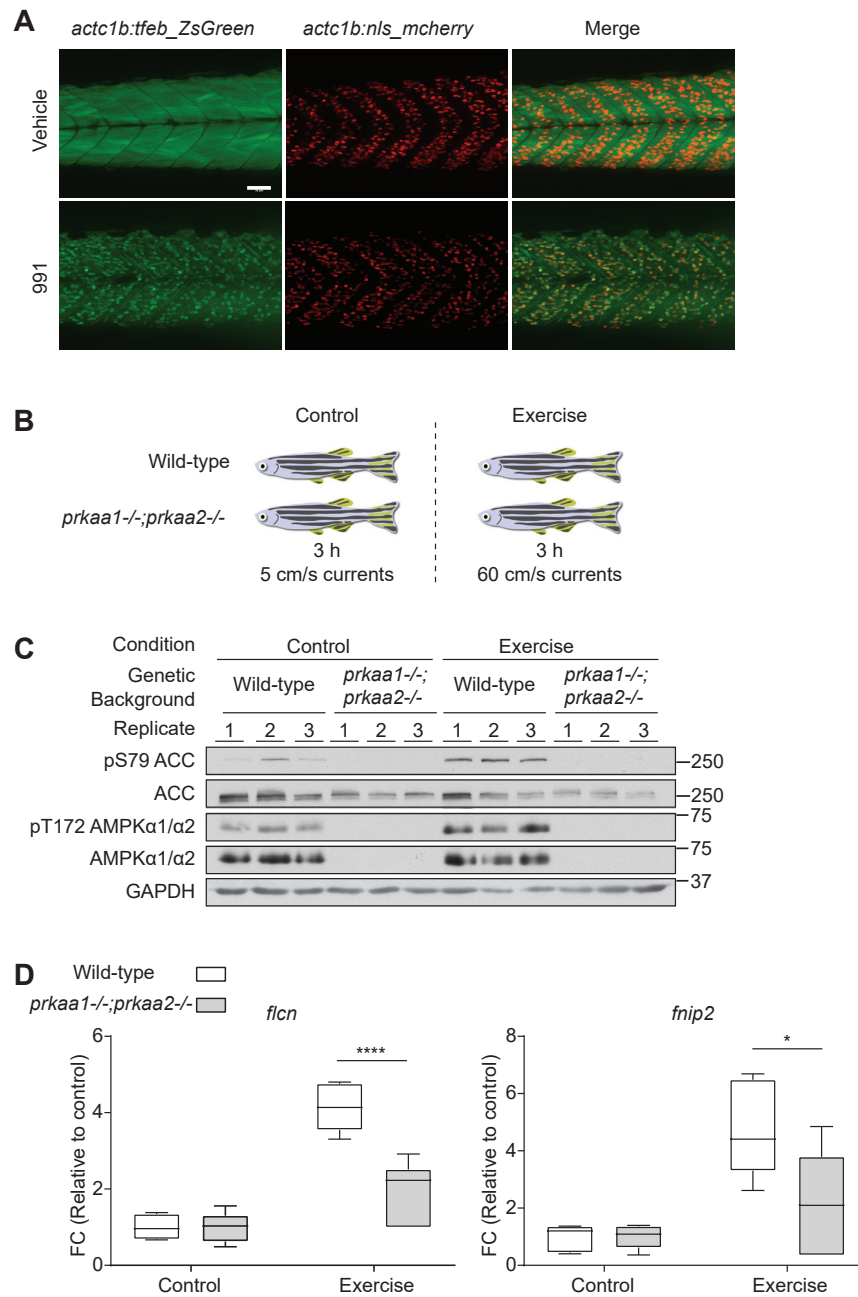
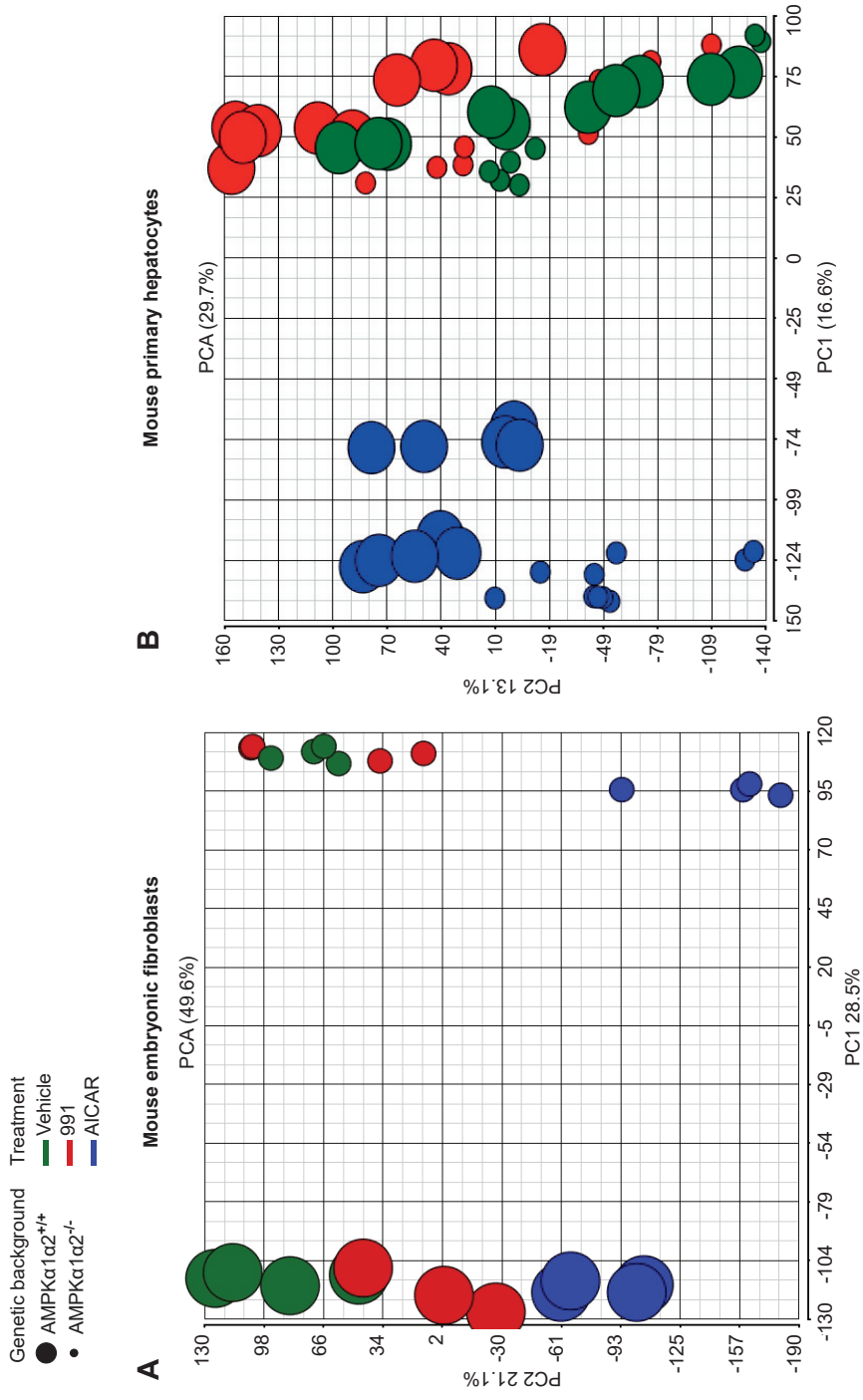
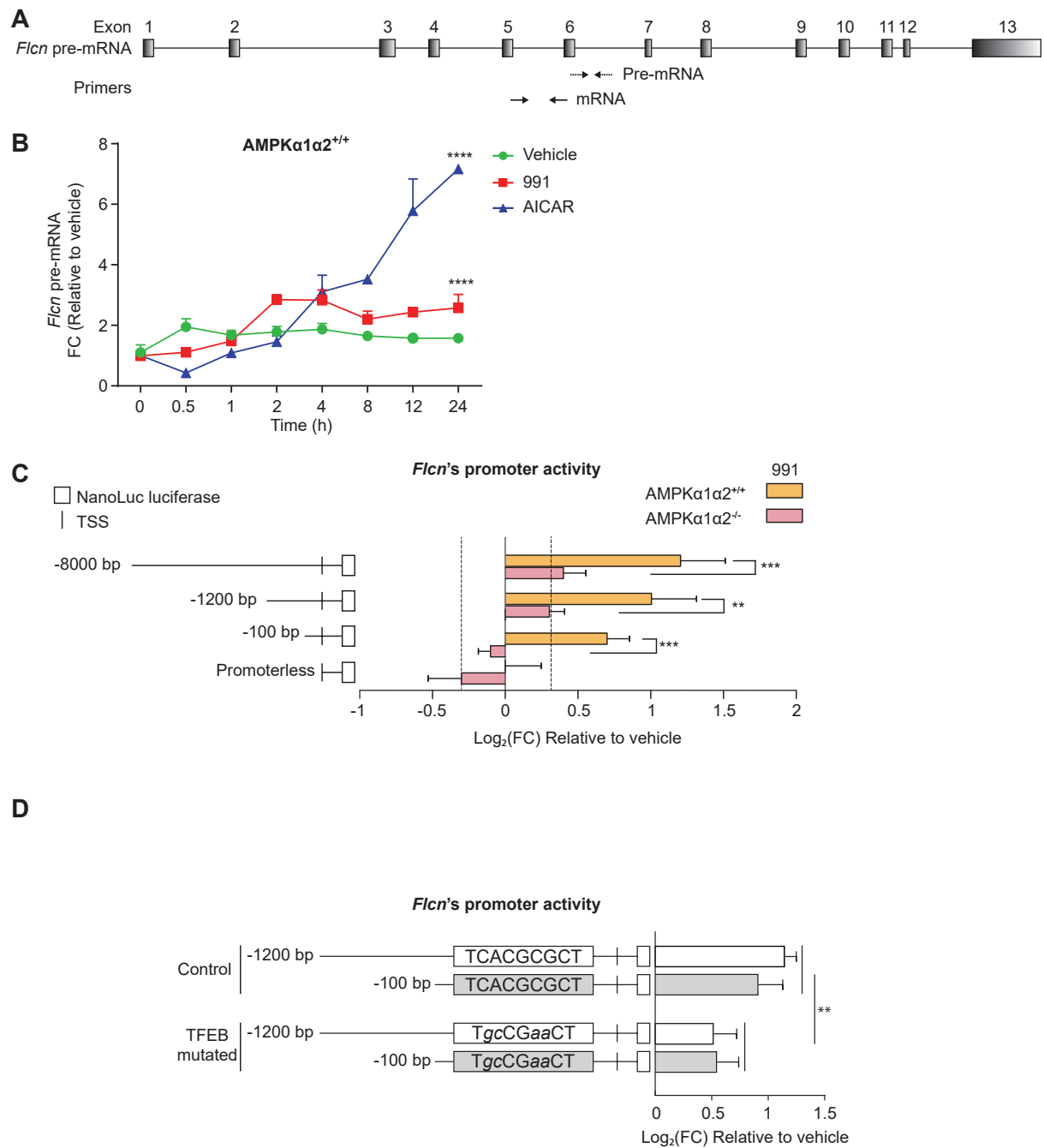


Fig. 8



Supplementary Fig. 1



Supplementary Fig. 2

9.5 List of genes regulated by 991 in MEFs

Gene symbol	Gene title	FC 991 vs Vehicle	FC AICAR vs Vehicle
<i>Ackr3</i>	atypical chemokine receptor 3	-1.7	
<i>Acot13</i>	acyl-CoA thioesterase 13	1.3	
<i>Acss2</i>	acyl-CoA synthetase short-chain family member 2	1.6	2.0
<i>Adar</i>	adenosine deaminase, RNA-specific	1.3	1.4
<i>Ahr</i>	aryl-hydrocarbon receptor repressor	1.5	
<i>AI413582</i>	expressed sequence AI413582	1.5	
<i>Ankrd12</i>	ankyrin repeat domain 12	1.4	
<i>Anln</i>	anillin, actin binding protein	1.3	
<i>Arl5b</i>	ADP-ribosylation factor-like 5B	1.3	1.4
<i>Armc8</i>	armadillo repeat containing 8	1.3	-1.5
<i>Atf3</i>	activating transcription factor 3	1.3	
<i>Atp6v0b</i>	ATPase, H+ transporting, lysosomal V0 subunit B	1.3	1.4
<i>Atp6v1b2</i>	ATPase, H+ transporting, lysosomal V1 subunit B2	1.4	
<i>Avl9</i>	AVL9 homolog (S. cerevisiae)	1.5	2.6
<i>AW549877</i>	expressed sequence AW549877	1.5	
<i>BC022687</i>	cDNA sequence BC022687	1.3	
<i>Bhlhe40</i>	basic helix-loop-helix family, member e40	1.7	
<i>Blvrb</i>	biliverdin reductase B (flavin reductase (NADPH))	1.4	
<i>Bri3</i>	brain protein I3	1.3	
<i>Bsdc1</i>	BSD domain containing 1	1.3	1.3
<i>Ccdc25</i>	coiled-coil domain containing 25	1.5	3.8
<i>Cmtm3</i>	CKLF-like MARVEL transmembrane domain containing 3	1.3	-1.3
<i>Cpt2</i>	carnitine palmitoyltransferase 2	1.3	
<i>Crebrf</i>	CREB3 regulatory factor	2.1	1.6
<i>Cxcl1</i>	chemokine (C-X-C motif) ligand 1	-1.5	-2.5
<i>Cxcl10</i>	chemokine (C-X-C motif) ligand 10	1.4	
<i>Cxcl5</i>	chemokine (C-X-C motif) ligand 5	-2.2	-5.7
<i>Cyp1a1</i>	cytochrome P450, family 1, subfamily a, polypeptide 1	1.4	-1.3
<i>Dars2</i>	aspartyl-tRNA synthetase 2 (mitochondrial)	1.3	
<i>Dbp</i>	D site albumin promoter binding protein	1.4	
<i>Ddit3</i>	DNA-damage inducible transcript 3	1.6	
<i>Dhcr7</i>	7-dehydrocholesterol reductase	1.3	1.3
<i>Dido1</i>	death inducer-obliterators 1	-1.4	-4.0
<i>Dlx4</i>	distal-less homeobox 4	-1.4	
<i>Dnajb6</i>	DnaJ (Hsp40) homolog, subfamily B, member 6	1.3	
<i>Dpp7</i>	dipeptidylpeptidase 7	1.6	1.7
<i>Dscc1</i>	defective in sister chromatid cohesion 1 homolog	1.3	1.4
<i>Dusp3</i>	dual specificity phosphatase 3 (vaccinia virus phosphatase VH1-related)	1.4	1.4
<i>Efnb2</i>	ephrin B2	-1.3	
<i>Eno2</i>	enolase 2, gamma neuronal	1.5	-1.4
<i>Fam13b</i>	family with sequence similarity 13, member B	-1.3	
<i>Fbxl4</i>	F-box and leucine-rich repeat protein 4	1.3	
<i>Fbxo32</i>	F-box protein 32	1.3	-1.6
<i>Fdft1</i>	farnesyl diphosphate farnesyl transferase 1	1.4	1.5
<i>Fgfr1op</i>	Fgfr1 oncogene partner	1.4	1.6
<i>Flcn</i>	folliculin	1.6	1.3
<i>Fmod</i>	fibromodulin	-1.4	-1.4
<i>Fnip1</i>	folliculin interacting protein 1	1.7	2.0
<i>Fnip2</i>	folliculin interacting protein 2	1.6	1.6
<i>Gdap10</i>	ganglioside-induced differentiation-associated-protein 10	1.4	
<i>Gdnf</i>	glial cell line derived neurotrophic factor	1.3	
<i>Gm19651</i>	predicted gene, 19651	1.3	
<i>Gm19773</i>	predicted gene, 19773	1.4	1.6
<i>Lin52</i>	lin-52 homolog (C. elegans)	1.3	1.4
<i>Ubal2</i>	UBA-like domain containing 2	1.3	
<i>Gnpda1</i>	glucosamine-6-phosphate deaminase 1	1.4	
<i>Gns</i>	glucosamine (N-acetyl)-6-sulfatase	1.4	1.6

<i>Gpr137b-ps</i>	G protein-coupled receptor 137B, pseudogene	1.4	
<i>HagH</i>	hydroxyacyl glutathione hydrolase	1.3	
<i>Hbp1</i>	high mobility group box transcription factor 1	1.6	1.4
<i>Hmgcs1</i>	3-hydroxy-3-methylglutaryl-Coenzyme A synthase 1	1.5	1.4
<i>Hmox1</i>	heme oxygenase (decycling) 1	1.3	
<i>Hs1bp3</i>	HCLS1 binding protein 3	1.4	
<i>Hsd17b7</i>	hydroxysteroid (17-beta) dehydrogenase 7	1.6	2.1
<i>Hsd1l</i>	hydroxysteroid dehydrogenase like 1	1.3	
<i>Ifit1</i>	interferon-induced protein with tetratricopeptide repeats 1	1.7	1.8
<i>Ifit2</i>	interferon-induced protein with tetratricopeptide repeats 2	1.5	
<i>Ing5</i>	inhibitor of growth family, member 5	1.4	
<i>Jade1</i>	jade family PHD finger 1	1.4	
<i>Kantr</i>	Kdm5c adjacent non-coding transcript	1.3	1.9
<i>Klf11</i>	Kruppel-like factor 11	1.4	2.9
<i>Klf2</i>	Kruppel-like factor 2 (lung)	-1.5	
<i>Klf9</i>	Kruppel-like factor 9	1.5	1.5
<i>Klhl24</i>	kelch-like 24	1.6	
<i>Ldlr</i>	low density lipoprotein receptor	1.3	1.7
<i>Lonrf1</i>	LON peptidase N-terminal domain and ring finger 1	1.3	1.5
<i>Lpin1</i>	lipin 1	1.9	2.1
<i>Lrp8</i>	low density lipoprotein receptor-related protein 8	1.3	
<i>Lss</i>	lanosterol synthase	1.5	1.4
<i>Maff</i>	v-maf musculoaponeurotic fibrosarcoma oncogene family, protein F	1.3	
<i>Mafg</i>	v-maf musculoaponeurotic fibrosarcoma oncogene family, protein G	1.3	1.5
<i>Mblac2</i>	metallo-beta-lactamase domain containing 2	1.4	
<i>Mcoln1</i>	mucolipin 1	1.4	
<i>Med1</i>	mediator complex subunit 1	1.4	2.1
<i>Mnt</i>	max binding protein	1.4	2.0
<i>Mroh1</i>	maestro heat-like repeat family member 1	1.4	1.4
<i>Msmo1</i>	methylsterol monooxygenase 1	1.5	1.7
<i>Mt1</i>	metallothionein 1	1.5	
<i>Mvd</i>	mevalonate (diphospho) decarboxylase	1.6	1.5
<i>Naga</i>	N-acetyl galactosaminidase, alpha	1.3	
<i>Nbr1</i>	neighbor of Brca1 gene 1	1.3	1.4
<i>NdrG1</i>	N-myc downstream regulated gene 1	1.5	
<i>Nedd4l</i>	neural precursor cell expressed	1.3	
<i>Neil3</i>	nei like 3 (E. coli)	1.3	1.3
<i>Neu1</i>	neuraminidase 1	1.7	
<i>Nub1</i>	negative regulator of ubiquitin-like proteins 1	1.3	1.4
<i>Olfm1</i>	olfactomedin 1	1.3	
<i>Ostm1</i>	osteopetrosis associated transmembrane protein 1	1.3	
<i>P2rx4</i>	purinergic receptor P2X, ligand-gated ion channel 4	1.4	
<i>Pde4b</i>	phosphodiesterase 4B, cAMP specific	-1.6	-1.8
<i>Plau</i>	plasminogen activator, urokinase	-1.6	-1.8
<i>Pparg</i>	peroxisome proliferator activated receptor gamma	1.3	
<i>Pqlc2</i>	PQ loop repeat containing 2	1.4	
<i>Ptgs2</i>	prostaglandin-endoperoxide synthase 2	1.3	
<i>Ptpdc1</i>	protein tyrosine phosphatase domain containing 1	1.4	
<i>Pvr</i>	poliovirus receptor	1.3	
<i>Rab20</i>	RAB20, member RAS oncogene family	1.3	
<i>Rdh11</i>	retinol dehydrogenase 11	1.4	1.6
<i>Runx1t1</i>	runt-related transcription factor 1	1.5	1.4
<i>Sc5d</i>	sterol-C5-desaturase	1.4	2.2
<i>Serac1</i>	serine active site containing 1	1.5	
<i>Slc1a3</i>	solute carrier family 1	-1.3	-1.5
<i>Slc25a40</i>	solute carrier family 25, member 40	1.3	
<i>Slc35f5</i>	solute carrier family 35, member F5	1.3	
<i>Slc4a7</i>	solute carrier family 4, sodium bicarbonate cotransporter, member 7	1.3	
<i>Smad2</i>	SMAD family member 2	1.3	1.5
<i>Smc2</i>	structural maintenance of chromosomes 2	1.3	1.8
<i>Snx16</i>	sorting nexin 16	1.3	1.5
<i>Sox11</i>	SRY (sex determining region Y)-box 11	-1.4	-1.9
<i>Stard4</i>	StAR-related lipid transfer (START) domain containing 4	1.4	1.4

<i>Stat2</i>	signal transducer and activator of transcription 2	1.4	
<i>Stx3</i>	syntaxin 3	1.4	1.6
<i>Tbcel</i>	tubulin folding cofactor E-like	1.3	1.3
<i>Thumpd2</i>	THUMP domain containing 2	1.3	
<i>Tiparp</i>	TCDD-inducible poly(ADP-ribose) polymerase	1.5	1.6
<i>Tmem55b</i>	transmembrane protein 55b	1.6	
<i>Tnfrsf10b</i>	tumor necrosis factor receptor superfamily, member 10b	1.3	
<i>Tollip</i>	toll interacting protein	1.4	1.6
<i>Tsc1</i>	tuberous sclerosis 1	1.3	
<i>Tslp</i>	thymic stromal lymphopoietin	1.3	
<i>Txnip</i>	thioredoxin interacting protein	1.6	3.6
<i>Uap1l1</i>	UDP-N-acetylglucosamine pyrophosphorylase 1-like 1	1.3	
<i>Ube2t</i>	ubiquitin-conjugating enzyme E2T (putative)	1.5	
<i>Vash2</i>	vasohibin 2	1.3	
<i>Vldlr</i>	very low density lipoprotein receptor	1.4	
<i>Wbp2</i>	WW domain binding protein 2	1.3	1.3
<i>Ypel5</i>	yippee-like 5 (Drosophila)	1.5	
<i>Zfp467</i>	zinc finger protein 467	-1.3	
<i>Zfp655</i>	zinc finger protein 655	1.3	1.5
<i>Zfyve26</i>	zinc finger, FYVE domain containing 26	1.4	

Appendix Table 1. List of genes regulated by 991 in MEFs.

The table reports the genes modulated following 991 treatment in MEFs, indicating gene symbol and title, together with the fold change (FC) following treatment with 991 or AICAR (when present). For filtering the corresponding transcripts, the moderated *P*-value was set at 0.05 and a FC cutoff of 1.3 was applied.

9.6 List of genes regulated by 991 in mouse primary hepatocytes

Gene symbol	Gene title	FC 991 vs Vehicle	FC AICAR vs Vehicle
<i>Aacs</i>	acetoacetyl-CoA synthetase	1.5	
<i>Abca1</i>	ATP-binding cassette, sub-family A (ABC1), member 1	1.4	
<i>Acacb</i>	acetyl-Coenzyme A carboxylase beta	1.4	1.8
<i>Acot6</i>	acyl-CoA thioesterase 6	1.5	
<i>Acp1</i>	acid phosphatase 1, soluble	-1.6	-1.8
<i>Adh1</i>	alcohol dehydrogenase 1 (class I)	1.3	
<i>Adnp2</i>	ADNP homeobox 2	1.4	
<i>Adrb2</i>	adrenergic receptor, beta 2	-1.5	-1.4
<i>Aen</i>	apoptosis enhancing nuclease	-1.4	
<i>AgI</i>	amylase-1,6-glucosidase, 4-alpha-glucanotransferase	-1.3	
<i>Agpat9</i>	1-acylglycerol-3-phosphate O-acyltransferase 9	1.4	
<i>Ahr</i>	aryl-hydrocarbon receptor	-2.0	1.4
<i>Airn</i>	antisense Igf2r RNA	-1.5	-1.5
<i>Ajuba</i>	ajuba LIM protein	-1.7	
<i>Akap13</i>	A kinase (PRKA) anchor protein 13	-1.4	-1.5
<i>Amn1</i>	antagonist of mitotic exit network 1	1.6	
<i>Amotl2</i>	angiomin-like 2	-1.8	1.4
<i>Ankrd12</i>	ankyrin repeat domain 12	1.5	
<i>Ankrd23</i>	ankyrin repeat domain 23	1.8	1.4
<i>Ankrd33b</i>	ankyrin repeat domain 33B	1.9	
<i>Ankrd50</i>	ankyrin repeat domain 50	1.3	
<i>Anks4b</i>	ankyrin repeat and sterile alpha motif domain containing 4B	-1.3	
<i>Aox1</i>	aldehyde oxidase 1	-1.4	
<i>Ap5s1</i>	adaptor-related protein 5 complex, sigma 1 subunit	1.6	
<i>Appl2</i>	adaptor protein, phosphotyrosine interaction	1.5	
<i>Areg</i>	amphiregulin	3.9	
<i>Arf2</i>	ADP-ribosylation factor 2	-1.3	
<i>Arhgap12</i>	Rho GTPase activating protein 12	1.4	
<i>Arhgap22</i>	Rho GTPase activating protein 22	1.5	
<i>Arhgap29</i>	Rho GTPase activating protein 29	-1.5	
<i>Arl4a</i>	ADP-ribosylation factor-like 4A	1.5	
<i>Arl5b</i>	ADP-ribosylation factor-like 5B	1.4	
<i>Arm66</i>	armadillo repeat containing 6	-1.3	
<i>Arntl</i>	aryl hydrocarbon receptor nuclear translocator-like	-1.3	
<i>Arsa</i>	arylsulfatase A	1.3	
<i>Asb11</i>	ankyrin repeat and SOCS box-containing 11	1.4	
<i>Atf3</i>	activating transcription factor 3	2.7	1.7
<i>Atf7ip</i>	activating transcription factor 7 interacting protein	1.3	
<i>Atp6v1b2</i>	ATPase, H+ transporting, lysosomal V1 subunit B2	1.6	
<i>Atp6v1h</i>	ATPase, H+ transporting, lysosomal V1 subunit H	2.0	2.3
<i>Avl9</i>	AVL9 homolog (S. cerevisiae)	1.4	
<i>B3gnt2</i>	UDP-GlcNAc:betaGal beta-1,3-N-acetylglucosaminyltransferase 2	1.4	
<i>B630005N14Rik</i>	RIKEN cDNA B630005N14 gene	-1.4	
<i>Baat</i>	bile acid-Coenzyme A: amino acid N-acyltransferase	-1.3	
<i>Bach2</i>	BTB and CNC homology 2	1.6	2.2
<i>Bag2</i>	BCL2-associated athanogene 2	-1.4	
<i>Bcl2l11</i>	BCL2-like 11 (apoptosis facilitator)	-1.3	
<i>Bcl3</i>	B cell leukemia/lymphoma 3	-1.6	-1.3
<i>Bex2</i>	brain expressed X-linked 2	1.4	
<i>Bhlhe40</i>	basic helix-loop-helix family, member e40	1.4	
<i>Bik</i>	BCL2-interacting killer	-1.3	-1.6
<i>Birc2</i>	baculoviral IAP repeat-containing 2	-1.7	
<i>Bmp4</i>	bone morphogenetic protein 4	1.5	
<i>Btc</i>	betacellulin, epidermal growth factor family member	2.0	
<i>Btg2</i>	B cell translocation gene 2, anti-proliferative	1.4	1.5
<i>C1qb</i>	complement component 1, q subcomponent, beta polypeptide	-1.4	

<i>Camk1d</i>	Mus musculus calcium/calmodulin-dependent protein kinase ID	-1.8	-1.8
<i>Camk2d</i>	calcium/calmodulin-dependent protein kinase II, delta	1.3	2.6
<i>Carf</i>	calcium response factor	1.4	
<i>Cblb</i>	Casitas B-lineage lymphoma b	-2.0	-7.4
<i>Cbr3</i>	carbonyl reductase 3	-1.5	-2.0
<i>Ccdc71l</i>	coiled-coil domain containing 71 like	1.4	
<i>Ccl20</i>	chemokine (C-C motif) ligand 20	-1.6	-1.7
<i>Ccl3</i>	chemokine (C-C motif) ligand 3	1.5	1.6
<i>Ccng2</i>	cyclin G2	1.4	
<i>Cda</i>	cytidine deaminase	1.3	
<i>Cdc42ep5</i>	CDC42 effector protein (Rho GTPase binding) 5	-1.5	
<i>Cdt1</i>	chromatin licensing and DNA replication factor 1	1.3	
<i>Cebpa</i>	CCAAT/enhancer binding protein (C/EBP), alpha	-1.4	
<i>Cep85</i>	centrosomal protein 85	1.5	
<i>Chac1</i>	ChaC, cation transport regulator 1	2.1	
<i>Chd3os</i>	chromodomain helicase DNA binding protein 3, opposite strand	1.3	
<i>Chd7</i>	chromodomain helicase DNA binding protein 7	1.3	
<i>Chka</i>	choline kinase alpha	1.6	
<i>Chsy3</i>	chondroitin sulfate synthase 3	1.6	-1.4
<i>Clart</i>	circadian associated repressor of transcription	1.5	
<i>Cited2</i>	Cbp/p300-interacting transactivator	-2.1	
<i>Clcn6</i>	chloride channel 6	1.3	
<i>Clcn7</i>	chloride channel 7	1.3	
<i>Cldn14</i>	claudin 14	1.3	1.4
<i>Cldn4</i>	claudin 4	2.0	
<i>Clec2d</i>	C-type lectin domain family 2, member d	2.0	-2.2
<i>Cln6</i>	ceroid-lipofuscinosis, neuronal 6	1.7	1.4
<i>Cnm2</i>	cyclin M2	1.3	
<i>Coq10a</i>	coenzyme Q10 homolog A	1.4	
<i>Cp</i>	ceruloplasmin	-1.5	-2.3
<i>Cpeb2</i>	cytoplasmic polyadenylation element binding protein 2	1.4	1.4
<i>Cpeb4</i>	cytoplasmic polyadenylation element binding protein 4	1.5	1.3
<i>Creb3l3</i>	cAMP responsive element binding protein 3-like 3	1.5	
<i>Creb5</i>	cAMP responsive element binding protein 5	1.6	
<i>Crebrf</i>	CREB3 regulatory factor	1.3	1.4
<i>Crebzf</i>	CREB/ATF bZIP transcription factor	1.3	-1.6
<i>Cry2</i>	cryptochrome 2 (photolyase-like)	-1.3	
<i>Ctns</i>	cystinosis, nephropathic	1.7	
<i>Ctsb</i>	cathepsin B	1.6	-2.0
<i>Ctsl</i>	cathepsin L	2.1	2.1
<i>Cxcl1</i>	chemokine (C-X-C motif) ligand 1	-1.4	-4.4
<i>Cxcl10</i>	chemokine (C-X-C motif) ligand 10	-1.5	
<i>Cyp26a1</i>	cytochrome P450, family 26, subfamily a, polypeptide 1	1.5	2.3
<i>Cyth1</i>	cytohesin 1	-1.3	
<i>D630045M09Rik</i>	RIKEN cDNA D630045M09 gene	-1.4	-1.5
<i>Dab2ip</i>	disabled 2 interacting protein	-1.4	
<i>Dcbld2</i>	discoidin, CUB and LCCL domain containing 2	1.3	
<i>Ddit3</i>	DNA-damage inducible transcript 3	2.4	1.5
<i>Dennd4a</i>	DENN/MADD domain containing 4A	1.4	
<i>Dgat2</i>	diacylglycerol O-acyltransferase 2	1.5	
<i>Dhrs3</i>	dehydrogenase/reductase (SDR family) member 3	1.3	1.3
<i>Dkc1</i>	dyskeratosis congenita 1, dyskerin	-1.3	-1.3
<i>Dlc1</i>	deleted in liver cancer 1	-1.8	
<i>Dna2</i>	DNA replication helicase 2 homolog (yeast)	1.3	-1.9
<i>Dnaja1</i>	DnaJ (Hsp40) homolog, subfamily A, member 1	-1.4	-1.3
<i>Dnajb4</i>	DnaJ (Hsp40) homolog, subfamily B, member 4	-1.9	
<i>Dnmbp</i>	dynamin binding protein	1.3	1.5
<i>Dnmt3a</i>	DNA methyltransferase 3A	1.6	1.4
<i>Dot1l</i>	DOT1-like, histone H3 methyltransferase (S. cerevisiae)	1.3	
<i>Dpp7</i>	dipeptidylpeptidase 7	1.4	
<i>Dusp10</i>	dual specificity phosphatase 10	1.4	

<i>Dusp16</i>	dual specificity phosphatase 16	-1.3	-2.6
<i>Dusp4</i>	dual specificity phosphatase 4	1.8	
<i>Dvl2</i>	dishevelled 2, dsh homolog (Drosophila)	1.4	
<i>Dynll1</i>	dynein light chain LC8-type 1	-1.4	-1.4
<i>E2f8</i>	E2F transcription factor 8	1.6	
<i>Eea1</i>	early endosome antigen 1	1.5	
<i>Egln3</i>	egl-9 family hypoxia-inducible factor 3	-2.0	
<i>Egr1</i>	early growth response 1	2.9	7.5
<i>Eif2a</i>	eukaryotic translation initiation factor 2A	-1.4	
<i>Eif2ak2</i>	eukaryotic translation initiation factor 2-alpha kinase 2	-1.4	
<i>Eif4ebp1</i>	eukaryotic translation initiation factor 4E binding protein 1	1.4	
<i>Elmsan1</i>	ELM2 and Myb/SANT-like domain containing 1	1.5	1.6
<i>Enc1</i>	ectodermal-neural cortex 1	-1.9	
<i>Enpp5</i>	ectonucleotide pyrophosphatase/phosphodiesterase 5	1.4	
<i>Eny2</i>	enhancer of yellow 2 homolog (Drosophila)	-1.3	
<i>Epg5</i>	ectopic P-granules autophagy protein 5 homolog (C. elegans)	1.4	
<i>Epha1</i>	Eph receptor A1	-1.4	1.4
<i>ErbB3</i>	v-erb-b2 erythroblastic leukemia viral oncogene homolog 3 (avian)	-1.3	1.7
<i>Ern1</i>	endoplasmic reticulum (ER) to nucleus signalling 1	1.4	-1.9
<i>Etl4</i>	enhancer trap locus 4	-1.6	
<i>Ets2</i>	E26 avian leukemia oncogene 2, 3' domain	1.6	
<i>Eva1a</i>	eva-1 homolog A (C. elegans)	1.9	
<i>Exph5</i>	exophilin 5	1.3	
<i>Fads1</i>	fatty acid desaturase 1	1.4	
<i>Fam102a</i>	family with sequence similarity 102, member A	1.5	
<i>Fam124a</i>	family with sequence similarity 124, member A	-1.4	
<i>Fam13b</i>	family with sequence similarity 13, member B	-1.4	
<i>Fam178a</i>	family with sequence similarity 178, member A	1.4	
<i>Fam21</i>	family with sequence similarity 21	1.4	-1.5
<i>Fam84b</i>	family with sequence similarity 84, member B	1.4	-1.4
<i>Farp2</i>	FERM, RhoGEF and pleckstrin domain protein 2	-1.3	
<i>Fbxo22</i>	F-box protein 22	-1.3	-1.4
<i>Fbxo33</i>	F-box protein 33	-1.4	
<i>Fgd3</i>	FYVE, RhoGEF and PH domain containing 3	-1.8	-2.5
<i>Fgf1</i>	fibroblast growth factor 1	-1.4	
<i>Fln</i>	folliculin	1.5	
<i>Fn1</i>	fibronectin 1	-2.0	-3.0
<i>Fnip1</i>	folliculin interacting protein 1	1.6	1.5
<i>Fnip2</i>	folliculin interacting protein 2	1.7	
<i>Fuca2</i>	fucosidase, alpha-L- 2, plasma	2.1	
<i>Fundc1</i>	FUN14 domain containing 1	1.4	
<i>G6pc</i>	glucose-6-phosphatase, catalytic	-2.9	1.7
<i>Gab2</i>	growth factor receptor bound protein 2-associated protein 2	1.5	
<i>Gadd45a</i>	growth arrest and DNA-damage-inducible 45 alpha	1.5	
<i>Gadd45b</i>	growth arrest and DNA-damage-inducible 45 beta	-2.3	-1.9
<i>Galc</i>	galactosylceramidase	1.5	
<i>Gas2l3</i>	growth arrest-specific 2 like 3	1.4	
<i>Gck</i>	glucokinase	2.0	
<i>Gcnt2</i>	glucosaminyl (N-acetyl) transferase 2, l-branching enzyme	1.3	
<i>Gdap10</i>	ganglioside-induced differentiation-associated-protein 10	1.3	
<i>Gdf15</i>	growth differentiation factor 15	1.9	1.7
<i>Gga2</i>	golgi associated, gamma adaptin ear containing, ARF binding protein 2	1.3	
<i>Gla</i>	galactosidase, alpha	1.4	
<i>Glrx3 /// Gm12669</i>	glutaredoxin 3 /// glutaredoxin 3 pseudogene	-1.3	-1.3
<i>Glt28d2</i>	glycosyltransferase 28 domain containing 2	-1.4	
<i>Glytk</i>	glycerate kinase	-1.6	1.5
<i>Gm12942 /// Zmym6</i>	predicted gene 12942 /// zinc finger, MYM-type 6	1.6	
<i>Gm19773</i>	predicted gene, 19773	1.6	-1.3
<i>Gm20604 /// Moap1</i>	predicted gene 20604 /// modulator of apoptosis 1	1.3	
<i>Gm21399 /// Prdx1</i>	peroxiredoxin 1 pseudogene /// peroxiredoxin 1	-1.3	-1.4
<i>Gm22</i>	predicted gene 22	1.3	

<i>Gm2990</i>	predicted gene 2990	1.3	
<i>Gm4354</i>	predicted gene 4354	1.3	
<i>Gm4944</i>	predicted gene 4944	1.4	
<i>Gm8615</i> /// <i>Gnpda1</i>	glucosamine-6-phosphate deaminase 1	2.0	-1.3
<i>Gm8801</i> /// <i>Ppp1r10</i>	protein phosphatase 1, regulatory subunit 10	-1.3	
<i>Gnpda1</i>	glucosamine-6-phosphate deaminase 1	1.8	
<i>Gns</i>	glucosamine (N-acetyl)-6-sulfatase	1.5	-1.8
<i>Gpd2</i>	glycerol phosphate dehydrogenase 2, mitochondrial	1.4	
<i>Gpnmb</i>	glycoprotein (transmembrane) nmb	1.3	
<i>Grpel2</i>	GrpE-like 2, mitochondrial	2.2	
<i>Gtf2a1</i>	general transcription factor II A, 1	1.4	
<i>Hbegf</i>	heparin-binding EGF-like growth factor	1.6	2.2
<i>Hbp1</i>	high mobility group box transcription factor 1	1.5	1.5
<i>Hectd2</i>	HECT domain containing 2	1.9	
<i>Hgsnat</i>	heparan-alpha-glucosaminide N-acetyltransferase	1.4	
<i>Hif1a</i>	hypoxia inducible factor 1, alpha subunit	1.4	
<i>Hilpda</i>	hypoxia inducible lipid droplet associated	3.2	
<i>Hist3h2a</i>	histone cluster 3, H2a	1.3	-1.6
<i>Hivep2</i>	human immunodeficiency virus type I enhancer binding protein 2	1.3	
<i>Hkdc1</i>	hexokinase domain containing 1	1.5	
<i>Hmgcr</i>	3-hydroxy-3-methylglutaryl-Coenzyme A reductase	1.4	
<i>Hmgcs1</i>	3-hydroxy-3-methylglutaryl-Coenzyme A synthase 1	1.4	
<i>Hook2</i>	hook homolog 2 (Drosophila)	1.3	
<i>Hps4</i>	Hermansky-Pudlak syndrome 4 homolog (human)	1.6	
<i>Hs1bp3</i>	HCLS1 binding protein 3	1.3	
<i>Hspa1b</i>	heat shock protein 1B	-3.0	
<i>Hspa8</i>	heat shock protein 8	-1.6	-1.3
<i>Hspb8</i>	heat shock protein 8	1.5	
<i>Hsph1</i>	heat shock 105kDa/110kDa protein 1	-1.4	
<i>Huwe1</i>	HECT, UBA and WWE domain containing 1	1.6	
<i>Icam1</i>	intercellular adhesion molecule 1	-1.3	
<i>Ier2</i>	immediate early response 2	1.4	
<i>Ier3</i>	immediate early response 3	1.4	-1.5
<i>Ifi47</i>	interferon gamma inducible protein 47	-1.6	
<i>Igfbp3</i>	insulin-like growth factor binding protein 3	-1.4	-1.3
<i>Il1rn</i>	interleukin 1 receptor antagonist	1.5	
<i>Il22ra1</i>	interleukin 22 receptor, alpha 1	-1.5	
<i>Ilf3</i>	interleukin enhancer binding factor 3	1.3	
<i>Impact</i>	impact, RWD domain protein	1.4	
<i>Insig1</i>	insulin induced gene 1	1.7	
<i>Irak2</i>	interleukin-1 receptor-associated kinase 2	1.3	
<i>Irf1</i>	interferon regulatory factor 1	-1.4	
<i>Irf2</i>	interferon regulatory factor 2	-1.4	
<i>Irf2bp1</i>	interferon regulatory factor 2 binding protein-like	-1.4	
<i>Irs1</i>	insulin receptor substrate 1	-1.8	
<i>Jph1</i>	junctophilin 1	1.3	
<i>Kantr</i>	Kdm5c adjacent non-coding transcript	1.4	
<i>Kcnk5</i>	potassium channel, subfamily K, member 5	1.4	1.6
<i>Kctd15</i>	potassium channel tetramerisation domain containing 15	1.6	
<i>Kif1b</i>	kinesin family member 1B	-1.6	
<i>Kifc3</i>	kinesin family member C3	-1.4	
<i>Klf11</i>	Kruppel-like factor 11	1.4	1.6
<i>Klf4</i>	Kruppel-like factor 4 (gut)	1.4	-1.3
<i>Klf6</i>	Kruppel-like factor 6	1.3	1.4
<i>Klhl24</i>	kelch-like 24	1.5	1.5
<i>Klhl25</i>	kelch-like 25	-1.3	
<i>Lamc1</i>	laminin, gamma 1	1.3	
<i>Lats2</i>	large tumor suppressor 2	-1.3	
<i>Lce1d</i>	late cornified envelope 1D	3.5	
<i>Lcmt2</i>	leucine carboxyl methyltransferase 2	1.6	
<i>Lcorl</i>	ligand dependent nuclear receptor corepressor-like	1.6	

<i>Lgr4</i>	leucine-rich repeat-containing G protein-coupled receptor 4	-1.3	
<i>Lhfpl2</i>	lipoma HMGIC fusion partner-like 2	1.4	
<i>Lmna</i>	lamin A	-1.4	
<i>LOC102634034</i>	uncharacterized LOC102634034	1.6	
<i>Lonrf1</i>	LON peptidase N-terminal domain and ring finger 1	1.7	
<i>Lonrf3</i>	LON peptidase N-terminal domain and ring finger 3	1.8	
<i>Lpin1</i>	lipin 1	1.5	2.3
<i>Lpin2</i>	lipin 2	1.4	1.4
<i>Lrrc28</i>	leucine rich repeat containing 28	1.4	
<i>Lurap1l</i>	leucine rich adaptor protein 1-like	-1.4	
<i>Ly96</i>	lymphocyte antigen 96	1.4	
<i>Maff</i>	v-maf musculoaponeurotic fibrosarcoma oncogene family, protein F (avian)	1.3	
<i>Mal2</i>	mal, T cell differentiation protein 2	-1.3	
<i>Mapk4</i>	mitogen-activated protein kinase 4	1.5	
<i>Mapk6</i>	mitogen-activated protein kinase 6	1.3	
<i>March3</i>	membrane-associated ring finger (C3HC4) 3	1.3	
<i>Mavs</i>	mitochondrial antiviral signaling protein	1.3	
<i>Mcoln1</i>	mucolipin 1	1.4	
<i>Mdm2</i>	transformed mouse 3T3 cell double minute 2	1.4	
<i>Mfsd11</i>	major facilitator superfamily domain containing 11	1.5	
<i>Micu1</i>	mitochondrial calcium uptake 1	1.3	
<i>Mkln1os</i>	muskelin 1, intracellular mediator containing kelch motifs, opposite strand	1.4	
<i>Mmp19</i>	matrix metalloproteinase 19	-1.3	
<i>Mn1</i>	meningioma 1	1.4	
<i>Mospd1</i>	motile sperm domain containing 1	1.4	
<i>Mpp6</i>	membrane protein, palmitoylated 6 (MAGUK p55 subfamily member 6)	2.0	-1.8
<i>Mreg</i>	melanoregulin	1.3	
<i>Mroh1</i>	maestro heat-like repeat family member 1	1.5	
<i>Msmo1</i>	methylsterol monooxygenase 1	1.3	
<i>Mt1</i>	metallothionein 1	1.8	-5.6
<i>Mthfd1</i>	methylenetetrahydrofolate dehydrogenase	-1.3	
<i>Mtss1</i>	metastasis suppressor 1	-1.4	-2.7
<i>Myc</i>	myelocytomatosis oncogene	1.4	1.4
<i>Myo1b</i>	myosin IB	-1.4	
<i>N4bp2l1</i>	NEDD4 binding protein 2-like 1	1.9	1.9
<i>Nab1</i>	Ngfi-A binding protein 1	-1.3	
<i>Nabp1</i>	nucleic acid binding protein 1	1.3	-1.4
<i>Nagk</i>	N-acetylglucosamine kinase	1.4	-2.7
<i>Nav2</i>	neuron navigator 2	1.3	1.5
<i>Nbeal1</i>	neurobeachin like 1	-1.4	-2.9
<i>Ncapd2</i>	non-SMC condensin I complex, subunit D2	-1.4	1.3
<i>Ndrg1</i>	N-myc downstream regulated gene 1	1.4	1.5
<i>Neat1</i>	nuclear paraspeckle assembly transcript 1	1.3	-7.5
<i>Nedd4l</i>	neural precursor cell expressed, developmentally down-regulated gene 4-like	1.3	1.3
<i>Nedd9</i>	neural precursor cell expressed, developmentally down-regulated gene 9	-2.1	
<i>Neo1</i>	neogenin	1.3	
<i>Neu1</i>	neuraminidase 1	1.4	
<i>Nfe2l1</i>	nuclear factor, erythroid derived 2,-like 1	1.3	
<i>Nfkbia</i>	nuclear factor of kappa light polypeptide gene enhancer in B cells inhibitor, alpha	-1.5	
<i>Nfkbie</i>	nuclear factor of kappa light polypeptide gene enhancer in B cells inhibitor, epsilon	-1.7	-1.5
<i>Nhlrc3</i>	NHL repeat containing 3	1.5	
<i>Nlrc5</i>	NLR family, CARD domain containing 5	1.4	
<i>Npc1</i>	Niemann-Pick type C1	1.7	
<i>Nr0b2</i>	nuclear receptor subfamily 0, group B, member 2	-1.6	
<i>Nr2f2</i>	nuclear receptor subfamily 2, group F, member 2	-1.4	
<i>Nr3c1</i>	nuclear receptor subfamily 3, group C, member 1	-1.5	
<i>Nr3c2</i>	nuclear receptor subfamily 3, group C, member 2	1.4	
<i>Nr6a1</i>	nuclear receptor subfamily 6, group A, member 1	1.8	1.9
<i>Nrg1</i>	neuregulin 1	1.4	
<i>Nrg4</i>	neuregulin 4	1.3	1.7
<i>Nrip1</i>	nuclear receptor interacting protein 1	1.3	1.4

<i>Nrp1</i>	neuropilin 1	-1.7	-2.1
<i>Nt5e</i>	5' nucleotidase, ecto	-1.3	
<i>Nuak2</i>	NUAK family, SNF1-like kinase, 2	-1.4	
<i>Nupr1</i>	nuclear protein transcription regulator 1	2.4	
<i>Oasl1</i>	2'-5' oligoadenylate synthetase-like 1	1.6	
<i>Ostm1</i>	osteopetrosis associated transmembrane protein 1	1.5	
<i>Pagr1a</i>	PAXIP1 associated glutamate rich protein 1A	-1.3	
<i>Paics</i>	phosphoribosylaminoimidazole carboxylase	-1.3	-1.4
<i>Pak3</i>	p21 protein (Cdc42/Rac)-activated kinase 3	-1.3	
<i>Palld</i>	palladin, cytoskeletal associated protein	1.4	-1.5
<i>Palmd</i>	palmdelphin	-1.5	
<i>Pard6a</i>	par-6 family cell polarity regulator alpha	1.3	
<i>Parp16</i>	poly (ADP-ribose) polymerase family, member 16	-1.5	
<i>Pdk4</i>	pyruvate dehydrogenase kinase, isoenzyme 4	4.6	2.1
<i>Pdlim5</i>	PDZ and LIM domain 5	-1.6	-1.5
<i>Pdlim7</i>	PDZ and LIM domain 7	-1.3	-1.4
<i>Phip</i>	pleckstrin homology domain interacting protein	-1.4	
<i>Phlda3</i>	pleckstrin homology-like domain, family A, member 3	-1.5	
<i>Phldb1</i>	pleckstrin homology-like domain, family B, member 1	-1.3	
<i>Piga</i>	phosphatidylinositol glycan anchor biosynthesis, class A	1.7	
<i>Pim1</i>	proviral integration site 1	1.7	
<i>Pip4k2b</i>	phosphatidylinositol-5-phosphate 4-kinase, type II, beta	-1.3	
<i>Pja1</i>	praja ring finger 1, E3 ubiquitin protein ligase	-1.4	-1.3
<i>Plat</i>	plasminogen activator, tissue	1.4	
<i>Plekhf1</i>	pleckstrin homology domain containing, family F	1.3	
<i>Plin3</i>	perilipin 3	1.4	
<i>Plin4</i>	perilipin 4	1.6	1.7
<i>Plk3</i>	polo-like kinase 3	1.6	1.6
<i>Plscr1</i>	phospholipid scramblase 1	-1.4	-4.6
<i>Plscr2</i>	phospholipid scramblase 2	-1.5	
<i>Pmepa1</i>	prostate transmembrane protein, androgen induced 1	-1.4	-1.3
<i>Pmm1</i>	phosphomannomutase 1	1.3	
<i>Ppap2b</i>	phosphatidic acid phosphatase type 2B	-1.7	
<i>Ppargc1a</i>	peroxisome proliferative activated receptor, gamma, coactivator 1 alpha	1.5	1.4
<i>Ppargc1b</i>	peroxisome proliferative activated receptor, gamma, coactivator 1 beta	1.4	
<i>Ppm1h</i>	protein phosphatase 1H (PP2C domain containing)	1.6	1.4
<i>Ppp1r12a</i>	protein phosphatase 1, regulatory (inhibitor) subunit 12A	1.3	
<i>Ppp1r15a</i>	protein phosphatase 1, regulatory (inhibitor) subunit 15A	2.2	1.9
<i>Ppp1r3g</i>	protein phosphatase 1, regulatory (inhibitor) subunit 3G	1.7	1.7
<i>Ppp2r5e</i>	protein phosphatase 2, regulatory subunit B', epsilon	-1.3	
<i>Prdx4</i>	peroxiredoxin 4	-1.3	-1.4
<i>Prdx6</i>	peroxiredoxin 6	-1.7	-5.0
<i>Prkag3</i>	protein kinase, AMP-activated, gamma 3 non-catalytic subunit	-1.5	
<i>Proser2</i>	proline and serine rich 2	-2.3	
<i>Prox1</i>	prospero homeobox 1	1.6	1.4
<i>Prr5l</i>	proline rich 5 like	1.4	
<i>Psmc4</i>	proteasome (prosome, macropain) 26S subunit, ATPase, 4	-1.3	-1.3
<i>Ptpn21</i>	protein tyrosine phosphatase, non-receptor type 21	-1.3	-2.3
<i>Pvr</i>	poliovirus receptor	1.6	
<i>Pvrl3</i>	poliovirus receptor-related 3	-1.4	
<i>Rab20</i>	RAB20, member RAS oncogene family	1.4	-1.7
<i>Rab30</i>	RAB30, member RAS oncogene family	3.0	
<i>Ralb</i>	v-ral simian leukemia viral oncogene homolog B (ras related)	1.3	
<i>Rap1gap2</i>	RAP1 GTPase activating protein 2	1.5	
<i>Rasa2</i>	RAS p21 protein activator 2	1.4	
<i>Rbm12</i>	RNA binding motif protein 12	-1.5	
<i>Rel1</i>	RELT-like 1	1.4	
<i>Rhobtb1</i>	Rho-related BTB domain containing 1	1.8	1.5
<i>Rhou</i>	ras homolog gene family, member U	1.5	
<i>Rhpn2</i>	rhophilin, Rho GTPase binding protein 2	1.5	
<i>Rnf135</i>	ring finger protein 135	-1.4	

<i>Rnf169</i>	ring finger protein 169	-1.3	1.3
<i>Rnf186</i>	ring finger protein 186	1.4	
<i>Rnf19a</i>	ring finger protein 19A	-1.3	
<i>Rnf24</i>	ring finger protein 24	1.4	
<i>Rnf41</i>	ring finger protein 41	1.4	
<i>Rpia</i>	ribose 5-phosphate isomerase A	1.6	
<i>Rragd</i>	Ras-related GTP binding D	1.5	
<i>Rrm2b</i>	ribonucleotide reductase M2 B (TP53 inducible)	1.3	
<i>Rsad2</i>	radical S-adenosyl methionine domain containing 2	1.8	1.7
<i>Rtn4rl1</i>	reticulin 4 receptor-like 1	-1.5	
<i>Rtp3</i>	receptor transporter protein 3	-1.7	
<i>Rusc2</i>	RUN and SH3 domain containing 2	1.4	
<i>Samd4</i>	sterile alpha motif domain containing 4	-1.3	
<i>Sbk1</i>	SH3-binding kinase 1	-1.3	1.5
<i>Sbno2</i>	strawberry notch homolog 2 (Drosophila)	-1.4	-2.2
<i>Sbsn</i>	suprabasin	1.3	
<i>Sc5d</i>	sterol-C5-desaturase	1.4	
<i>Scly</i>	selenocysteine lyase	1.5	
<i>Scpep1</i>	serine carboxypeptidase 1	1.4	
<i>septin 7</i>	septin 7	-1.3	-1.4
<i>Serpina7</i>	serine (or cysteine) peptidase inhibitor, clade A	-1.3	-1.6
<i>Sfpq</i>	splicing factor proline/glutamine rich	-1.4	
<i>Sgk1</i>	serum/glucocorticoid regulated kinase 1	-1.5	
<i>Sgpp1</i>	sphingosine-1-phosphate phosphatase 1	-1.4	-1.3
<i>Sh2d4a</i>	SH2 domain containing 4A	-1.6	
<i>Sh3bp5</i>	SH3-domain binding protein 5 (BTK-associated)	-1.4	
<i>Siah1a</i>	seven in absentia 1A	1.3	
<i>Slc16a10</i>	solute carrier family 16, member 10	1.5	1.3
<i>Slc16a6</i>	solute carrier family 16, member 6	1.5	
<i>Slc1a4</i>	solute carrier family 1, member 4	-1.3	
<i>Slc20a1</i>	solute carrier family 20, member 1	1.8	
<i>Slc25a25</i>	solute carrier family 25, member a25	1.4	1.5
<i>Slc25a5</i>	solute carrier family 25, member a5	-1.3	-1.4
<i>Slc26a1</i>	solute carrier family 26, member 1	-1.3	
<i>Slc26a11</i>	solute carrier family 26, member 11	1.3	
<i>Slc2a1</i>	solute carrier family 2, member 1	1.4	
<i>Slc35d1</i> /// <i>Slc35d1</i>	Mus musculus solute carrier family 35	-1.5	-6.8
<i>Slc7a1</i>	solute carrier family 7, member 1	1.4	1.4
<i>Slc7a2</i>	solute carrier family 7, member 2	1.4	1.8
<i>Sltm</i>	SAFB-like, transcription modulator	-1.3	
<i>Smcr8</i>	Smith-Magenis syndrome chromosome region	1.4	
<i>Smpd3</i>	sphingomyelin phosphodiesterase 3, neutral	-1.4	
<i>Snai2</i>	snail family zinc finger 2	2.6	
<i>Snhg1</i>	small nucleolar RNA host gene 1	1.3	
<i>Snx30</i>	sorting nexin family member 30	2.0	
<i>Snx33</i>	sorting nexin 33	1.5	
<i>Socs2</i>	suppressor of cytokine signaling 2	-1.5	
<i>Sorbs2</i>	sorbin and SH3 domain containing 2	-1.3	1.5
<i>Sox4</i>	SRY (sex determining region Y)-box 4	-2.0	-2.0
<i>Spag9</i>	sperm associated antigen 9	1.3	1.4
<i>Spin4</i>	spindlin family, member 4	2.2	
<i>Srrm4</i>	serine/arginine repetitive matrix 4	1.8	1.4
<i>St3gal4</i>	ST3 beta-galactoside alpha-2,3-sialyltransferase 4	1.6	
<i>Stat3</i>	signal transducer and activator of transcription 3	1.5	
<i>Stat5a</i>	signal transducer and activator of transcription 5A	1.4	
<i>Stk17b</i>	serine/threonine kinase 17b (apoptosis-inducing)	1.5	1.4
<i>Stx3</i>	syntaxin 3	1.9	
<i>Swap70</i>	SWA-70 protein	1.3	
<i>Synj2</i>	synaptojanin 2	1.4	
<i>Taf15</i>	TAF15 RNA polymerase II, TATA box binding protein	1.4	2.2
<i>Tagap</i> /// <i>Tagap1</i>	T cell activation Rho GTPase activating protein	1.3	

<i>Tanc1</i>	tetratricopeptide repeat, ankyrin repeat and coiled-coil containing 1	1.4	
<i>Tat</i>	tyrosine aminotransferase	1.5	1.4
<i>Tbc1d14</i>	TBC1 domain family, member 14	-1.4	
<i>Tbl1xr1</i>	transducin (beta)-like 1X-linked receptor 1	-1.5	-1.8
<i>Tbpl1</i>	TATA box binding protein-like 1	1.4	
<i>Tc2n</i>	tandem C2 domains, nuclear	1.3	
<i>Tceal1</i>	transcription elongation factor A (SII)-like 1	1.4	
<i>Tdrd7</i>	tudor domain containing 7	-1.8	-1.8
<i>Tecpr1</i>	tectonin beta-propeller repeat containing 1	1.4	
<i>Tenm3</i>	teneurin transmembrane protein 3	1.5	1.3
<i>Tes</i>	testis derived transcript	1.3	
<i>Tet2</i>	tet methylcytosine dioxygenase 2	1.4	
<i>Tgfb3</i>	transforming growth factor, beta receptor III	1.3	1.4
<i>Tgif1</i>	TGFB-induced factor homeobox 1	1.3	
<i>Tgoln1</i> /// <i>Tgoln2</i>	trans-golgi network protein /// trans-golgi network protein 2	1.4	
<i>Tifa</i>	TRAF-interacting protein with forkhead-associated domain	1.7	
<i>Timd2</i>	T cell immunoglobulin and mucin domain containing 2	-1.4	
<i>Tiparp</i>	TCDD-inducible poly(ADP-ribose) polymerase	1.4	1.4
<i>Tm9sf2</i>	transmembrane 9 superfamily member 2	-1.4	-1.3
<i>Tmem123</i>	transmembrane protein 123	-1.4	-1.4
<i>Tmem144</i>	transmembrane protein 144	1.6	
<i>Tmem154</i>	transmembrane protein 154	1.5	
<i>Tmem177</i>	transmembrane protein 177	1.3	
<i>Tmem219</i>	transmembrane protein 219	-1.4	1.5
<i>Tmem41a</i>	transmembrane protein 41a	-1.3	
<i>Tmem41b</i>	transmembrane protein 41B	1.5	
<i>Tmem55b</i>	transmembrane protein 55b	1.4	
<i>Tmem87b</i>	transmembrane protein 87B	1.6	1.4
<i>Tnfaip3</i>	tumor necrosis factor, alpha-induced protein 3	-1.6	
<i>Tnip2</i>	TNFAIP3 interacting protein 2	1.3	
<i>Tnrc18</i>	trinucleotide repeat containing 18	-1.3	
<i>Tnrc6a</i>	trinucleotide repeat containing 6a	-1.3	
<i>Tollip</i>	toll interacting protein	1.3	
<i>Tox</i>	thymocyte selection-associated high mobility group box	1.6	1.3
<i>Tpra1</i>	transmembrane protein, adipocyte associated 1	1.3	
<i>Tra2a</i>	transformer 2 alpha homolog (Drosophila)	-1.3	-1.3
<i>Trim7</i>	tripartite motif-containing 7	-1.7	-3.1
<i>Tsc1</i>	tuberous sclerosis 1	1.4	
<i>Tsc22d1</i>	TSC22 domain family, member 1	-1.3	-1.3
<i>Tsply1</i>	testis-specific protein, Y-encoded-like 1	-1.3	
<i>Ttbk2</i>	tau tubulin kinase 2	1.3	
<i>Ttc23</i>	tetratricopeptide repeat domain 23	1.6	
<i>Uap1l1</i>	UDP-N-actylglucosamine pyrophosphorylase 1-like 1	1.4	
<i>Ube2t</i>	ubiquitin-conjugating enzyme E2T (putative)	1.4	-1.4
<i>Ubttd2</i>	ubiquitin domain containing 2	-1.4	
<i>Ugcg</i>	UDP-glucose ceramide glucosyltransferase	1.4	
<i>Ung</i>	uracil DNA glycosylase	1.6	
<i>Usp18</i>	ubiquitin specific peptidase 18	1.5	1.7
<i>Usp2</i>	ubiquitin specific peptidase 2	-1.8	1.7
<i>Vasn</i>	vasorin	-1.4	
<i>Vps18</i>	vacuolar protein sorting 18 (yeast)	1.4	
<i>Vps29</i>	vacuolar protein sorting 29 (S. pombe)	1.3	-1.7
<i>Vps37b</i>	vacuolar protein sorting 37B (yeast)	1.6	
<i>Wasf1</i>	WAS protein family, member 1	-1.4	
<i>Wdr47</i>	WD repeat domain 47	1.4	
<i>Wdr62</i>	WD repeat domain 62	1.3	
<i>Wnt8b</i>	wingless-type MMTV integration site family, member 8B	1.4	
<i>Yars2</i>	tyrosyl-tRNA synthetase 2 (mitochondrial)	-1.5	
<i>Ypel2</i>	yippee-like 2 (Drosophila)	1.9	1.3
<i>Zbtb10</i>	zinc finger and BTB domain containing 10	1.3	1.4
<i>Zbtb2</i>	zinc finger and BTB domain containing 2	1.3	

<i>Zbtb21</i>	zinc finger and BTB domain containing 21	1.6	
<i>Zc2hc1a</i>	zinc finger, C2HC-type containing 1A	-1.4	
<i>Zc3h6</i>	zinc finger CCCH type containing 6	1.6	1.4
<i>Zcchc10</i>	zinc finger, CCHC domain containing 10	-1.4	-1.4
<i>Zcchc11</i>	zinc finger, CCHC domain containing 11	1.4	
<i>Zdhhc13</i>	zinc finger, DHHC domain containing 13	1.4	
<i>Zfand2a</i>	zinc finger, AN1-type domain 2A	2.0	
<i>Zfmx3</i>	zinc finger homeobox 3	-1.4	
<i>Zfp36</i>	zinc finger protein 36	1.3	2.0
<i>Zfp385b</i>	zinc finger protein 385B	2.5	
<i>Zfp398</i>	zinc finger protein 398	1.3	
<i>Zfp493</i>	zinc finger protein 493	1.3	
<i>Zfp516</i>	zinc finger protein 516	1.4	
<i>Zfp58</i>	zinc finger protein 58	1.3	-1.5
<i>Zfp655</i>	zinc finger protein 655	1.7	
<i>Zfp709</i>	zinc finger protein 709	1.4	-1.5
<i>Zfp945</i>	zinc finger protein 945	1.4	-2.3
<i>Zfyve26</i>	zinc finger, FYVE domain containing 26	1.3	
<i>Zkscan1</i>	zinc finger with KRAB and SCAN domains 1	1.5	
<i>Zswim8</i>	zinc finger SWIM-type containing 8	1.4	-1.4

Appendix Table 2. List of genes regulated by 991 in mouse primary hepatocytes.

The table reports the genes modulated upon 991 stimulation in isolated mouse hepatocytes, reporting gene symbol and title, together with the fold change (FC) following treatment with 991 or AICAR (when present). For filtering the corresponding transcripts, the moderated *P*-value was set at 0.05 and a FC cutoff of 1.3 was applied.

Bibliography

- 1 Hardie, D. G. Keeping the home fires burning: AMP-activated protein kinase. *J R Soc Interface* **15**, doi:10.1098/rsif.2017.0774 (2018).
- 2 Hardie, D. G. & Hawley, S. A. AMP-activated protein kinase: the energy charge hypothesis revisited. *Bioessays* **23**, 1112-1119, doi:10.1002/bies.10009 (2001).
- 3 Hardie, D. G. AMP-activated/SNF1 protein kinases: conserved guardians of cellular energy. *Nat Rev Mol Cell Biol* **8**, 774-785, doi:10.1038/nrm2249 (2007).
- 4 Salt, I. P., Johnson, G., Ashcroft, S. J. & Hardie, D. G. AMP-activated protein kinase is activated by low glucose in cell lines derived from pancreatic beta cells, and may regulate insulin release. *Biochem J* **335 (Pt 3)**, 533-539 (1998).
- 5 Choi, S. L. *et al.* The regulation of AMP-activated protein kinase by H(2)O(2). *Biochem Biophys Res Commun* **287**, 92-97, doi:10.1006/bbrc.2001.5544 (2001).
- 6 Qi, D. & Young, L. H. AMPK: energy sensor and survival mechanism in the ischemic heart. *Trends Endocrinol Metab* **26**, 422-429, doi:10.1016/j.tem.2015.05.010 (2015).
- 7 Jakobsen, J. S. *et al.* Temporal mapping of CEBPA and CEBPB binding during liver regeneration reveals dynamic occupancy and specific regulatory codes for homeostatic and cell cycle gene batteries. *Genome Res* **23**, 592-603, doi:10.1101/gr.146399.112 (2013).
- 8 Garcia, D. & Shaw, R. J. AMPK: Mechanisms of Cellular Energy Sensing and Restoration of Metabolic Balance. *Mol Cell* **66**, 789-800, doi:10.1016/j.molcel.2017.05.032 (2017).
- 9 Ruderman, N. B. *et al.* AMPK as a metabolic switch in rat muscle, liver and adipose tissue after exercise. *Acta Physiol Scand* **178**, 435-442, doi:10.1046/j.1365-201X.2003.01164.x (2003).
- 10 Viollet, B. *et al.* Targeting the AMPK pathway for the treatment of Type 2 diabetes. *Front Biosci (Landmark Ed)* **14**, 3380-3400 (2009).
- 11 Fujii, N. *et al.* Role of AMP-activated protein kinase in exercise capacity, whole body glucose homeostasis, and glucose transport in skeletal muscle -insight from analysis of a transgenic mouse model. *Diabetes Res Clin Pract* **77 Suppl 1**, S92-98, doi:10.1016/j.diabres.2007.01.040 (2007).
- 12 Cokorinos, E. C. *et al.* Activation of Skeletal Muscle AMPK Promotes Glucose Disposal and Glucose Lowering in Non-human Primates and Mice. *Cell Metab* **25**, 1147-1159 e1110, doi:10.1016/j.cmet.2017.04.010 (2017).
- 13 Esquejo, R. M. *et al.* Activation of Liver AMPK with PF-06409577 Corrects NAFLD and Lowers Cholesterol in Rodent and Primate Preclinical Models. *EBioMedicine* **31**, 122-132, doi:10.1016/j.ebiom.2018.04.009 (2018).
- 14 Zhang, B. B., Zhou, G. & Li, C. AMPK: an emerging drug target for diabetes and the metabolic syndrome. *Cell Metab* **9**, 407-416, doi:10.1016/j.cmet.2009.03.012 (2009).
- 15 Lochhead, P. A., Salt, I. P., Walker, K. S., Hardie, D. G. & Sutherland, C. 5-aminoimidazole-4-carboxamide riboside mimics the effects of insulin on the expression of the 2 key gluconeogenic genes PEPCK and glucose-6-phosphatase. *Diabetes* **49**, 896-903 (2000).
- 16 Li, Y. *et al.* AMPK phosphorylates and inhibits SREBP activity to attenuate hepatic steatosis and atherosclerosis in diet-induced insulin-resistant mice. *Cell Metab* **13**, 376-388, doi:10.1016/j.cmet.2011.03.009 (2011).
- 17 Tomita, K. *et al.* AICAR, an AMPK activator, has protective effects on alcohol-induced fatty liver in rats. *Alcohol Clin Exp Res* **29**, 240S-245S (2005).
- 18 Foretz, M. *et al.* Short-term overexpression of a constitutively active form of AMP-activated protein kinase in the liver leads to mild hypoglycemia and fatty liver. *Diabetes* **54**, 1331-1339 (2005).

- 19 Um, J. H. *et al.* AMP-activated protein kinase-deficient mice are resistant to the metabolic effects of resveratrol. *Diabetes* **59**, 554-563, doi:10.2337/db09-0482 (2010).
- 20 Niu, Y. *et al.* Exercise-induced GLUT4 transcription via inactivation of HDAC4/5 in mouse skeletal muscle in an AMPKalpha2-dependent manner. *Biochim Biophys Acta Mol Basis Dis* **1863**, 2372-2381, doi:10.1016/j.bbadis.2017.07.001 (2017).
- 21 Viollet, B. *et al.* AMPK inhibition in health and disease. *Crit Rev Biochem Mol Biol* **45**, 276-295, doi:10.3109/10409238.2010.488215 (2010).
- 22 Fujii, N. *et al.* Exercise induces isoform-specific increase in 5'AMP-activated protein kinase activity in human skeletal muscle. *Biochem Biophys Res Commun* **273**, 1150-1155, doi:10.1006/bbrc.2000.3073 (2000).
- 23 Thornton, C., Snowden, M. A. & Carling, D. Identification of a novel AMP-activated protein kinase beta subunit isoform that is highly expressed in skeletal muscle. *J Biol Chem* **273**, 12443-12450 (1998).
- 24 Barnes, B. R. *et al.* The 5'-AMP-activated protein kinase gamma3 isoform has a key role in carbohydrate and lipid metabolism in glycolytic skeletal muscle. *J Biol Chem* **279**, 38441-38447, doi:10.1074/jbc.M405533200 (2004).
- 25 Yu, H., Fujii, N., Hirshman, M. F., Pomerleau, J. M. & Goodyear, L. J. Cloning and characterization of mouse 5'-AMP-activated protein kinase gamma3 subunit. *Am J Physiol Cell Physiol* **286**, C283-292, doi:10.1152/ajpcell.00319.2003 (2004).
- 26 Bultot, L. *et al.* Benzimidazole derivative small-molecule 991 enhances AMPK activity and glucose uptake induced by AICAR or contraction in skeletal muscle. *Am J Physiol Endocrinol Metab* **311**, E706-E719, doi:10.1152/ajpendo.00237.2016 (2016).
- 27 Deshmukh, A. S., Glund, S., Tom, R. Z. & Zierath, J. R. Role of the AMPKgamma3 isoform in hypoxia-stimulated glucose transport in glycolytic skeletal muscle. *Am J Physiol Endocrinol Metab* **297**, E1388-1394, doi:10.1152/ajpendo.00125.2009 (2009).
- 28 Richter, E. A. & Hargreaves, M. Exercise, GLUT4, and skeletal muscle glucose uptake. *Physiol Rev* **93**, 993-1017, doi:10.1152/physrev.00038.2012 (2013).
- 29 Birk, J. B. & Wojtaszewski, J. F. Predominant alpha2/beta2/gamma3 AMPK activation during exercise in human skeletal muscle. *J Physiol* **577**, 1021-1032, doi:10.1113/jphysiol.2006.120972 (2006).
- 30 Costford, S. R. *et al.* Gain-of-function R225W mutation in human AMPKgamma(3) causing increased glycogen and decreased triglyceride in skeletal muscle. *PLoS One* **2**, e903, doi:10.1371/journal.pone.0000903 (2007).
- 31 Milan, D. *et al.* A mutation in PRKAG3 associated with excess glycogen content in pig skeletal muscle. *Science* **288**, 1248-1251 (2000).
- 32 Cheung, P. C., Salt, I. P., Davies, S. P., Hardie, D. G. & Carling, D. Characterization of AMP-activated protein kinase gamma-subunit isoforms and their role in AMP binding. *Biochem J* **346 Pt 3**, 659-669 (2000).
- 33 Gollob, M. H., Green, M. S., Tang, A. S. & Roberts, R. PRKAG2 cardiac syndrome: familial ventricular preexcitation, conduction system disease, and cardiac hypertrophy. *Curr Opin Cardiol* **17**, 229-234 (2002).
- 34 Arad, M. *et al.* Constitutively active AMP kinase mutations cause glycogen storage disease mimicking hypertrophic cardiomyopathy. *J Clin Invest* **109**, 357-362, doi:10.1172/JCI14571 (2002).
- 35 Vaughan, C. J. *et al.* Molecular genetic analysis of PRKAG2 in sporadic Wolff-Parkinson-White syndrome. *J Cardiovasc Electrophysiol* **14**, 263-268 (2003).
- 36 Gollob, M. H. *et al.* Identification of a gene responsible for familial Wolff-Parkinson-White syndrome. *N Engl J Med* **344**, 1823-1831, doi:10.1056/NEJM200106143442403 (2001).
- 37 Wu, J. *et al.* Chemoproteomic analysis of intertissue and interspecies isoform diversity of AMP-activated protein kinase (AMPK). *J Biol Chem* **288**, 35904-35912, doi:10.1074/jbc.M113.508747 (2013).

- 38 Viollet, B. & Foretz, M. Animal Models to Study AMPK. *Exp Suppl* **107**, 441-469, doi:10.1007/978-3-319-43589-3_18 (2016).
- 39 Carling, D. *et al.* Mammalian AMP-activated protein kinase is homologous to yeast and plant protein kinases involved in the regulation of carbon metabolism. *J Biol Chem* **269**, 11442-11448 (1994).
- 40 Pang, T. *et al.* Conserved alpha-helix acts as autoinhibitory sequence in AMP-activated protein kinase alpha subunits. *J Biol Chem* **282**, 495-506, doi:10.1074/jbc.M605790200 (2007).
- 41 Crute, B. E., Seefeld, K., Gamble, J., Kemp, B. E. & Witters, L. A. Functional domains of the alpha1 catalytic subunit of the AMP-activated protein kinase. *J Biol Chem* **273**, 35347-35354 (1998).
- 42 Chen, L. *et al.* Structural insight into the autoinhibition mechanism of AMP-activated protein kinase. *Nature* **459**, 1146-1149, doi:10.1038/nature08075 (2009).
- 43 Hawley, S. A. *et al.* Complexes between the LKB1 tumor suppressor, STRAD alpha/beta and MO25 alpha/beta are upstream kinases in the AMP-activated protein kinase cascade. *J Biol* **2**, 28, doi:10.1186/1475-4924-2-28 (2003).
- 44 Woods, A. *et al.* LKB1 is the upstream kinase in the AMP-activated protein kinase cascade. *Curr Biol* **13**, 2004-2008 (2003).
- 45 Shaw, R. J. *et al.* The tumor suppressor LKB1 kinase directly activates AMP-activated kinase and regulates apoptosis in response to energy stress. *Proc Natl Acad Sci U S A* **101**, 3329-3335, doi:10.1073/pnas.0308061100 (2004).
- 46 Sakamoto, K., Goransson, O., Hardie, D. G. & Alessi, D. R. Activity of LKB1 and AMPK-related kinases in skeletal muscle: effects of contraction, phenformin, and AICAR. *Am J Physiol Endocrinol Metab* **287**, E310-317, doi:10.1152/ajpendo.00074.2004 (2004).
- 47 Sakamoto, K. *et al.* Deficiency of LKB1 in skeletal muscle prevents AMPK activation and glucose uptake during contraction. *EMBO J* **24**, 1810-1820, doi:10.1038/sj.emboj.7600667 (2005).
- 48 Zhang, Y. L. *et al.* AMP as a low-energy charge signal autonomously initiates assembly of AXIN-AMPK-LKB1 complex for AMPK activation. *Cell Metab* **18**, 546-555, doi:10.1016/j.cmet.2013.09.005 (2013).
- 49 Zhang, C. S. *et al.* The lysosomal v-ATPase-Ragulator complex is a common activator for AMPK and mTORC1, acting as a switch between catabolism and anabolism. *Cell Metab* **20**, 526-540, doi:10.1016/j.cmet.2014.06.014 (2014).
- 50 Hawley, S. A. *et al.* Calmodulin-dependent protein kinase kinase-beta is an alternative upstream kinase for AMP-activated protein kinase. *Cell Metab* **2**, 9-19, doi:10.1016/j.cmet.2005.05.009 (2005).
- 51 Hurley, R. L. *et al.* The Ca²⁺/calmodulin-dependent protein kinase kinases are AMP-activated protein kinase kinases. *J Biol Chem* **280**, 29060-29066, doi:10.1074/jbc.M503824200 (2005).
- 52 Woods, A. *et al.* Ca²⁺/calmodulin-dependent protein kinase kinase-beta acts upstream of AMP-activated protein kinase in mammalian cells. *Cell Metab* **2**, 21-33, doi:10.1016/j.cmet.2005.06.005 (2005).
- 53 Mitchelhill, K. I. *et al.* Posttranslational modifications of the 5'-AMP-activated protein kinase beta1 subunit. *J Biol Chem* **272**, 24475-24479 (1997).
- 54 Valentine, R. J., Coughlan, K. A., Ruderman, N. B. & Saha, A. K. Insulin inhibits AMPK activity and phosphorylates AMPK Ser(4)(8)(5)/(4)(9)(1) through Akt in hepatocytes, myotubes and incubated rat skeletal muscle. *Arch Biochem Biophys* **562**, 62-69, doi:10.1016/j.abb.2014.08.013 (2014).
- 55 Sanders, M. J. *et al.* Defining the mechanism of activation of AMP-activated protein kinase by the small molecule A-769662, a member of the thienopyridone family. *J Biol Chem* **282**, 32539-32548, doi:10.1074/jbc.M706543200 (2007).

- 56 Oligschlaeger, Y. *et al.* The recruitment of AMP-activated protein kinase to glycogen is regulated by autophosphorylation. *J Biol Chem* **290**, 11715-11728, doi:10.1074/jbc.M114.633271 (2015).
- 57 Lopez-Mejia, I. C. *et al.* CDK4 Phosphorylates AMPKalpha2 to Inhibit Its Activity and Repress Fatty Acid Oxidation. *Mol Cell* **68**, 336-349 e336, doi:10.1016/j.molcel.2017.09.034 (2017).
- 58 Scott, J. W. *et al.* CBS domains form energy-sensing modules whose binding of adenosine ligands is disrupted by disease mutations. *J Clin Invest* **113**, 274-284, doi:10.1172/JCI19874 (2004).
- 59 Bateman, A. The structure of a domain common to archaeobacteria and the homocystinuria disease protein. *Trends Biochem Sci* **22**, 12-13 (1997).
- 60 Xiao, B. *et al.* Structural basis for AMP binding to mammalian AMP-activated protein kinase. *Nature* **449**, 496-500, doi:10.1038/nature06161 (2007).
- 61 Xiao, B. *et al.* Structural basis of AMPK regulation by small molecule activators. *Nat Commun* **4**, 3017, doi:10.1038/ncomms4017 (2013).
- 62 Xiao, B. *et al.* Structure of mammalian AMPK and its regulation by ADP. *Nature* **472**, 230-233, doi:10.1038/nature09932 (2011).
- 63 Hardie, D. G. AMPK--sensing energy while talking to other signaling pathways. *Cell Metab* **20**, 939-952, doi:10.1016/j.cmet.2014.09.013 (2014).
- 64 Ross, F. A., Jensen, T. E. & Hardie, D. G. Differential regulation by AMP and ADP of AMPK complexes containing different gamma subunit isoforms. *Biochem J* **473**, 189-199, doi:10.1042/BJ20150910 (2016).
- 65 Hardie, D. G., Ross, F. A. & Hawley, S. A. AMP-activated protein kinase: a target for drugs both ancient and modern. *Chem Biol* **19**, 1222-1236, doi:10.1016/j.chembiol.2012.08.019 (2012).
- 66 Hardie, D. G. & Alessi, D. R. LKB1 and AMPK and the cancer-metabolism link - ten years after. *BMC Biol* **11**, 36, doi:10.1186/1741-7007-11-36 (2013).
- 67 Cool, B. *et al.* Identification and characterization of a small molecule AMPK activator that treats key components of type 2 diabetes and the metabolic syndrome. *Cell Metab* **3**, 403-416, doi:10.1016/j.cmet.2006.05.005 (2006).
- 68 Goransson, O. *et al.* Mechanism of action of A-769662, a valuable tool for activation of AMP-activated protein kinase. *J Biol Chem* **282**, 32549-32560, doi:10.1074/jbc.M706536200 (2007).
- 69 Scott, J. W. *et al.* Thienopyridone drugs are selective activators of AMP-activated protein kinase beta1-containing complexes. *Chem Biol* **15**, 1220-1230, doi:10.1016/j.chembiol.2008.10.005 (2008).
- 70 Polekhina, G. *et al.* Structural basis for glycogen recognition by AMP-activated protein kinase. *Structure* **13**, 1453-1462, doi:10.1016/j.str.2005.07.008 (2005).
- 71 Scott, J. W. *et al.* Small molecule drug A-769662 and AMP synergistically activate naive AMPK independent of upstream kinase signaling. *Chem Biol* **21**, 619-627, doi:10.1016/j.chembiol.2014.03.006 (2014).
- 72 Treebak, J. T., Birk, J. B., Hansen, B. F., Olsen, G. S. & Wojtaszewski, J. F. A-769662 activates AMPK beta1-containing complexes but induces glucose uptake through a PI3-kinase-dependent pathway in mouse skeletal muscle. *Am J Physiol Cell Physiol* **297**, C1041-1052, doi:10.1152/ajpcell.00051.2009 (2009).
- 73 Willows, R., Navaratnam, N., Lima, A., Read, J. & Carling, D. Effect of different gamma-subunit isoforms on the regulation of AMPK. *Biochem J* **474**, 1741-1754, doi:10.1042/BCJ20170046 (2017).
- 74 Hardie, D. G. AMPK: positive and negative regulation, and its role in whole-body energy homeostasis. *Curr Opin Cell Biol* **33**, 1-7, doi:10.1016/j.ceb.2014.09.004 (2015).

- 75 Vavvas, D. *et al.* Contraction-induced changes in acetyl-CoA carboxylase and 5'-AMP-activated kinase in skeletal muscle. *J Biol Chem* **272**, 13255-13261 (1997).
- 76 Winder, W. W. & Hardie, D. G. Inactivation of acetyl-CoA carboxylase and activation of AMP-activated protein kinase in muscle during exercise. *Am J Physiol* **270**, E299-304, doi:10.1152/ajpendo.1996.270.2.E299 (1996).
- 77 Wojtaszewski, J. F., Nielsen, P., Hansen, B. F., Richter, E. A. & Kiens, B. Isoform-specific and exercise intensity-dependent activation of 5'-AMP-activated protein kinase in human skeletal muscle. *J Physiol* **528 Pt 1**, 221-226 (2000).
- 78 Stephens, T. J. *et al.* Progressive increase in human skeletal muscle AMPK α 2 activity and ACC phosphorylation during exercise. *Am J Physiol Endocrinol Metab* **282**, E688-694, doi:10.1152/ajpendo.00101.2001 (2002).
- 79 Yang, Y., Atasoy, D., Su, H. H. & Sternson, S. M. Hunger states switch a flip-flop memory circuit via a synaptic AMPK-dependent positive feedback loop. *Cell* **146**, 992-1003, doi:10.1016/j.cell.2011.07.039 (2011).
- 80 Iwabuchi, M. *et al.* Adiponectin and AdipoR1 regulate PGC-1 α and mitochondria by Ca²⁺ and AMPK/SIRT1. *Nature* **464**, 1313-1319, doi:10.1038/nature08991 (2010).
- 81 Kubota, N. *et al.* Adiponectin stimulates AMP-activated protein kinase in the hypothalamus and increases food intake. *Cell Metab* **6**, 55-68, doi:10.1016/j.cmet.2007.06.003 (2007).
- 82 Yamauchi, T. *et al.* Adiponectin stimulates glucose utilization and fatty-acid oxidation by activating AMP-activated protein kinase. *Nat Med* **8**, 1288-1295, doi:10.1038/nm788 (2002).
- 83 Tamas, P. *et al.* Regulation of the energy sensor AMP-activated protein kinase by antigen receptor and Ca²⁺ in T lymphocytes. *J Exp Med* **203**, 1665-1670, doi:10.1084/jem.20052469 (2006).
- 84 Jenkins, Y. *et al.* AMPK activation through mitochondrial regulation results in increased substrate oxidation and improved metabolic parameters in models of diabetes. *PLoS One* **8**, e81870, doi:10.1371/journal.pone.0081870 (2013).
- 85 Grahame Hardie, D. Regulation of AMP-activated protein kinase by natural and synthetic activators. *Acta Pharm Sin B* **6**, 1-19, doi:10.1016/j.apsb.2015.06.002 (2016).
- 86 Gadalla, A. E. *et al.* AICA riboside both activates AMP-activated protein kinase and competes with adenosine for the nucleoside transporter in the CA1 region of the rat hippocampus. *J Neurochem* **88**, 1272-1282 (2004).
- 87 Gomez-Galeno, J. E. *et al.* A Potent and Selective AMPK Activator That Inhibits de Novo Lipogenesis. *ACS Med Chem Lett* **1**, 478-482, doi:10.1021/ml100143q (2010).
- 88 Olivier, S., Foretz, M. & Viollet, B. Promise and challenges for direct small molecule AMPK activators. *Biochem Pharmacol* **153**, 147-158, doi:10.1016/j.bcp.2018.01.049 (2018).
- 89 Zadra, G. *et al.* A novel direct activator of AMPK inhibits prostate cancer growth by blocking lipogenesis. *EMBO Mol Med* **6**, 519-538, doi:10.1002/emmm.201302734 (2014).
- 90 Benziane, B. *et al.* AMP-activated protein kinase activator A-769662 is an inhibitor of the Na⁺-K⁺-ATPase. *Am J Physiol Cell Physiol* **297**, C1554-1566, doi:10.1152/ajpcell.00010.2009 (2009).
- 91 Moreno, D., Knecht, E., Viollet, B. & Sanz, P. A769662, a novel activator of AMP-activated protein kinase, inhibits non-proteolytic components of the 26S proteasome by an AMPK-independent mechanism. *FEBS Lett* **582**, 2650-2654, doi:10.1016/j.febslet.2008.06.044 (2008).
- 92 Myers, R. W. *et al.* Systemic pan-AMPK activator MK-8722 improves glucose homeostasis but induces cardiac hypertrophy. *Science* **357**, 507-511, doi:10.1126/science.aah5582 (2017).

- 93 Coughlan, K. A., Valentine, R. J., Ruderman, N. B. & Saha, A. K. AMPK activation: a therapeutic target for type 2 diabetes? *Diabetes Metab Syndr Obes* **7**, 241-253, doi:10.2147/DMSO.S43731 (2014).
- 94 Day, E. A., Ford, R. J. & Steinberg, G. R. AMPK as a Therapeutic Target for Treating Metabolic Diseases. *Trends Endocrinol Metab* **28**, 545-560, doi:10.1016/j.tem.2017.05.004 (2017).
- 95 Zhou, G. *et al.* Role of AMP-activated protein kinase in mechanism of metformin action. *J Clin Invest* **108**, 1167-1174, doi:10.1172/JCI13505 (2001).
- 96 Fullerton, M. D. *et al.* Single phosphorylation sites in Acc1 and Acc2 regulate lipid homeostasis and the insulin-sensitizing effects of metformin. *Nat Med* **19**, 1649-1654, doi:10.1038/nm.3372 (2013).
- 97 Foretz, M. *et al.* Metformin inhibits hepatic gluconeogenesis in mice independently of the LKB1/AMPK pathway via a decrease in hepatic energy state. *J Clin Invest* **120**, 2355-2369, doi:10.1172/JCI40671 (2010).
- 98 Hunter, R. W. *et al.* Metformin reduces liver glucose production by inhibition of fructose-1-6-bisphosphatase. *Nat Med* **24**, 1395-1406, doi:10.1038/s41591-018-0159-7 (2018).
- 99 Bergeron, R. *et al.* Effect of 5-aminoimidazole-4-carboxamide-1-beta-D-ribofuranoside infusion on in vivo glucose and lipid metabolism in lean and obese Zucker rats. *Diabetes* **50**, 1076-1082 (2001).
- 100 Buhl, E. S. *et al.* Long-term AICAR administration reduces metabolic disturbances and lowers blood pressure in rats displaying features of the insulin resistance syndrome. *Diabetes* **51**, 2199-2206 (2002).
- 101 Iglesias, M. A. *et al.* AICAR administration causes an apparent enhancement of muscle and liver insulin action in insulin-resistant high-fat-fed rats. *Diabetes* **51**, 2886-2894 (2002).
- 102 Pold, R. *et al.* Long-term AICAR administration and exercise prevents diabetes in ZDF rats. *Diabetes* **54**, 928-934 (2005).
- 103 Song, X. M. *et al.* 5-Aminoimidazole-4-carboxamide ribonucleoside treatment improves glucose homeostasis in insulin-resistant diabetic (ob/ob) mice. *Diabetologia* **45**, 56-65, doi:10.1007/s001250200006 (2002).
- 104 Boon, H. *et al.* Intravenous AICAR administration reduces hepatic glucose output and inhibits whole body lipolysis in type 2 diabetic patients. *Diabetologia* **51**, 1893-1900, doi:10.1007/s00125-008-1108-7 (2008).
- 105 Salatto, C. T. *et al.* Selective Activation of AMPK beta1-Containing Isoforms Improves Kidney Function in a Rat Model of Diabetic Nephropathy. *J Pharmacol Exp Ther* **361**, 303-311, doi:10.1124/jpet.116.237925 (2017).
- 106 Rawlins, J., Bhan, A. & Sharma, S. Left ventricular hypertrophy in athletes. *Eur J Echocardiogr* **10**, 350-356, doi:10.1093/ejehocardi/jep017 (2009).
- 107 Celenza, J. L. & Carlson, M. A yeast gene that is essential for release from glucose repression encodes a protein kinase. *Science* **233**, 1175-1180 (1986).
- 108 Lo, W. S. *et al.* Snf1--a histone kinase that works in concert with the histone acetyltransferase Gcn5 to regulate transcription. *Science* **293**, 1142-1146, doi:10.1126/science.1062322 (2001).
- 109 Bungard, D. *et al.* Signaling kinase AMPK activates stress-promoted transcription via histone H2B phosphorylation. *Science* **329**, 1201-1205, doi:10.1126/science.1191241 (2010).
- 110 Abate, G. *et al.* Snf1/AMPK regulates Gcn5 occupancy, H3 acetylation and chromatin remodelling at *S. cerevisiae* ADY2 promoter. *Biochim Biophys Acta* **1819**, 419-427, doi:10.1016/j.bbagr.2012.01.009 (2012).
- 111 McGee, S. L. *et al.* AMP-activated protein kinase regulates GLUT4 transcription by phosphorylating histone deacetylase 5. *Diabetes* **57**, 860-867, doi:10.2337/db07-0843 (2008).

- 112 McGee, S. L. *et al.* Exercise increases nuclear AMPK alpha2 in human skeletal muscle. *Diabetes* **52**, 926-928 (2003).
- 113 Steinberg, G. R. *et al.* Reduced glycogen availability is associated with increased AMPKalpha2 activity, nuclear AMPKalpha2 protein abundance, and GLUT4 mRNA expression in contracting human skeletal muscle. *Appl Physiol Nutr Metab* **31**, 302-312, doi:10.1139/h06-003 (2006).
- 114 Suzuki, A. *et al.* Leptin stimulates fatty acid oxidation and peroxisome proliferator-activated receptor alpha gene expression in mouse C2C12 myoblasts by changing the subcellular localization of the alpha2 form of AMP-activated protein kinase. *Mol Cell Biol* **27**, 4317-4327, doi:10.1128/MCB.02222-06 (2007).
- 115 Wu, D. *et al.* Glucose-regulated phosphorylation of TET2 by AMPK reveals a pathway linking diabetes to cancer. *Nature* **559**, 637-641, doi:10.1038/s41586-018-0350-5 (2018).
- 116 Salt, I. *et al.* AMP-activated protein kinase: greater AMP dependence, and preferential nuclear localization, of complexes containing the alpha2 isoform. *Biochem J* **334** (Pt 1), 177-187 (1998).
- 117 Kodiha, M., Rassi, J. G., Brown, C. M. & Stochaj, U. Localization of AMP kinase is regulated by stress, cell density, and signaling through the MEK-->ERK1/2 pathway. *Am J Physiol Cell Physiol* **293**, C1427-1436, doi:10.1152/ajpcell.00176.2007 (2007).
- 118 Vara-Ciruelos, D. *et al.* Genotoxic Damage Activates the AMPK-alpha1 Isoform in the Nucleus via Ca(2+)/CaMKK2 Signaling to Enhance Tumor Cell Survival. *Mol Cancer Res* **16**, 345-357, doi:10.1158/1541-7786.MCR-17-0323 (2018).
- 119 Kazgan, N., Williams, T., Forsberg, L. J. & Brenman, J. E. Identification of a nuclear export signal in the catalytic subunit of AMP-activated protein kinase. *Mol Biol Cell* **21**, 3433-3442, doi:10.1091/mbc.E10-04-0347 (2010).
- 120 Zuleger, N., Kerr, A. R. & Schirmer, E. C. Many mechanisms, one entrance: membrane protein translocation into the nucleus. *Cell Mol Life Sci* **69**, 2205-2216, doi:10.1007/s00018-012-0929-1 (2012).
- 121 Wang, R. & Brattain, M. G. The maximal size of protein to diffuse through the nuclear pore is larger than 60kDa. *FEBS Lett* **581**, 3164-3170, doi:10.1016/j.febslet.2007.05.082 (2007).
- 122 Marin, T. L. *et al.* Identification of AMP-activated protein kinase targets by a consensus sequence search of the proteome. *BMC Syst Biol* **9**, 13, doi:10.1186/s12918-015-0156-0 (2015).
- 123 Gong, H., Xie, J., Zhang, N., Yao, L. & Zhang, Y. MEF2A binding to the Glut4 promoter occurs via an AMPKalpha2-dependent mechanism. *Med Sci Sports Exerc* **43**, 1441-1450, doi:10.1249/MSS.0b013e31820f6093 (2011).
- 124 Chen, L. *et al.* Chronic ethanol feeding impairs AMPK and MEF2 expression and is associated with GLUT4 decrease in rat myocardium. *Exp Mol Med* **42**, 205-215, doi:10.3858/emm.2010.42.3.021 (2010).
- 125 Holmes, B. F., Sparling, D. P., Olson, A. L., Winder, W. W. & Dohm, G. L. Regulation of muscle GLUT4 enhancer factor and myocyte enhancer factor 2 by AMP-activated protein kinase. *Am J Physiol Endocrinol Metab* **289**, E1071-1076, doi:10.1152/ajpendo.00606.2004 (2005).
- 126 Holmes, B. F., Kurth-Kraczek, E. J. & Winder, W. W. Chronic activation of 5'-AMP-activated protein kinase increases GLUT-4, hexokinase, and glycogen in muscle. *J Appl Physiol (1985)* **87**, 1990-1995, doi:10.1152/jappl.1999.87.5.1990 (1999).
- 127 Thomson, D. M. *et al.* AMP-activated protein kinase phosphorylates transcription factors of the CREB family. *J Appl Physiol (1985)* **104**, 429-438, doi:10.1152/japplphysiol.00900.2007 (2008).
- 128 Jorgensen, S. B. *et al.* Role of AMPKalpha2 in basal, training-, and AICAR-induced GLUT4, hexokinase II, and mitochondrial protein expression in mouse muscle. *Am J Physiol Endocrinol Metab* **292**, E331-339, doi:10.1152/ajpendo.00243.2006 (2007).

- 129 Reznick, R. M. & Shulman, G. I. The role of AMP-activated protein kinase in mitochondrial biogenesis. *J Physiol* **574**, 33-39, doi:10.1113/jphysiol.2006.109512 (2006).
- 130 Fentz, J. *et al.* AMPKalpha is essential for acute exercise-induced gene responses but not for exercise training-induced adaptations in mouse skeletal muscle. *Am J Physiol Endocrinol Metab* **309**, E900-914, doi:10.1152/ajpendo.00157.2015 (2015).
- 131 Zong, H. *et al.* AMP kinase is required for mitochondrial biogenesis in skeletal muscle in response to chronic energy deprivation. *Proc Natl Acad Sci U S A* **99**, 15983-15987, doi:10.1073/pnas.252625599 (2002).
- 132 Suwa, M., Nakano, H. & Kumagai, S. Effects of chronic AICAR treatment on fiber composition, enzyme activity, UCP3, and PGC-1 in rat muscles. *J Appl Physiol (1985)* **95**, 960-968, doi:10.1152/japplphysiol.00349.2003 (2003).
- 133 Winder, W. W. *et al.* Activation of AMP-activated protein kinase increases mitochondrial enzymes in skeletal muscle. *J Appl Physiol (1985)* **88**, 2219-2226, doi:10.1152/jappl.2000.88.6.2219 (2000).
- 134 Garcia-Roves, P. M., Osler, M. E., Holmstrom, M. H. & Zierath, J. R. Gain-of-function R225Q mutation in AMP-activated protein kinase gamma3 subunit increases mitochondrial biogenesis in glycolytic skeletal muscle. *J Biol Chem* **283**, 35724-35734, doi:10.1074/jbc.M805078200 (2008).
- 135 Irrcher, I., Ljubicic, V., Kirwan, A. F. & Hood, D. A. AMP-activated protein kinase-regulated activation of the PGC-1alpha promoter in skeletal muscle cells. *PLoS One* **3**, e3614, doi:10.1371/journal.pone.0003614 (2008).
- 136 Jager, S., Handschin, C., St-Pierre, J. & Spiegelman, B. M. AMP-activated protein kinase (AMPK) action in skeletal muscle via direct phosphorylation of PGC-1alpha. *Proc Natl Acad Sci U S A* **104**, 12017-12022, doi:10.1073/pnas.0705070104 (2007).
- 137 Canto, C. *et al.* AMPK regulates energy expenditure by modulating NAD⁺ metabolism and SIRT1 activity. *Nature* **458**, 1056-1060, doi:10.1038/nature07813 (2009).
- 138 Lemercier, C. *et al.* mHDA1/HDAC5 histone deacetylase interacts with and represses MEF2A transcriptional activity. *J Biol Chem* **275**, 15594-15599, doi:10.1074/jbc.M908437199 (2000).
- 139 Narkar, V. A. *et al.* AMPK and PPARdelta agonists are exercise mimetics. *Cell* **134**, 405-415, doi:10.1016/j.cell.2008.06.051 (2008).
- 140 Ju, J. S., Smith, J. L., Oppelt, P. J. & Fisher, J. S. Creatine feeding increases GLUT4 expression in rat skeletal muscle. *Am J Physiol Endocrinol Metab* **288**, E347-352, doi:10.1152/ajpendo.00238.2004 (2005).
- 141 Boudaba, N. *et al.* AMPK Re-Activation Suppresses Hepatic Steatosis but its Downregulation Does Not Promote Fatty Liver Development. *EBioMedicine* **28**, 194-209, doi:10.1016/j.ebiom.2018.01.008 (2018).
- 142 Foretz, M., Even, P. C. & Viollet, B. AMPK Activation Reduces Hepatic Lipid Content by Increasing Fat Oxidation In Vivo. *Int J Mol Sci* **19**, doi:10.3390/ijms19092826 (2018).
- 143 You, M., Matsumoto, M., Pacold, C. M., Cho, W. K. & Crabb, D. W. The role of AMP-activated protein kinase in the action of ethanol in the liver. *Gastroenterology* **127**, 1798-1808 (2004).
- 144 Woods, A. *et al.* Characterization of the role of AMP-activated protein kinase in the regulation of glucose-activated gene expression using constitutively active and dominant negative forms of the kinase. *Mol Cell Biol* **20**, 6704-6711 (2000).
- 145 Guigas, B. *et al.* AMP-activated protein kinase-independent inhibition of hepatic mitochondrial oxidative phosphorylation by AICA riboside. *Biochem J* **404**, 499-507, doi:10.1042/BJ20070105 (2007).
- 146 Berasi, S. P. *et al.* Inhibition of gluconeogenesis through transcriptional activation of EGR1 and DUSP4 by AMP-activated kinase. *J Biol Chem* **281**, 27167-27177, doi:10.1074/jbc.M602416200 (2006).

- 147 Woods, A. *et al.* Liver-Specific Activation of AMPK Prevents Steatosis on a High-Fructose Diet. *Cell Rep* **18**, 3043-3051, doi:10.1016/j.celrep.2017.03.011 (2017).
- 148 Viollet, B. *et al.* AMP-activated protein kinase in the regulation of hepatic energy metabolism: from physiology to therapeutic perspectives. *Acta Physiol (Oxf)* **196**, 81-98, doi:10.1111/j.1748-1716.2009.01970.x (2009).
- 149 Andreelli, F. *et al.* Liver adenosine monophosphate-activated kinase- α 2 catalytic subunit is a key target for the control of hepatic glucose production by adiponectin and leptin but not insulin. *Endocrinology* **147**, 2432-2441, doi:10.1210/en.2005-0898 (2006).
- 150 Lee, J. M. *et al.* AMPK-dependent repression of hepatic gluconeogenesis via disruption of CREB-CRTC2 complex by orphan nuclear receptor small heterodimer partner. *J Biol Chem* **285**, 32182-32191, doi:10.1074/jbc.M110.134890 (2010).
- 151 Yang, W. *et al.* Regulation of transcription by AMP-activated protein kinase: phosphorylation of p300 blocks its interaction with nuclear receptors. *J Biol Chem* **276**, 38341-38344, doi:10.1074/jbc.C100316200 (2001).
- 152 Viana, A. Y. *et al.* Role of hepatic AMPK activation in glucose metabolism and dexamethasone-induced regulation of AMPK expression. *Diabetes Res Clin Pract* **73**, 135-142, doi:10.1016/j.diabres.2005.12.011 (2006).
- 153 Kawaguchi, T., Osatomi, K., Yamashita, H., Kabashima, T. & Uyeda, K. Mechanism for fatty acid "sparing" effect on glucose-induced transcription: regulation of carbohydrate-responsive element-binding protein by AMP-activated protein kinase. *J Biol Chem* **277**, 3829-3835, doi:10.1074/jbc.M107895200 (2002).
- 154 Hong, Y. H., Varanasi, U. S., Yang, W. & Leff, T. AMP-activated protein kinase regulates HNF4 α transcriptional activity by inhibiting dimer formation and decreasing protein stability. *J Biol Chem* **278**, 27495-27501, doi:10.1074/jbc.M304112200 (2003).
- 155 Leclerc, I. *et al.* Hepatocyte nuclear factor-4 α involved in type 1 maturity-onset diabetes of the young is a novel target of AMP-activated protein kinase. *Diabetes* **50**, 1515-1521 (2001).
- 156 Chiang, J. Y. Negative feedback regulation of bile acid metabolism: impact on liver metabolism and diseases. *Hepatology* **62**, 1315-1317, doi:10.1002/hep.27964 (2015).
- 157 Watanabe, M. *et al.* Bile acids lower triglyceride levels via a pathway involving FXR, SHP, and SREBP-1c. *J Clin Invest* **113**, 1408-1418, doi:10.1172/JCI21025 (2004).
- 158 Arab, J. P., Karpen, S. J., Dawson, P. A., Arrese, M. & Trauner, M. Bile acids and nonalcoholic fatty liver disease: Molecular insights and therapeutic perspectives. *Hepatology* **65**, 350-362, doi:10.1002/hep.28709 (2017).
- 159 Imamura, K., Ogura, T., Kishimoto, A., Kaminishi, M. & Esumi, H. Cell cycle regulation via p53 phosphorylation by a 5'-AMP activated protein kinase activator, 5-aminoimidazole-4-carboxamide-1- β -D-ribofuranoside, in a human hepatocellular carcinoma cell line. *Biochem Biophys Res Commun* **287**, 562-567, doi:10.1006/bbrc.2001.5627 (2001).
- 160 He, G. *et al.* AMP-activated protein kinase induces p53 by phosphorylating MDMX and inhibiting its activity. *Mol Cell Biol* **34**, 148-157, doi:10.1128/MCB.00670-13 (2014).
- 161 Lamia, K. A. *et al.* AMPK regulates the circadian clock by cryptochrome phosphorylation and degradation. *Science* **326**, 437-440, doi:10.1126/science.1172156 (2009).
- 162 Um, J. H. *et al.* Activation of 5'-AMP-activated kinase with diabetes drug metformin induces casein kinase I ϵ (CKI ϵ)-dependent degradation of clock protein mPer2. *J Biol Chem* **282**, 20794-20798, doi:10.1074/jbc.C700070200 (2007).
- 163 Vieira, E. *et al.* Relationship between AMPK and the transcriptional balance of clock-related genes in skeletal muscle. *Am J Physiol Endocrinol Metab* **295**, E1032-1037, doi:10.1152/ajpendo.90510.2008 (2008).
- 164 Fu, A., Eberhard, C. E. & Sreter, R. A. Role of AMPK in pancreatic beta cell function. *Mol Cell Endocrinol* **366**, 127-134, doi:10.1016/j.mce.2012.06.020 (2013).

- 165 Rourke, J. L., Hu, Q. & Srean, R. A. AMPK and Friends: Central Regulators of beta Cell Biology. *Trends Endocrinol Metab* **29**, 111-122, doi:10.1016/j.tem.2017.11.007 (2018).
- 166 Kone, M. *et al.* LKB1 and AMPK differentially regulate pancreatic beta-cell identity. *FASEB J* **28**, 4972-4985, doi:10.1096/fj.14-257667 (2014).
- 167 Martinez-Sanchez, A. *et al.* MiR-184 expression is regulated by AMPK in pancreatic islets. *FASEB J* **32**, 2587-2600, doi:10.1096/fj.201701100R (2018).
- 168 Pullen, T. J. *et al.* Identification of genes selectively disallowed in the pancreatic islet. *Islets* **2**, 89-95, doi:10.4161/isl.2.2.11025 (2010).
- 169 Yun, H. *et al.* AMP-activated protein kinase mediates the antioxidant effects of resveratrol through regulation of the transcription factor FoxO1. *FEBS J* **281**, 4421-4438, doi:10.1111/febs.12949 (2014).
- 170 Greer, E. L. *et al.* The energy sensor AMP-activated protein kinase directly regulates the mammalian FOXO3 transcription factor. *J Biol Chem* **282**, 30107-30119, doi:10.1074/jbc.M705325200 (2007).
- 171 Greer, E. L. *et al.* An AMPK-FOXO pathway mediates longevity induced by a novel method of dietary restriction in *C. elegans*. *Curr Biol* **17**, 1646-1656, doi:10.1016/j.cub.2007.08.047 (2007).
- 172 Hoppe, S. *et al.* AMP-activated protein kinase adapts rRNA synthesis to cellular energy supply. *Proc Natl Acad Sci U S A* **106**, 17781-17786, doi:10.1073/pnas.0909873106 (2009).
- 173 Lien, F. *et al.* Metformin interferes with bile acid homeostasis through AMPK-FXR crosstalk. *J Clin Invest* **124**, 1037-1051, doi:10.1172/JCI68815 (2014).
- 174 Lim, C. Y. & Zoncu, R. The lysosome as a command-and-control center for cellular metabolism. *J Cell Biol* **214**, 653-664, doi:10.1083/jcb.201607005 (2016).
- 175 Zoncu, R. *et al.* mTORC1 senses lysosomal amino acids through an inside-out mechanism that requires the vacuolar H⁺-ATPase. *Science* **334**, 678-683, doi:10.1126/science.1207056 (2011).
- 176 Young, N. P. *et al.* AMPK governs lineage specification through Tfeb-dependent regulation of lysosomes. *Genes Dev* **30**, 535-552, doi:10.1101/gad.274142.115 (2016).
- 177 Steingrimsson, E., Copeland, N. G. & Jenkins, N. A. Melanocytes and the microphthalmia transcription factor network. *Annu Rev Genet* **38**, 365-411, doi:10.1146/annurev.genet.38.072902.092717 (2004).
- 178 Napolitano, G. & Ballabio, A. TFEB at a glance. *J Cell Sci* **129**, 2475-2481, doi:10.1242/jcs.146365 (2016).
- 179 Aksan, I. & Goding, C. R. Targeting the microphthalmia basic helix-loop-helix-leucine zipper transcription factor to a subset of E-box elements in vitro and in vivo. *Mol Cell Biol* **18**, 6930-6938 (1998).
- 180 Pogenberg, V. *et al.* Restricted leucine zipper dimerization and specificity of DNA recognition of the melanocyte master regulator MITF. *Genes Dev* **26**, 2647-2658, doi:10.1101/gad.198192.112 (2012).
- 181 Hartman, M. L. & Czyz, M. MITF in melanoma: mechanisms behind its expression and activity. *Cell Mol Life Sci* **72**, 1249-1260, doi:10.1007/s00018-014-1791-0 (2015).
- 182 Argani, P. *et al.* Primary renal neoplasms with the ASPL-TFE3 gene fusion of alveolar soft part sarcoma: a distinctive tumor entity previously included among renal cell carcinomas of children and adolescents. *Am J Pathol* **159**, 179-192, doi:10.1016/S0002-9440(10)61684-7 (2001).
- 183 Kauffman, E. C. *et al.* Molecular genetics and cellular features of TFE3 and TFEB fusion kidney cancers. *Nat Rev Urol* **11**, 465-475, doi:10.1038/nrurol.2014.162 (2014).
- 184 Mahony, C. B., Fish, R. J., Pasche, C. & Bertrand, J. Y. tfec controls the hematopoietic stem cell vascular niche during zebrafish embryogenesis. *Blood* **128**, 1336-1345, doi:10.1182/blood-2016-04-710137 (2016).

- 185 Steingrimsón, E. *et al.* Mitf and Tfe3, two members of the Mitf-Tfe family of bHLH-Zip transcription factors, have important but functionally redundant roles in osteoclast development. *Proc Natl Acad Sci U S A* **99**, 4477-4482, doi:10.1073/pnas.072071099 (2002).
- 186 Hershey, C. L. & Fisher, D. E. Mitf and Tfe3: members of a b-HLH-ZIP transcription factor family essential for osteoclast development and function. *Bone* **34**, 689-696, doi:10.1016/j.bone.2003.08.014 (2004).
- 187 Martina, J. A. *et al.* The nutrient-responsive transcription factor TFE3 promotes autophagy, lysosomal biogenesis, and clearance of cellular debris. *Sci Signal* **7**, ra9, doi:10.1126/scisignal.2004754 (2014).
- 188 Settembre, C. *et al.* TFEB links autophagy to lysosomal biogenesis. *Science* **332**, 1429-1433, doi:10.1126/science.1204592 (2011).
- 189 Settembre, C. *et al.* TFEB controls cellular lipid metabolism through a starvation-induced autoregulatory loop. *Nat Cell Biol* **15**, 647-658, doi:10.1038/ncb2718 (2013).
- 190 Salma, N., Song, J. S., Arany, Z. & Fisher, D. E. Transcription Factor Tfe3 Directly Regulates Pgc-1alpha in Muscle. *J Cell Physiol* **230**, 2330-2336, doi:10.1002/jcp.24978 (2015).
- 191 Huan, C. *et al.* Transcription factors TFE3 and TFEB are critical for CD40 ligand expression and thymus-dependent humoral immunity. *Nat Immunol* **7**, 1082-1091, doi:10.1038/ni1378 (2006).
- 192 Pastore, N. *et al.* TFEB and TFE3 cooperate in the regulation of the innate immune response in activated macrophages. *Autophagy* **12**, 1240-1258, doi:10.1080/15548627.2016.1179405 (2016).
- 193 Pastore, N. *et al.* TFE3 regulates whole-body energy metabolism in cooperation with TFEB. *EMBO Mol Med* **9**, 605-621, doi:10.15252/emmm.201607204 (2017).
- 194 Steingrimsón, E., Tessarollo, L., Reid, S. W., Jenkins, N. A. & Copeland, N. G. The bHLH-Zip transcription factor Tfeb is essential for placental vascularization. *Development* **125**, 4607-4616 (1998).
- 195 Medina, D. L. *et al.* Transcriptional activation of lysosomal exocytosis promotes cellular clearance. *Dev Cell* **21**, 421-430, doi:10.1016/j.devcel.2011.07.016 (2011).
- 196 Palmieri, M. *et al.* Characterization of the CLEAR network reveals an integrated control of cellular clearance pathways. *Hum Mol Genet* **20**, 3852-3866, doi:10.1093/hmg/ddr306 (2011).
- 197 Sardiello, M. *et al.* A gene network regulating lysosomal biogenesis and function. *Science* **325**, 473-477, doi:10.1126/science.1174447 (2009).
- 198 Mansueto, G. *et al.* Transcription Factor EB Controls Metabolic Flexibility during Exercise. *Cell Metab* **25**, 182-196, doi:10.1016/j.cmet.2016.11.003 (2017).
- 199 Vega-Rubin-de-Celis, S., Pena-Llopis, S., Konda, M. & Brugarolas, J. Multistep regulation of TFEB by MTORC1. *Autophagy* **13**, 464-472, doi:10.1080/15548627.2016.1271514 (2017).
- 200 Settembre, C. *et al.* A lysosome-to-nucleus signalling mechanism senses and regulates the lysosome via mTOR and TFEB. *EMBO J* **31**, 1095-1108, doi:10.1038/emboj.2012.32 (2012).
- 201 Roczniak-Ferguson, A. *et al.* The transcription factor TFEB links mTORC1 signaling to transcriptional control of lysosome homeostasis. *Sci Signal* **5**, ra42, doi:10.1126/scisignal.2002790 (2012).
- 202 Martina, J. A., Chen, Y., Gucek, M. & Puertollano, R. MTORC1 functions as a transcriptional regulator of autophagy by preventing nuclear transport of TFEB. *Autophagy* **8**, 903-914, doi:10.4161/auto.19653 (2012).
- 203 Li, L. *et al.* A TFEB nuclear export signal integrates amino acid supply and glucose availability. *Nat Commun* **9**, 2685, doi:10.1038/s41467-018-04849-7 (2018).
- 204 Medina, D. L. *et al.* Lysosomal calcium signalling regulates autophagy through calcineurin and TFEB. *Nat Cell Biol* **17**, 288-299, doi:10.1038/ncb3114 (2015).

- 205 Martina, J. A., Diab, H. I., Brady, O. A. & Puertollano, R. TFEB and TFE3 are novel components of the integrated stress response. *EMBO J* **35**, 479-495, doi:10.15252/embj.201593428 (2016).
- 206 Li, X. *et al.* Nucleus-Translocated ACS2 Promotes Gene Transcription for Lysosomal Biogenesis and Autophagy. *Mol Cell* **66**, 684-697 e689, doi:10.1016/j.molcel.2017.04.026 (2017).
- 207 Spampanato, C. *et al.* Transcription factor EB (TFEB) is a new therapeutic target for Pompe disease. *EMBO Mol Med* **5**, 691-706, doi:10.1002/emmm.201202176 (2013).
- 208 Song, W. *et al.* TFEB regulates lysosomal proteostasis. *Hum Mol Genet* **22**, 1994-2009, doi:10.1093/hmg/ddt052 (2013).
- 209 Martini-Stoica, H., Xu, Y., Ballabio, A. & Zheng, H. The Autophagy-Lysosomal Pathway in Neurodegeneration: A TFEB Perspective. *Trends Neurosci* **39**, 221-234, doi:10.1016/j.tins.2016.02.002 (2016).
- 210 Decressac, M. *et al.* TFEB-mediated autophagy rescues midbrain dopamine neurons from alpha-synuclein toxicity. *Proc Natl Acad Sci U S A* **110**, E1817-1826, doi:10.1073/pnas.1305623110 (2013).
- 211 Merrill, G. F., Kurth, E. J., Hardie, D. G. & Winder, W. W. AICA riboside increases AMP-activated protein kinase, fatty acid oxidation, and glucose uptake in rat muscle. *Am J Physiol* **273**, E1107-1112 (1997).
- 212 Guigas, B. *et al.* Beyond AICA riboside: in search of new specific AMP-activated protein kinase activators. *IUBMB Life* **61**, 18-26, doi:10.1002/iub.135 (2009).
- 213 Guigas, B. *et al.* 5-Aminoimidazole-4-carboxamide-1-beta-D-ribofuranoside and metformin inhibit hepatic glucose phosphorylation by an AMP-activated protein kinase-independent effect on glucokinase translocation. *Diabetes* **55**, 865-874 (2006).
- 214 Napolitano, G. *et al.* mTOR-dependent phosphorylation controls TFEB nuclear export. *Nat Commun* **9**, 3312, doi:10.1038/s41467-018-05862-6 (2018).
- 215 Meng, J. & Ferguson, S. M. GATOR1-dependent recruitment of FLCN-FNIP to lysosomes coordinates Rag GTPase heterodimer nucleotide status in response to amino acids. *J Cell Biol* **217**, 2765-2776, doi:10.1083/jcb.201712177 (2018).
- 216 Yan, M. *et al.* The tumor suppressor folliculin regulates AMPK-dependent metabolic transformation. *J Clin Invest* **124**, 2640-2650, doi:10.1172/JCI71749 (2014).
- 217 Yan, M. *et al.* Chronic AMPK activation via loss of FLCN induces functional beige adipose tissue through PGC-1alpha/ERRalpha. *Genes Dev* **30**, 1034-1046, doi:10.1101/gad.281410.116 (2016).
- 218 Laderoute, K. R. *et al.* 5'-AMP-activated protein kinase (AMPK) is induced by low-oxygen and glucose deprivation conditions found in solid-tumor microenvironments. *Mol Cell Biol* **26**, 5336-5347, doi:10.1128/MCB.00166-06 (2006).
- 219 Kirchner, J., Brune, B. & Namgaladze, D. AICAR inhibits NFkappaB DNA binding independently of AMPK to attenuate LPS-triggered inflammatory responses in human macrophages. *Sci Rep* **8**, 7801, doi:10.1038/s41598-018-26102-3 (2018).
- 220 Green, G. H. & Diggle, P. J. On the operational characteristics of the Benjamini and Hochberg False Discovery Rate procedure. *Stat Appl Genet Mol Biol* **6**, Article27, doi:10.2202/1544-6115.1302 (2007).
- 221 Huang, D. W., Sherman, B. T. & Lempicki, R. A. Systematic and integrative analysis of large gene lists using DAVID bioinformatics resources. *Nature Protocols* **4**, 44, doi:10.1038/nprot.2008.211
<https://www.nature.com/articles/nprot.2008.211#supplementary-information> (2008).
- 222 Huang da, W., Sherman, B. T. & Lempicki, R. A. Bioinformatics enrichment tools: paths toward the comprehensive functional analysis of large gene lists. *Nucleic Acids Res* **37**, 1-13, doi:10.1093/nar/gkn923 (2009).

- 223 Soyombo, A. A. *et al.* TRP-ML1 regulates lysosomal pH and acidic lysosomal lipid hydrolytic activity. *J Biol Chem* **281**, 7294-7301, doi:10.1074/jbc.M508211200 (2006).
- 224 Mok, A., Cao, H. & Hegele, R. A. Genomic basis of mucopolysaccharidosis type IIID (MIM 252940) revealed by sequencing of GNS encoding N-acetylglucosamine-6-sulfatase. *Genomics* **81**, 1-5 (2003).
- 225 Pshezhetsky, A. V. & Hinek, A. Where catabolism meets signalling: neuraminidase 1 as a modulator of cell receptors. *Glycoconj J* **28**, 441-452, doi:10.1007/s10719-011-9350-5 (2011).
- 226 Kramer, A., Green, J., Pollard, J., Jr. & Tugendreich, S. Causal analysis approaches in Ingenuity Pathway Analysis. *Bioinformatics* **30**, 523-530, doi:10.1093/bioinformatics/btt703 (2014).
- 227 Huang, Z. *et al.* ACS2 promotes systemic fat storage and utilization through selective regulation of genes involved in lipid metabolism. *Proc Natl Acad Sci U S A* **115**, E9499-E9506, doi:10.1073/pnas.1806635115 (2018).
- 228 Kondo, A. *et al.* Extracellular Acidic pH Activates the Sterol Regulatory Element-Binding Protein 2 to Promote Tumor Progression. *Cell Rep* **18**, 2228-2242, doi:10.1016/j.celrep.2017.02.006 (2017).
- 229 Zhang, Y., Ma, K. L., Ruan, X. Z. & Liu, B. C. Dysregulation of the Low-Density Lipoprotein Receptor Pathway Is Involved in Lipid Disorder-Mediated Organ Injury. *Int J Biol Sci* **12**, 569-579, doi:10.7150/ijbs.14027 (2016).
- 230 Sharpe, L. J. & Brown, A. J. Controlling cholesterol synthesis beyond 3-hydroxy-3-methylglutaryl-CoA reductase (HMGCR). *J Biol Chem* **288**, 18707-18715, doi:10.1074/jbc.R113.479808 (2013).
- 231 Peterson, T. R. *et al.* mTOR complex 1 regulates lipin 1 localization to control the SREBP pathway. *Cell* **146**, 408-420, doi:10.1016/j.cell.2011.06.034 (2011).
- 232 Audas, T. E., Li, Y., Liang, G. & Lu, R. A novel protein, Luman/CREB3 recruitment factor, inhibits Luman activation of the unfolded protein response. *Mol Cell Biol* **28**, 3952-3966, doi:10.1128/MCB.01439-07 (2008).
- 233 Zhou, R., Tardivel, A., Thorens, B., Choi, I. & Tschopp, J. Thioredoxin-interacting protein links oxidative stress to inflammasome activation. *Nat Immunol* **11**, 136-140, doi:10.1038/ni.1831 (2010).
- 234 Lu, K., Psakhye, I. & Jentsch, S. Autophagic clearance of polyQ proteins mediated by ubiquitin-Atg8 adaptors of the conserved CUET protein family. *Cell* **158**, 549-563, doi:10.1016/j.cell.2014.05.048 (2014).
- 235 Siggs, O. M. *et al.* Mutation of Fnip1 is associated with B-cell deficiency, cardiomyopathy, and elevated AMPK activity. *Proc Natl Acad Sci U S A* **113**, E3706-3715, doi:10.1073/pnas.1607592113 (2016).
- 236 Baba, M. *et al.* Folliculin encoded by the BHD gene interacts with a binding protein, FNIP1, and AMPK, and is involved in AMPK and mTOR signaling. *Proc Natl Acad Sci U S A* **103**, 15552-15557, doi:10.1073/pnas.0603781103 (2006).
- 237 Possik, E. *et al.* Folliculin regulates ampk-dependent autophagy and metabolic stress survival. *PLoS Genet* **10**, e1004273, doi:10.1371/journal.pgen.1004273 (2014).
- 238 Hellemans, J. & Vandesompele, J. Selection of reliable reference genes for RT-qPCR analysis. *Methods Mol Biol* **1160**, 19-26, doi:10.1007/978-1-4939-0733-5_3 (2014).
- 239 Gut, P., Reischauer, S., Stainier, D. Y. R. & Arnaout, R. Little Fish, Big Data: Zebrafish as a Model for Cardiovascular and Metabolic Disease. *Physiol Rev* **97**, 889-938, doi:10.1152/physrev.00038.2016 (2017).
- 240 Gilbert, M. J., Zerulla, T. C. & Tierney, K. B. Zebrafish (*Danio rerio*) as a model for the study of aging and exercise: physical ability and trainability decrease with age. *Exp Gerontol* **50**, 106-113, doi:10.1016/j.exger.2013.11.013 (2014).

- 241 Vincent, M. F., Marangos, P. J., Gruber, H. E. & Van den Berghe, G. Inhibition by AICA riboside of gluconeogenesis in isolated rat hepatocytes. *Diabetes* **40**, 1259-1266 (1991).
- 242 Longnus, S. L., Wambolt, R. B., Parsons, H. L., Brownsey, R. W. & Allard, M. F. 5-Aminoimidazole-4-carboxamide 1-beta -D-ribofuranoside (AICAR) stimulates myocardial glycogenolysis by allosteric mechanisms. *Am J Physiol Regul Integr Comp Physiol* **284**, R936-944, doi:10.1152/ajpregu.00319.2002 (2003).
- 243 Ojuka, E. O., Nolte, L. A. & Holloszy, J. O. Increased expression of GLUT-4 and hexokinase in rat epitrochlearis muscles exposed to AICAR in vitro. *J Appl Physiol* (1985) **88**, 1072-1075, doi:10.1152/jappl.2000.88.3.1072 (2000).
- 244 Stoppani, J. *et al.* AMP-activated protein kinase activates transcription of the UCP3 and HKII genes in rat skeletal muscle. *Am J Physiol Endocrinol Metab* **283**, E1239-1248, doi:10.1152/ajpendo.00278.2002 (2002).
- 245 Sanchez, A. M. *et al.* AMPK promotes skeletal muscle autophagy through activation of forkhead FoxO3a and interaction with ULK1. *J Cell Biochem* **113**, 695-710, doi:10.1002/jcb.23399 (2012).
- 246 Tikhanovich, I., Cox, J. & Weinman, S. A. Forkhead box class O transcription factors in liver function and disease. *J Gastroenterol Hepatol* **28 Suppl 1**, 125-131, doi:10.1111/jgh.12021 (2013).
- 247 Eberle, D., Hegarty, B., Bossard, P., Ferre, P. & Foulle, F. SREBP transcription factors: master regulators of lipid homeostasis. *Biochimie* **86**, 839-848, doi:10.1016/j.biochi.2004.09.018 (2004).
- 248 Hua, X., Sakai, J., Ho, Y. K., Goldstein, J. L. & Brown, M. S. Hairpin orientation of sterol regulatory element-binding protein-2 in cell membranes as determined by protease protection. *J Biol Chem* **270**, 29422-29427 (1995).
- 249 Nohturfft, A., Brown, M. S. & Goldstein, J. L. Topology of SREBP cleavage-activating protein, a polytopic membrane protein with a sterol-sensing domain. *J Biol Chem* **273**, 17243-17250 (1998).
- 250 Wang, X., Sato, R., Brown, M. S., Hua, X. & Goldstein, J. L. SREBP-1, a membrane-bound transcription factor released by sterol-regulated proteolysis. *Cell* **77**, 53-62 (1994).
- 251 Hua, X., Wu, J., Goldstein, J. L., Brown, M. S. & Hobbs, H. H. Structure of the human gene encoding sterol regulatory element binding protein-1 (SREBF1) and localization of SREBF1 and SREBF2 to chromosomes 17p11.2 and 22q13. *Genomics* **25**, 667-673 (1995).
- 252 Horton, J. D. *et al.* Combined analysis of oligonucleotide microarray data from transgenic and knockout mice identifies direct SREBP target genes. *Proc Natl Acad Sci U S A* **100**, 12027-12032, doi:10.1073/pnas.1534923100 (2003).
- 253 Horton, J. D. *et al.* Activation of cholesterol synthesis in preference to fatty acid synthesis in liver and adipose tissue of transgenic mice overproducing sterol regulatory element-binding protein-2. *J Clin Invest* **101**, 2331-2339, doi:10.1172/JCI2961 (1998).
- 254 Schmidt, L. S. & Linehan, W. M. FLCN: The causative gene for Birt-Hogg-Dube syndrome. *Gene* **640**, 28-42, doi:10.1016/j.gene.2017.09.044 (2018).
- 255 Nahorski, M. S. *et al.* Folliculin interacts with p0071 (plakophilin-4) and deficiency is associated with disordered RhoA signalling, epithelial polarization and cytokinesis. *Hum Mol Genet* **21**, 5268-5279, doi:10.1093/hmg/dd3378 (2012).
- 256 Dunlop, E. A. *et al.* FLCN, a novel autophagy component, interacts with GABARAP and is regulated by ULK1 phosphorylation. *Autophagy* **10**, 1749-1760, doi:10.4161/auto.29640 (2014).
- 257 Luijten, M. N. *et al.* Birt-Hogg-Dube syndrome is a novel ciliopathy. *Hum Mol Genet* **22**, 4383-4397, doi:10.1093/hmg/ddt288 (2013).
- 258 Possik, E. *et al.* FLCN and AMPK Confer Resistance to Hyperosmotic Stress via Remodeling of Glycogen Stores. *PLoS Genet* **11**, e1005520, doi:10.1371/journal.pgen.1005520 (2015).

- 259 Goncharova, E. A. *et al.* Folliculin controls lung alveolar enlargement and epithelial cell survival through E-cadherin, LKB1, and AMPK. *Cell Rep* **7**, 412-423, doi:10.1016/j.celrep.2014.03.025 (2014).
- 260 Hasumi, H. *et al.* Folliculin-interacting proteins Fnip1 and Fnip2 play critical roles in kidney tumor suppression in cooperation with Flcn. *Proc Natl Acad Sci U S A* **112**, E1624-1631, doi:10.1073/pnas.1419502112 (2015).
- 261 Reyes, N. L. *et al.* Fnip1 regulates skeletal muscle fiber type specification, fatigue resistance, and susceptibility to muscular dystrophy. *Proc Natl Acad Sci U S A* **112**, 424-429, doi:10.1073/pnas.1413021112 (2015).
- 262 Hasumi, H. *et al.* Identification and characterization of a novel folliculin-interacting protein FNIP2. *Gene* **415**, 60-67, doi:10.1016/j.gene.2008.02.022 (2008).
- 263 Wang, L. *et al.* Serine 62 is a phosphorylation site in folliculin, the Birt-Hogg-Dube gene product. *FEBS Lett* **584**, 39-43, doi:10.1016/j.febslet.2009.11.033 (2010).
- 264 Puertollano, R., Ferguson, S. M., Brugarolas, J. & Ballabio, A. The complex relationship between TFEB transcription factor phosphorylation and subcellular localization. *EMBO J* **37**, doi:10.15252/embj.201798804 (2018).
- 265 Marz, A. M., Fabian, A. K., Kozany, C., Bracher, A. & Hausch, F. Large FK506-binding proteins shape the pharmacology of rapamycin. *Mol Cell Biol* **33**, 1357-1367, doi:10.1128/MCB.00678-12 (2013).
- 266 Liu, Q. *et al.* Characterization of Torin2, an ATP-competitive inhibitor of mTOR, ATM, and ATR. *Cancer Res* **73**, 2574-2586, doi:10.1158/0008-5472.CAN-12-1702 (2013).
- 267 Hunter, R. W. *et al.* Mechanism of action of compound-13: an alpha1-selective small molecule activator of AMPK. *Chem Biol* **21**, 866-879, doi:10.1016/j.chembiol.2014.05.014 (2014).
- 268 Schlegel, A. & Gut, P. Metabolic insights from zebrafish genetics, physiology, and chemical biology. *Cell Mol Life Sci* **72**, 2249-2260, doi:10.1007/s00018-014-1816-8 (2015).
- 269 Shaw, R. J. *et al.* The LKB1 tumor suppressor negatively regulates mTOR signaling. *Cancer Cell* **6**, 91-99, doi:10.1016/j.ccr.2004.06.007 (2004).
- 270 Gwinn, D. M. *et al.* AMPK phosphorylation of raptor mediates a metabolic checkpoint. *Mol Cell* **30**, 214-226, doi:10.1016/j.molcel.2008.03.003 (2008).
- 271 Inoki, K. *et al.* TSC2 integrates Wnt and energy signals via a coordinated phosphorylation by AMPK and GSK3 to regulate cell growth. *Cell* **126**, 955-968, doi:10.1016/j.cell.2006.06.055 (2006).
- 272 Brady, O. A., Martina, J. A. & Puertollano, R. Emerging roles for TFEB in the immune response and inflammation. *Autophagy* **14**, 181-189, doi:10.1080/15548627.2017.1313943 (2018).
- 273 Wada, S. *et al.* The tumor suppressor FLCN mediates an alternate mTOR pathway to regulate browning of adipose tissue. *Genes Dev* **30**, 2551-2564, doi:10.1101/gad.287953.116 (2016).

Glossary

2-DG	2-deoxyglucose
ACC	Acetyl-CoA carboxylase
<i>Actc1b</i>	Actin alpha cardiac muscle 1b
ACSS2	Acetyl-CoA synthetase-2
AD	Activation domain
ADaM-site	Allosteric drug and metabolite binding site
ADP	Adenosine diphosphate
ATP	Adenosine triphosphate
AdipoR1	Adiponectin receptor-1
AICAR	5-aminoimidazole-4-carboxamide-1- β -D-ribofuranoside
AID	Auto-inhibitory domain
AMPK	AMP-activated protein kinase
ANOVA	Analysis of variance
ATP	Adenosine triphosphate
<i>B2m</i>	β 2 microglobulin
BHD	Birt-Hogg-Dubé
bHLH	Basic helix-loop-helix
BMAL1	Brain and muscle ARNT-like-1
C13	Compound 13
C2	Compound 2
Ca ²⁺	Calcium
CAMKK β	Ca ²⁺ -calmodulin-dependent protein kinase kinase β
CBP/p300	CREB-binding protein
CBS	Cystathionine β -synthase
ChREBP	Carbohydrate-responsive element-binding protein
CKI ϵ	Casein kinase I ϵ
CLEAR	Coordinated lysosomal expression and regulation

CREB	cAMP response element-binding protein
<i>Crebrf</i>	CREB3 regulatory factor
CRM1	Chromosomal maintenance-1
CRTC2	CREB regulated transcription coactivator-2
CRY1	Cryptochrome
CTD	C-terminal domain
DAVID	Database for Annotation, Visualization and Integrated Discovery
DMEM	Dulbecco's modified eagle medium
dpf	Days post fertilization
DKO	Double knockout
ESCs	Embryonic stem cells
EIF2AK3	Eukaryotic translation initiation factor 2 α kinase 3
FBP1	Fructose-1,6-biphosphatase-1
FC	Fold change
FDR	False discover rate
FKBP12	FK506-binding protein-12
FLCN	Folliculin
FNIP	Folliculin interacting protein
FOXO	Forkhead box O
FXR	Farnesoid X receptor
GAS	Gastrocnemius
G6Pase	Glucose 6-phosphatase
GEF	GLUT4 enhancer factor
GHSR1	Growth hormone secretagogue receptor type 1
GLUT4	Glucose transporter 4
<i>Gns</i>	N-acetylglucosamine-6-sulfatase
GSK3 β	Glycogen synthase kinase-3 β
H	Histone
HDACs	Histone deacetylases
HIF α	Hypoxia-inducible factor- α

HKII	Hexokinase II
HMGCR	3-hydroxy-3-methylglutaryl-CoA reductase
HNF4 α	Hepatocyte nuclear factor-4 α
IP	Immunoprecipitated
IPA	Ingenuity Pathway Analysis
KD	Kinase domain
KO	Knockout
LAMTOR1	Late endosomal/lysosomal adaptor MAPK and mTOR Activator-1
<i>Ldlr</i>	Low density lipoprotein receptor
LKB1	Liver kinase B1
<i>Lpin1</i>	Lipin-1
L-PK	L-pyruvate kinase
LSDs	Lysosomal storage disorders
MAPK	Mitogen-activated protein kinase
MCOLN1	Mucolipin-1
MDM4	Mouse double minute 4
MEF2	Myocyte enhancer factor-2
MEFs	Mouse embryonic fibroblasts
MiT	Microphthalmia
MITF	Microphthalmia-associated transcription factor
MO25 α/β	Mouse protein 25 α and β
<i>Msmo1</i>	Methylsterol monooxygenase-1
mTORC1 or 2	Mammalian target of rapamycin complex 1 or 2
NES	Nuclear export signal
<i>Neu1</i>	Neuraminidase-1
NLS	Nuclear localization signal
P70 S6K	p70-S6 kinase-1
PC	Principal component
PCA	Principal component analysis
PEPCK	Phosphoenolpyruvate carboxykinase

PER	Period
PGC1 α	Peroxisome proliferator-activated receptor gamma coactivator 1- α
Pi	Phosphate ions
PKB	Protein kinase B
Pol I	RNA polymerase I
<i>Ppara</i>	Peroxisome proliferator-activated receptor α
PPAR δ	Peroxisome proliferator-activated receptor δ
<i>Ppia</i>	Peptidylprolyl isomerase-a
PTMs	Post-translational modifications
RMA	Robust multiarray averaging
ROS	Reactive oxygen species
rRNA	Ribosomal RNA
S6RP	S6 ribosomal protein
SIRT1	Sirtuin-1
SNF1	Sucrose non fermenting
SREBP	Sterol regulatory element-binding protein
STRAD α/β	STE20-related kinase adaptor α and β
TCA	Tricarboxylic acid cycle
TET2	Ten-eleven translocation-2
TFEB	Transcription factor EB
TIF-1A	Transcription initiation factor-1A
<i>Tollip</i>	Toll interacting protein
TSS	Transcription start site
<i>Txnip</i>	Thioredoxin interacting protein
U2OS	Human osteosarcoma
USF1	Upstream stimulatory factor-1
v-ATPase	Vacuolar-type H ⁺ -ATPase
WB	Western blot
WT	Wild-type
ZDF	Zucker diabetic fatty

Zip	Zipper motif
ZMP	AICAR monophosphate
α -RIM	α -subunit regulatory interacting motif
β -CBM	β -subunit carbohydrate-binding module

Caterina Collodet

Address:

Ch. des Triaudes 4,
1024 Ecublens, Switzerland
caterina.collodet@gmail.com

Personal information:

Date of birth: 28.08.1990
Nationality: Italian
Marital status: Single



RESEARCH EXPERIENCE

- 03.2015 – 03.2019: **PhD candidate**
Nestlé Institute of Health Sciences (NIHS) and École Polytechnique Fédérale de Lausanne (EPFL)
Thesis directors: Dr Patrick Descombes (NIHS) and Prof Bart Deplancke (EPFL)
- 01.2014 – 06.2014: **Master's project**
École Normale Supérieure (ENS), Paris, France
Supervision: Dr Claire Dugast-Darzacq (ENS) and Prof Anna Savoia (University of Trieste)
- 04.2012 – 07.2012: **Bachelor's project**
University of Padova (Unipd)
Supervision: Prof Elisa Greggio (Unipd)

EDUCATION

- 2015 – 2019: **PhD in molecular life sciences**
Nestlé Institute of Health Sciences and École polytechnique fédérale de Lausanne
- 2013 – 2014: **MSc in Génétique**
University of Paris VII
15.6/20
- 2012 – 2014: **MSc in Functional Genomics**
University of Trieste
110/110 *summa cum laude*
- 2009 – 2012: **BSc in Biotechnology**
University of Padova
110/110

SCOLARSHIPS

Admitted to the 1-year double degree program within the University of Trieste and the University Paris VII. In this context, I obtained two fellowships:

- Erasmus studies, 6 months
- Erasmus placement, 6 months

PUBLICATIONS

Collodet C, Foretz M, Deak M, Bultot L, Metaïron S, Viollet B, Lefebvre G, Raymond F, Parisi A, Civiletto G, Gut P, Descombes P, Sakamoto K. AMPK promotes induction of a tumor suppressor FLCN through activation of TFEB independently of mTOR. *BioRxiv*. 2018 Dec 20. doi: <https://doi.org/10.1101/499921>. Preprint.

Kfoury A, Armaro M, **Collodet C**, Sordet-Dessimoz J, Giner MP, Christen S, Moco S, Leleu M, de Leval L, Koch U, Trumpp A, Sakamoto K, Beermann F, Radtke F. AMPK promotes survival of c-Myc-positive melanoma cells by suppressing oxidative stress. *EMBO J*. 2018 Feb 12. PMID: 29440228.

Lopez-Mejia IC, Lagarrigue S, Giralto A, Martinez-Carreres L, Zanou N, Denechaud PD, Castillo-Armengol J, Chavey C, Orpinell M, Delacuisine B, Nasrallah A, **Collodet C**, Zhang L, Viollet B, Hardie DG, Fajas L. CDK4 Phosphorylates AMPK α 2 to Inhibit Its Activity and Repress Fatty Acid Oxidation. *Mol Cell*. 2017 Oct 19. PMID: 29053957.

Theret M, Gsaier L, Schaffer B, Juban G, Ben Larbi S, Weiss-Gayet M, Bultot L, **Collodet C**, Foretz M, Desplanches D, Sanz P, Zang Z, Yang L, Vial G, Viollet B, Sakamoto K, Brunet A, Chazaud B, Mounier R. AMPK α 1-LDH pathway regulates muscle stem cell self-renewal by controlling metabolic homeostasis. *EMBO J*. 2017 Jul 3. PMID: 28515121.

Bultot L, Jensen TE, Lai YC, Madsen AL, **Collodet C**, Kviklyte S, Deak M, Yavari A, Foretz M, Ghaffari S, Bellahcene M, Ashrafian H, Rider MH, Richter EA, Sakamoto K. A benzimidazole derivative small molecule 991 enhances AMPK activity and glucose uptake induced by AICAR or contraction in skeletal muscle. *Am J Physiol Endocrinol Metab*. 2016 Aug 30. PMID: 27577855.

POSTERS AND ORAL COMMUNICATIONS

Talk: “Gene expression profiling and analysis identify a key metabolic mediator of the master energy sensor, AMP-activated protein kinase”
Nebion-Novartis Workshop in Basel (2018)

Poster: “AMPK-dependent gene expression profiles in response to small molecule AMPK activators”
Life Science Symposium in Lausanne (2017)

Poster: “AMPK-dependent gene expression profiles in response to small molecule AMPK activators”
International Symposium on AMPK in Xiamen (2016)

Poster: “AMPK-dependent gene expression profiles in response to small molecule AMPK activators”
Lausanne Integrative Metabolism Nutrition Alliance symposium in Lausanne (2016)

Poster: “Analysis of AMPK: response to small molecule AMPK activator-dependent gene expression profiles”
European Workshop on AMPK in Maastricht (2015)

VOLUNTEERING

2016 – 2019: **BioScience Network Lausanne**
Web manager and event organizer

2015 – 2017: **NIHS PhD Students Association**
Co-founder/Coordinator

SKILLS

Field of expertise	Metabolism, cell biology, transcription regulation
Technical expertise	Cell culture: primary hepatocytes and various cell lines, transfections Molecular biology and biochemistry: RNA extraction, qPCR, Western blotting, sample preparation for mass spectrometry, kinase activity, promoter activity assay Animal models: mouse and zebrafish Informatics: basic microarray analysis, Microsoft Office, GraphPad prism, Adobe Illustrator, ImageJ, EndNote.
License for animal experimentation	RESAL module 1
Languages	Native speaker of Italian, fluent in English, intermediate level of French and basic knowledge of Swedish

